AD-A046 358 CALIFORNIA UNIV BERKELEY DEPT OF CIVIL ENGINEERING F/G 13/13
A FIELD STUDY OF SPILING REINFORCEMENT IN UNDERGROUND OPENINGS.(U)
JUN 77 G E KORBIN, T L BREKKE DACW45-74-C-0026

UNCLASSIFIED MRD-TR-1-77 NL

1 OF 3
ADA
046358

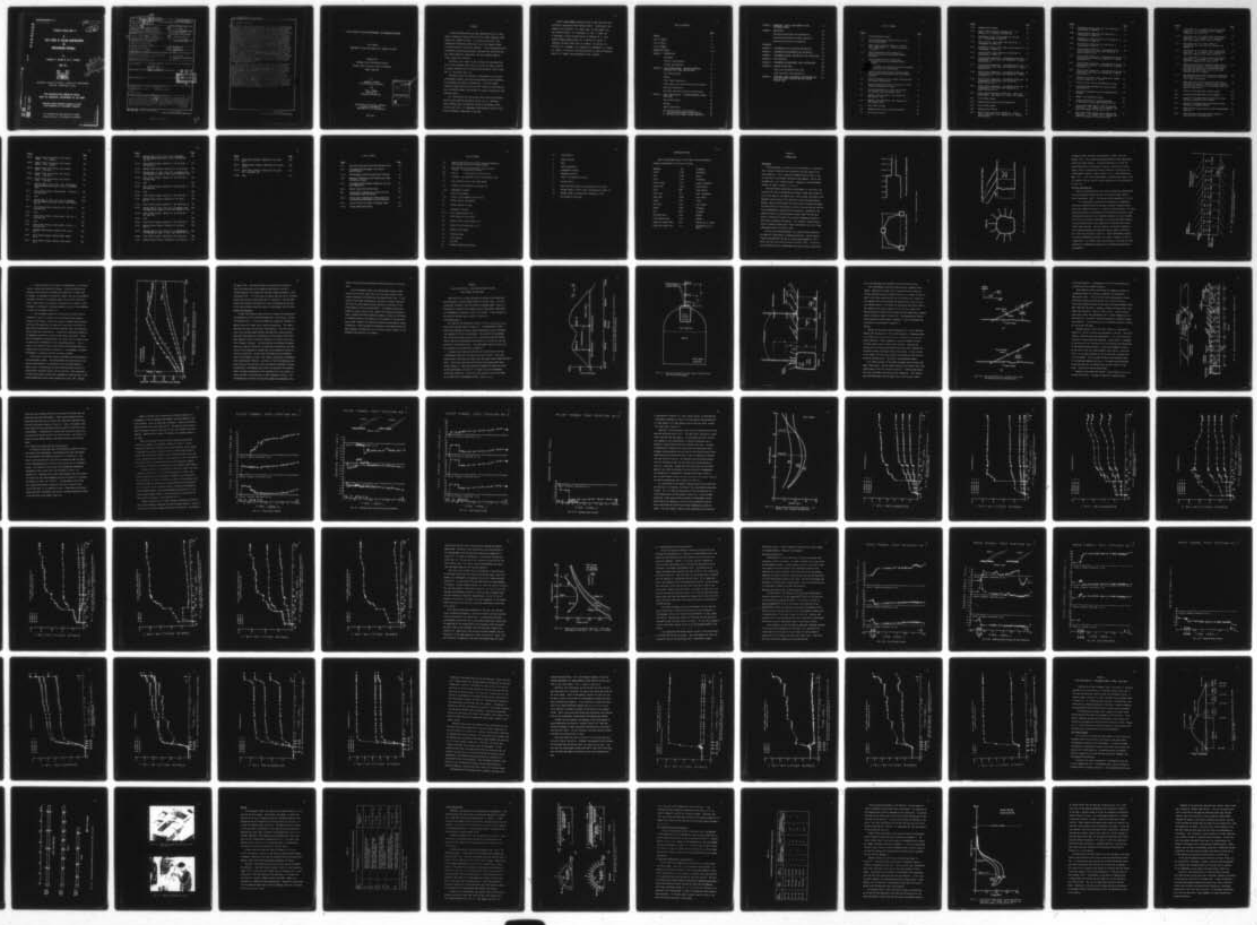

12

TECHNICAL REPORT MRD-1-77

A FIELD STUDY OF SPILING REINFORCEMENT IN UNDERGROUND OPENINGS

by

Gregory E. Korbin & Tor L. Brekke

JUNE 1977

MISSOURI RIVER DIVISION, CORPS OF ENGINEERS
OMAHA, NEBRASKA 68101

THIS RESEARCH WAS FUNDED BY OFFICE,
CHIEF OF ENGINEERS, DEPARTMENT OF THE ARMY

PREPARED UNDER CONTRACT DACW45-74-C-0026
WITH UNIVERSITY OF CALIFORNIA, BERKELEY

Unclassified

SECURITY CLASSIFICATION OF THIS PAGE (When Data Entered)

REPORT DOCUMENTATION PAGE	READ INSTRUCTIONS BEFORE COMPLETING FORM
1. REPORT NUMBER: Technical Report MRD-1-77	2. GOVT ACCESSION NO. / 3. RECIPIENT'S CATALOG NUMBER
4. TITLE (and Subtitle): Rational Design of Tunnel Supports Subtitle: A Field Study of Spiling Reinforcement in Underground Openings.	5. TYPE OF REPORT & PERIOD COVERED: Final report. / 6. PERFORMING ORG. REPORT NUMBER
7. AUTHOR(s): Gregory E. Korbin and Tor L. Brekke	8. CONTRACT OR GRANT NUMBER(s): DACW45-74-C-0026
9. PERFORMING ORGANIZATION NAME AND ADDRESS: Department of Civil Engineering, University of California, Berkeley, California 94720	10. PROGRAM ELEMENT, PROJECT, TASK AREA & WORK UNIT NUMBERS
11. CONTROLLING OFFICE NAME AND ADDRESS: Department of the Army, Office, Chief of Engineers, Washington, D. C. 20314	12. REPORT DATE: June 1977 / 13. NUMBER OF PAGES: 228
14. MONITORING AGENCY NAME & ADDRESS (if different from Controlling Office): Department of the Army, Missouri River Division, Corps of Engineers, P. O. Box 103, Downtown Station, Omaha, Nebraska 68101	15. SECURITY CLASS. (of this report): Unclassified / 15a. DECLASSIFICATION/DOWNGRADING SCHEDULE

16. DISTRIBUTION STATEMENT (of this Report)

This document has been approved for public release and sale; its distribution is unlimited.

232p.

17. DISTRIBUTION STATEMENT (of the abstract entered in Block 20, if different from Report)

DDC RECEIVED NOV 4 1977 F.

18. SUPPLEMENTARY NOTES

19. KEY WORDS (Continue on reverse side if necessary and identify by block number)

Instrumentation
Reinforcement (structures)
Spiling
Tunnel supports
Tunnels
Underground openings

20. ABSTRACT (Continue on reverse side if necessary and identify by block number)

This report covers the second phase of a two part research effort. The previous study (Technical Report MRD-2-75) largely considered the effectiveness of prereinforcement systems. From measurements and observations of the physical model behavior in conjunction with calibrated numerical model results, the mechanisms by which prereinforcement displays its effectiveness was implied, but not verified. → next page (Continued)

DD FORM 1 JAN 73 1473 EDITION OF 1 NOV 65 IS OBSOLETE

Unclassified

SECURITY CLASSIFICATION OF THIS PAGE (When Data Entered)

401 105

20. ABSTRACT (Continued)

Further investigations were required to examine and substantiate the mechanisms by which prereinforcement and, in particular, spiling reinforcement work. A field instrumentation program was designed to monitor the spiling under actual tunneling conditions. This report describes the results of two such investigations. The first was carried out at the Burlington Northern Railroad pilot tunnel and main bore near North Bonneville, Washington, and the second at the Eisenhower Memorial Tunnel, South Bore. The investigation was designed to address questions primarily related to the magnitude, distribution, and time history of the deformation induced tension and bending of spiles as a result of excavation. Deformation induced tension was shown to be the major mechanism by which spiling reinforcement displays its effectiveness, while bending was of minor significance. Results from the Bonneville and Eisenhower tunnels were compared as their size, depth, and geologic environment were significantly different. The results indicated that the reinforced arch thickness was strongly dependent on ground type, while arch capacity was largely a function of opening size, shape, and depth. Variations in the instrumentation program at each of the two field sites provided for additional findings. At Bonneville, instrumented spiles used in conjunction with extensometers furnished information on the compatibility of the strains in spiles and that of rock mass in their immediate vicinity. All instrumentation installed for the pilot tunnel was designed to also monitor and rock mass behavior during excavation of the main bore.

At the Eisenhower Tunnel, the reinforcement/support system consisted of spiling, steel sets, and a two stage concrete liner. Support loads were calculated from instrumented steel sets. A comparison of the loads anticipated on the basis of ground conditions with that of actual measured loads provided a strong indication of the effectiveness of spiling reinforcement. It revealed that the rock mass-reinforcement system was the primary factor in the permanent stabilization of the tunnel opening; whereas, the internal support system performed a secondary role in the control of local loosening. Instrumented spiles placed in various types of rock, ranging from moderately jointed to highly crushed and altered squeezing ground, revealed the influence of different geologic environments on the response of the reinforcement system. Based on the observed reinforced ground-support system interaction, a design procedure incorporating instrumented spiles has been proposed, including the role of internal support systems in the permanent stabilization of an opening.

A FIELD STUDY OF SPILING REINFORCEMENT IN UNDERGROUND OPENINGS

Final Report

Department of the Army Contract No. DACW45-74-C-0026

Prepared for

Geology, Soils and Materials Branch

Missouri River Division, Corps of Engineers

Omaha, Nebraska

by

GREGORY E. KORBIN
Assistant Research Engineer

and

TOR L. BREKKE
Professor of
Geological Engineering

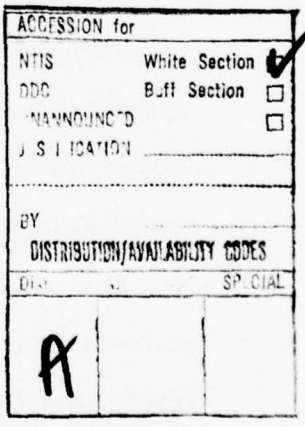

University of California, Berkeley
College of Engineering
Department of Civil Engineering

June 1977

PREFACE

The work reported herein has been sponsored by the U.S. Army Corps of Engineers, Missouri River Division, Omaha, Nebraska, under Contract No. DACW45-74-C-0026. It has been carried out in the Geotechnical Engineering Laboratories and at the Computer Center of the University of California, Berkeley. Field investigations were performed at the Burlington Northern Railroad pilot tunnel and main bore, North Bonneville, Washington, and the Eisenhower Memorial Tunnel, South Bore, Colorado.

Included in this report are the findings from some additional work at the Eisenhower Tunnel that was carried out under a Service to Industry Contract with the Construction Contractor, Peter Kiewit Sons' Co. and Brown & Root, Inc.

The report covers field studies on the behavior of rock mass-reinforcement systems, reinforced ground-support system interaction, and reinforced arch design considerations. A previous report (Technical Report MRD-2-75) discussed the findings on the effectiveness of prereinforcement systems based on studies using physical and numerical models.

This investigation has been greatly facilitated by the helpful advice of the technical monitoring officer, Mr. J.F. Redlinger, Chief, Geology, Soils and Materials Branch of the Missouri River Division, and of Mr. L.B. Underwood, Chief Geologist, Office of the Chief of Engineers, Department of the Army.

Further acknowledgment gratefully goes to many others who also assisted in carrying out this research effort. In particular, the authors wish to thank Mr. T.A. Lang, Leeds, Hill and Jewett, Inc., San Francisco; Messrs. P.R. McOllough, J.E. Gay, R. Lange, and W. Mystkowski of the Colorado Division of Highways; Mr. L. Lutz, Federal Highway Administration; Mr. R. Poulson Jr. and Mr. R. Sundstrom, of Peter Kiewit Sons' Co.; Messrs. H.D. Barnes, J.B. Griffiths, P.L. Grubaugh, L.A. Gustafson, R.D. MacDonald, E.L. McCoy, J.W. Sager, P.N. White, of the Portland District, Corps of Engineers; and Mr. D.E. Hansen, Jenny Geotechnical Corp., Seattle.

TABLE OF CONTENTS

		Page
PREFACE		ii
LIST OF FIGURES		vi
LIST OF TABLES		xv
LIST OF SYMBOLS		xvi
CONVERSION FACTORS		xviii
CHAPTER 1.	INTRODUCTION	1
	Background	1
	Previous Investigations	4
	Current Investigations	10
CHAPTER 2.	FIELD INVESTIGATION: BURLINGTON NORTHERN RAILROAD PILOT TUNNEL AND MAIN BORE	12
	Test Station Design	12
	Geology	16
	Pilot Tunnel Construction	21
	Pilot Tunnel Test Station Results and Discussion	22
	Main Bore Construction	43
	Main Bore Test Station Results and Discussion	43
CHAPTER 3.	FIELD INVESTIGATION: EISENHOWER MEMORIAL TUNNEL, SOUTH BORE	60
	Test Station Design	60
	Geology	66
	Tunnel Construction	68
	Test Station Results and Discussion	70
	a. Rock Mass-Reinforcement System Behavior	70
	b. Reinforced Arch-Support System Interaction	91

CHAPTER 4.	COMPARISON: RESULTS FROM BONNEVILLE AND EISENHOWER TUNNELS	97
CHAPTER 5.	CONCLUSIONS	100
	Rock Mass-Reinforcement System Mechanisms	100
	Reinforced Ground-Support System Interaction	102
	Reinforced Arch Design Considerations	103
REFERENCES		106
APPENDIX 1.	INSTRUMENTED SPILE DESIGN AND CONSTRUCTION	108
APPENDIX 2.	INSTRUMENTATION PERFORMANCE AND CALIBRATION	122
APPENDIX 3.	EXTENSOMETER DESIGN, CONSTRUCTION, AND INSTALLATION	125
APPENDIX 4.	DATA REDUCTION	132
APPENDIX 5.	INSTRUMENTED REINFORCEMENT STRESS DISTRIBUTIONS	139
APPENDIX 6.	SUPPORT SYSTEM LOADS	168
	Loads From Instrumented Steel Sets	168
	Loads From Spile Stress Relaxation	171
APPENDIX 7.	EISENHOWER TUNNEL INSTRUMENTED REINFORCEMENT AND STEEL SET STRESS HISTORIES AND TEST STATION GEOLOGIC MAPS	174

LIST OF FIGURES

Figure		Page
1-1	Prereinforcement Systems	2
1-2	Spiling Reinforcement Ahead of Face (a form of prereinforcement)	3
1-3	Model Tunnel Excavation Sequence in Profile (Rn = Round Number n, t = Time at Excavation of Round n)	5
1-4	Radial Deformation History Comparison: Unreinforced and Spiling Reinforced Models, Position A	6
1-5	Axial Deformation History Comparison: Unreinforced and Spiling Reinfored Models, Position F	7
1-6	Computed Radial and Tangential Stress Distributions with and without Prereinforcement	9
2-1	Profile of Burlington Northern Railroad Tunnel, North Bonneville, Washington, and Test Station Locations	13
2-2	Section of Bonneville Pilot Tunnel, Main Bore and Test Station Extensometer	14
2-3	Section and Profile Vertical Projections of Test Station Instrumentation Layout	15
2-4	Insitu Orientation of a) Axial and b) Axial Plus Bending Type Instrumented Spiles	17
2-5	Geologic Plan and Profile, Test Station No. 1 (Mac Donald, 1976)	19
2-6	Geologic Plan and Profile, Test Station No. 2 (Mac Donald, 1976)	20
2-7	Axial Stress History	24
2-8	Bending Stress History and Sign Convention	25
2-9	Axial Stress History	26

Figure		Page
2-10	Bending Stress History	27
2-11	Radial Stress Distribution Comparison: 5 ft. Advance, 15 ft. Advance, and Long Term	29
2-12	Deformation History, Pilot Tunnel Test Station No. 1, Extensometer TA (MPBX-TA)	30
2-13	Strain History, Pilot Tunnel Test Station No. 1, Extensometer TA (MPBX-TA)	31
2-14	Deformation History, Pilot Tunnel Test Station No. 2, Extensometer TC (MPBX-TC)	32
2-15	Strain History, Pilot Tunnel Test Station No. 2, Extensometer TC (MPBX-TC)	33
2-16	Strain History Comparison: Instrumented Spiles and Extensometer, Pilot Tunnel Test Station No. 2, Radial Position 28 in.	35
2-17	Strain History Comparison: Instrumented Spiles and Extensometers, Pilot Tunnel Test Station No. 1, Radial Position 32 in.	36
2-18	Strain History Comparison: Instrumented Spiles and Extensometer, Pilot Tunnel Test Station No. 2, Radial Position 32 in.	37
2-19	Strain History Comparison: Instrumented Spiles and Extensometers, Pilot Tunnel Test Station No. 1, Radial Position 40 in.	38
2-20	Strain History Comparison: Instrumented Spiles and Extensometer, Pilot Tunnel Test Station No. 2, Radial Position 40 in.	39
2-21	Radial Strain Distribution Comparison: Spiles and Extensometers (Rock Mass),1 hr. after 5 ft. Advance	41
2-22	Axial Stress History	44
2-23	Bending Stress History and Sign Convention	45
2-24	Axial Stress History	46
2-25	Bending Stress History	47
2-26	Radial Stress Distribution Comparison: Initial (before excavation), 5 ft. Advance, 25 ft. Advance, and Long Term	49

Figure		Page
2-27	Deformation History, Main Bore Test Station No. 1, Extensometer TA (MPBX-TA)	50
2-28	Strain History, Main Bore Test Station No. 1, Extensometer TA (MPBX-TA)	51
2-29	Deformation History, Main Bore Test Station No. 2, Extensometer TC (MPBX-TC)	52
2-30	Strain History, Main Bore Test Station No. 2, Extensometer TC (MPBX-TC)	53
2-31	Strain History Comparison: Instrumented Spiles and Extensometer, Main Bore Test Station No. 2, Radial Position 18 in.	56
2-32	Strain History Comparison: Instrumented Spiles and Extensometer, Main Bore Test Station No. 1, Radial Position 22 in.	57
2-33	Strain History Comparison: Instrumented Spiles and Extensometer, Main Bore Test Station No. 1, Radial Position 30 in.	58
2-34	Strain History Comparison: Instrumented Spiles and Extensometer, Main Bore Test Station No. 2, Radial Position 30 in.	59
3-1	Profile of Eisenhower Tunnel, Second Bore, Denver, Colorado (Hopper et. al., 1972)	61
3-2	Profile of Test Station Instrumentation Layout	62
3-3	Instrumented Reinforcement Bar Type and Strain Gauge Positions	64
3-4	Installed Instrumented Spile with Readout Cable Attached	65
3-5	Readout Instrumentation System	65
3-6	Section and Profile of Rock Reinforcement a) Rock Class II and b) Rock Classes III & IV	69
3-7	Test Station 58+86, Radial Stress Distribution Comparison: 8 ft. Advance, 50 ft. Advance, and Long Term (summary of Fig. A5-8 to 10)	73
3-8	Test Station 73+42, Radial Stress Distribution Comparison: 8 ft. Advance, 50 ft. Advance, and Long Term (summary of Fig. A5-22 to 24)	76

Figure		Page
3-9	Test Station 70 + 14, Radial Stress Distribution Comparison: 6 ft. Advance and 50 ft. Advance (summary of Fig. A5-15, 16)	77
3-10	Test Station 63 + 01, Radial Stress Distribution Comparison: 8 ft. Advance, 50 ft. Advance and Long Term (summary of Fig. A5-12 to 14, 28)	79
3-11	Test Station 63 + 01, Stress History of Instrumented Spile and Steel Set (excerpt from Appendix 7)	80
3-12	Test Station 72 + 36, Radial Stress Distribution Comparison: 12 ft. Advance, 50 ft. Advance and Long Term (summary of Fig. A5-18 to 20, 29)	83
3-13	Test Station 80 + 87, Radial Stress Distribution Comparison: 8 ft Advance, 50 ft. Advance and Long Term (summary of Fig. A5-25 to 27)	85
3-14	Normalized Stress Ratio (measured to peak stress) Distribution Comparison: Absolute Radial Position and Radii (one radius equals top heading height plus width divided by four, 200 in.), All Test Stations after 8 ft. Advance	86
3-15	Pre-Excavation Stress Rate Distribution Comparison: Test Stations 63 + 01, 72 + 36 and 73 + 42, First 5 hrs. after Installation	89
4-1	Normalized Stress Ratio (measured to peak stress) Distribution Comparison: Absolute Radial Position and Radii (one radius equals top heading height plus width divided by four)	98
A1-1	Section of Instrument Head, General Layout	109
A1-2	Instrumented Reinforcement Wiring Schematic	110
A1-3	Section of Instrument Head, Shop Drawing, Design Employed at Bonneville Pilot Tunnel	112
A1-4	Section of Instrument Head, Shop Drawing, Design Employed at Eisenhower Tunnel	115
A1-5	Weldable Strain Gauge Installed within Reinforcement Steel Slot	117
A1-6	Wired Receptacle and Retaining Ring Ready for Insertion within Instrument Head	117

Figure		Page
A1-7	Alignment Jig Used to Position Receptacle after Setting Retaining Ring	119
A1-8	Filling Slot Containing Strain Gauge Lead Wires with Structural Adhesive	119
A3-1	Extensometer Design, Construction, and Installation (Terrametrics Inc.)	126
A3-2	Extensometer Anchor, Hydraulicly Activated	127
A3-3	Setting Anchors with Hydraulic Pump	127
A3-4	Reference Head and Measuring Rods	129
A3-5	Grout Mix Tank and Pump	129
A4-1	Radial Deformation Distribution as Derived from Extensometer Results	134
A4-2	Interpolation on Deformation Surface in Terms of Time and Radial Position	134
A4-3	Linear Interpolation	137
A4-4	Interpolation by Parabolic Fairing with Blend	137
A5-1	Bonneville Pilot Tunnel Radial Stress Distribution, 5 ft. Advance	141
A5-2	Bonneville Pilot Tunnel Radial Stress Distribution, 15 ft. Advance	142
A5-3	Bonneville Pilot Tunnel Radial Stress Distribution, Long Term	143
A5-4	Bonneville Main Bore Radial Stress Distribution, Initial	144
A5-5	Bonneville Main Bore Radial Stress Distribution, 5 ft. Advance	144
A5-6	Bonneville Main Bore Radial Stress Distribution, 25 ft. Advance	145
A5-7	Bonneville Main Bore Radial Stress Distribution, Long Term	145
A5-8	Radial Stress Distribution, Test Station 58 + 86, 8 ft. Advance	146

Figure		Page
A5-9	Radial Stress Distribution, Test Station 58+86, 50 ft. Advance	147
A5-10	Radial Stress Distribution, Test Station 58+86, Long Term	148
A5-11	Radial Stress Distribution, Test Station 63+01, Pre-excavation	149
A5-12	Radial Stress Distribution, Test Station 63+01, 8 ft. Advance	150
A5-13	Radial Stress Distribution, Test Station 63+01, 50 ft. Advance	151
A5-14	Radial Stress Distribution, Test Station 63+01, Long Term	152
A5-15	Radial Stress Distribution, Test Station 70+14, 6 ft. Advance	153
A5-16	Radial Stress Distribution, Test Station 70+14, 50 ft. Advance	154
A5-17	Radial Stress Distribution, Test Station 72+36, Pre-excavation	155
A5-18	Radial Stress Distribution, Test Station 72+36, 12 ft. Advance	156
A5-19	Radial Stress Distribution, Test Station 72+36, 50 ft. Advance	157
A5-20	Radial Stress Distribution, Test Station 72+36, Long Term	158
A5-21	Radial Stress Distribution, Test Station 73+42, Pre-excavation	159
A5-22	Radial Stress Distributi , Test Station 73+42, 8 ft. Advance	160
A5-23	Radial Stress Distribu' on, Test Station 73+42, 50 ft. Advanc.	161
A5-24	Radial Stress Distribution, Test Station 73+42, Long Term	162

Figure		Page
A5-25	Radial Stress Distribution, Test Station 80+87, 8 ft. Advance	163
A5-26	Radial Stress Distribution, Test Station 80+87, 50 ft. Advance	164
A5-27	Radial Stress Distribution, Test Station 80+87, Long Term	165
A5-28	Radial Stress Distribution, Test Station 63+06, Long Term	166
A5-29	Radial Stress Distribution, Test Station 72+46, Long Term	167
A7-1	Geologic Map (J. Post, Colo. Div. of Highways) and Instrumentation Layout in Plan, Test Station 58+86	177
A7-2	Axial Stress History, Station 58+86, Spile No. 1, and Steel Set	178
A7-2	Cont.	179
A7-3	Geologic Map (J. Post, Colo. Div. of Highways) and Instrumentation Layout in Plan, Test Station 63 + 01	180
A7-4	Axial Stress History, Station 63+01, Spile No. 1 and Steel Set	181
A7-4	Cont.	182
A7-5	Axial Stress History, Station 63+01, Spile No. 2 and Steel Set	183
A7-5	Cont.	184
A7-6	Axial Stress History, Station 63+01, Spile No. 3 and Steel Set	185
A7-7	Bending Stress History, Station 63+01, Spile No. 3	186
A7-8	Axial Stress History, Station 63+06, Radial No. 4	187
A7-9	Axial Stress History, Station 63+06, Radial No. 5	188

Figure		Page
A7-10	Geologic Map (J. Post, Colo. Div. of Highways) and Instrumentation Layout in Plan, Test Station 70 + 14	189
A7-11	Axial Stress History, Station 70 + 14, Spile No. 1 and Steel Set	190
A7-12	Bending Stress History, Station 70 + 14, Spile No.1	191
A7-13	Geologic Map (J. Post, Colo. Div. of Highways) and Instrumentation Layout in Plan, Test Station 72 + 36	192
A7-14	Axial Stress History, Station 72 + 36, Spile No. 1 and Steel Set	193
A7-14	Cont.	194
A7-15	Axial Stress History, Station 72 + 36, Spile No. 2 and Steel Set	195
A7-15	Cont.	196
A7-16	Axial Stress History, Station 72 + 36, Spile No. 3	197
A7-17	Bending Stress History, Station 72 + 36, Spile No. 3	198
A7-18	Axial Stress History, Station 72 + 46, Radial No. 5	199
A7-19	Geologic Map (J. Post, Colo. Div. of Highways) and Instrumentation Layout in Plan, Test Station 73 + 42	200
A7-20	Axial Stress History, Station 73 + 42, Spile No. 1 and Steel Set	201
A7-20	Cont.	202
A7-21	Axial Stress History, Station 73 + 42, Spile No. 2	203
A7-22	Bending Stress History, Station 73 + 42, Spile No. 2	204
A7-23	Geologic Map (J. Post, Colo. Div. of Highways) and Instrumentation Layout in Plan, Test Station 80 + 87	205
A7-24	Axial Stress History, Station 80 + 87, Spile No. 1	206
A7-25	Bending Stress History, Station 80 + 87, Spile No. 1	207

Figure		Page
A7-26	Axial Stress History, Station 80 + 87, Spile No. 2	208
A7-27	Bending Stress History, Station 80 + 87, Spile No. 2	209
A7-28	Axial Stress History, Station 80 + 87, Spile No. 3 and Steel Set	210
A7-28	Cont.	211

LIST OF TABLES

Table		Page
3-I	Rock Class Description and Predicted Rock Load	67
3-II	Instrumented Reinforcement Test Station Specifications	71
3-III	Reinforcement System Peak Equivalent Pressure	88
3-IV	Measured, Predicted and Anticipated Rock Loads on Internal Supports	94
A1-I	Instrumented Reinforcement Components List and Parts Manufactor	121
A5-I	Radial Stress Distribution Index	140
A6-I	Values Used In Computation of Rock Load from Instrumented Steel Set Results	170
A6-II	Values Used in Computation of Rock Load from Instrumented Reinforcement Stress Relaxation	173
A7-I	Stress History Plot Index, Eisenhower Tunnel	175
A7-II	Figure Symbol Descriptions	176

LIST OF SYMBOLS

↑	time of excavation shot at which round was advanced or when labeled time at which event occurred
(A)	face located at initial position, point at which instrumented spiles were installed
(n)	face advanced n feet beyond initial position
A_c	tributary cross sectional area of the concrete liner
A_s	cross sectional area of the steel member
A_t	tributary area supported by the steel set
a,b,c	independent constants
B	width of top heading
C.G.	contact grout between rock and liner
E_c	elastic modulus of concrete
E_s	elastic modulus of steel
e	exponential function
F.S.L.	first stage concrete liner
H_p	total height of rock column
H'_p	height of rock column before F.S.L.
H''_p	height of rock column after F.S.L.
H_t	height of top heading
I.P.	inflection point
J.S.	joint spacing
L.T.	long term
P_o	external hydrostatic pressure

R_n	round number n
r	radial position
t	time
u	radial deformation
x	independent variable
y	dependent variable
ε_s	strain in orientation of spile
ε_v	vertical strain
θ	angle from the vertical to orientation of spile axis
$\Delta\sigma'$	average change in stress after installation of steel set
$\Delta\sigma''$	average change in stress after placement of liner
γ	unit weight of rock mass

CONVERSION FACTORS

Units of measurement used in this report can be converted to Standard International (SI) units as follows:

Multiply	By	To Obtain
inches	2.540	centimeters
feet	0.305	meters
miles	1.700	kilometers
square inches	6.45	square centimeters
square feet	0.093	square meters
acres	4047	square meters
cubic inch	16.4	cubic centimeters
cubic foot	0.028	cubic meters
gallon	3.80	liters
acre-feet	1233	cubic meters
pounds	0.454	kilograms
tons	907.2	kilograms
one pound force	4.45	newtons
one kilogram force	9.81	newtons
pounds per square foot	47.9	newtons per sq. meter
pounds per square inch	6.9	kilonewtons per sq. meter

CHAPTER 1

INTRODUCTION

Background

Prereinforcement, of which spiling reinforcement is a particular form, involves reinforcing the surrounding rock mass ahead of the main excavation. This is generally accomplished by placing in predrilled holes fully grouted untensioned steel members such as reinforcement bars, on a regular pattern. Examples of prereinforcement systems are shown in Figures 1-1 and 1-2.

Prereinforcement and ordinary reinforcement, or rock bolts, are basically the same in methodology and design, though each system differs in the scope of its capabilities. Both systems contribute to the permanent stabilization of the opening by restricting deformations. However, only prereinforcement can significantly influence the immediate stabilization of the heading in terms of stand-up time by restricting the deformations concurrent with excavation. Essentially, the added efficiency of prereinforcement systems stems from the early point of installation relative to the total deformation history of the ground surrounding the opening. This concept is equally applicable to support systems and is under investigation for use in large underground caverns (Stillborg, 1977).

The fact that prereinforcement can improve ground conditions has been well established in engineering practice. Case histories largely concerned with the use of spiling reinforcement in civil works have been described by Brekke and Korbin (1974). The particularly successful use of reinforcement from small drifts at the first

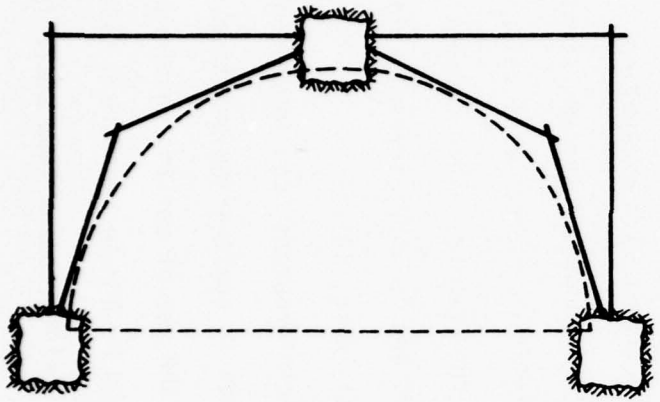

Pre-reinforcing From Small Drifts

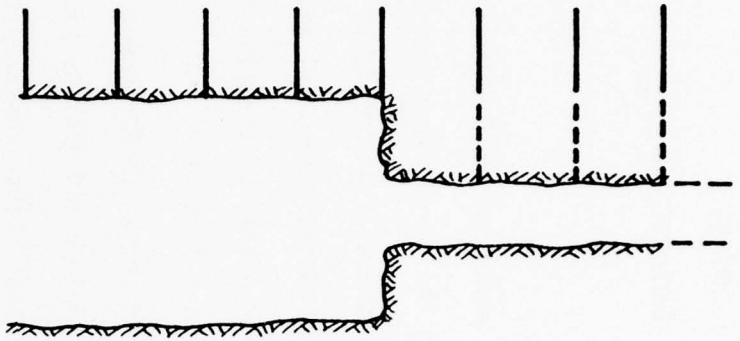

Pre-reinforcing From an Exploration Drift

FIG. 1-1. Prereinforcement Systems

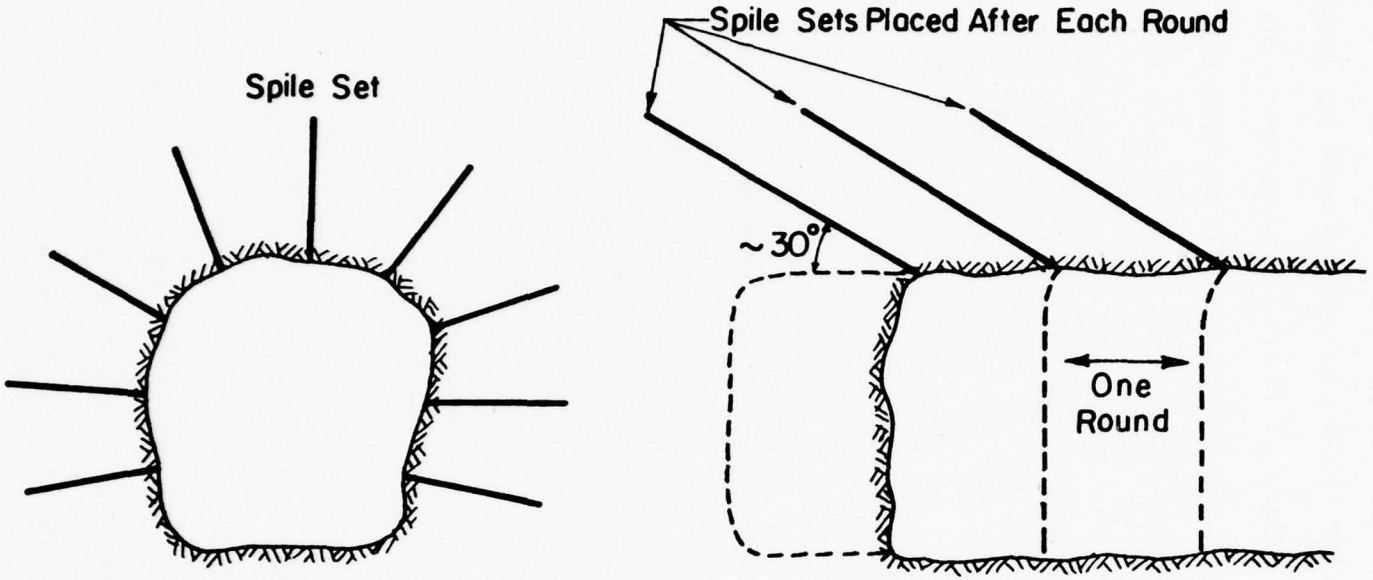

FIG. 1-2. Spiling Reinforcement Ahead of Face (a form of prereinforcement)

Eisenhower Tunnel, Colorado, was examined by Hopper, Lang and Mathews (1972). More recently,prereinforcement has found application within the mining industry. If ground conditions in cut and fill stopes deteriorate to the extent of requiring conversion to timber stopes, there is considerable economic advantage in installing pre-reinforcement instead of timber (Palmer, et. al., 1976; Mathews and Meek, 1975). Long, fully grouted dowels, extending over several lifts, are placed in the ore roof for ground control prior to the extraction of each lift.

Previous Investigations

Previous investigations by the writers examined the effectiveness of prereinforcement through physical and numerical model studies (Korbin and Brekke, 1976). The findings can be summarized as follows:

1. A reinforcement system with the capability to immediately stabilize an opening should be designed to prevent loosening and to attain this capability quickly. In terms of ground response, this means reduced deformations, and thereby decreased deterioration due to work softening and reduction in the inherent available rock mass strength. The ability of spiling reinforcement to significantly reduce deformations was demonstrated by the comparison of reinforced with unreinforced tunnel openings. Physical models of cylindrical openings in stiff squeezing ground were excavated round by round to simulate a drill and blast operation, Figure 1-3. Radial deformation at point A and axial deformation at point F are shown in Figures 1-4 and 1-5 respectively. For similar times and positions of the tunnel face the reductions in deformation exhibited by the reinforced opening were considerable.

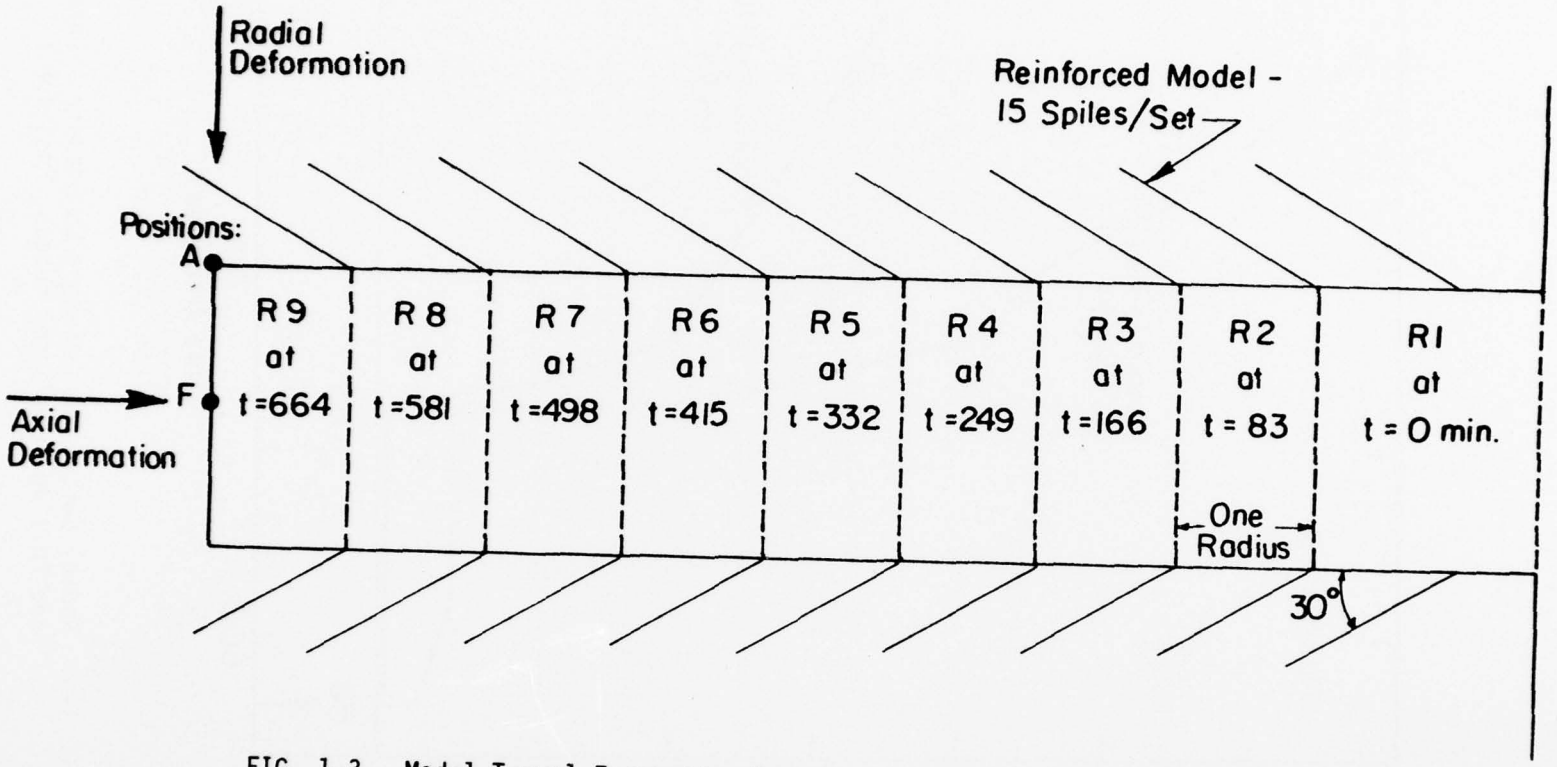

FIG. 1-3. Model Tunnel Excavation Sequence in Profile (Rn = Round Number n, t = Time at Excavation of Round n)

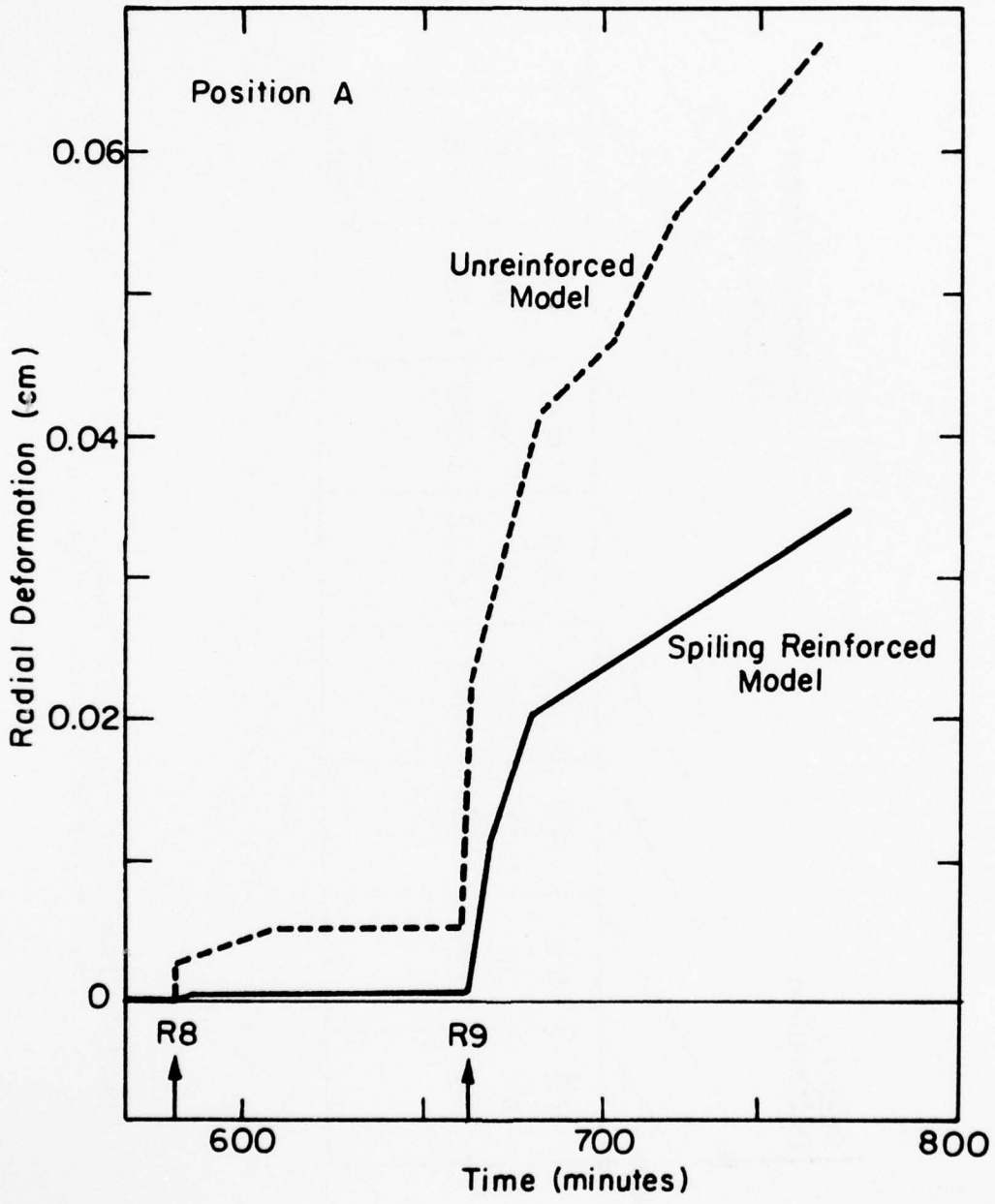

FIG. 1-4. Radial Deformation History Comparison: Unreinforced and Spiling Reinforced Models, Position A

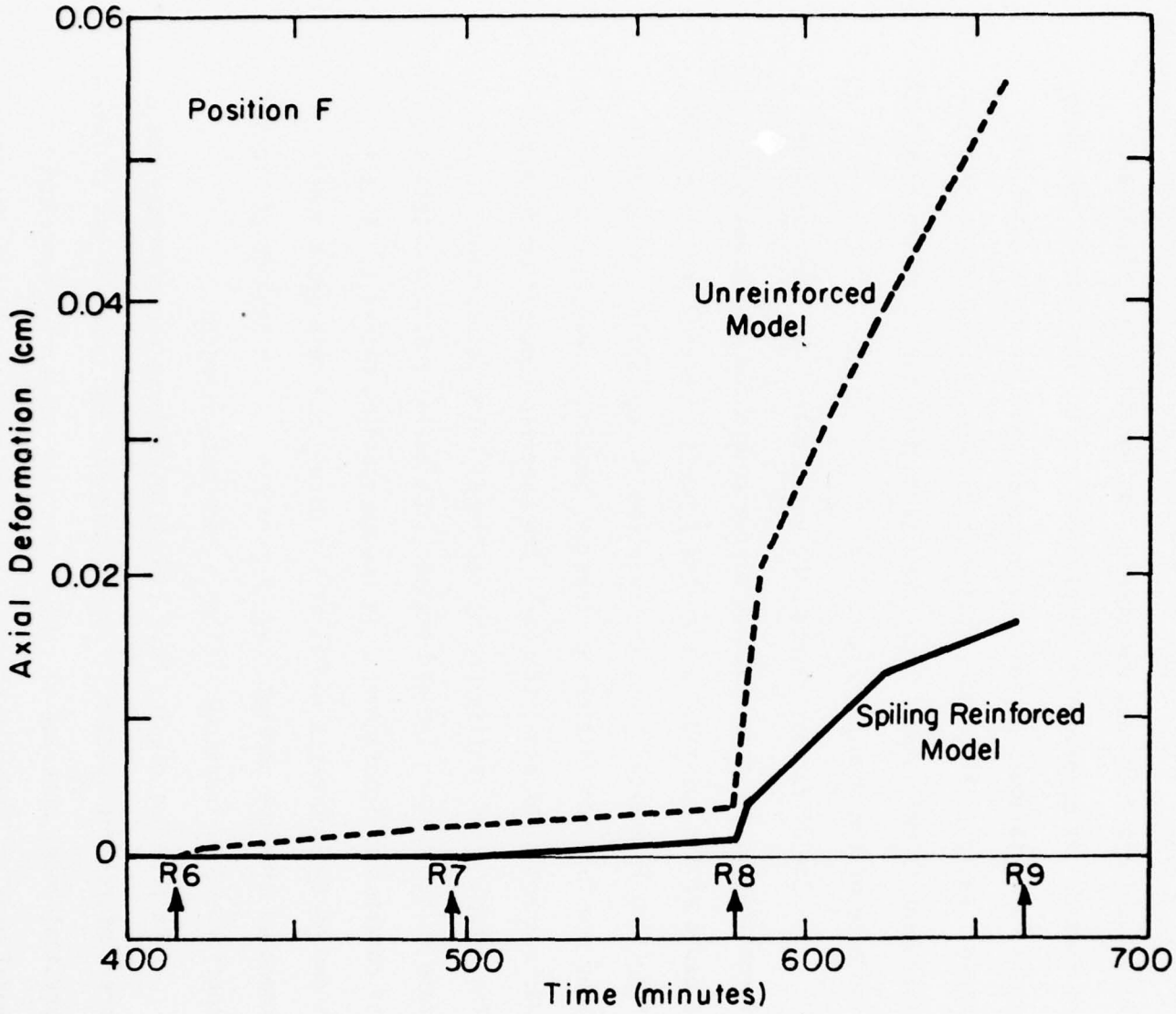

FIG. 1-5. Axial Deformation History Comparison: Unreinforced and Spiling Reinforced Models, Position F

2. Closely related to the control of deformations is the formation of a stable arch around the opening. Only by maintaining continuity of the rock mass surrounding the opening can a stable arch be formed. As observed in the physical models, the loss of continuity resulted in fallouts of increasing number and size until total collapse. Analytically, the increase in continuity as a result of reinforcement is reflected in increased tangential stress in the immediate vicinity of the opening, Figure 1-6.

3. The difference between the unrestrained and restrained deformations is due to a reaction of the reinforced region against closure of the opening. During the process of energy redistribution, resulting from excavation, the reaction of each spile can result in many possible combinations of tension, bending, shear, and torsion at various positions along the bar. The specific combination depends on the geometry and quality of the rock mass being reinforced. In the case of deformation induced tension, the spiles react to create a zone of compression (confinement) in the surrounding material. This is shown as the increased radial stress within the reinforced model as compared with the unreinforced, Figure 1-6. A consequence of greater confinement is increased available rock mass strength.

The previous studies have largely considered the effectiveness of prereinforcement systems. From measurements and observations of the physical model behavior in conjunction with calibrated numerical model results, the mechanisms by which prereinforcement display its effectiveness have been implied, but not verified. Many researchers, including the writers, believe that deformation induced tension is the primary mechanism by which these systems work (Lang, 1961; Mathews

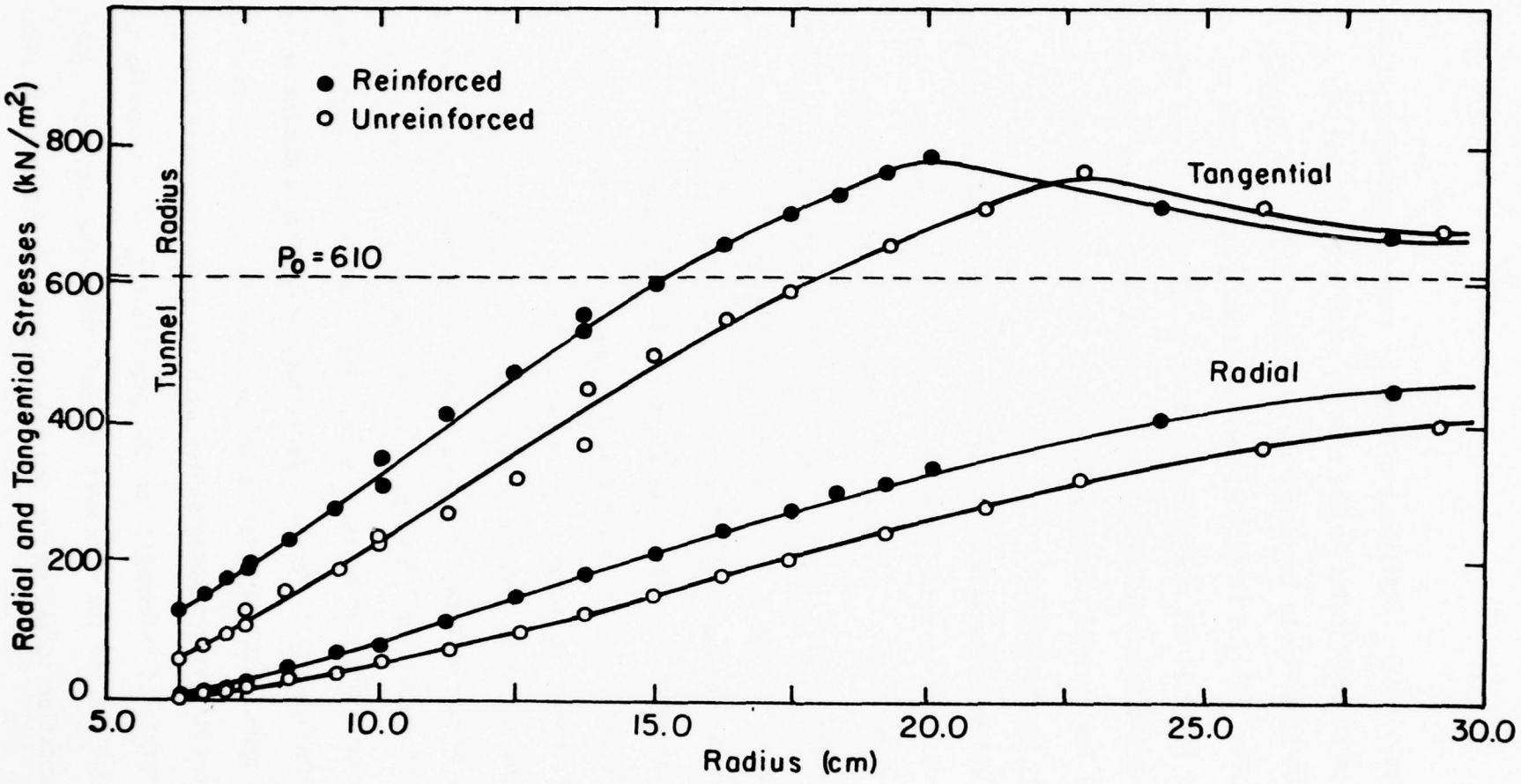

FIG. 1-6. Computed Radial and Tangential Stress Distributions with and without Prereinforcement (P_0 = External Pressure)

and Meek, 1975). Resistance offered by shearing the reinforcing steel also contributes to the opening stabilization, but has a limited capacity to influence the rock mass (Lande and Bonazzi, 1974; Bjurstrom, 1974). It is the shear resistance derived from an increased normal force across a shear plane that is influential and efficient. Bending and torsional resistance are small contributing factors due to the low stiffness offered by typical reinforcement steel sections.

Current Investigation

Further investigations were required to examine and substantiate the mechanisms by which prereinforcement and, in particular, spiling reinforcement work. A field instrumentation program was designed to monitor the spiling under actual tunneling conditions. This report describes the results of two such investigations. The first was carried out at the Burlington Northern Railroad pilot tunnel and main bore near North Bonneville, Washington, and the second at the Eisenhower Memorial Tunnel, South Bore located on I-70 about sixty miles west of Denver, Colorado. The investigation was designed to address questions primarily related to the magnitude, distribution, and time history of the deformation induced tension and bending of spiles as a result of excavation. Results from the Bonneville and Eisenhower tunnels were compared as their size, depth, and geologic environment were significantly different. Variations in the instrumentation program at each of the two field sites provided for additional findings. At Bonneville, instrumented spiles used in conjunction with extensometers furnished information on the compatibility of the strains in spiles and that of the rock mass in their immediate vicinity. All instrumentation installed for the pilot tunnel was designed to also

monitor spile and rock mass behavior during excavation of the main bore.

At the Eisenhower Tunnel, the reinforcement-support system consisted of spiling, steel sets, and a two stage concrete liner. Support loads were calculated from instrumented steel sets. A comparison of the loads anticipated on the basis of ground conditions with that of actual measured loads provided an indication of the effectiveness of spiling reinforcement. Instrumented spiles were placed in various types of rock, ranging from moderately jointed to highly crushed and altered squeezing ground, to assess the influence of different geologic environments on the response of the reinforcement system. Based on the observed reinforced ground-support system interaction, a design procedure incorporating instrumented spiles has been proposed, including the role of internal support systems in the permanent stabilization of an opening.

CHAPTER 2

FIELD INVESTIGATION: BURLINGTON NORTHERN RAILROAD PILOT TUNNEL AND MAIN BORE

Construction of a second powerhouse at Bonneville Dam necessitated relocation of the Burlington Northern railroad tracks. The relocation plan included a 1400 foot tunnel at moderate depth, Figure 2-1. Uncertainties related to the geology and the ground water regime made it advantageous to construct a small pilot tunnel. It was situated in the crown of the main bore as shown in Figure 2-2.

Test Station Design

As a part of the exploration program, two test stations were planned at the locations shown in Figure 2-1. Instrumentation at each station was designed to monitor ground deformation and the corresponding response of spiling reinforcement. Four-position rod extensometers installed from the surface prior to excavation provided information on the radial deformation distribution as a function of time and position of the advancing face. The extensometer design, construction, and installation are described in Appendix 3.

Contract specifications called for the installation of spiling reinforcement within the vicinity of each test station. Fifty foot sections were reinforced with eight foot long number seven thread (Dywidag) bolts. Spile sets consisting of four bolts were placed after every round, Figure 2-3. When the opening had advanced to within one round of the extensometer, position "A" in Figure 2-3, two instrumented spiles were installed. At the first test station, this was followed by a second set of instrumented spiles. Regular spiles

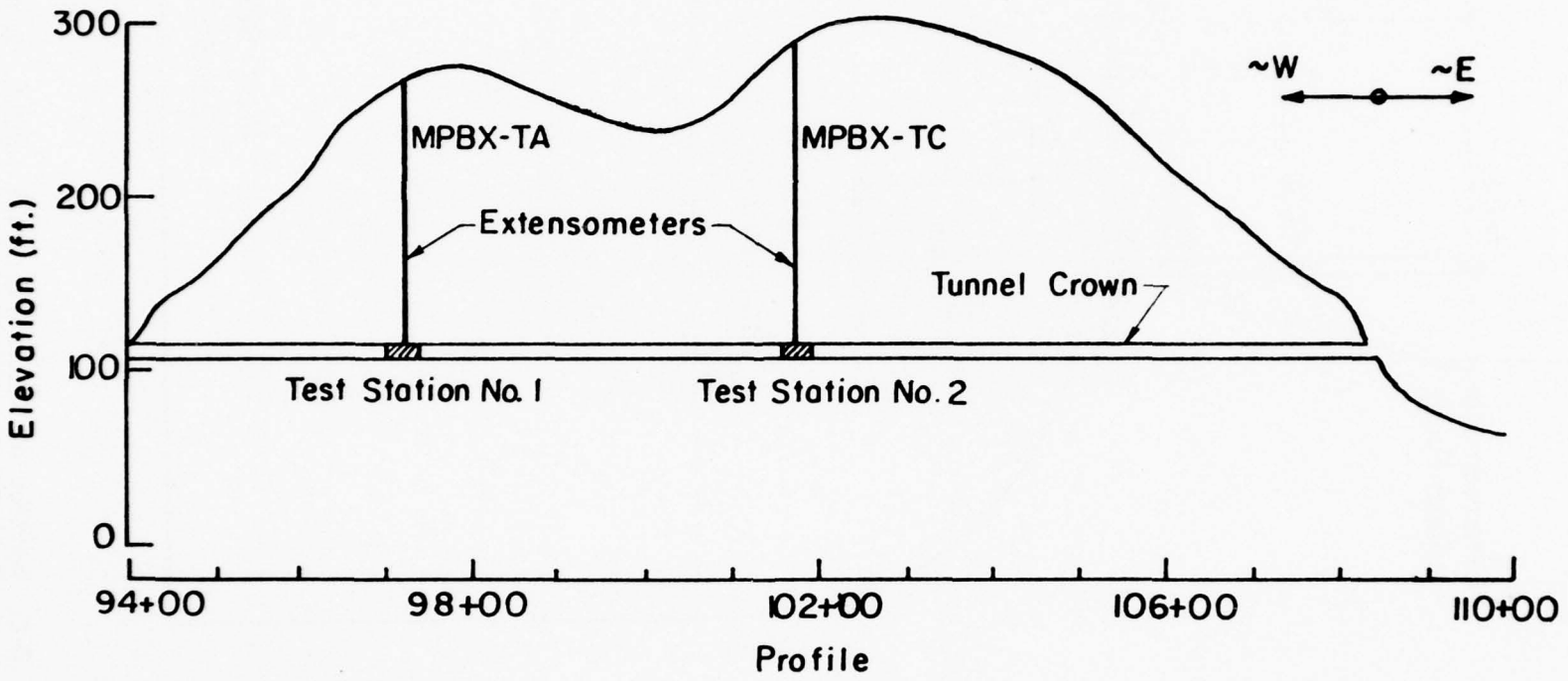

FIG. 2-1. Profile of Burlington Northern Railroad Tunnel, North Bonneville, Washington, and Test Station Locations

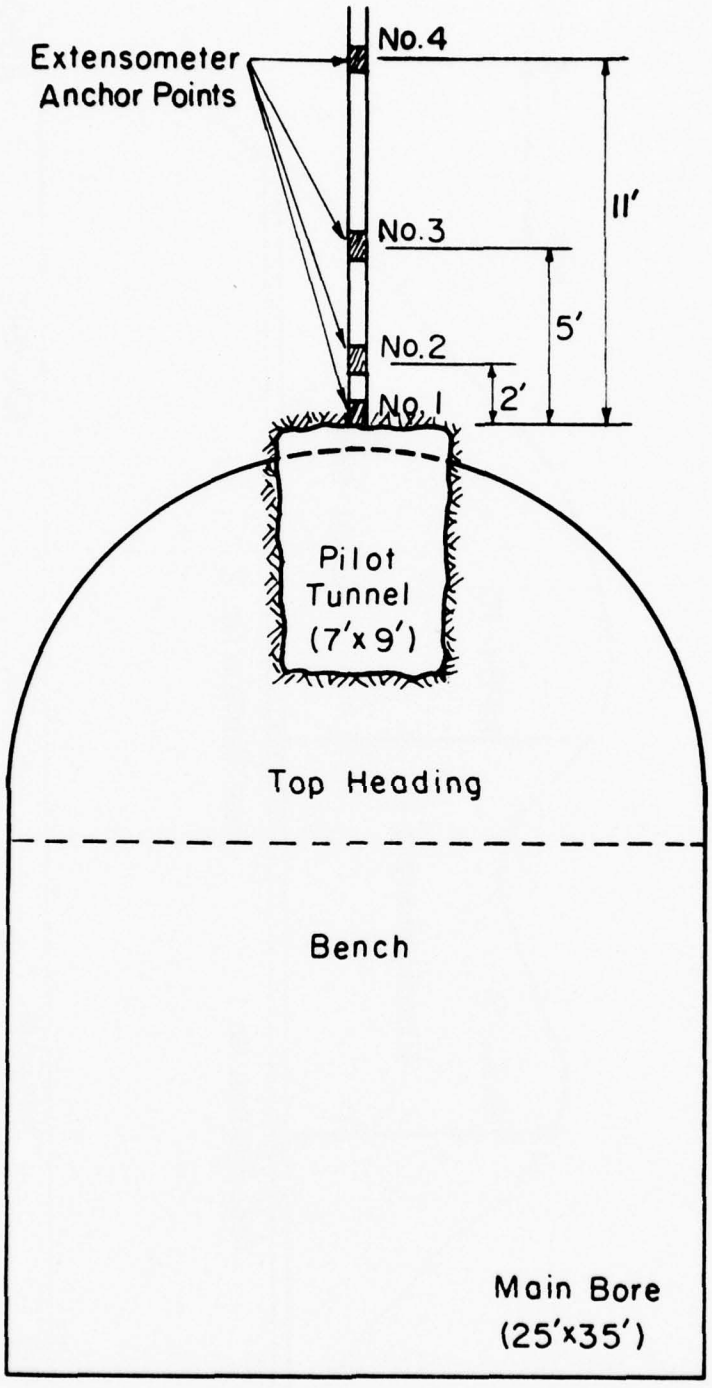

FIG. 2-2. Section of Bonneville Pilot Tunnel, Main Bore and Test Station Extensometer

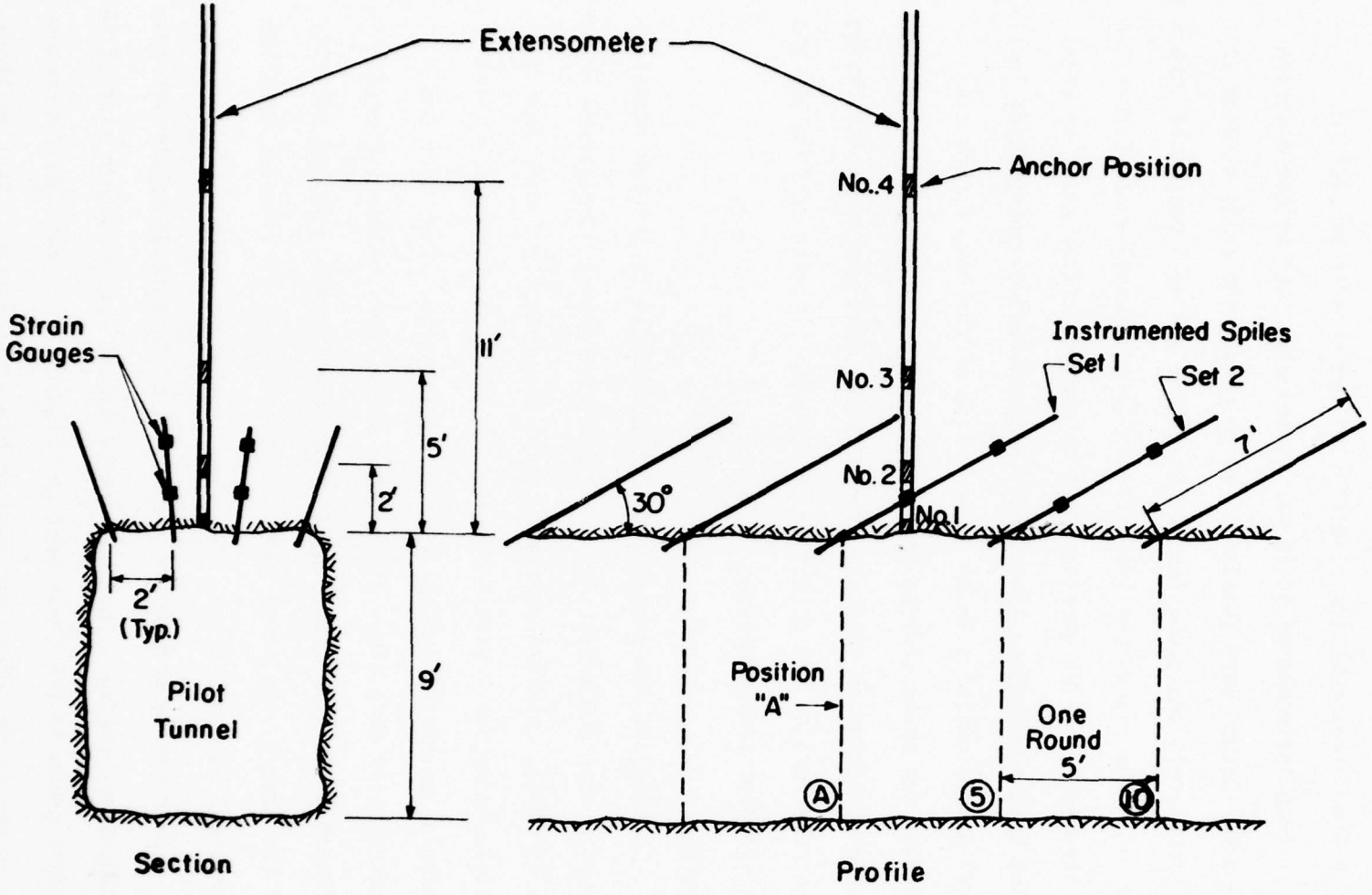

FIG. 2-3. Section and Profile Vertical Projections of Test Station Instrumentation Layout

were used throughout the remainder of the reinforced section.

Each instrumented spile was fitted with four weldable strain gauges. Gauges were located so as to record the axial strains at various positions along the length of the bar as a result of displacements in the plane containing the spile and tunnel axis, Figure 2-4. Instrumented spiles were designed to measure either axial or axial plus bending strains. The former was achieved by positioning individual gauges on the side or neutral axis of the bar, Figure 2-4a. Bending and axial strains were resolved from two diametrically opposed gauges oriented as shown in Figure 2-4b. Instrumented spile design and construction are described in Appendix 1, while performance and calibration are considered in Appendix 2.

Geology

Geology of the region under consideration is a large landslide deposit over 600 years old. The landslide debris is composed primarily of large, relatively intact blocks of sedimentary rock from the Weigle Formation. Blocks ranging in size up to hundreds of feet traveled several miles to their final location. Some made the journey with only minor disturbance while other blocks suffered considerable distress resulting in major shear zones. In the vicinity of the tunnel, the slide mass overlies a preslide alluvium from the ancestral Columbia River. The area is now considered stable.

Over eighty percent of the tunnel alignment passes through four major slide blocks. The two largest blocks are on either side of the saddle shown in the cross section, Figure 2-1. Other ground encountered was slide debris and sand at block boundaries. Test stations were positioned away from the saddle so as to be located within

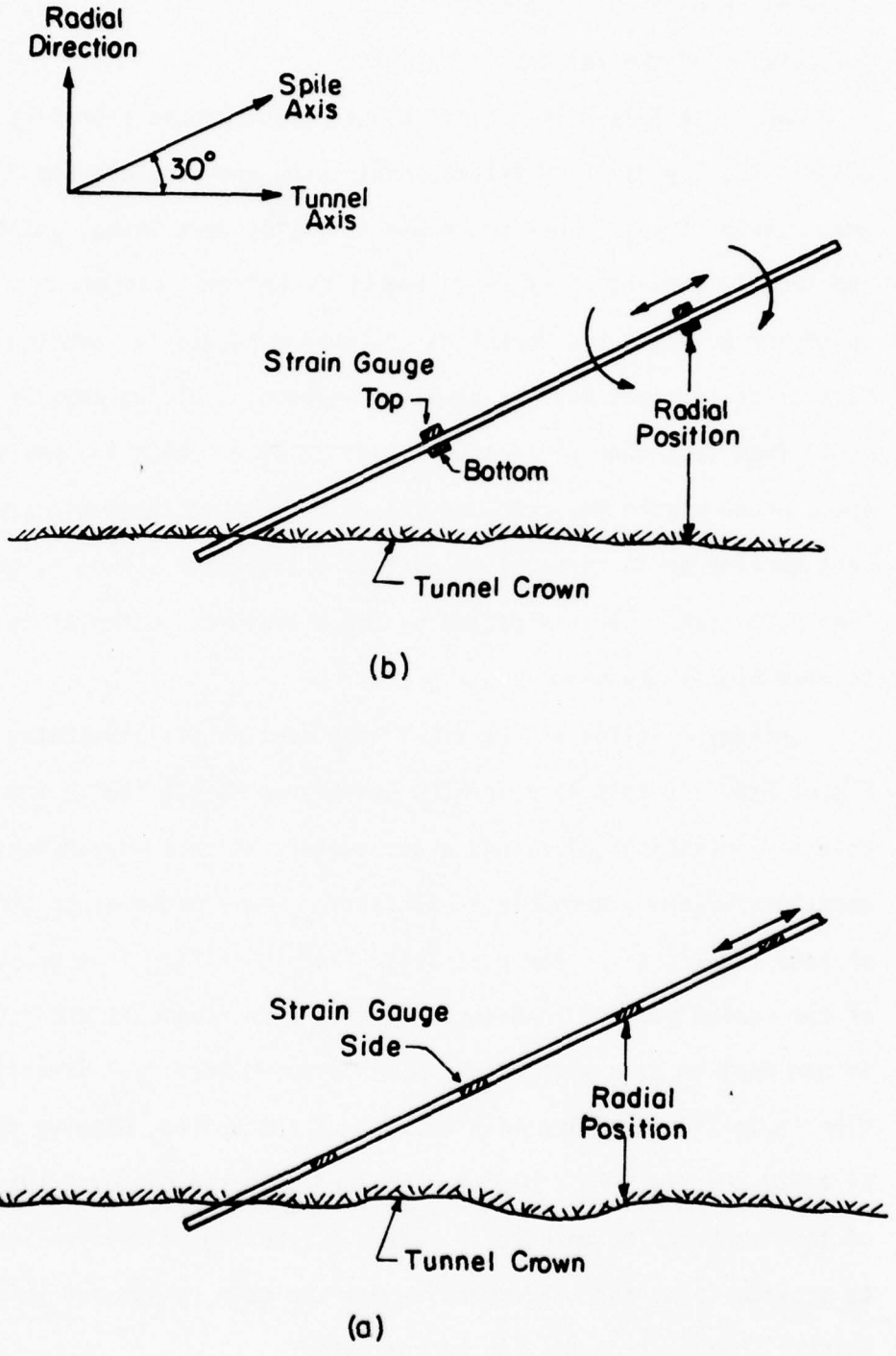

FIG. 2-4. Insitu Orientation of a) Axial and b) Axial Plus Bending Type Instrumented Spiles

slide block material. Extensometer drill hole logs confirmed the suitability of the selected locations.

Rock materials within slide blocks are composed primarily of alternating layers of siltstone, sandstone, and conglomerate (Mac Donald, 1976). They are fresh to partly decomposed, jointed, and locally sheared by preslide and slide induced deformation. Joints occur along and normal to the nearly horizontal bedding planes. Most often the rock mass is randomly jointed, yielding angular fragments from less than .1 foot to 2 feet in size. Locally, massive areas occur within the conglomerate unit. Intact fragments are of dent quality or in terms of unconfined compressive strength, greater than 3,000 psi. Classification of the slide block material is blocky to very blocky and seamy.

Geology specific to the first test station is illustrated in Figure 2-5. At this location the overburden is 156 feet. The entire station, including spiles and extensometer, is in a very blocky and occasionally seamy grey-black sandstone. Seamy material is composed of sand to silt size, low plasticity fines resulting from granulation of the medium grained sandstone. Intact rock fragments are from .1 to one foot in size with larger members found locally. Stratification is in the same direction as that of the spiles, dipping from 15 to 20 degrees. This had some influence on the sawtooth shape of the overbreak between spile sets. A blasting pattern designed to provide space for the forepoles was the main reason for this shape. There was no flowing ground water.

Geology of the second test station is more complex, yet similar to that of the first. As shown in Figure 2-6, numerous shears

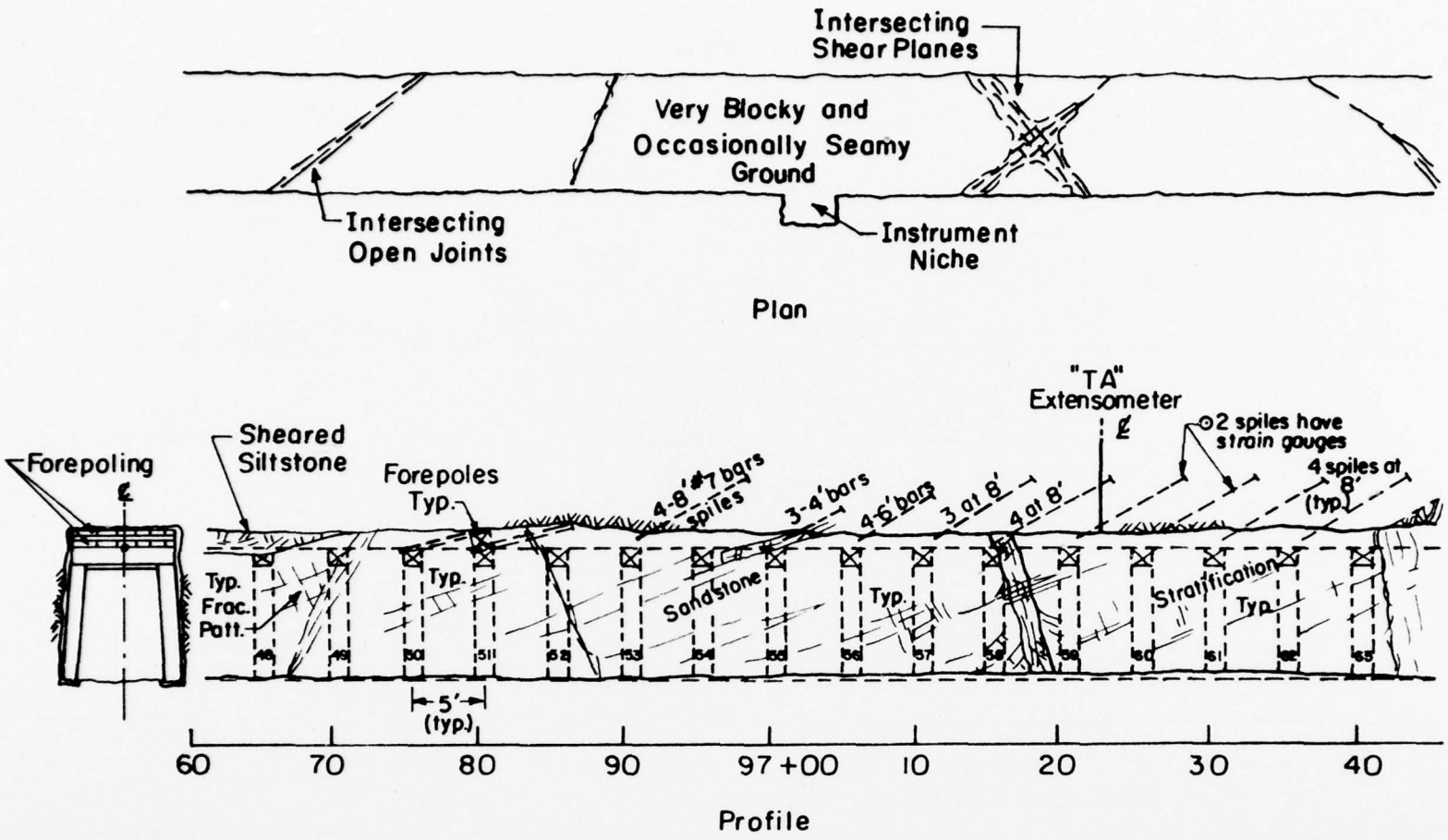

FIG. 2-5. Geologic Plan and Profile, Test Station No. 1 (MacDonald, 1976)

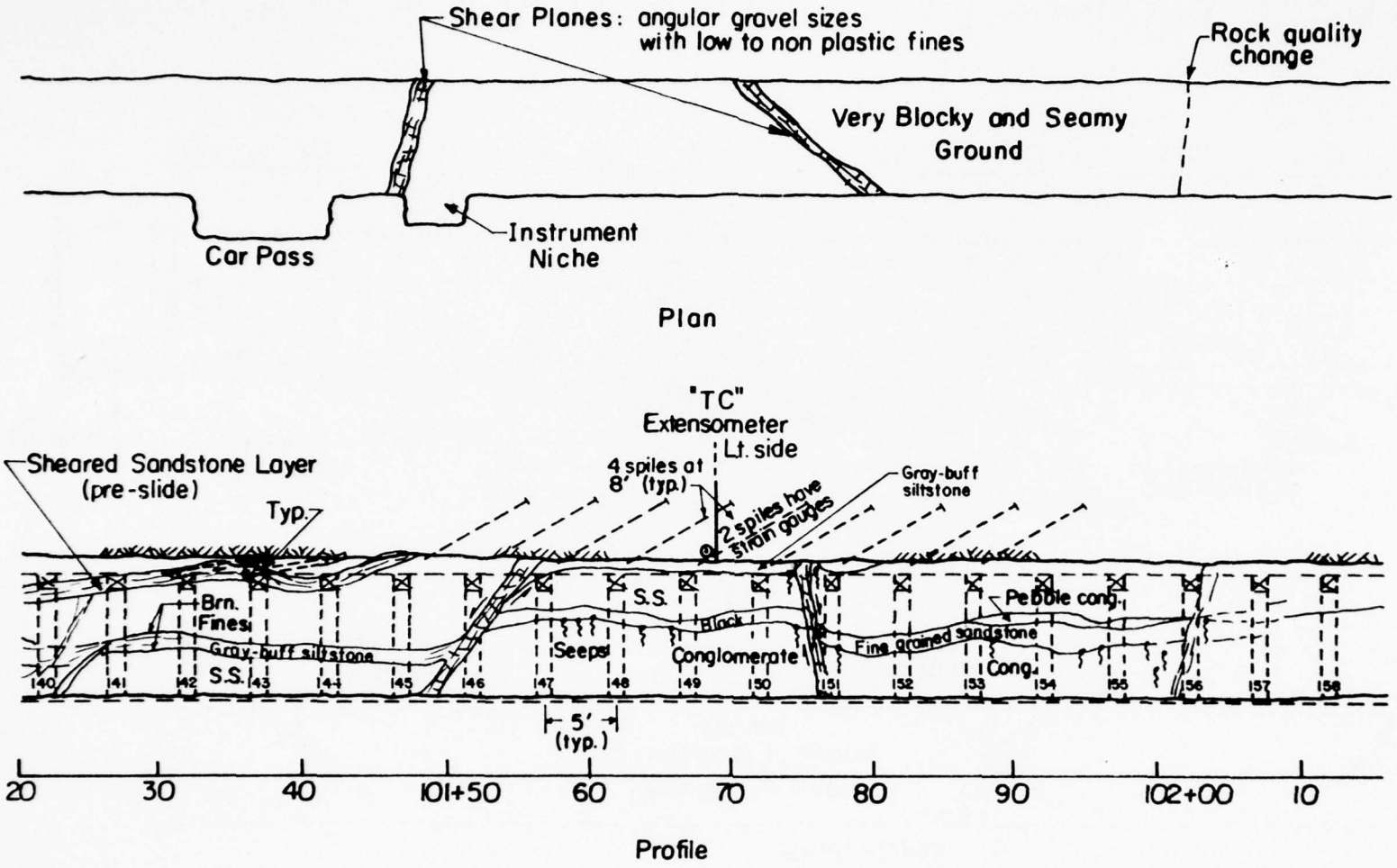

FIG. 2-6. Geologic Plan and Profile, Test Station No. 2 (MacDonald, 1976)

intersect the opening. They contain angular gravel and/or low plasticity fines. Water seepage from the shear zones was observed in small amounts. A horizontal shear, exposed at the tunnel walls, divides a sandstone and siltstone layer from a conglomerate unit. The fine grained sandstone which locally grades into siltstone is similar to the rock mass of the first test station. The conglomerate is composed of rounded cobble to pebble size inclusions in a matrix of sandstone-siltstone type material. Like the sandstone, it is randomly jointed, has granulation, and is characterized as very blocky and seamy ground. Spiles and extensometer anchors are located within alternating layers of sandstone, siltstone, and a three foot conglomerate unit directly above the crown. The exact position of the layers is uncertain on account of poor core recovery from the extensometer borehole. Overburden at the site of the second test station is 171 feet.

Pilot Tunnel Construction

Full face drill and blast was the primary method of excavation. Rounds were limited to five feet. Typical advance rates were one round per eight hour shift, three shifts per day. Pneumatic spades were used in soft ground between slide blocks and in shear zones.

Ground support consisted of one foot square timber posts and caps spaced on five foot centers. Fan tail and straight three inch planks in eight foot lengths were used for forepoles and lagging. Forepoles were installed after excavation rather than driven ahead before excavation began. Only a few sets between slide blocks showed any signs of significant loading.

The only difference between the method of excavation and support

within the test stations and that of the entire pilot tunnel was the addition of spiling reinforcement. After setting forepoles and removing the muck from the last round, four eight foot long holes were drilled in the pattern shown in Figure 2-3. Bags of polyester resin grout loaded into the holes were displaced with the insertion of the reinforcement. A combination of rotation and thrust were used to mix the resin and drive the spile to its final position. Set time of the grout was about twenty minutes, long before excavation of the next round.

Pilot Tunnel Test Station Results And Discussion

As previously described, when the heading was advanced to within one round of the extensometer, instrumented spiles were substituted for the ordinary reinforcement, position "A" of Figure 2-3. This point in position and time, just prior to advancing under the cover of the instrumented spiles, was the initial point for all instrumentation. The records of spile stress and extensometer deformation, subsequent to the initial time, are displayed in Figures 2-7 through 2-15. Although spile strains were measured, the terms stress and strain are used interchangeably as they only differ by a constant, the modulus of steel (30×10^6 psi). Circled numbers on the time axis indicate the present location of the face, relative to the initial position "A", as measured in feet. Arrows depict shot times. Radial position is defined as the vertical distance between the tunnel crown and spile strain gauge, Figure 2-4.

Results from both test stations were considered together as a consequence of similar geologic environment, rock mass behavior, and spile response. Also, as described in Appendix 1, many of the strain gauges did not survive the installation. The majority of the results were from gauges located on that part of the spile farthest from the opening. Combining test stations filled gaps and revealed trends in the data.

Those strain gauges that did survive revealed large tensile stresses in response to excavation, Figures 2-7 and 2-9. On advancing the tunnel one round from the initial position, spiles showed an average axial stress increase of 6 KSI (1.8 tons tensile force). Taking into account the tributary area reinforced by each spile, the stress increase was equivalent to a rock load of 0.7 KSF. Considering this force, there is strong evidence that the deformation induced tension was a significant contribution to the immediate stabilization.

Bending stresses, upon excavation of the first round, were minor relative to axial stress. For similar magnitudes of stress, the energy supplied by the reinforcement in bending is only one-fourth that in tension. As shown in Figures 2-8 and 2-10, the stresses were negative, which was indicative of concave deflection facing upward. This is contrary to the deflected shape of forepoles and emphasizes the difference between spiling reinforcement and forepoling, a temporary ground support method. On the average, the significance of bending did not increase in the long term (L.T.).

Radial distributions of stress increase, obtained at particular times, were plotted to summarize the reinforcement behavior. The form was similar to the bell shaped probability distribution. By employing

PILOT TUNNEL TEST STATION NO. 1

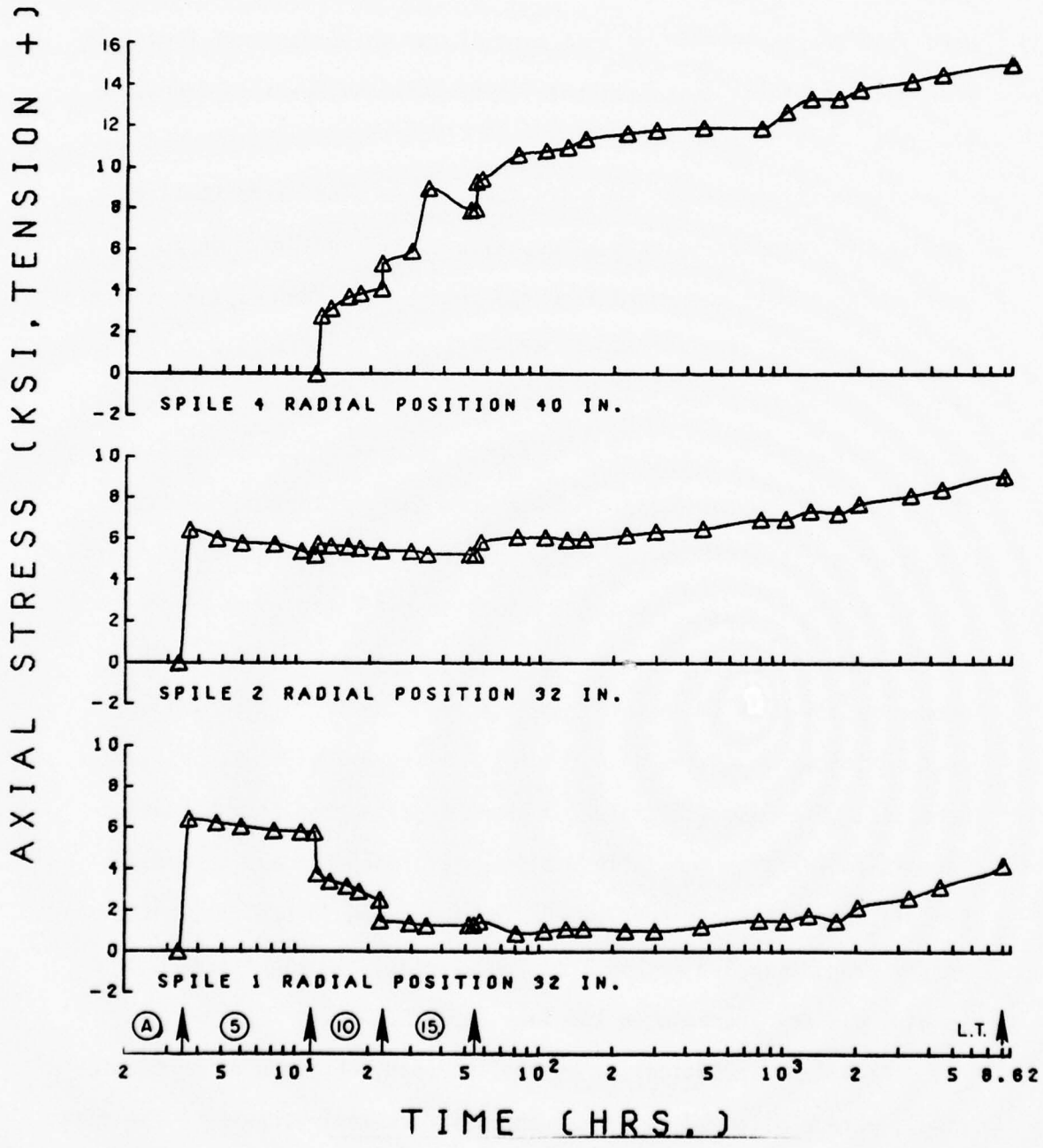

FIG. 2-7. Axial Stress History

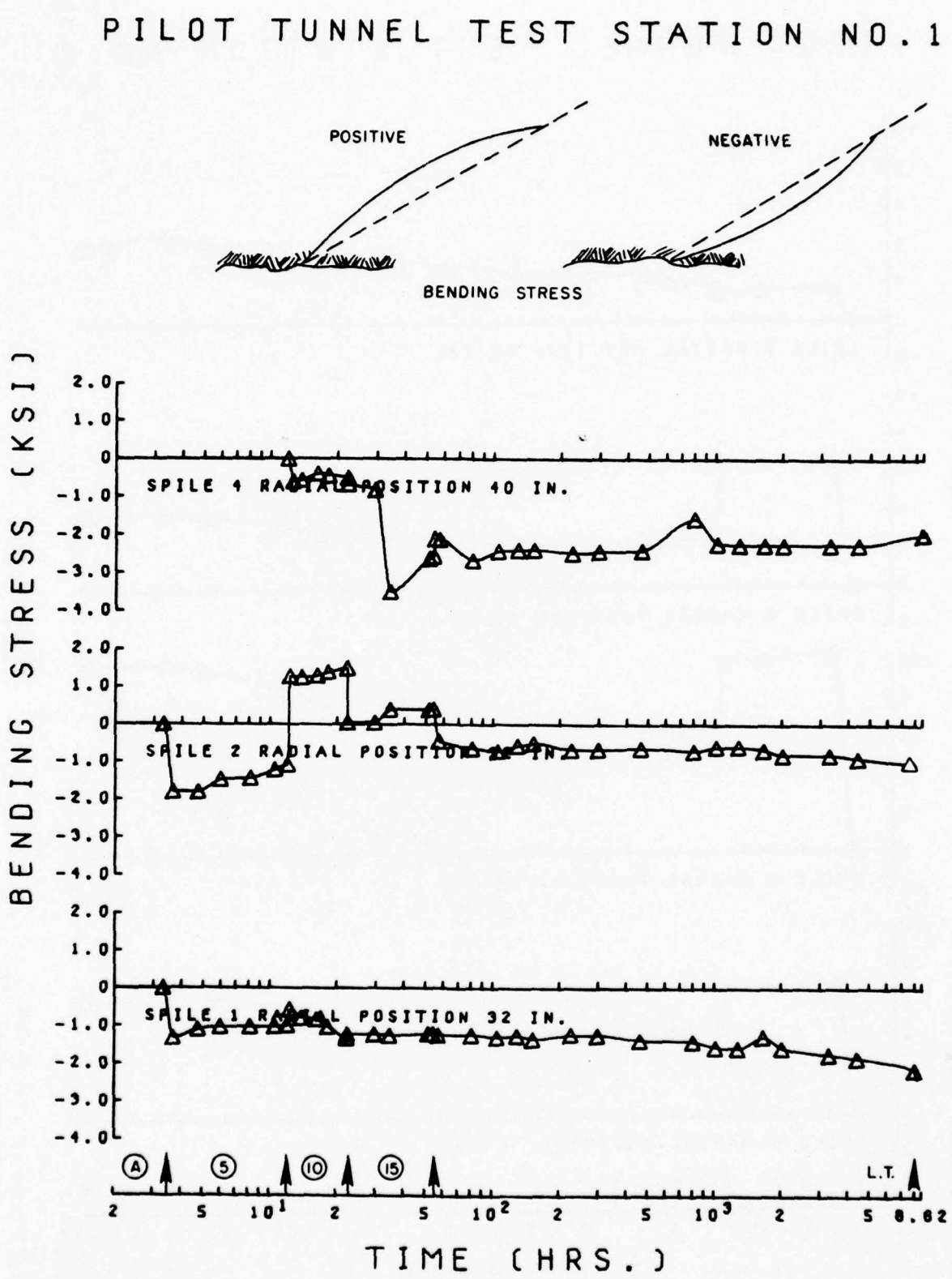

FIG. 2-8. Bending Stress History and Sign Convention

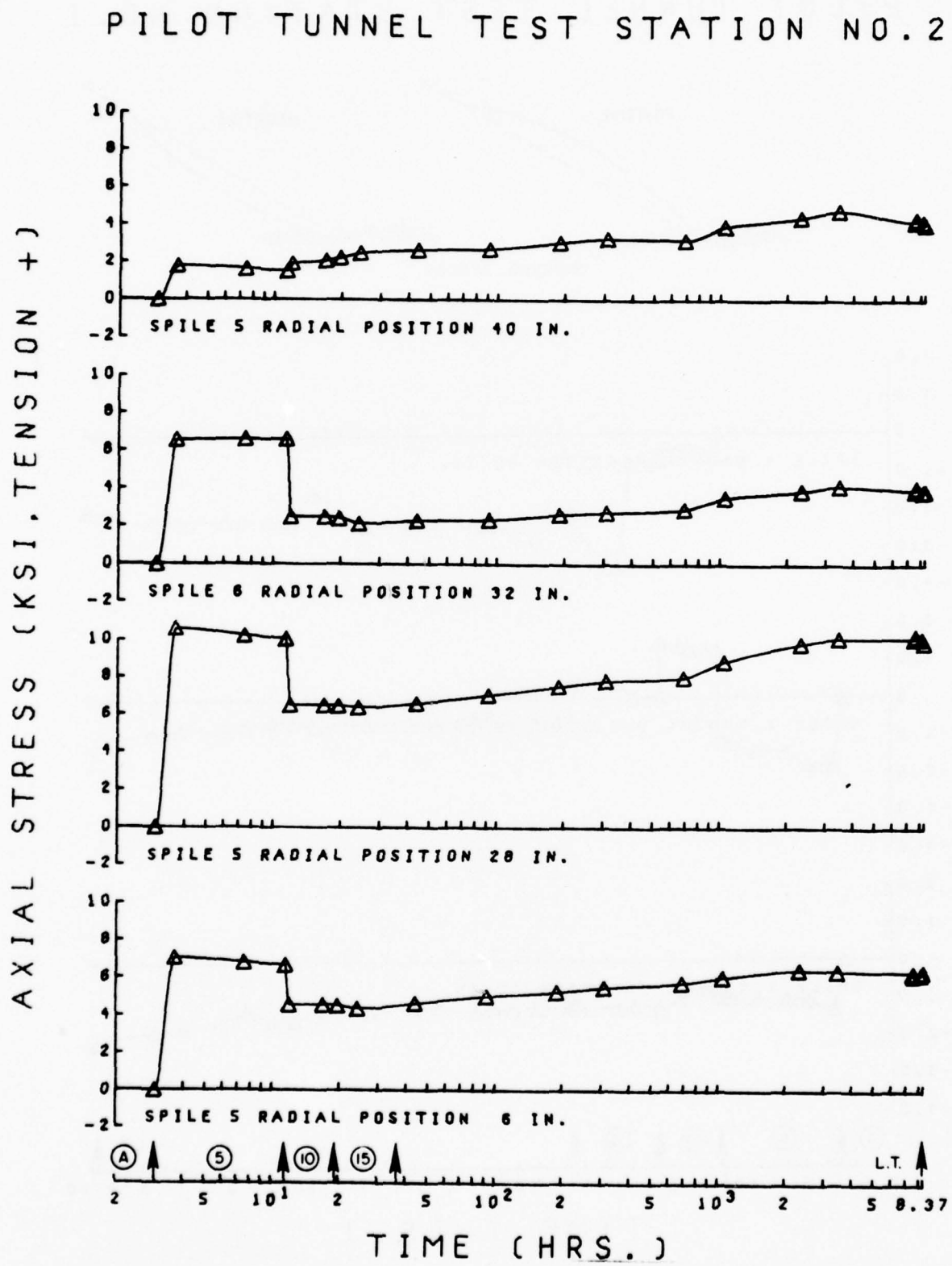

FIG. 2-9. Axial Stress History

PILOT TUNNEL TEST STATION NO. 2

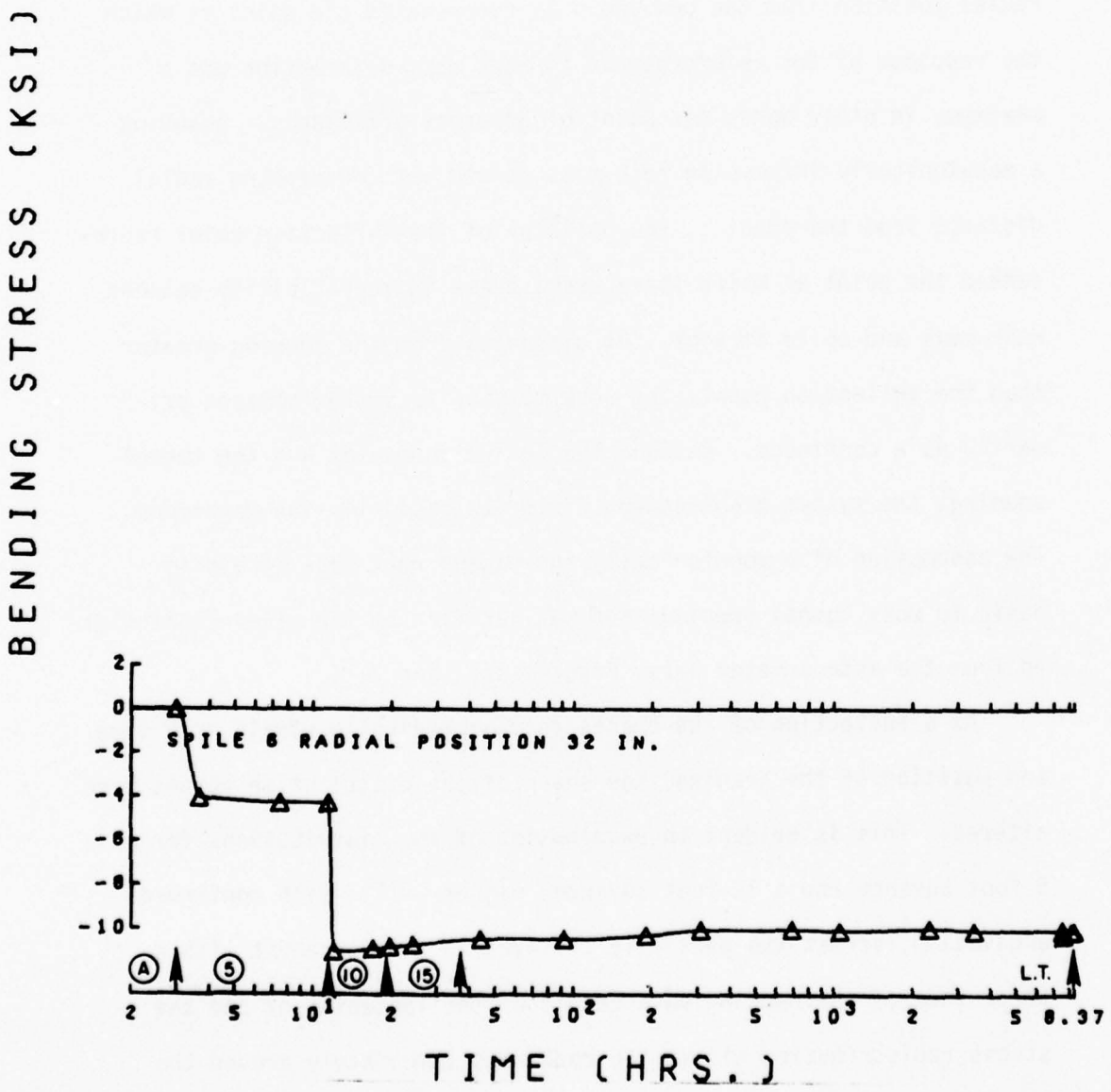

FIG. 2-10. Bending Stress History

a representative function in a least square routine, as described and illustrated in Appendix 5, "best" fit distributions were obtained for a 5 foot advance, a 15 foot advance, and for one year after excavation (long term), Figure 2-11.

Generally, the distribution curves could be characterized by their peak and inflection point (I.P.). The peak stress occurred at a given radial position from the opening. It represented the point at which the response of the reinforcement to rock mass deformation was a maximum, in other words the point of greatest efficiency. Assuming a monotonically increasing rock mass strain with decreasing radial distance from the opening, the position of the inflection point represented the point at which there was a break in compatibility between rock mass and spile strains. At distances from the opening greater than the inflection point, the rock mass-spile system behaved primarily as a continuum. Between the inflection point and the tunnel opening, the system displacement field was basically inhomogeneous. The assumption of a monotonically increasing rock mass strain is basic to most tunnel openings and was verified by the strains calculated from the extensometer data, Figures 2-13 and 2-15.

As a reflection of the change in measured spile strain with time and position of the heading, the shape of the distribution curves were altered. This is evident on examination of the distributions for a 5 foot advance and a 15 foot advance, Figure 2-11. With continued excavation, stress was partially relieved in reinforcement within three feet of the opening as a result of the loosening of and the stress redistribution within the rock mass immediately around the tunnel. This was largely a result of the vibrations due to blasting.

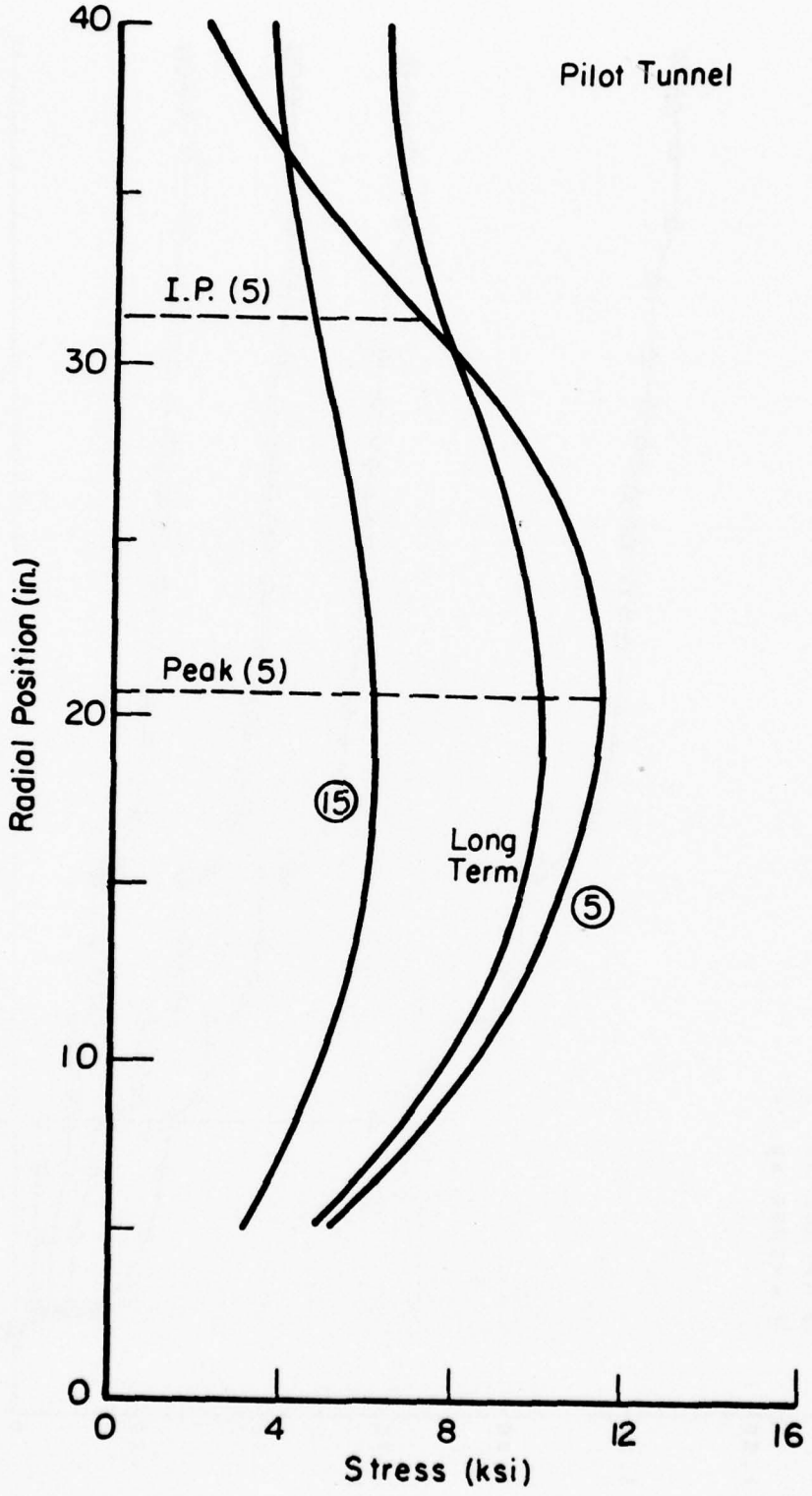

FIG. 2-11. Radial Stress Distribution Comparison: 5 ft. Advance, 15 ft. Advance, and Long Term

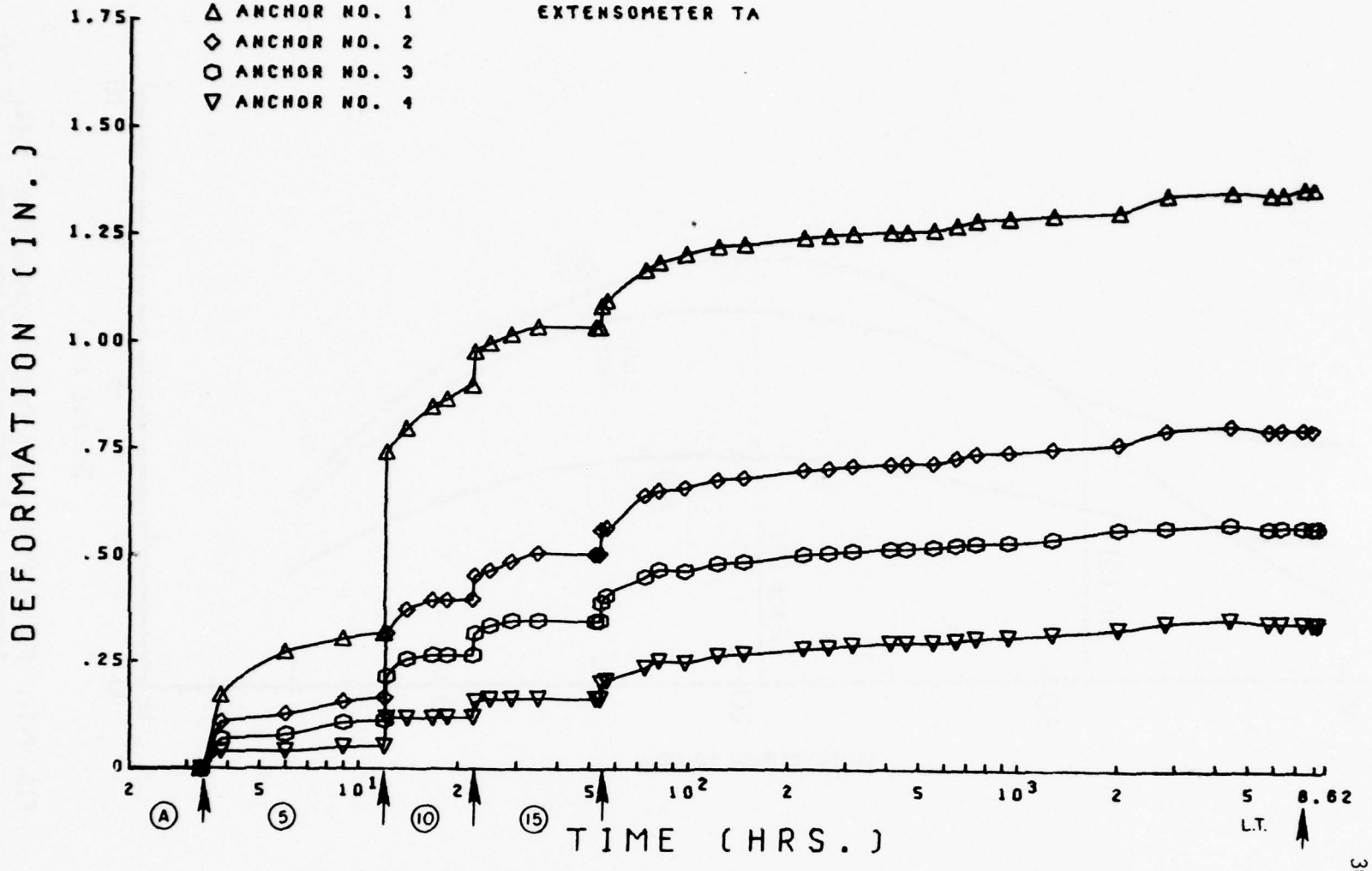

FIG. 2-12. Deformation History, Pilot Tunnel Test Station No. 1, Extensometer TA (MPBX-TA)

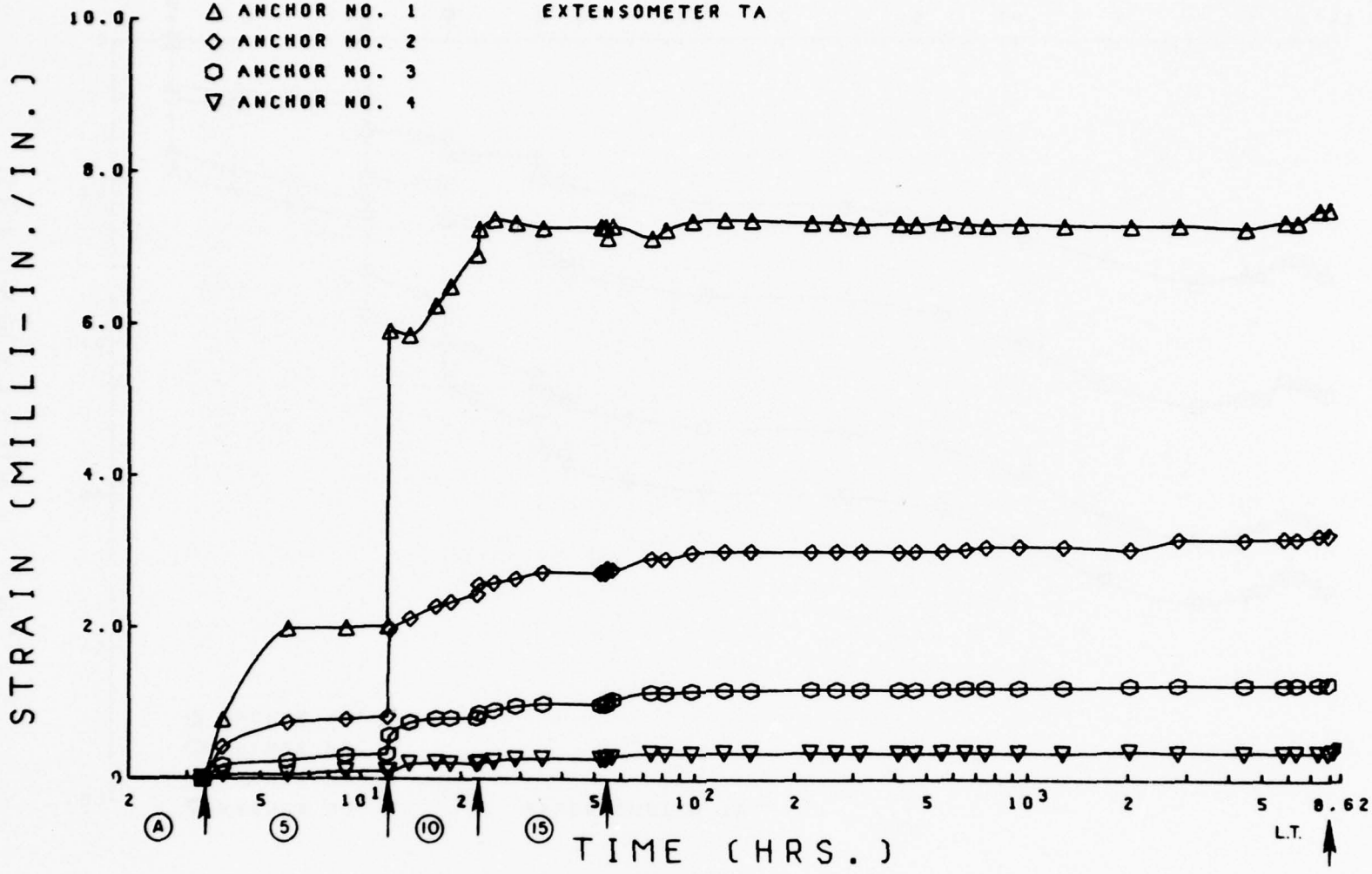

FIG. 2-13. Strain History, Pilot Tunnel Test Station No. 1, Extensometer TA (MPBX-TA)

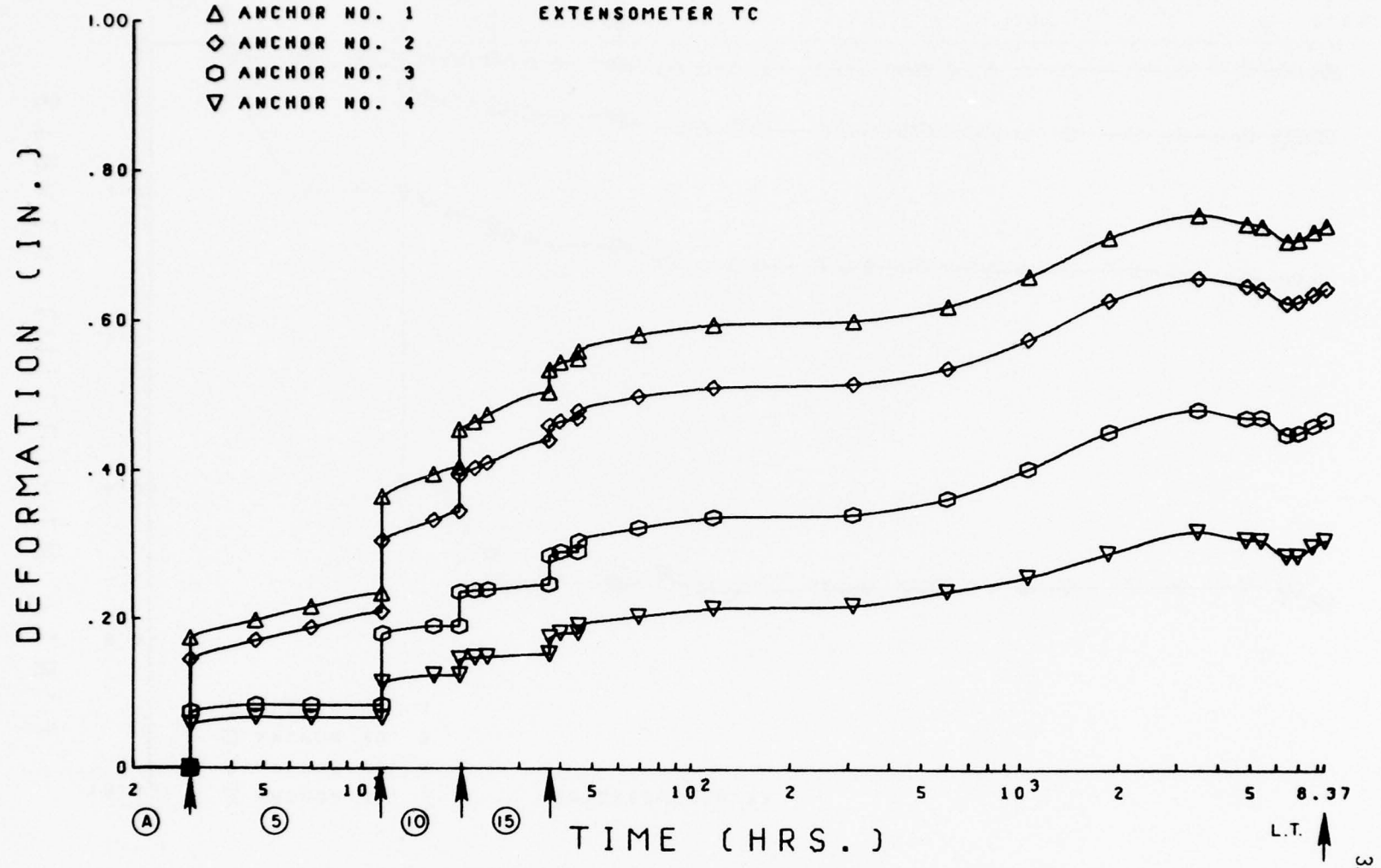

FIG. 2-14. Deformation History, Pilot Tunnel Test Station No. 2, Extensometer TC (MPBX-TC)

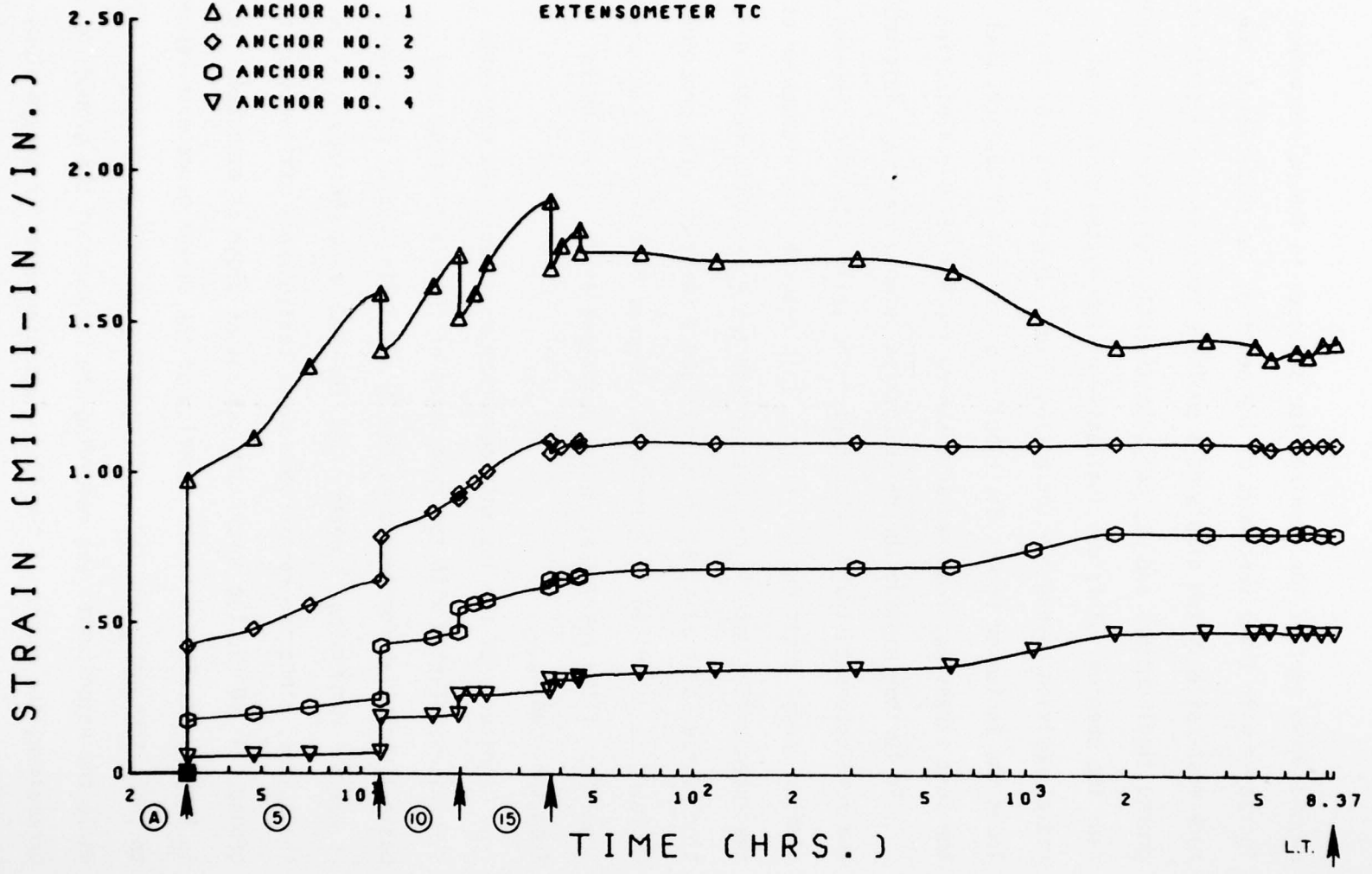

FIG. 2-15. Strain History, Pilot Tunnel Test Station No. 2, Extensometer TC (MPBX-TC)

Beyond three feet of the opening, the stresses in the reinforcement increased with the advancement of the heading. In this region, the rock mass-spile system displayed a positive response to the continued ground displacements and was not significantly influenced by loosening near the opening. This was indicative of the system behavior at a radial position beyond the inflection point. During the year that followed the indicated stress distribution at 15 feet of advance, much of the lost stress was regained as shown by the long term distribution.

To further examine the relationships between rock mass deformation and reinforcement strain, extensometer and spile data were compared at similar radial positions and times. This required transformation of the extensometer data in order to obtain the rock strain in the direction of the spile axis, at the strain gauge position. The procedure employed is described in Appendix 4. Figures 2-16 through 2-20 are summaries of the results at radial positions of 28, 32 and 40 in. from the opening.

Magnitudes of the instantaneous change in rock mass and spile strains, associated with the excavation of the first round, were basically similar for gauges at the 28 and 32 in. radial positions. It was not surprising, however, that the rock mass strained more than the spiles, since the reinforcement was considerably stiffer than the ground. At 40 in. the comparison was not as close as expected. This is largely attributed to the location of the strain gauge with respect to the extensometer and face position after advancing one round. While the extensometer was recording the response of the ground to excavation, the gauges at the 40 in. position were far enough along the bar so as to be ahead of the face. Consequently, it was the

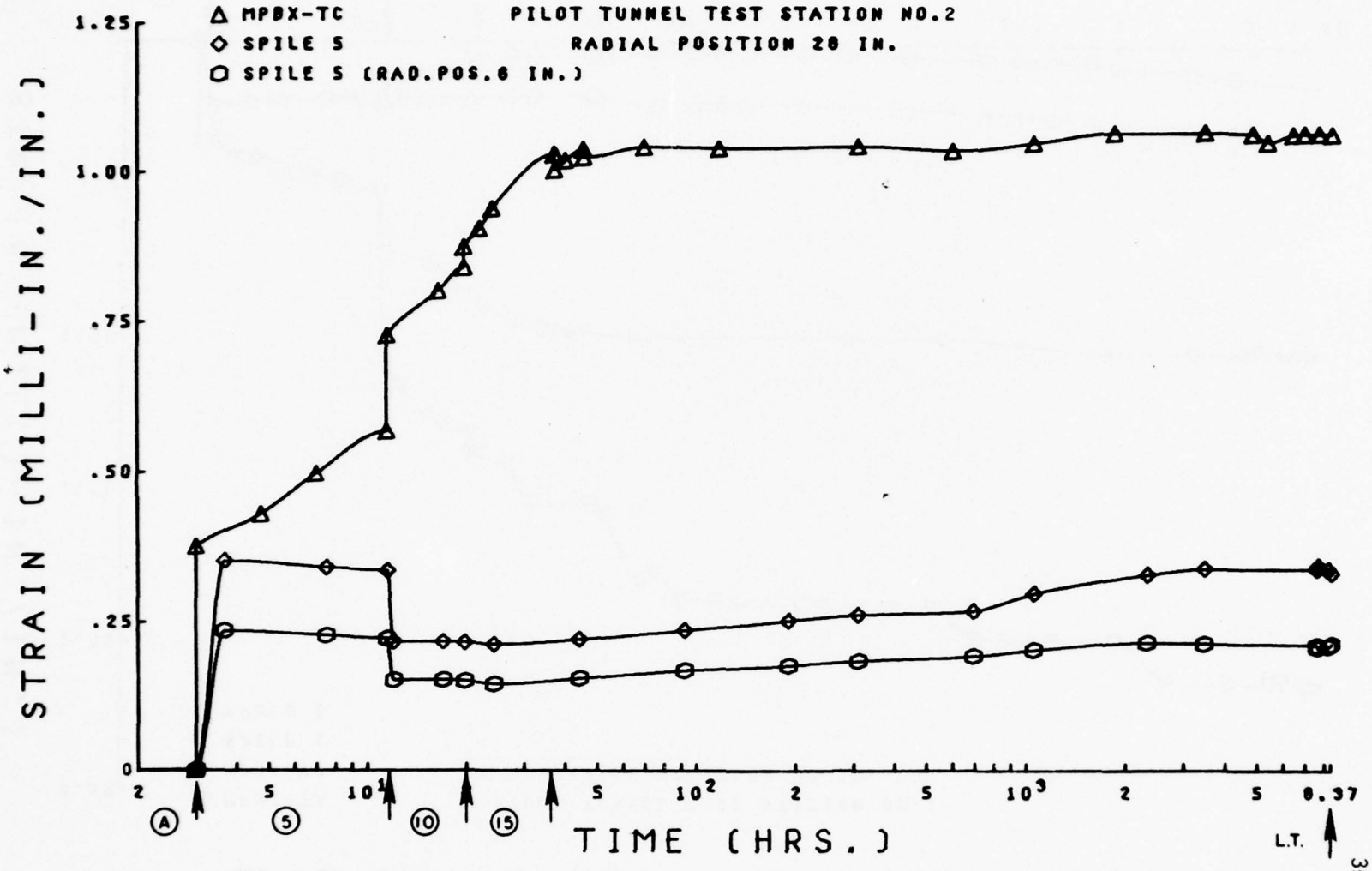

FIG. 2-16. Strain History Comparison: Instrumented Spiles and Extensometer, Pilot Tunnel Test Station No. 2, Radial Position 28 in.

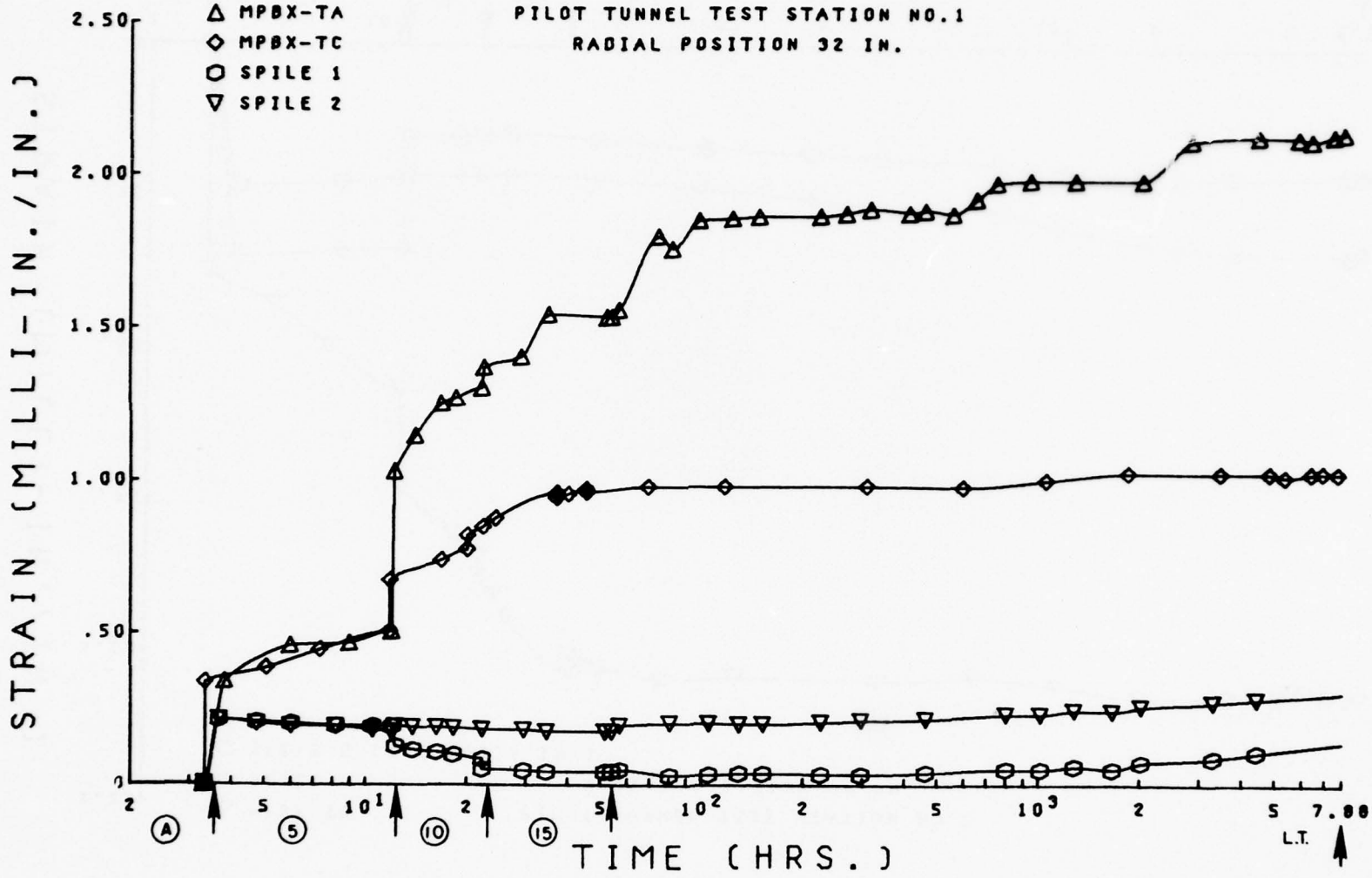

FIG. 2-17. Strain History Comparison: Instrumented Spiles and Extensometers, Pilot Tunnel Test Station No. 1, Radial Position 32 in.

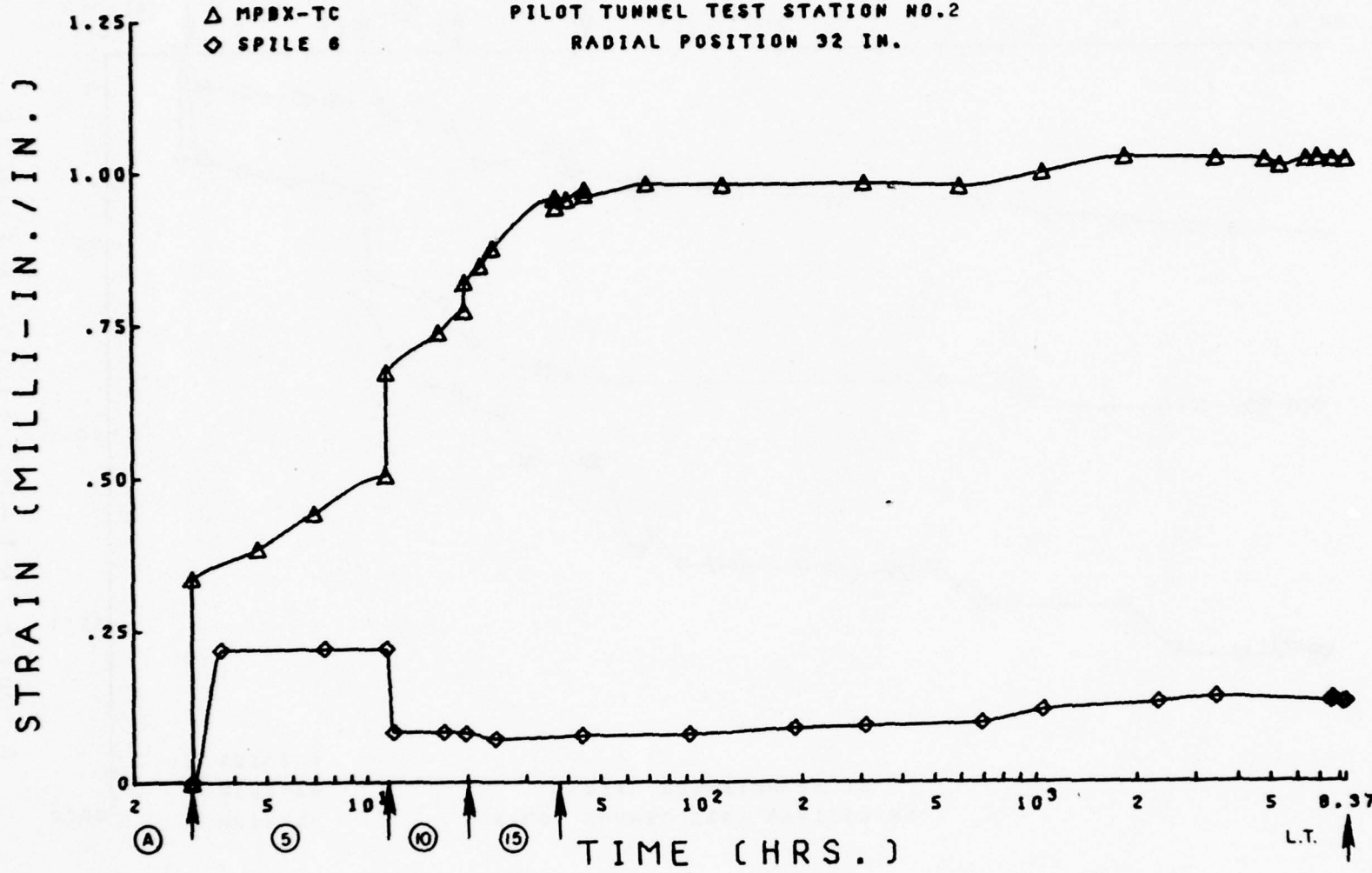

FIG. 2-18. Strain History Comparison: Instrumented Spiles and Extensometer, Pilot Tunnel Test Station No. 2, Radial Position 32 in.

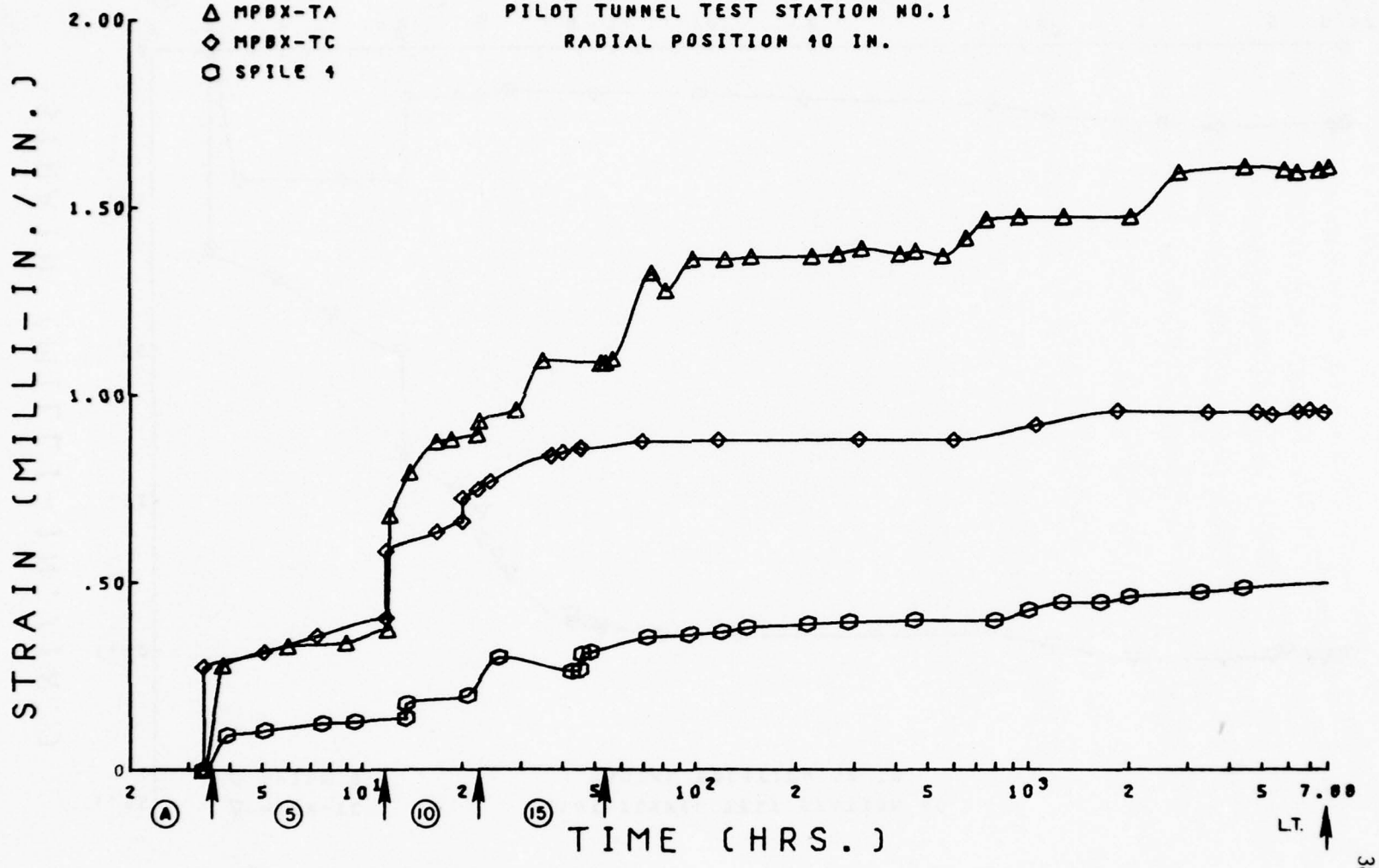

FIG. 2-19. Strain History Comparison: Instrumented Spiles and Extensometers, Pilot Tunnel Test Station No. 1, Radial Position 40 in.

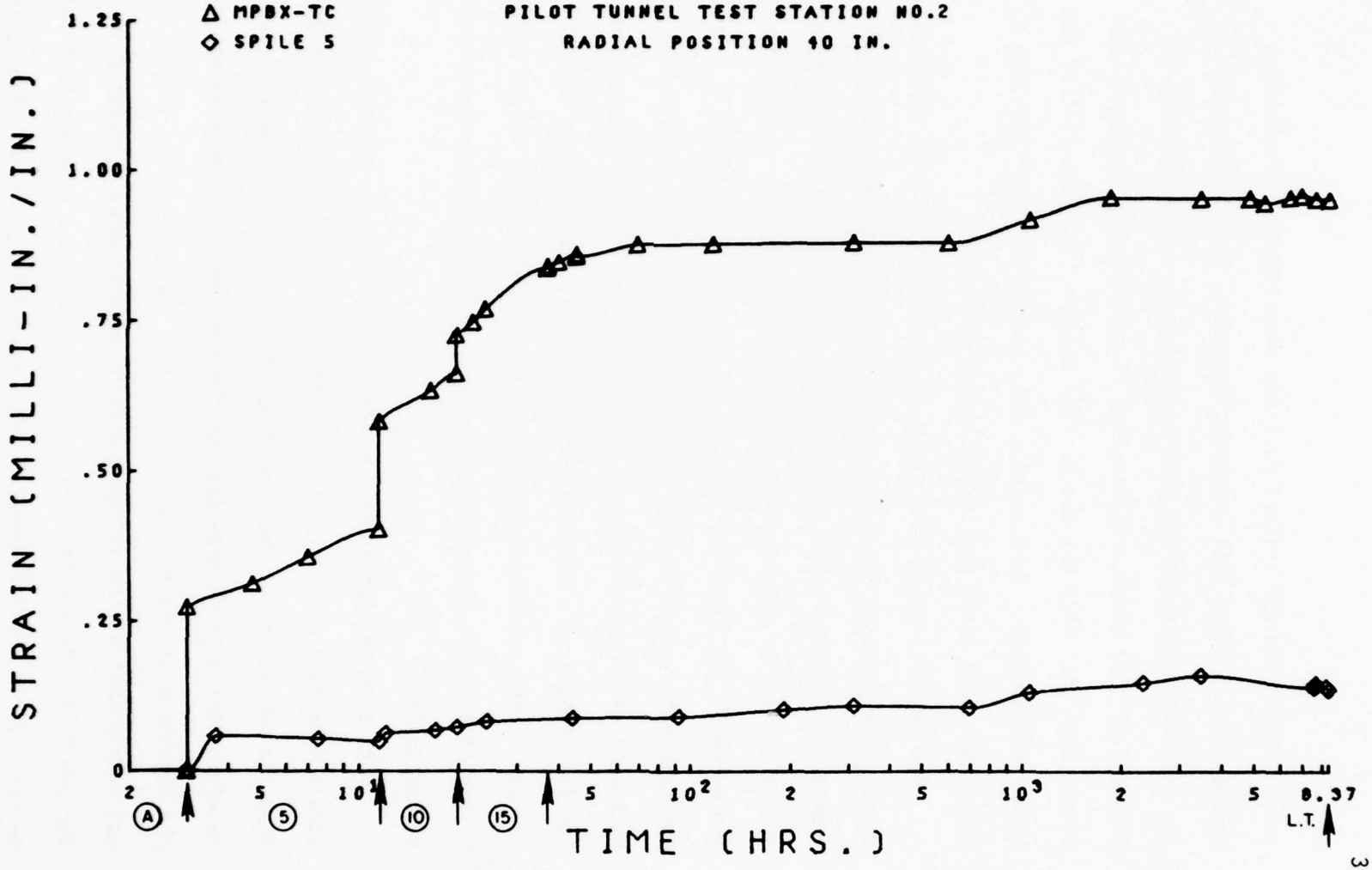

FIG. 2-20. Strain History Comparison: Instrumented Spiles and Extensometer, Pilot Tunnel Test Station No. 2, Radial Position 40 in.

second round from the initial position that advanced the heading beyond them. Taking this into consideration, the distributions of the instantaneous spile and rock mass response are summarized in Figure 2-21. As shown, extensometer TC consistantly recorded less strain than TA. This was due to its location, two feet left of the tunnel center line. As a result, the two extensometers provided a lower and upper bound for the rock mass behavior.

Due to the lack of data close to the opening, it was difficult to accurately locate the spile strain distribution peak, Figure 2-21. However, by interpolation it appeared to occur at a radial position around 20 in., at which point the rock mass strain was approximately 0.6 percent. At the inflection point, the strain was about 0.4 percent. For this early point in time after excavation, the strains within the rock-mass reinforcement system at a radial position of greater than two feet displayed a reasonable compatibility, considering the difference in the relative stiffness of the two components in the system. Within this region, the rock mass strain was approximately twice that of the spiles.

With time and continued advancement of the face, the rock mass strain increased considerably. One of the largest increases resulted from the excavation of the second round. As previously described, reinforcement within three feet of the opening exhibited a stress drop. The magnitude of the instantaneous strain decrease within the spiles was nearly that of the increase within the rock mass, Figures 2-16 through 2-18. Beyond three feet strains increased together, but not necessarily in the same proportion, Figure 2-19 and 2-20. Again, this was indicative of compatible rock mass-reinforcement behavior found

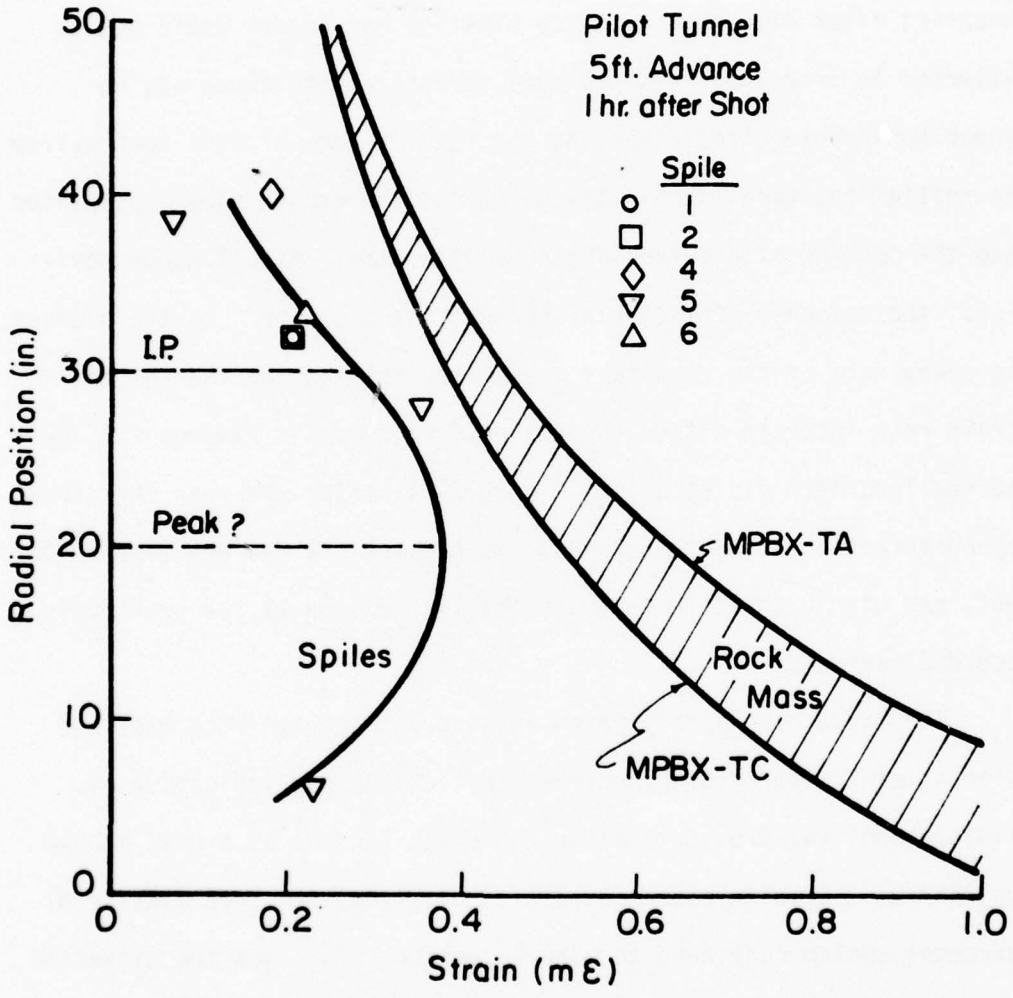

FIG. 2-21. Radial Strain Distribution Comparison: Spiles and Extensometers (Rock Mass), 1 hr. after 5 ft. Advance

at a location beyond the inflection point.

It can be argued that wherever increasing strains within the rock mass are accompanied by a reduction in reinforcement strain, the ground has deteriorated and the bond between the rock and spile destroyed or weakened. However, if this was the case, deformation occurring after disturbance due to blasting had ceased would not be reflected in increased reinforcement stress. Disturbance was no longer noticeable after advancing the face 20 feet or four rounds from the initial position. From this point on, the ground slowly displaced into the opening at a decreasing rate with time. At all gauge positions, the response of the reinforcement was positive. On the average, the creep rate of the rock mass was nearly the same as that of the strain rate increase within the spiles. As shown in Figures 2-7, 2-9, and the long term distribution, Figure 2-11, after one year the stress beyond three feet from the opening was greater than at any time in the past, and within three feet it was nearly the same as the previously recorded maximum.

The large discrepancy which existed between the rock mass and spile strains after vibration from blasting was not indicative of reinforcement failure, but rather the establishment of a new, stable equilibrium. Despite poor controls on blasting, the rock mass-reinforcement system continued to work in unison. This was the situation close to the tunnel opening as well as at the farthest extent of the spiles.

The influence of the wooden support system on the establishment of the new equilibrium was minimal. Gaps left between the posts and cap would close as the system took load. Measurements showed

negligible closure. Visual inspections revealed only a small amount of loosened material resting on the forepoles.

Main Bore Construction

Construction of the main bore was initiated nine months after completion of the pilot tunnel. As shown in Figure 2-2, it was driven by top heading and bench. Ground support primarily consisted of steel sets spaced on five foot centers and a reinforced concrete liner. Shotcrete was used for lagging in the lower half of the top heading. Depending on ground conditions, forepoles were placed after excavation or driven ahead before advancing the round. Spiling reinforcement was employed in a random manner; consequently, it was not considered to be of significant influence on ground stabilization.

Main Bore Test Station Results And Discussion

In many aspects, the response of the rock mass-reinforcement system to excavation of the top heading was similar to that observed during excavation of the pilot tunnel. The increase in stress on advancing beneath the cover of the spiles, the relaxation of the reinforcement nearest the opening with continued advancement of the heading, and the opposite behavior of the reinforcement farthest from the opening were all the same, Figures 2-22 to 2-25. However, the increased size of the opening and the lack of additional reinforcement within the arch had a pronounced effect on the overall results.

Upon excavation of the top heading, additional overbreak resulted in the spiles being embedded only five feet, i.e., equivalent to a reinforced arch of one-quarter of the radius of the main bore as compared to a pilot tunnel arch nearly one radius thick. Given this thin arch plus excess damage due to blasting and the

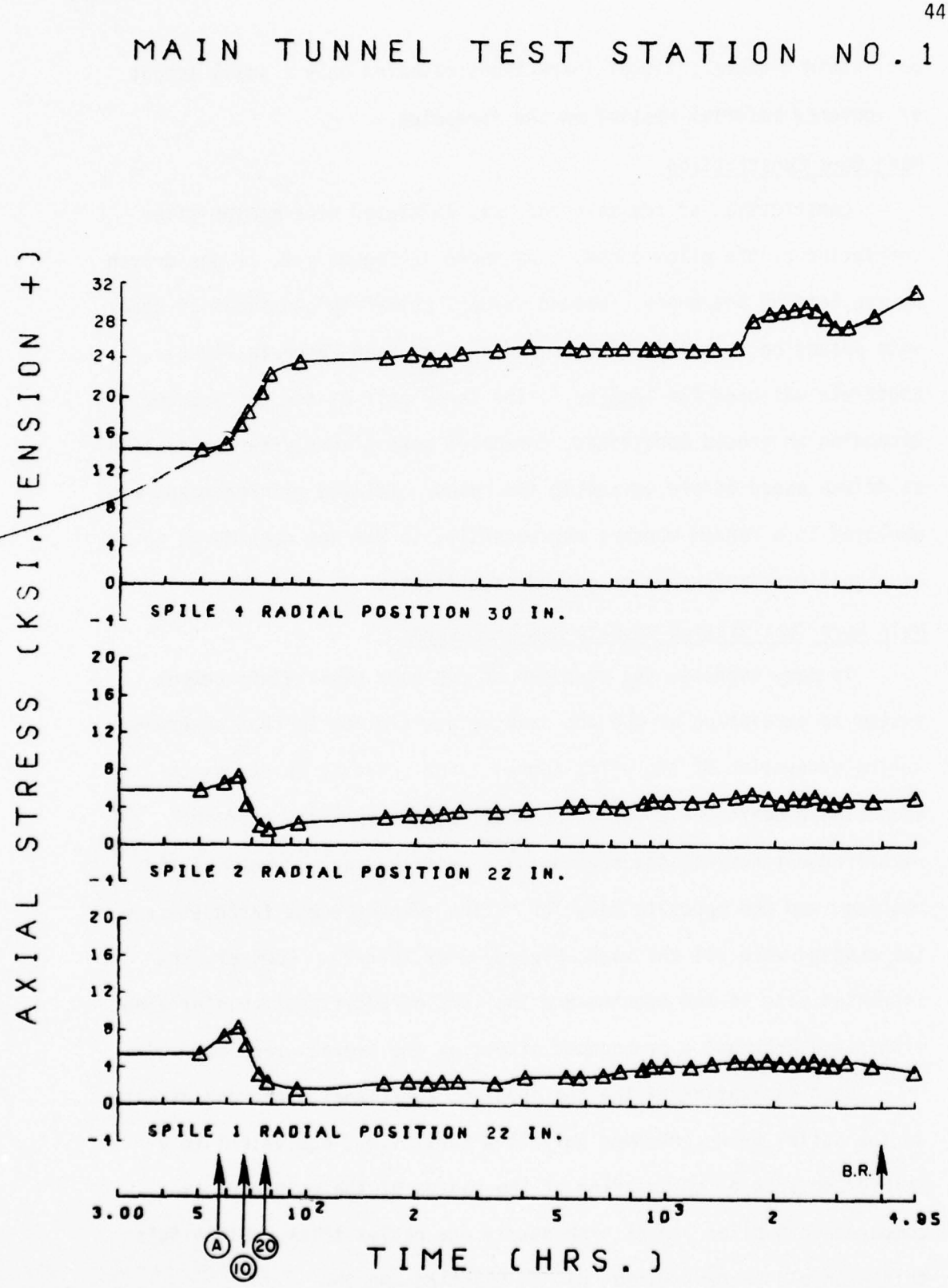

FIG. 2-22. Axial Stress History

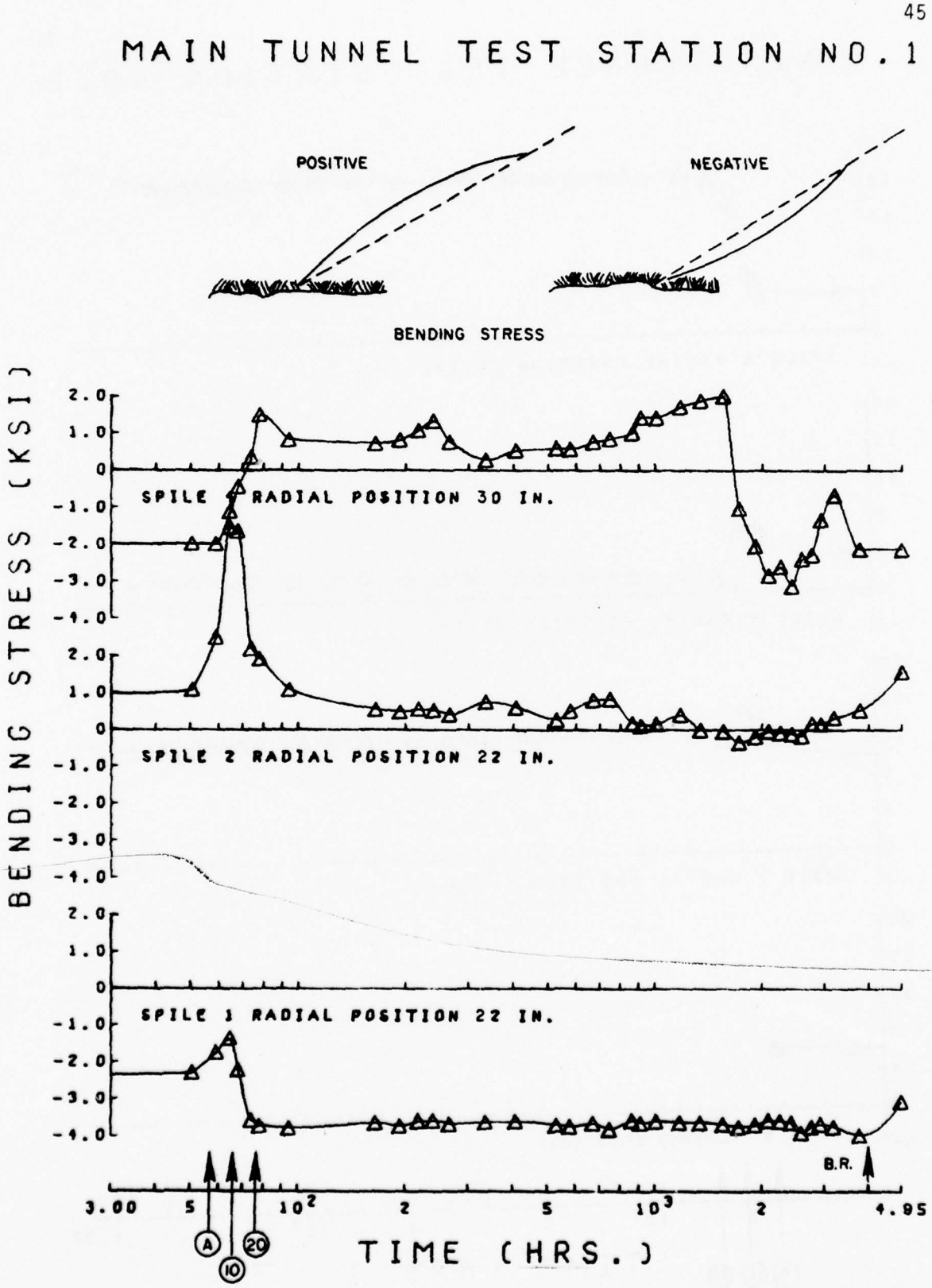

FIG. 2-23. Bending Stress History and Sign Convention

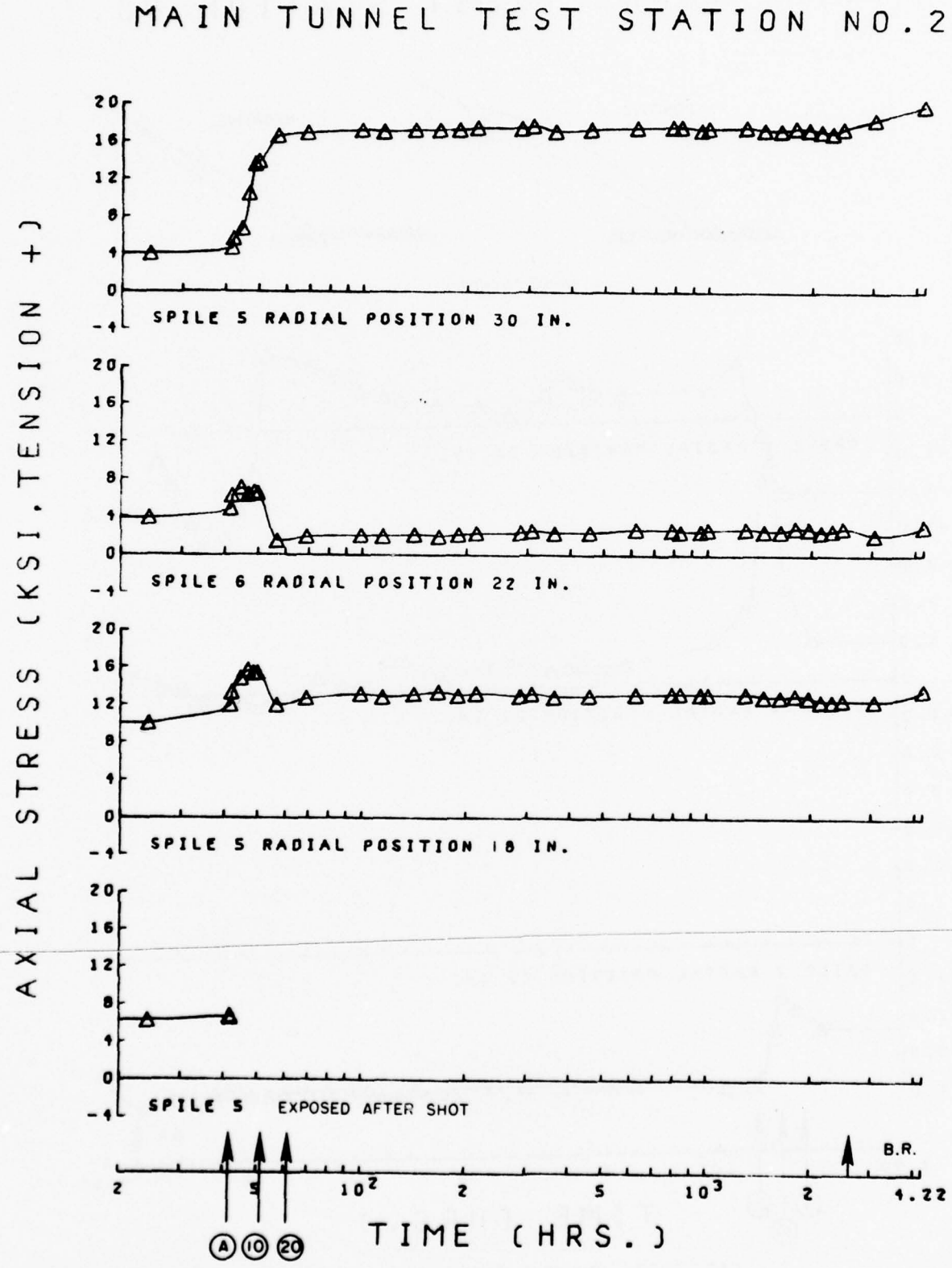

FIG. 2-24. Axial Stress History

MAIN TUNNEL TEST STATION NO. 2

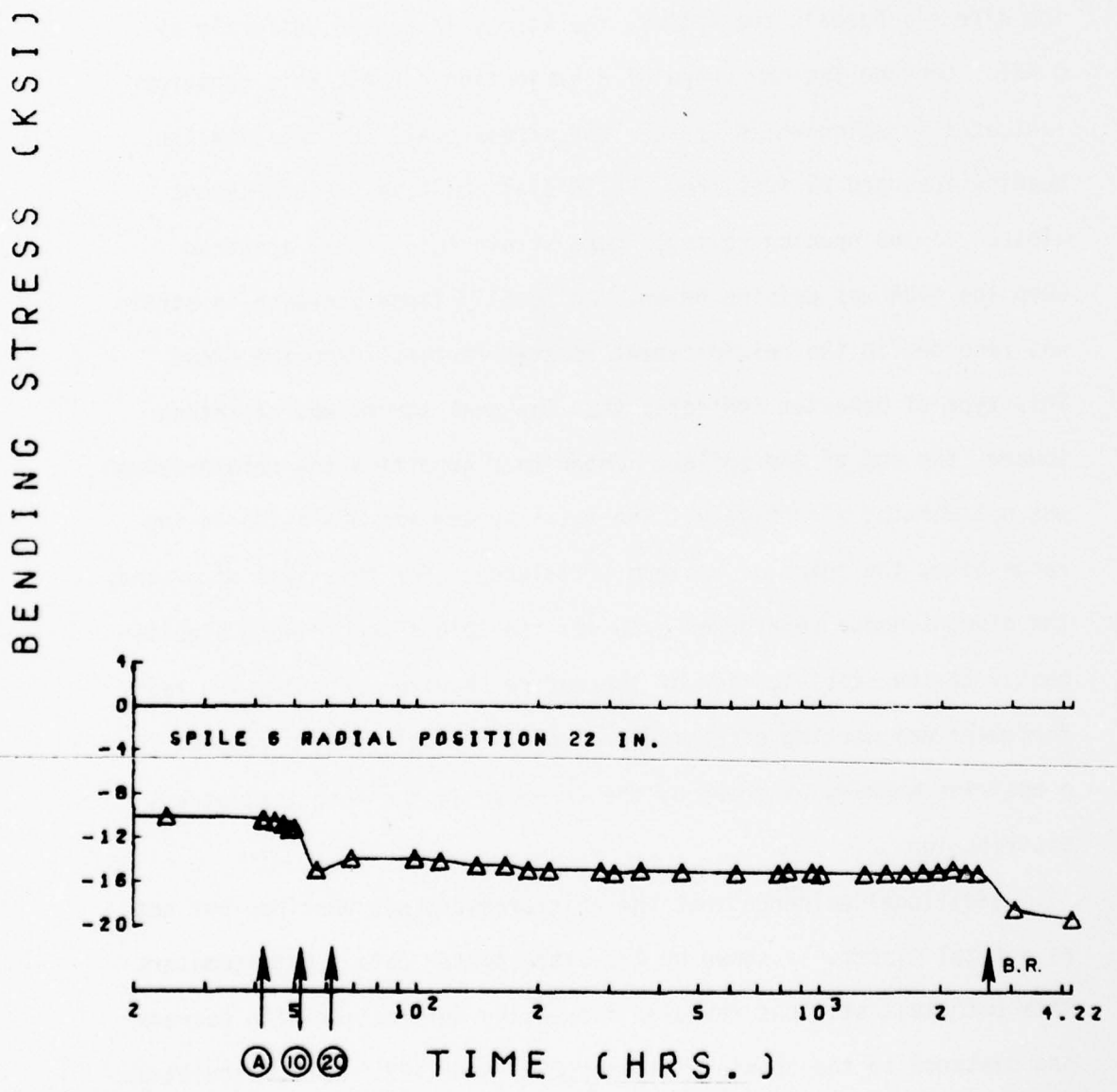

FIG. 2-25. Bending Stress History

lack of additional reinforcement, the results shown in Figure 2-26 were predictable.

Stress distributions (Figure 2-26) were obtained from the results of strain gauges located between 18 and 30 in. from the crown. Consequently, as compared to the size of the opening, only a small portion of the total distribution curve was produced. On advancing the top heading directly beneath the spiles, the stress increased uniformly by 4 KSI. Considering the shape of distribution curves, this behavior indicates a region which is near the stress peak. By the time the heading advanced 25 feet from the initial position, reinforcement closest to the opening relieved more strain than it had acquired when the face was passing below. An equally large increase in strain was recorded in the reinforcement located farthest from the crown. This type of behavior indicated that the peak stress was migrating toward the end of the spiles. Under this condition the reinforcement was not working effectively. The total system was operating in the range below the point of maximum efficiency. For this type of ground, the discontinuous reinforced arch was too thin to contribute significantly to the stabilization of the entire heading. Whether the reinforcement was working effectively or not, it continued to respond in a positive manner, as shown by the increase in the long term stress distribution.

Additional evidence that the reinforcement was working, but not as a total system, is shown by the extensometer data. Extensometers from both test stations revealed increasing deformation with decreasing distance to the opening, Figures 2-27 and 2-29. Upon calculation of the strains, it was evident that they were not monotonically

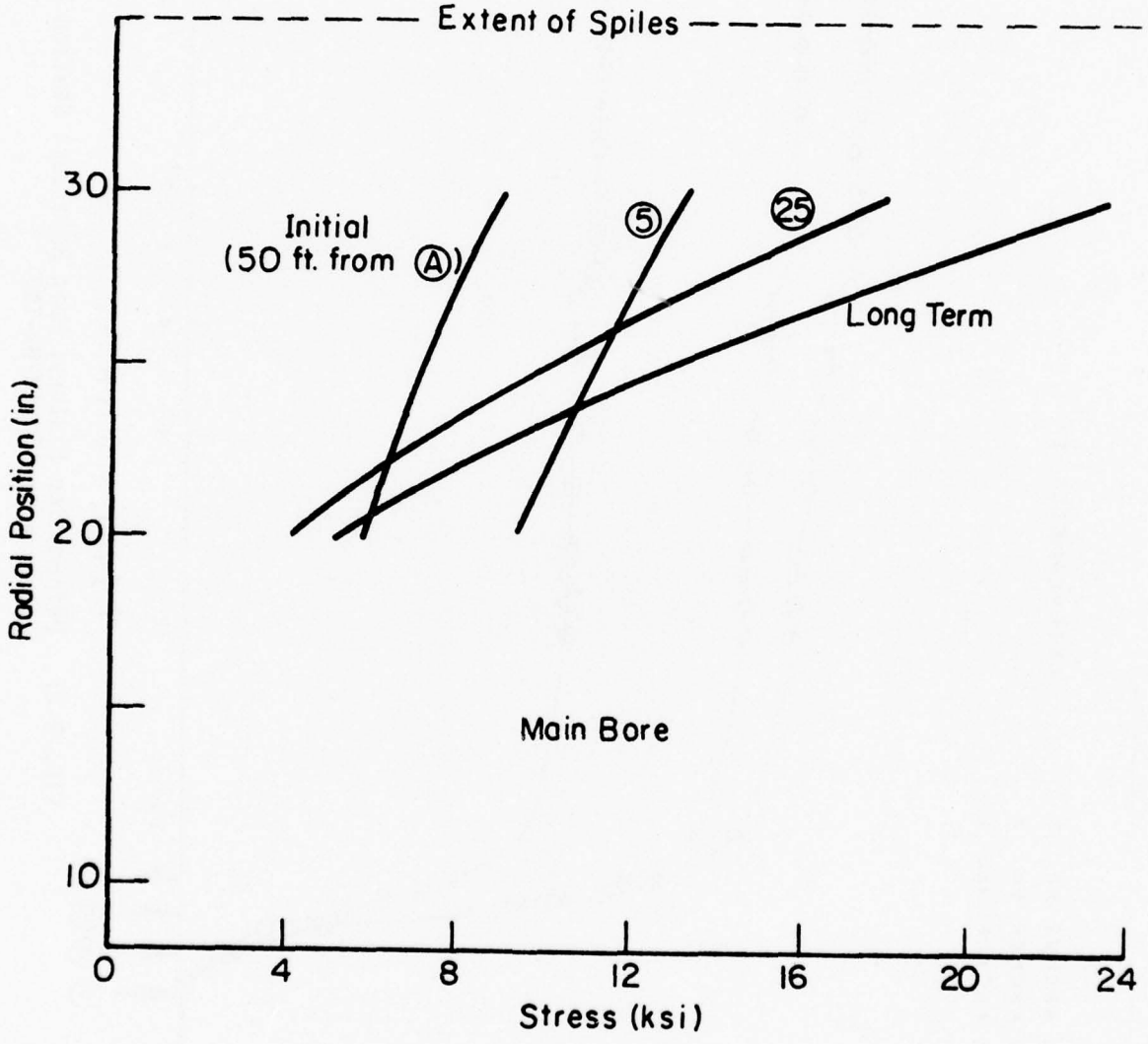

FIG. 2-26. Radial Stress Distribution Comparison: Initial (before excavation), 5 ft. Advance, 25 ft. Advance, and Long Term

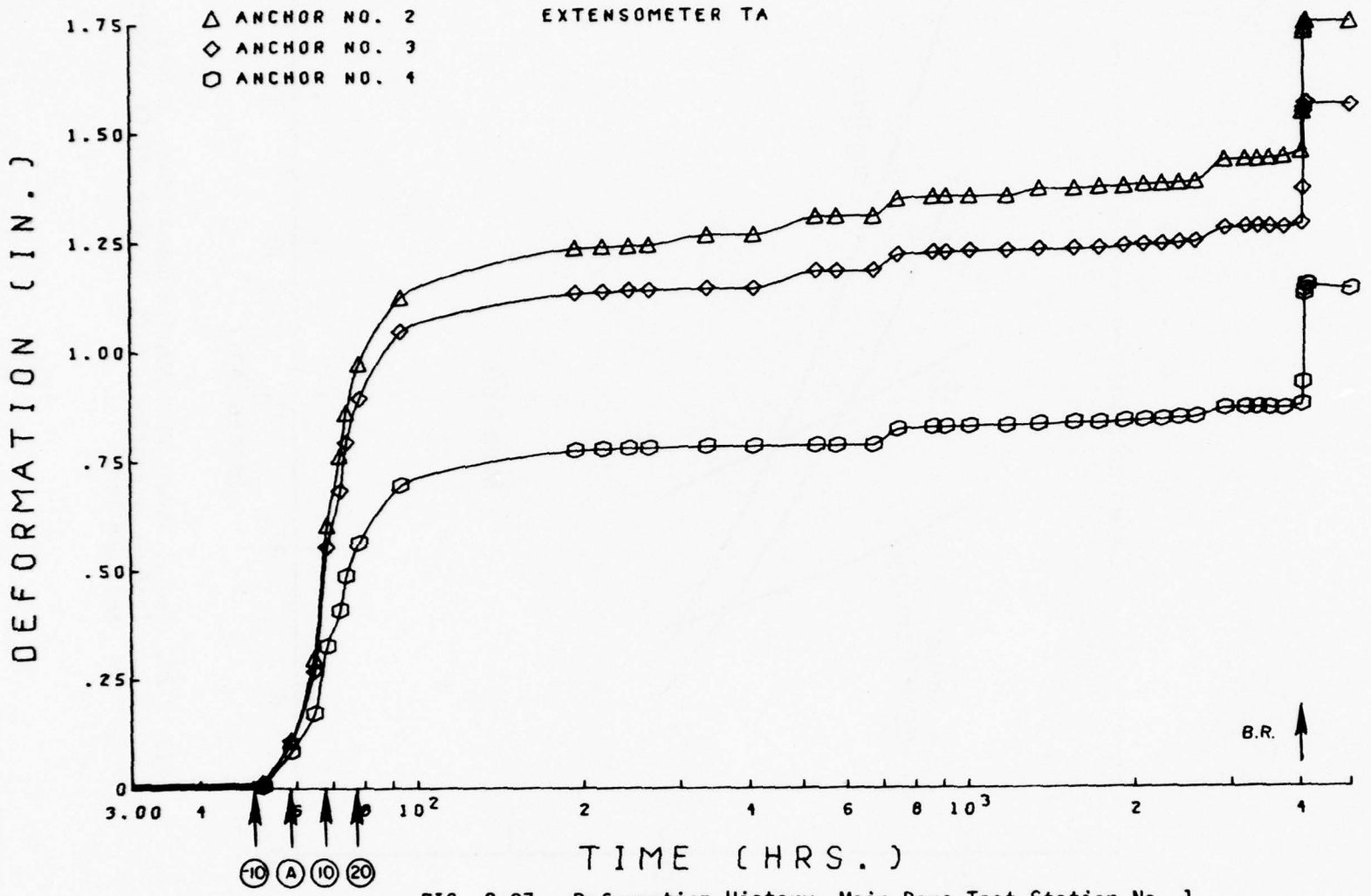

FIG. 2-27. Deformation History, Main Bore Test Station No. 1, Extensometer TA (MPBX-TA)

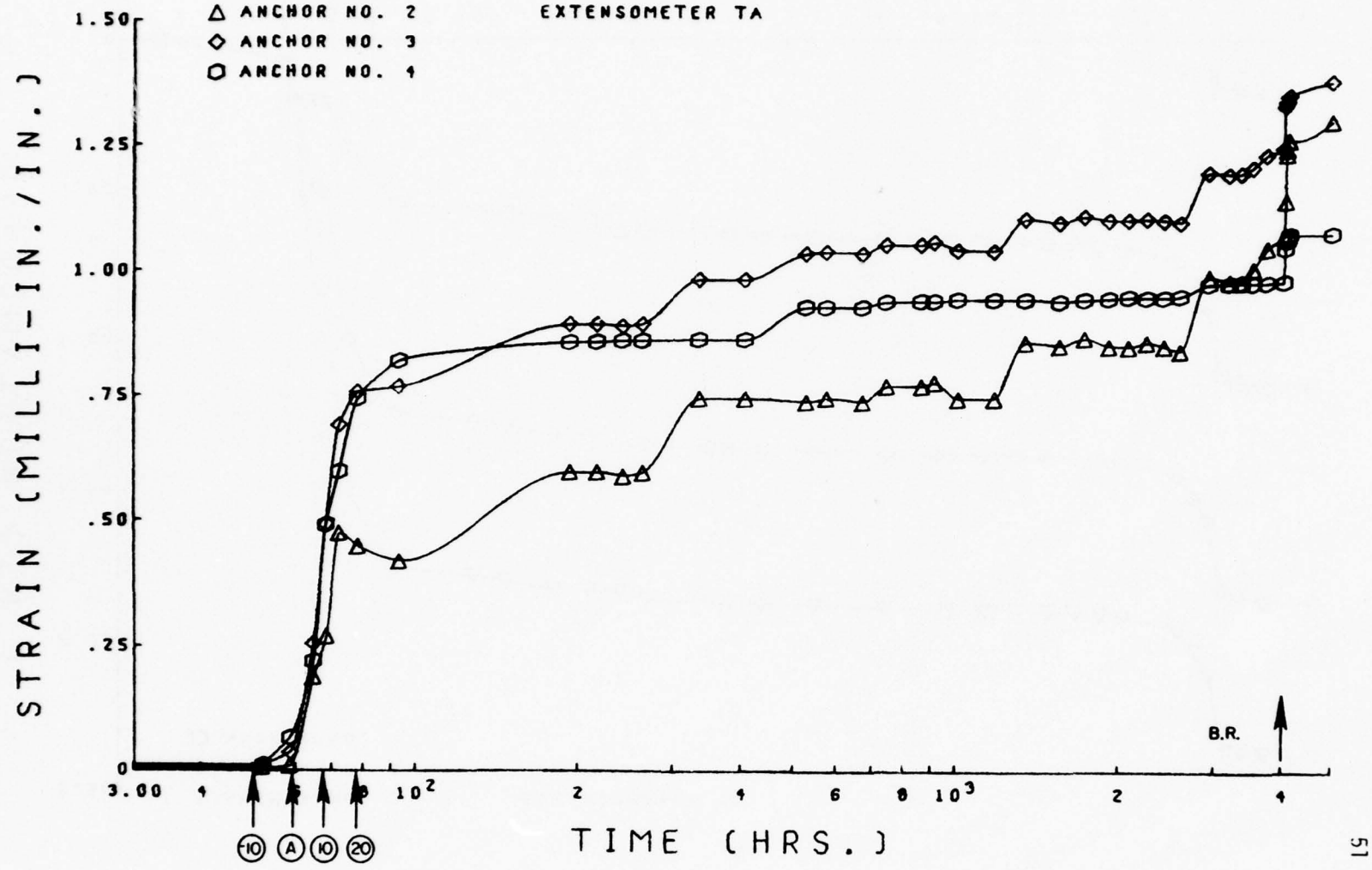

FIG. 2-28. Strain History, Main Bore Test Station No. 1, Extensometer TA (MPBX)

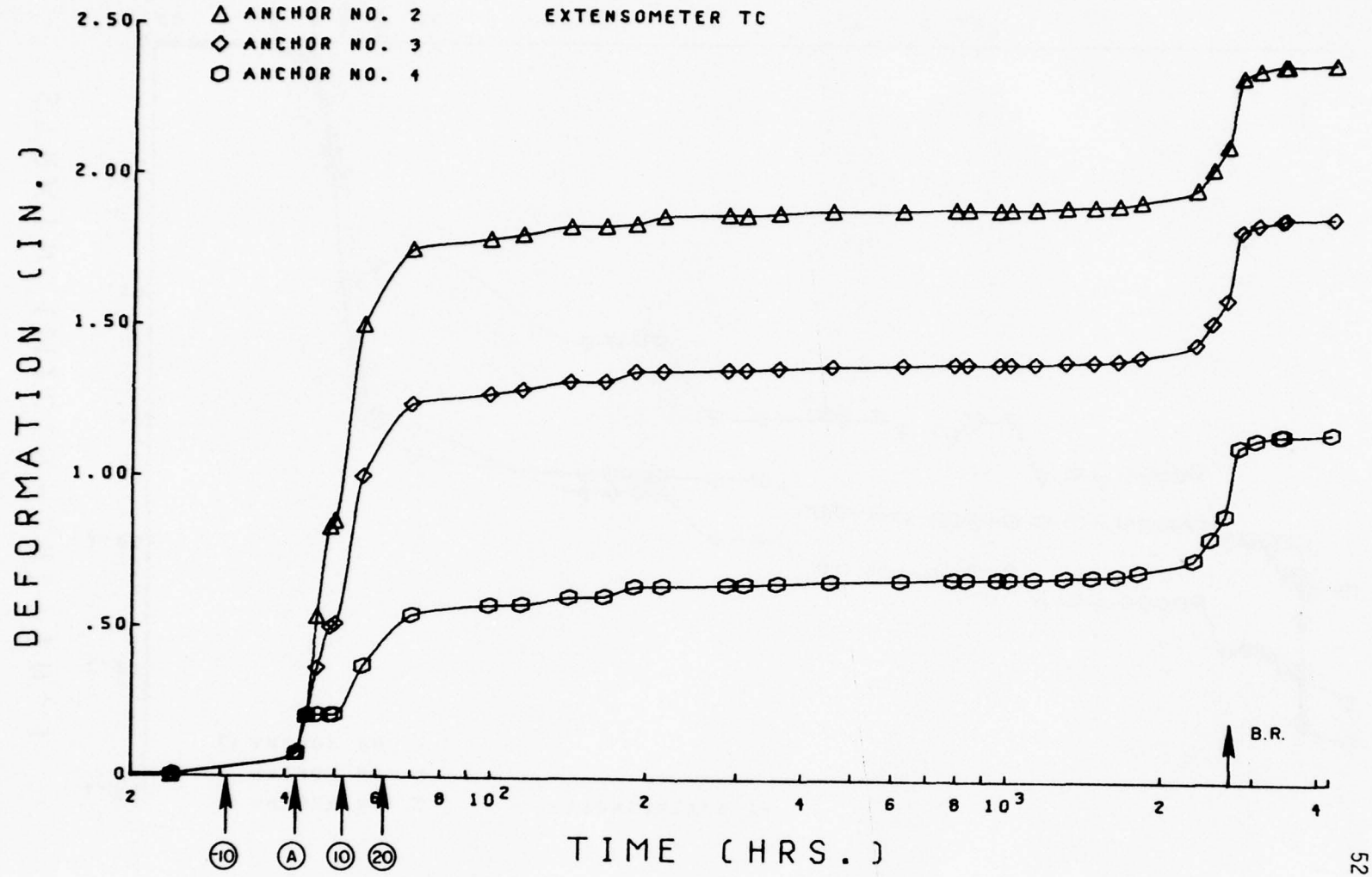

FIG. 2-29. Deformation History, Main Bore Test Station No. 2, Extensometer TC (MPBX-TC)

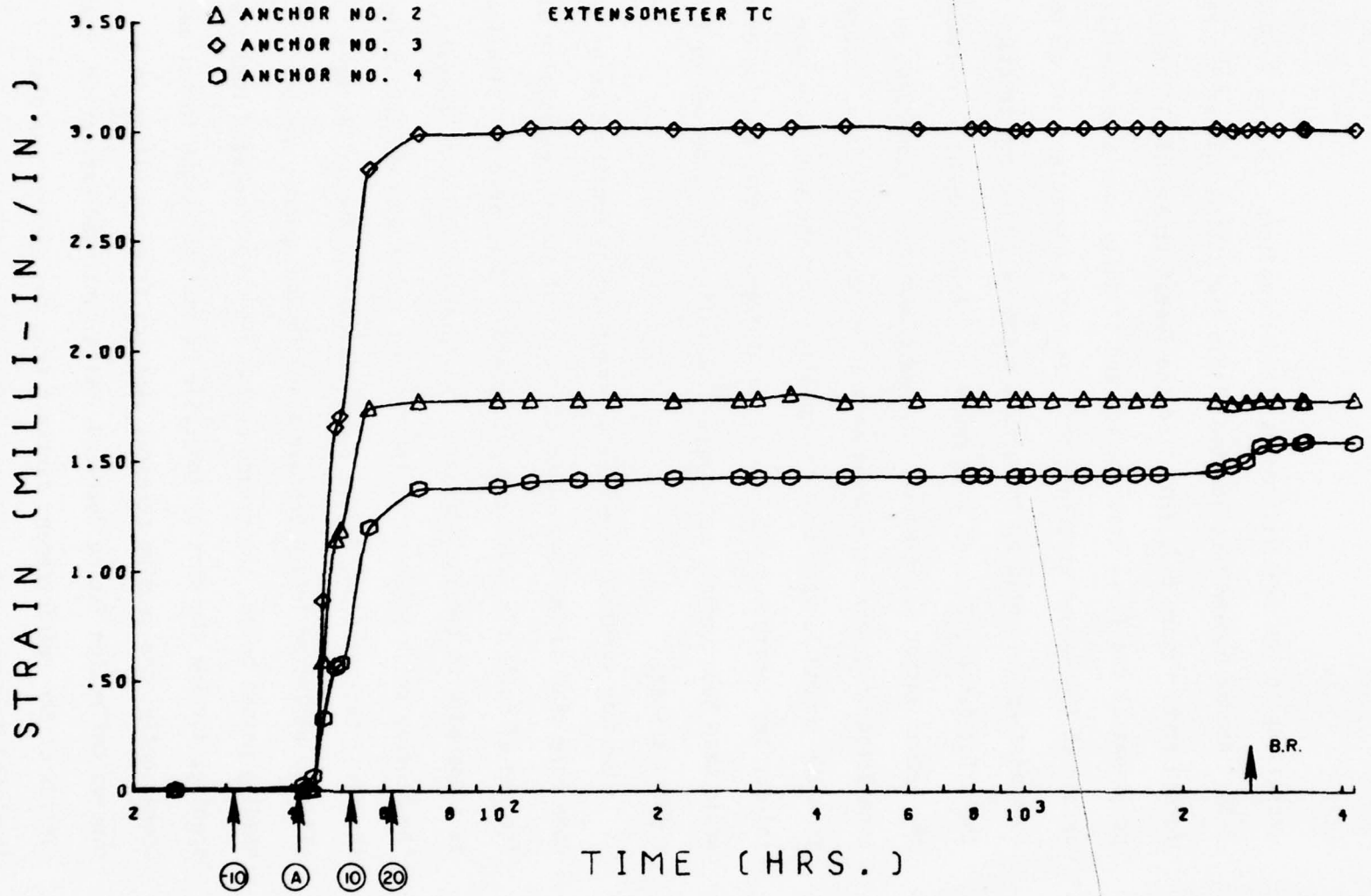

FIG. 2-30. Strain History, Main Bore Test Station No. 2, Extensometer TC (MPBX-TC)

increasing in the same fashion as the deformations, Figures 2-28 and 2-30. Anchor number two, located within the bottom half of the reinforced arch, Figure 2-3, exhibited the lowest strain of all anchor positions at the first test station and slightly more than the last anchor at the second station. This was not a characteristic of the rock mass as evidenced by the ground response during construction of the pilot tunnel, Figures 2-13 and 2-15. Reinforcement surrounding the second anchor had tied the rock mass together. Subsequent to excavation, the thin reinforced arch acted as a rigid body, separated from the ground farther from the opening. Had the arch been made thicker and continuous with longer reinforcement, that section of rock would have been largely self-supporting rather than a burden to the support system.

Bending stresses were more dominant during construction of the main bore than during excavation of the pilot tunnel, especially at the end of spile six, Figure 2-25. Overall, they were not significant as compared with tensile stresses. An interesting point, however, was the bending which occurred as the heading passed beneath the spiles at the first test station, Figure 2-23. Initially, the spiles were slightly deflected into a concave shape facing upward. As the heading passed below, the ground behind the face displaced into the opening, forcing the part of the spile nearest the crown to follow. Consequently, the bending stresses went positive, resulting in a concave deflection facing downward. With continued excavation, that portion of the reinforcement farthest from the opening was also displaced downward, returning the spile close to its original shape.

Instrumented spiles recorded strain increases long before the

excavation passed below. The first observed response, as the top heading approached, was approximately 10 feet from the initial position, or one radius ahead. This is shown in Figure 2-32.

Basically, the relationship of the rock mass and spile strains upon excavation was in principle the same as previously described for the pilot tunnel. Close to the opening, Figures 2-31 and 2-32, the net gain in spile strain after the instantaneous increase and subsequent relaxation was negative. It was difficult to assess the influence of the large differences between rock mass and spile strains, since there was no method to account for the effect of the support system. After a new stable equilibrium was established, the contribution of the reinforcement system nearest the opening was unknown.

Farther from the opening, the response of the reinforcement to ground deformation was positive, Figures 2-33 and 2-34. Both comparisons displayed a closer correlation than observed in the results from the pilot tunnel. At this location, rock mass and spile strains differed by an average factor of four.

Long term creep rates (80 to 4,000 hrs.) of the rock mass were similar to that of the spiles. Although the measured strain increase at the second test station was small, the comparison was good. The fact that the reinforcement system continued to take load in the long term indicated some degree of continuity with the surrounding rock mass.

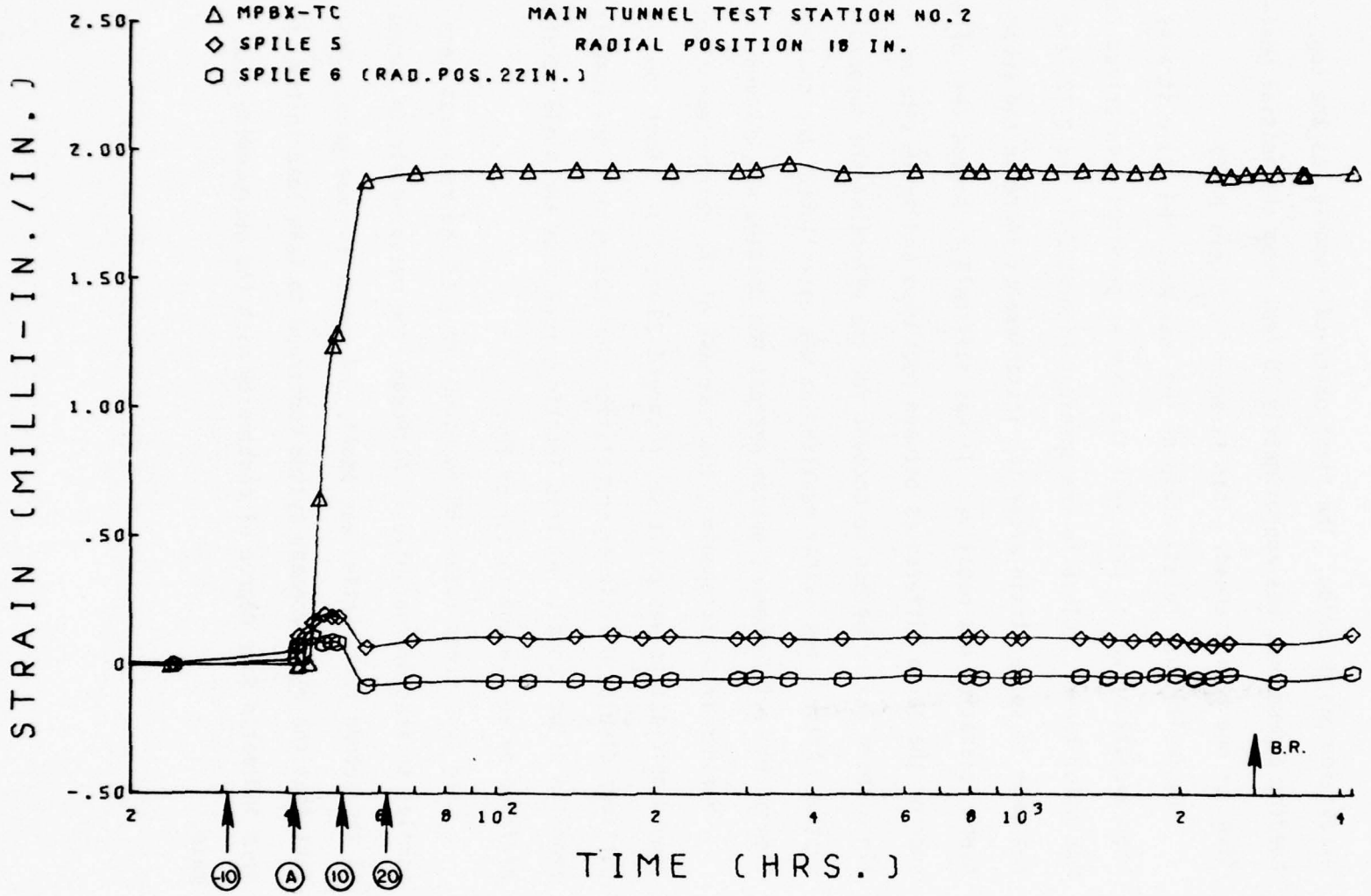

FIG. 2-31. Strain History Comparison: Instrumented Spiles and Extensometer, Main Bore Test Station No. 2, Radial Position 18 in.

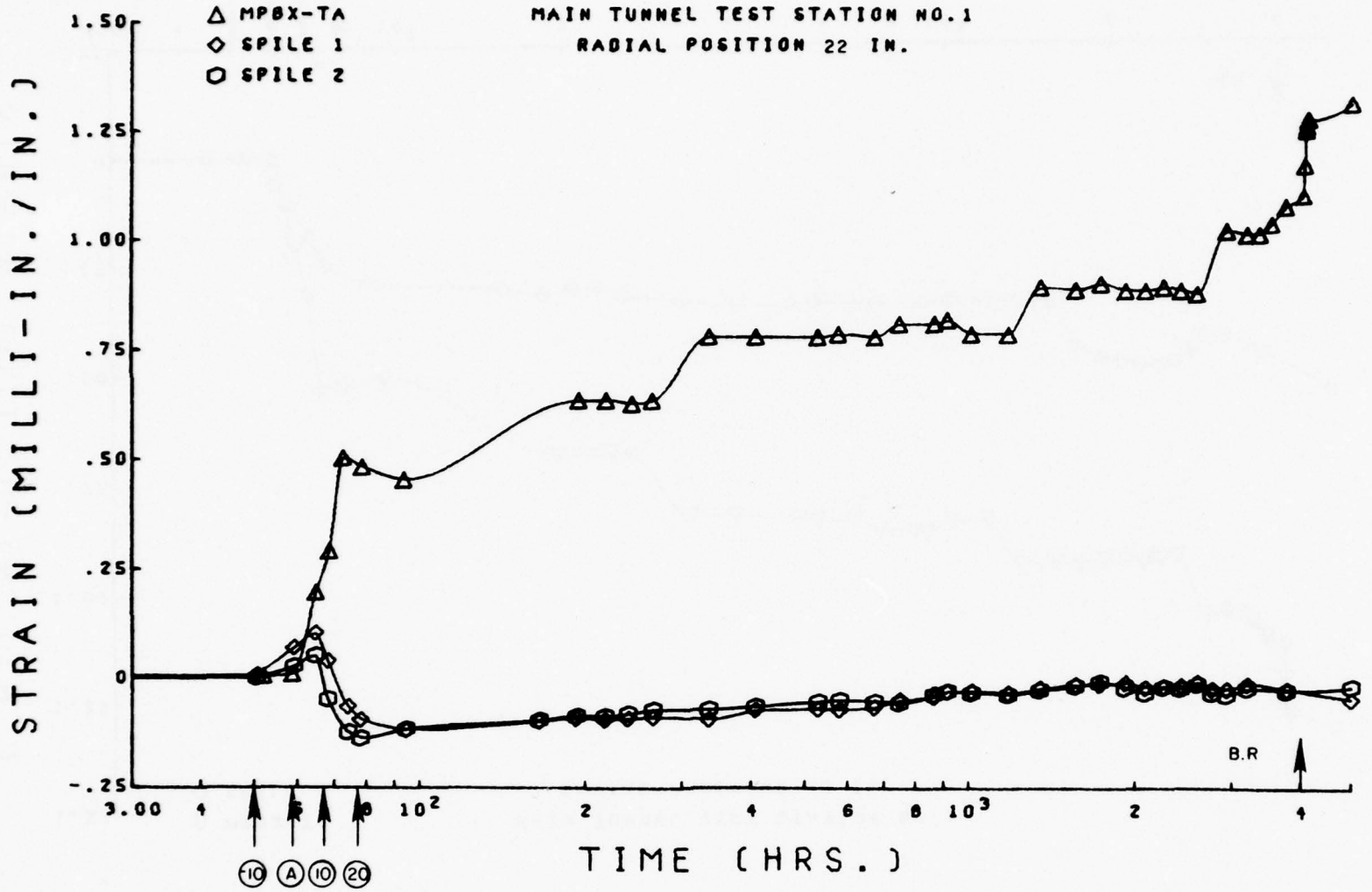

FIG. 2-32. Strain History Comparison: Instrumented Spiles and Extensometer, Main Bore Test Station No. 1, Radial Position 22 in.

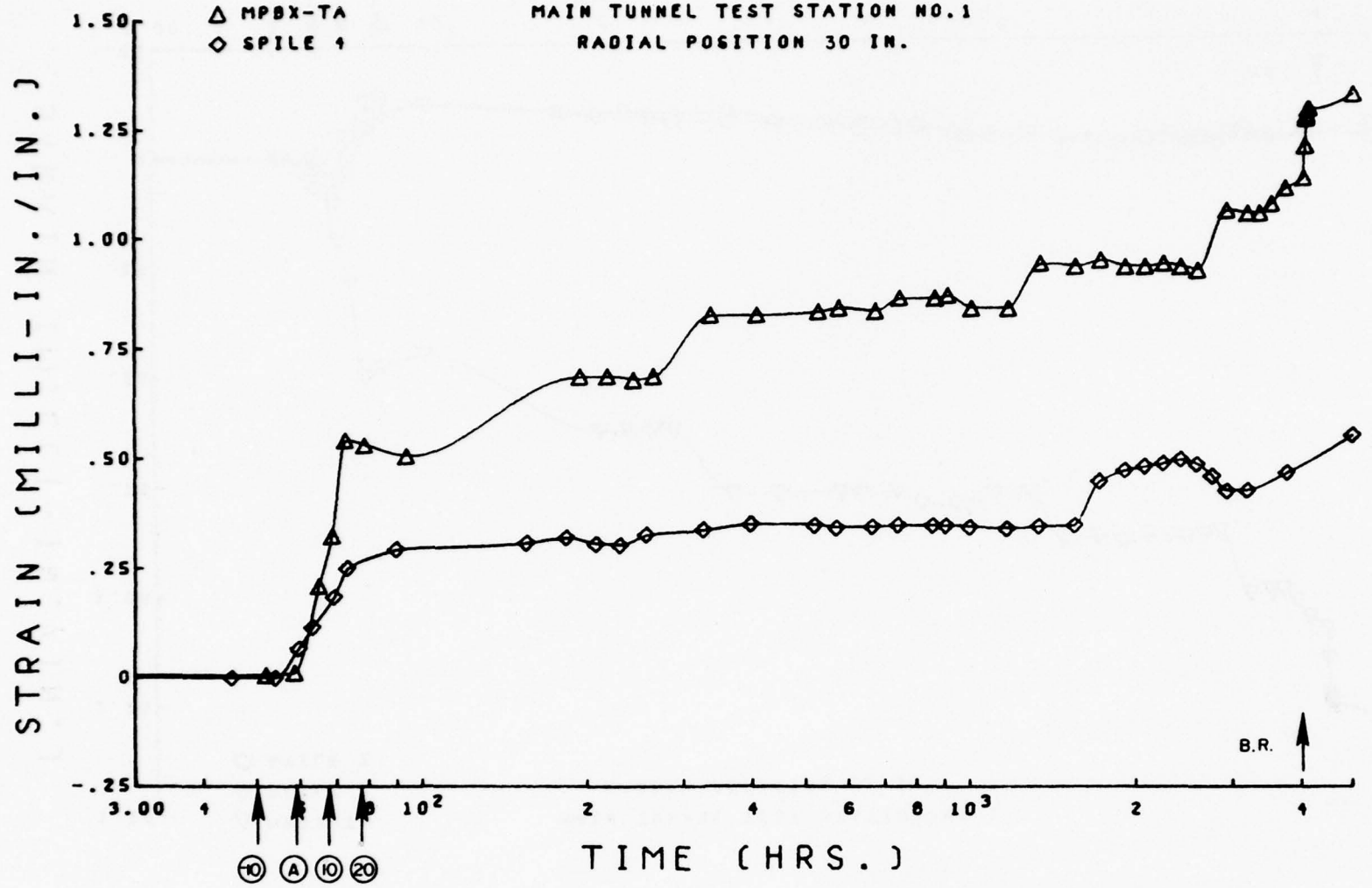

FIG. 2-33. Strain History Comparison: Instrumented Spiles and Extensometer, Main Bore Test Station No. 1, Radial Position 30 in.

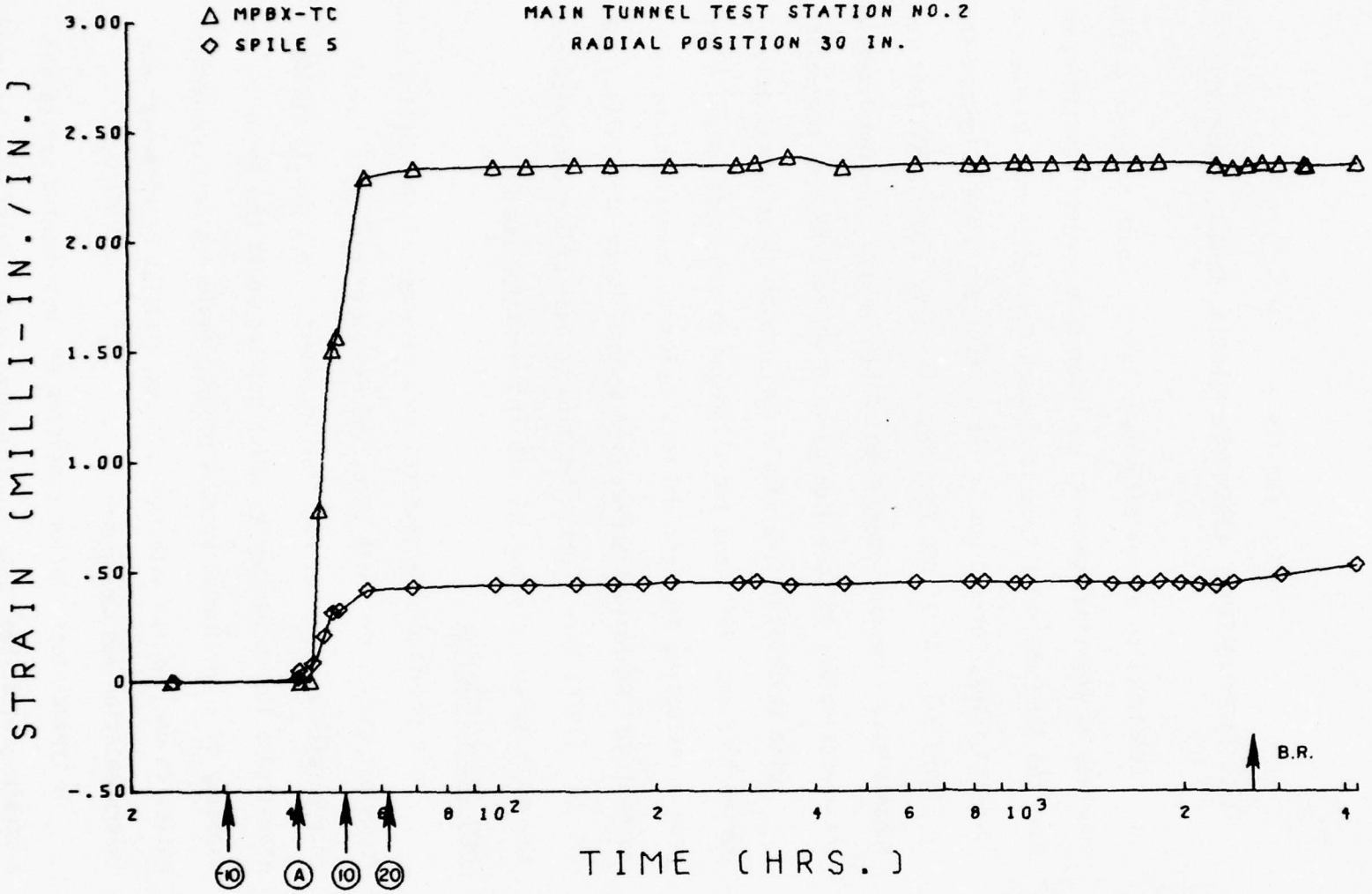

FIG. 2-34. Strain History Comparison: Instrumented Spiles and Extensometer, Main Bore Test Station No. 2, Radial Position 30 in.

CHAPTER 3

FIELD INVESTIGATION: EISENHOWER MEMORIAL TUNNEL, SOUTH BORE

Construction of the Eisenhower Tunnel, south bore, is presently underway as the final phase of an interstate project consisting of dual two lane vehicular tunnels through the Continental Divide. A location study, carried out in 1960, resulted in the alignment shown in Figure 3-1. At 11,000 feet above sea level, the 8,900 foot long tunnels have a maximum overburden of 1,450 feet. Opening dimensions are approximately 46 feet wide by 40 to 45 feet high as excavated.

Site exploration included a full length pilot tunnel driven during 1963 and 1964 along the alignment of the south bore. A program of extensive geologic and rock mechanics investigations were carried out (Geological Survey Professional Paper 815, 1974). Hooper, et. al., (1972) have given a detailed account of the construction of the north bore, including the use of prereinforcement.

Test Station Design

As a result of the observed effectiveness of the spiling reinforcement within the north bore, the design of the south tunnel incorporated a system of rock reinforcement. In order to further investigate the mechanisms by which spiling works and to verify the capacity of a reinforced arch, a program employing instrumented spiles in conjunction with the Colorado Division of Highways' own instrumentation was devised.

A typical test station consisted of instrumented spiles and a strain gauged steel set. Instrumented radial bolts were added in the most difficult ground, Figure 3-2. The instrumented spiles were

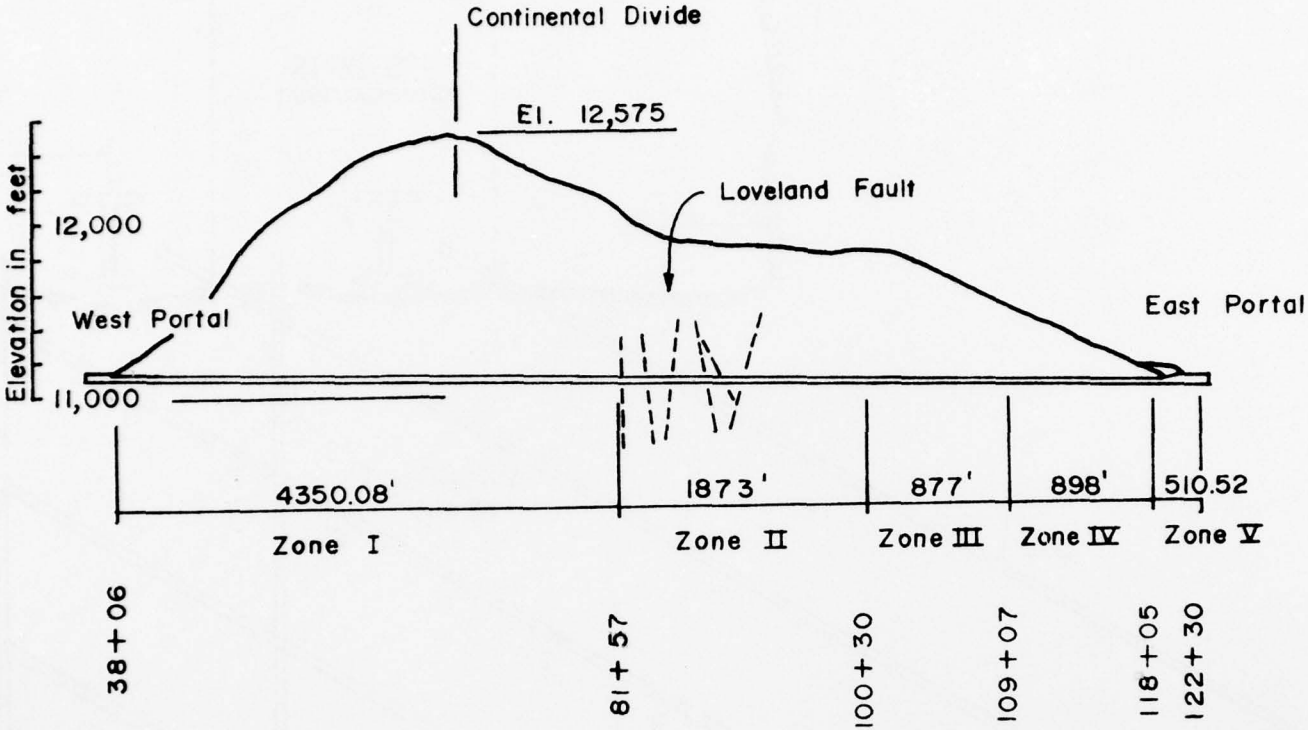

FIG. 3-1. Profile of Eisenhower Tunnel, Second Bore, Denver, Colorado (Hopper et. al., 1972)

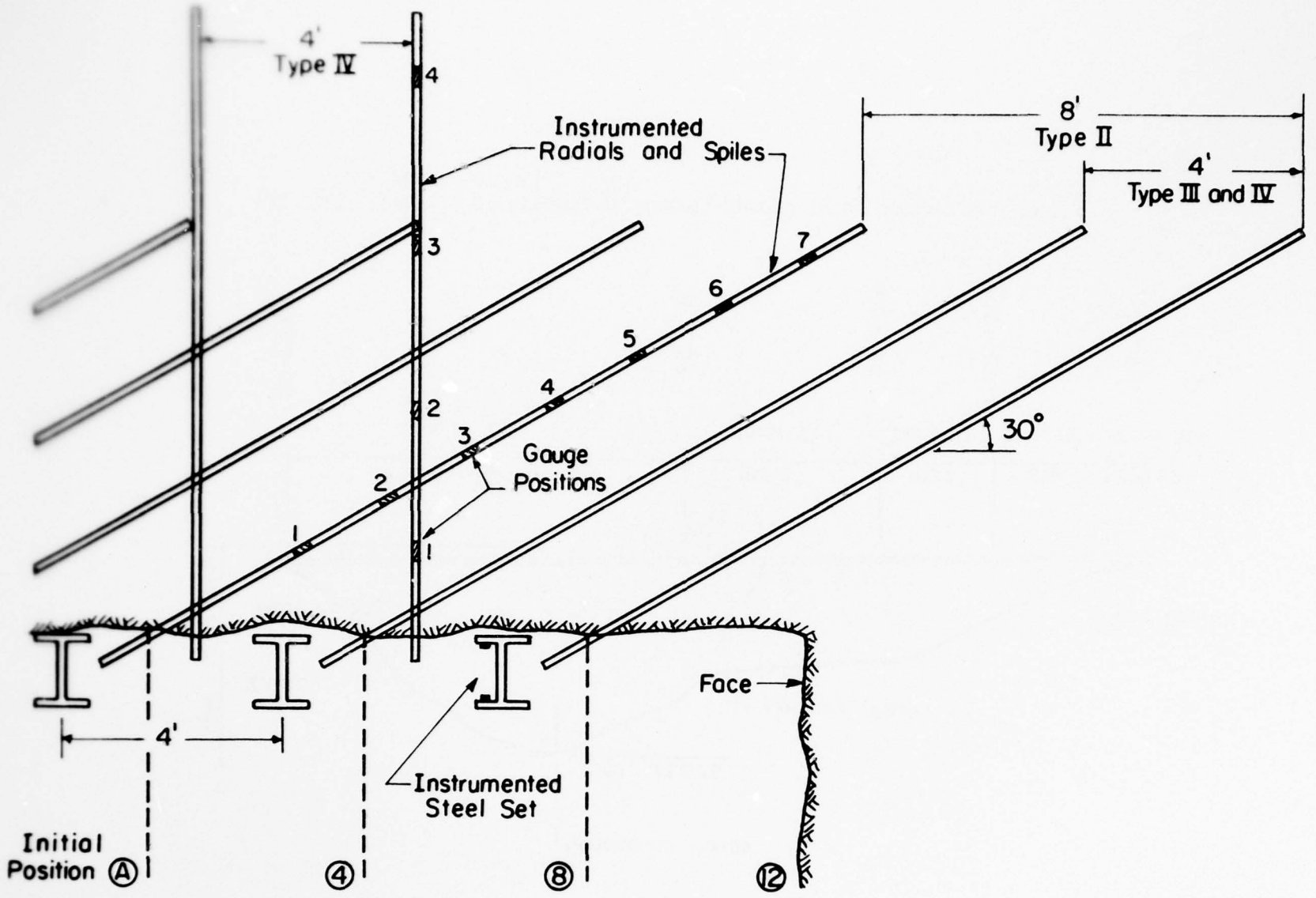

FIG. 3-2. Profile of Test Station Instrumentation Layout

designed, constructed, and installed as described in Appendix 1 and the previous chapter. When oriented properly, spiles were designed to measure axial and axial plus bending strains. Instrumented radial bolts were constructed in the same manner as spiles designed to record axial strains. Typical gauge layouts employed on the number eleven reinforcing bar are sketched in Figure 3-3. An installed instrumented spile with readout cable attached is pictured in Figure 3-4, while the readout system is illustrated in Figure 3-5.

Steel sets instrumented with weldable strain gauges on the inside of the top and bottom flanges at nine positions around the section were used to assess the support loads. In particular, the four gauges nearest the spring line were averaged to obtain the vertical rock load. The instrumented set was placed under the cover of the instrumented spiles as shown in Figure 3-2. Consequently, the response of the reinforcement-support system was monitored simultaneously. After placement of the first stage concrete liner, the strain gauges continued to provide information on the long term behavior of the composite support system.

As a result of the extensive geologic information derived from the pilot tunnel and north bore of the Eisenhower Tunnel, it was possible to identify the location of various ground types prior to construction of the south bore. This provided the opportunity to install and monitor several test stations in ground ranging from slightly blocky rock to that exhibiting squeezing behavior. A total of six stations were established in the top heading driven from the west portal, Zone I of Figure 3-1.

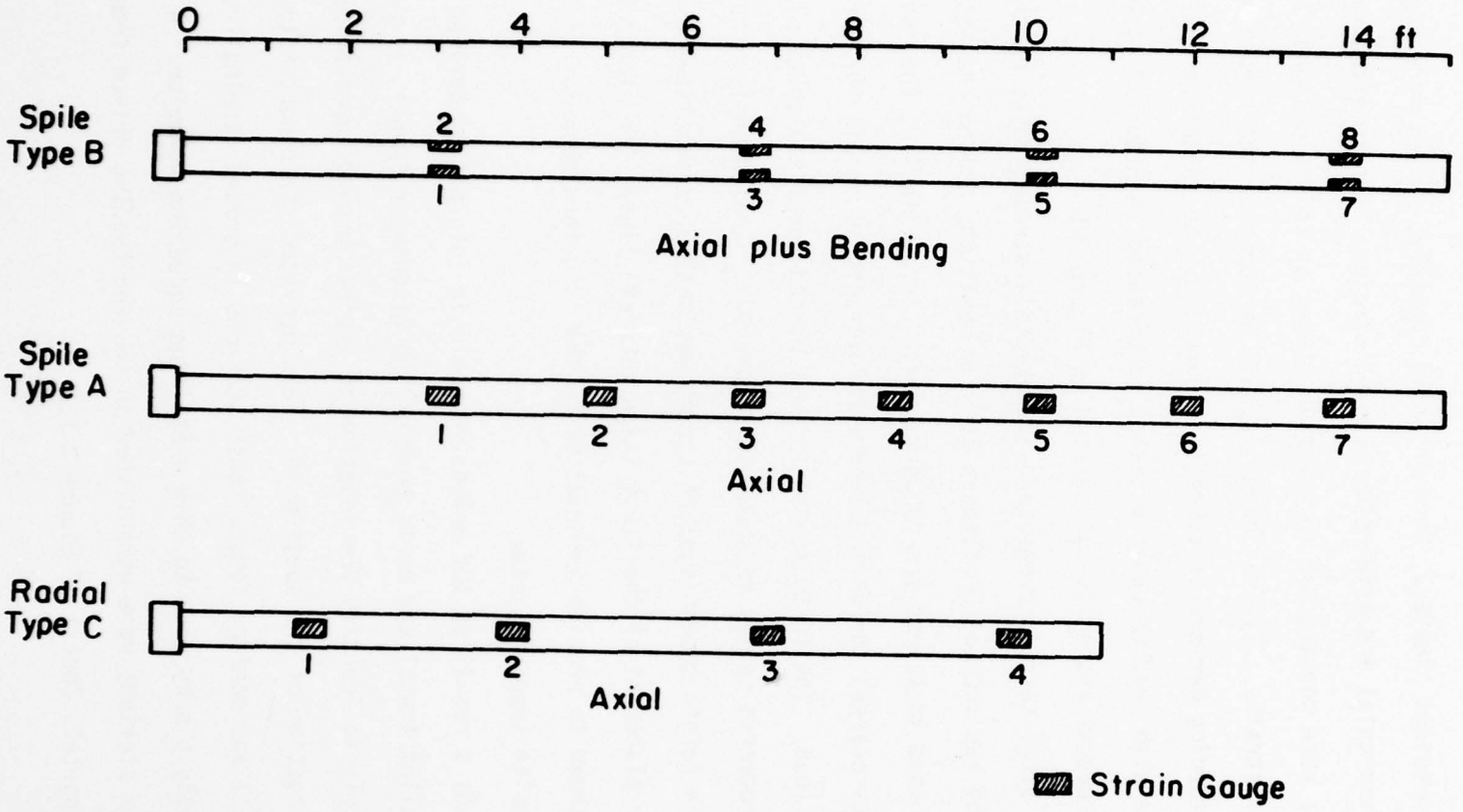

FIG. 3-3. Instrumented Reinforcement Bar Type and Strain Gauge Positions

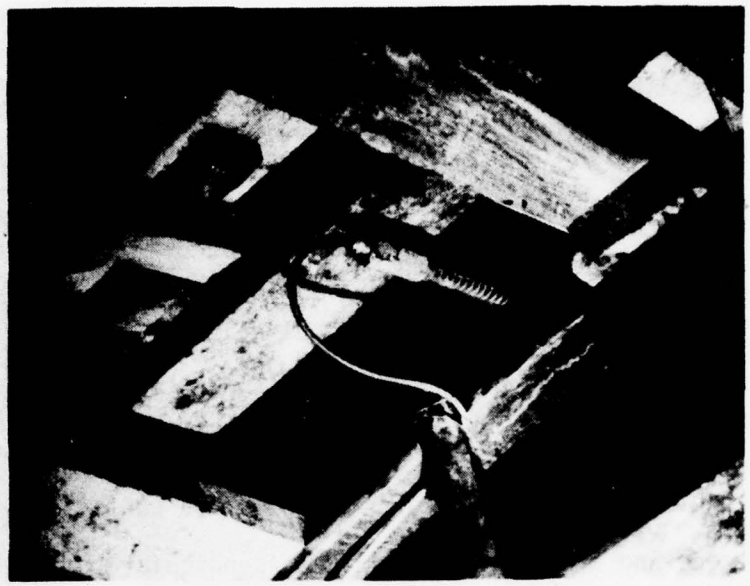

FIG. 3-4. Installed Instrumented Spile with Readout Cable Attached

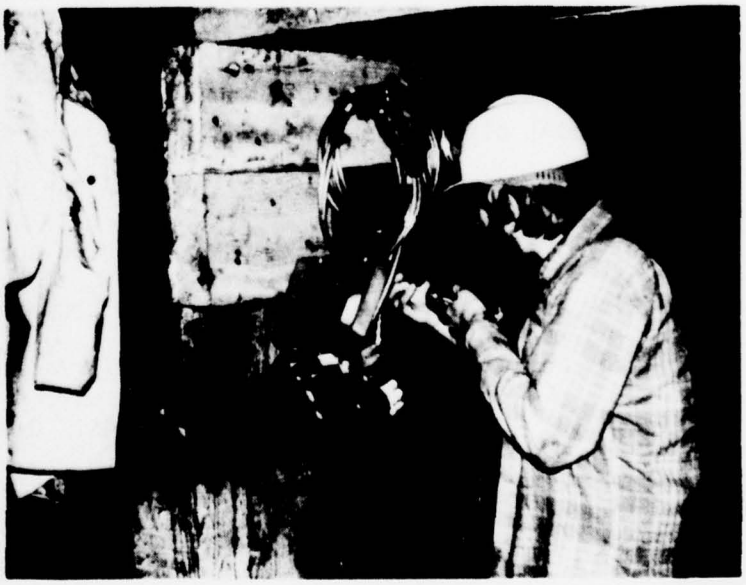

FIG. 3-5. Readout Instrumentation System

Geology

The Eisenhower Tunnels are located in the Rocky Mountains, at the crest of the Front Range. Structurally, the region is complex and consists primarily of Precambrian granitic and metasedimentary rocks. Deformation during Precambrian and Tertiary times was extensive, resulting in numerous shears and faults. The major structural feature in the area under consideration is the two mile wide Loveland Pass-Berthoud Pass shear zone, related to the Loveland Pass fault at its southern extension. Both tunnnels are contained within this shear zone and are oriented nearly perpendicular to it. As shown in the general profile, Figure 3-1, the Loveland fault is encountered at mid-length with more than 900 feet of vertical cover.

Ground conditions along the tunnel alignment are extremely varied, from massive granite to wide zones of squeezing fault gouge. In general, conditions improved with distance from the Loveland fault; however, major shears were encountered throughout the tunnel.

Rock mass classification was based on joint spacing and degree of alteration. Four rock classes, given in Table 3-I, were specified (Post, 1973). Each class was divided into two subcategories, a and b, indicative of the rock quality within each group. An estimate of rock loads on internal supports, based on Terzaghi (1946), was tabulated for comparison with measured loads. Dimensions incorporated in the formulation were that of the top heading, width (B) of 46 feet, and height (H_t) of 23 feet.

TABLE 3-I

Rock Class Descriptions and Predicted Rock Load

Rock Class [1]	Description [1,2]	Rock Load H_p (feet) [2]
Ia	Massive to slightly blocky, having a joint spacing of greater than 1.0 feet with no alteration.	0 to .25B
Ib		0 - 12 ft.
IIa	Moderately blocky and seamy having a joint spacing greater than 0.5 feet with little or no alteration.	.13 B to .35 $(B + H_t)$
IIb		6 - 25 ft.
IIIa	Very blocky and seamy, having a joint spacing less than 1.0 feet, moderately to highly altered with zones of moderate to intense shearing.	(.18 to 1.10) $(B + H_t)$
IIIb		12 - 76 ft.
IVa	Squeezing (low to moderate) ground, highly crushed and altered, non-plastic, abundant clay, joint spacing less than 0.5 ft.	(1.10 to 2.10) $(B + H_t)$
		76 - 145 ft.
IVb	Squeezing (moderate to high) and swelling, plastic highly altered, mainly clay gouge.	(2.10 to 4.50) $(B + H_t)$
		145 - 311 ft.

B, Width of Top Heading = 2 H_t, Height = 46 ft.

([1]From Post, 1973 & [2]Terzaghi, 1946)

Tunnel Construction

Presently, two headings are being advanced simultaneously. From the east portal two foot drifts, one being the remined pilot tunnel, and a crown drift were driven through Zone II, Figure 3-1. After placing reinforcement from the foot drifts, they were backfilled with concrete. Ground within the perimeter of the drifts will be removed by top heading and bench. Spiling reinforcement is planned for the stabilization of ground between drifts.

In the main gouge zone of the Loveland Fault, a series of stack drifts will be excavated and backfilled with concrete until the entire arch and sidewalls are constructed prior to removal of the central core.

From the west portal, excavation throughout Zone I was by top heading and bench. Rounds within the top heading were between four and eight feet long. Spiling reinforcement with the pattern shown in Figure 3-6b was required in all Type III and IV ground. Radial bolts were an added requirement in Type IV rock. Occasionally, a small stretch of included Type II ground was reinforced with the pattern shown in Figure 3-6a. Spiles were 16 foot long and radial bolts 12 foot long number eleven reinforcing bars. Using percussive drills mounted on the jumbo, the reinforcement was placed in pre-drilled holes filled with bags of polyester resin. With the exception of occasional problems in filling the entire hole with the resin grout, the installation of reinforcement went smoothly and rapidly.

In addition to reinforcement, the support system within the top heading consisted of steel sets spaced on four foot centers and a first stage concrete liner (F.S.L.). Set members were W14 x 61,

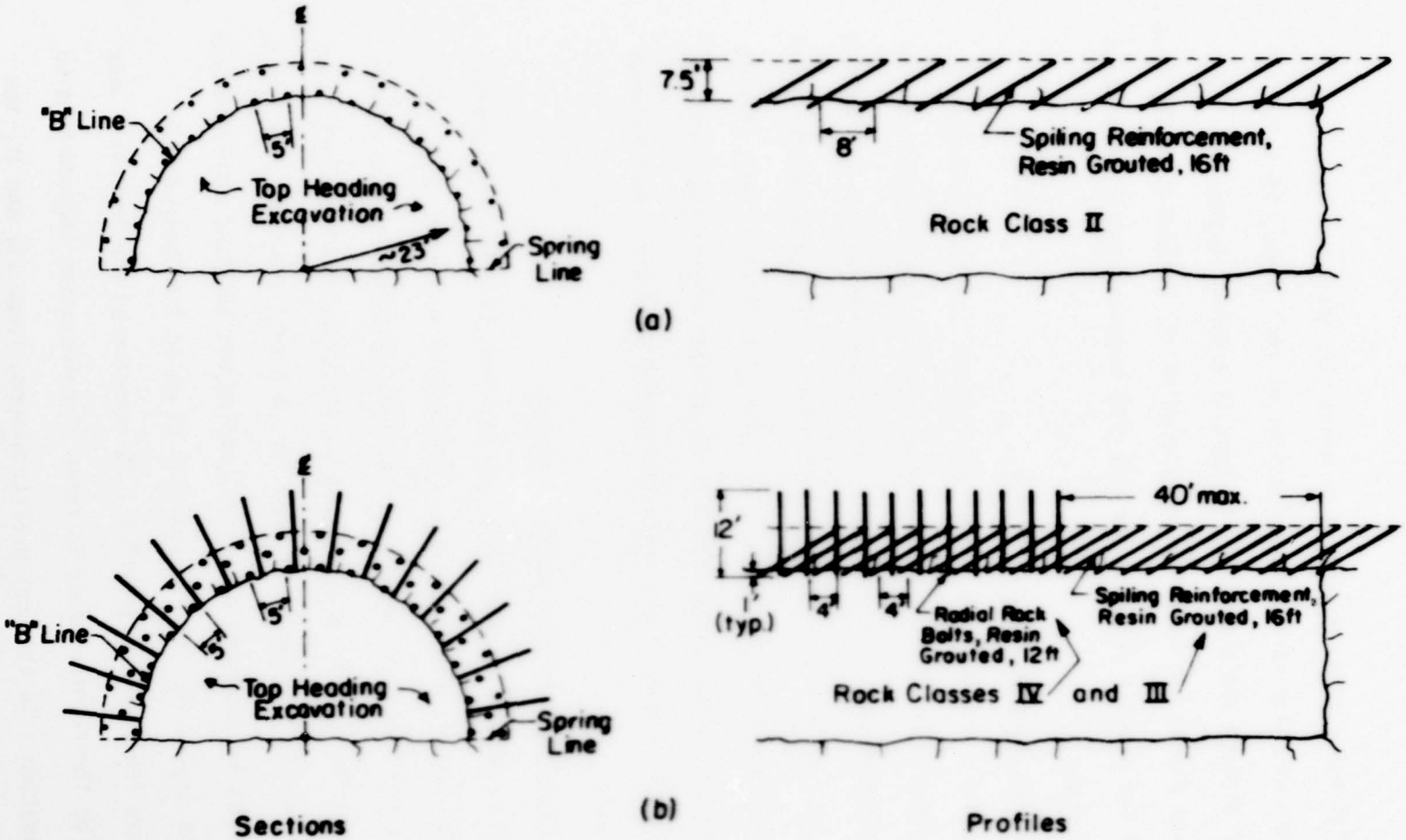

FIG. 3-6. Section and Profile of Rock Reinforcement, a) Rock Class II and b) Rock Classes III & IV

95 or 136 pound steel depending on ground conditions. Liner thickness was also varied as a function of rock class, 14 in. in Types I through III and 20 in. in Type IV ground. Typically, the liner was placed one month after excavation and contact grouting (C.G.) between the outside of the liner and rock occurred roughly one month after lining.

Test Station Results and Discussion

Six test stations consisting of from one to five instrumented reinforcement bars and an instrumented steel set were established in ground ranging from Type Ib to IVa, as defined in Table 3-I. Details related to rock class, number of instrumented bars, and reinforcement spacing are presented in Table 3-II. The rock class of each station is listed in a range to account for the variability of the rock mass. Even over the length of one spile the ground conditions could change considerably.

a. Rock Mass-Reinforcement System Behavior

Each of the 18 instrumented bars had from four to eight operating strain gauges, resulting in a considerable volume of data. To summarize the important aspects of the reinforcement behavior, three radial distributions of axial stress at different times and positions of the advancing face were obtained for each test station. The first distribution was produced after the heading was advanced approximately eight feet beyond the initial position at which the instrumented spiles were installed, Figure 3-2. It represented the immediate peak response of the reinforcement in terms of deformation induced tension upon excavation. In the poor quality ground, Types III and IV, the eight foot advance was made in two rounds.

TABLE 3-II

Instrumented Reinforcement Test Station Specifications

Test Station	Rock Class	Date Installed	Number of Instrumented Bars		Reinforcement Spacing (FT.)		
					Axial	Circumferential	
			Spiles	Radials		Spiles	Radials
58 + 86	Ib - IIa	9-15-76	1	-	-	-	-
63 + 01	IIIb-IVa	10-19-76	3	2	4	2.5	5
70 + 14	IIb -IIIa	12-27-76	2	-	4	5	-
72 + 36	IIIb-IVa	1-20-77	3	2	4	2.5	5
73 + 42	Ib-IIb	2-02-77	2	-	8	5	-
80 + 87	IIIa-IIIb	3-23-77	3	-	4	2.5	-

With continued advancement of the heading, a certain degree of stress relaxation occurred within the reinforcement. The magnitude of the relaxation was strongly dependent on the ground type. In any case, the majority had taken place by the time the face had advanced 50 feet from the initial position. A second distribution was obtained at this point. The final distribution was derived from the last set of data acquired from each test station. It represented the long term behavior of the reinforced rock mass.

Radial stress distributions were derived from the reinforcement stress histories as described and illustrated in Appendix 5. The stress history plot of each strain gauge is arranged by test station, bar number, and radial position in Appendix 7. A plot of the average vertical stress history of the instrumented steel set and a sketch of the specific geology and instrumentation location are also included for each station (Appendix 7).

Consider the set of radial stress distributions shown in Figure 3-7. Station 58+86 was established in competent ground of slightly to moderately blocky rock. Only one spile, the instrumented spile, was installed at this site to test a new design of strain gauge. Since there was no system of reinforcement, the instrumented spile was basically monitoring the rock mass behavior. In this type of ground, however, the reinforcement would be widely spaced. Consequently, the influence of a reinforcement system would not significantly alter the observed stress distributions.

The changing shape of the distribution curves as characterized by the position and magnitude of the peak and inflection point provided considerable insight into the rock mass-reinforcement behavior.

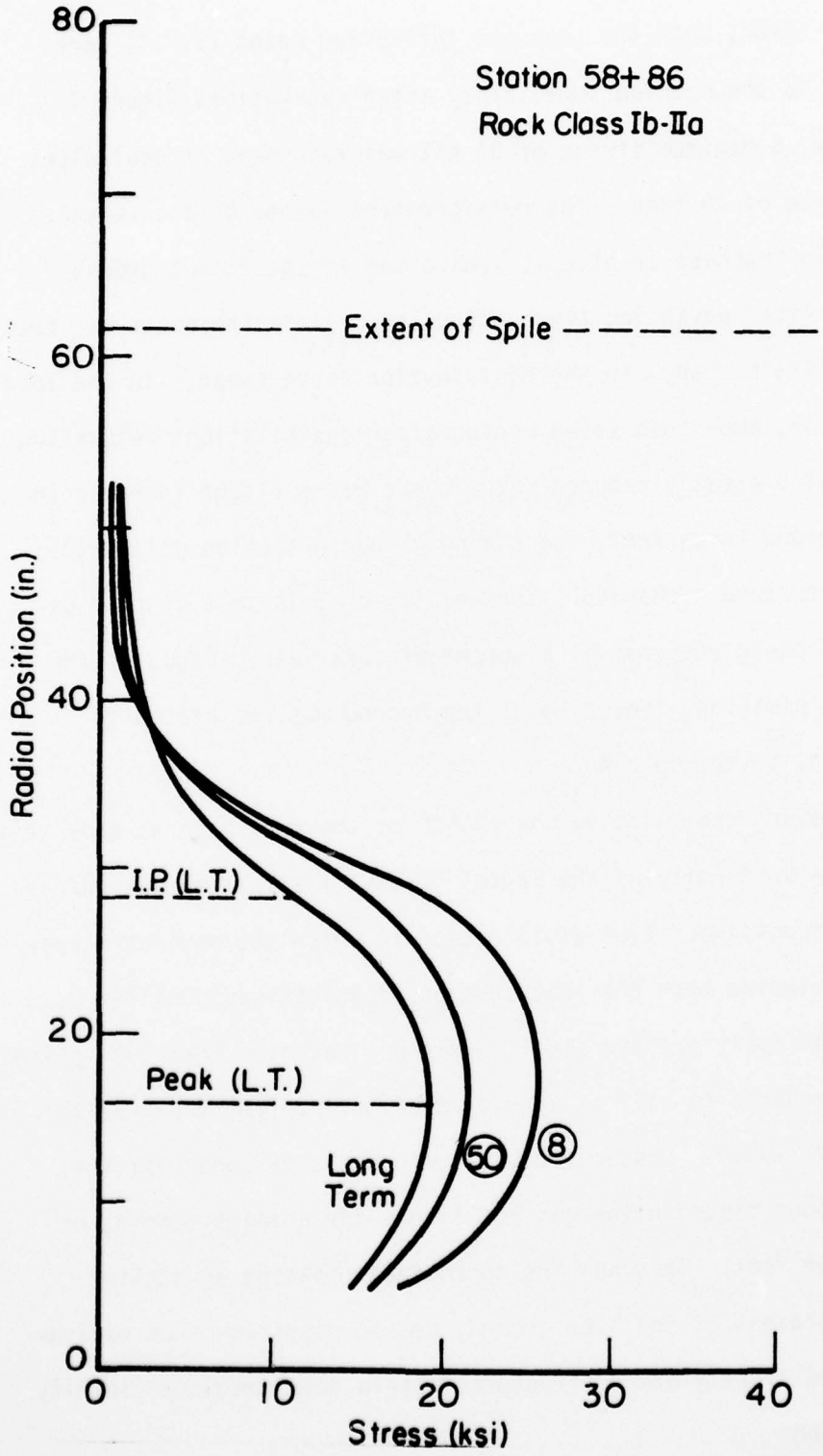

FIG. 3-7. Test Station 58+86, Radial Stress Distribution Comparison: 8 ft. Advance, 50 ft. Advance, and Long Term (summary of Fig. A5-8 to 10)

At station 58+86, both the peak and inflection point (I.P.), were very close to the opening immediately after excavation, Figure 3-7. At the peak, a maximum stress of 26 KSI was recorded, an equivalent tensile force of 20 tons. The reinforcement beyond 40 in. revealed a negligible increase in stress, indicating insignificant ground activity. After advancing the heading some relaxation occurred, but there was little change in the distribution curve shape. In the long term behavior, more than seven months after installation, relaxation continued at a greatly reduced rate, there was a slight increase in activity beyond three feet, and the peak and inflection point radial positions remained unchanged. The results of this test station exhibited the basic response of a competent rock mass. Based on the peak stress position, loosening of the ground was restricted to within 16 in. of the opening.

Considering the relative competence of the rock mass at this test station, the uniformity of the radial stress distribution was unforeseen. A discontinuous type distribution in which the maximum stress positions coincide with the intersection of joints was considered. Pull tests on fully grouted steel dowels has revealed that the applied stress was reduced to half at approximately 6 in. from the free surface (Dunham, 1976). Consequently, on the basis of superposition, a discontinuous distribution was not likely for a joint spacing of less than one foot. This was the approximate spacing at station 58+86. Regardless of the type ground, damage resulting from excavation produced closely spaced fractures within the immediate vicinity of the opening.

Compared to the previously described test station, station 73+42 was in ground of slightly lower quality. This was reflected by the shift in position of the peak and inflection point away from the opening, Figure 3-8, relative to that recorded at station 58+86. Although the pattern of the stress relaxation was similar, the peak stress recorded was greater and the ground activity beyond 40 in. from the opening was increased. There was also a small migration of the peak and inflection point away from the tunnel with advancement of the heading. This indicated a slight increase in rock mass deterioration, probably related to vibration during excavation. In the long term, the system continued to take load in a uniform manner, but without a noticeable shift in the peak and inflection point. Consequently, the rock mass-reinforcement system was in stable equilibrium. Loosening of the rock around the tunnel was limited to within 20 in. of the opening and significant ground activity to within 50 in.

Of the two instrumented spiles installed at station 70+14, only one survived for a few weeks. However, sufficient data was gathered to illustrate the increased ground activity away from the opening in this moderately to very blocky and seamy ground, Figure 3-9.

Basically, the characteristics of the previously discussed test stations were similar with small differences related to variations in rock quality (rock class Ib through IIIa). A major difference in rock mass-reinforcement response was observed for spiles installed within highly altered and sheared ground containing a significant proportion of clay (rock class IIIb-IVa). At the depths encountered, this rock mass exhibited a large component of creep deformation or squeezing behavior.

AD-A046 358 CALIFORNIA UNIV BERKELEY DEPT OF CIVIL ENGINEERING F/G 13/13
A FIELD STUDY OF SPILING REINFORCEMENT IN UNDERGROUND OPENINGS.(U)
JUN 77 G E KORBIN, T L BREKKE DACW45-74-C-0026

UNCLASSIFIED MRD-TR-1-77 NL

2 OF 3
ADA
046358

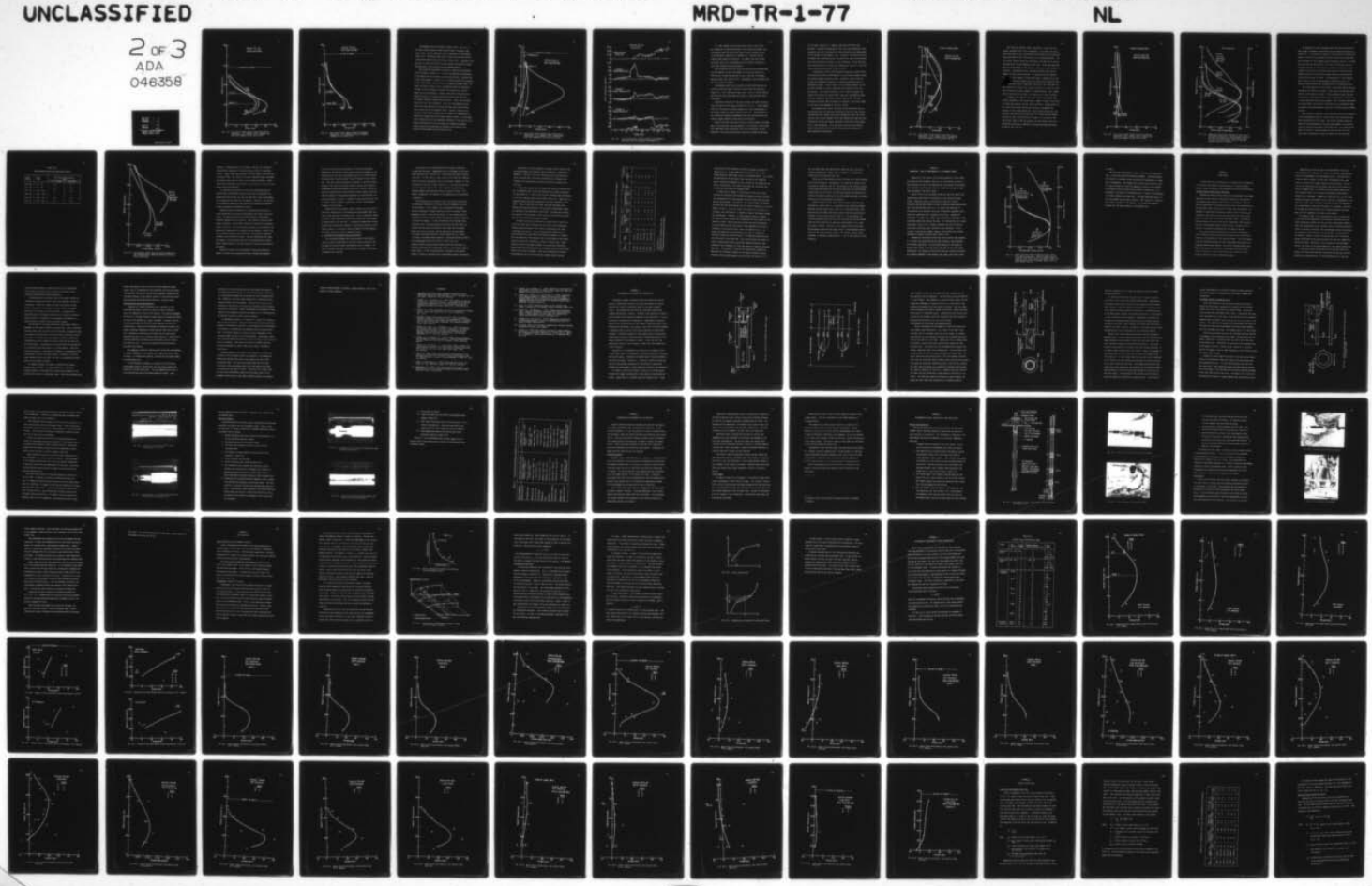

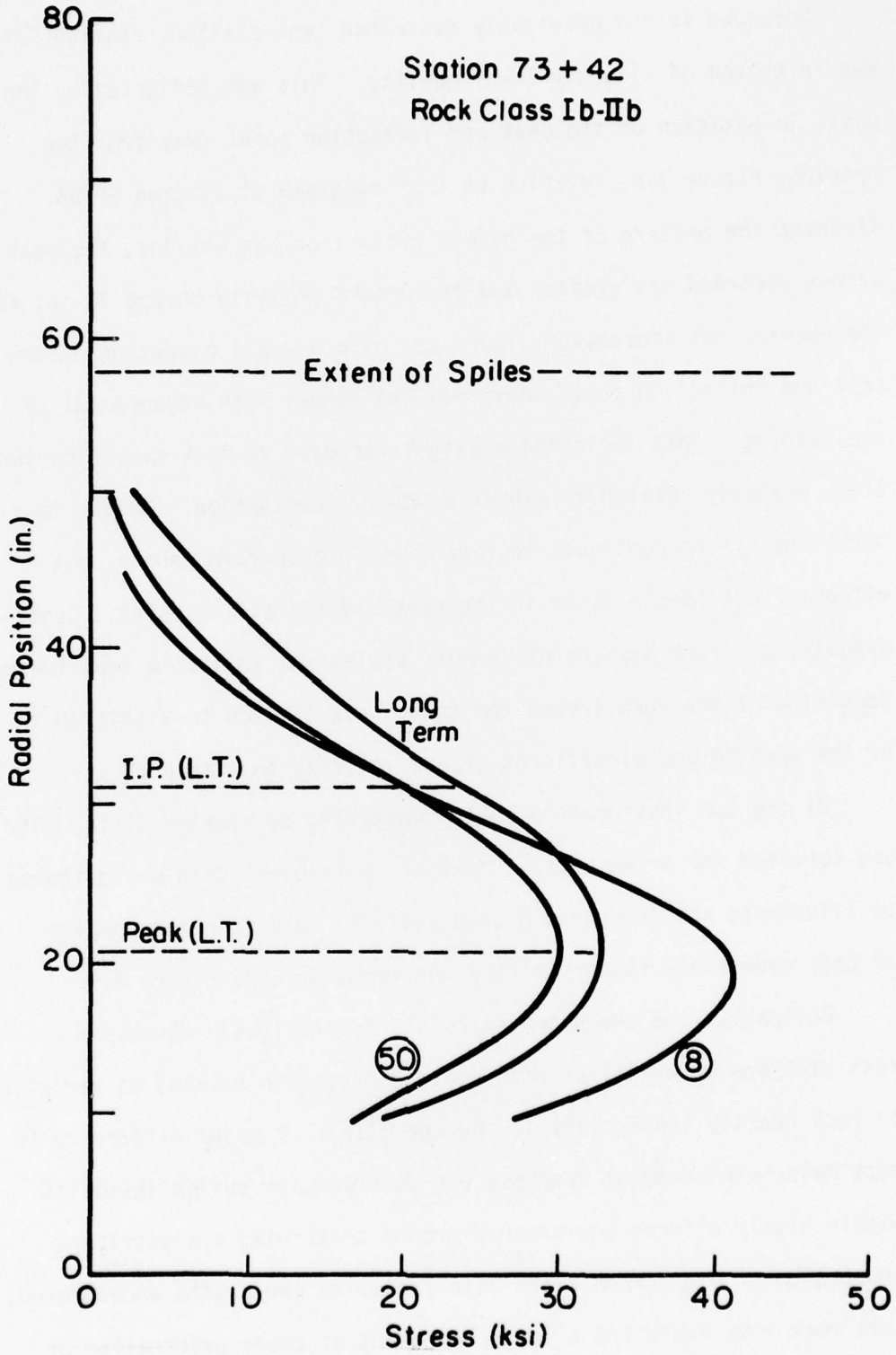

FIG. 3-8. Test Station 73+42, Radial Stress Distribution Comparison: 8 ft. Advance, 50 ft. Advance, and Long Term (summary of Fig. A5-22 to 24)

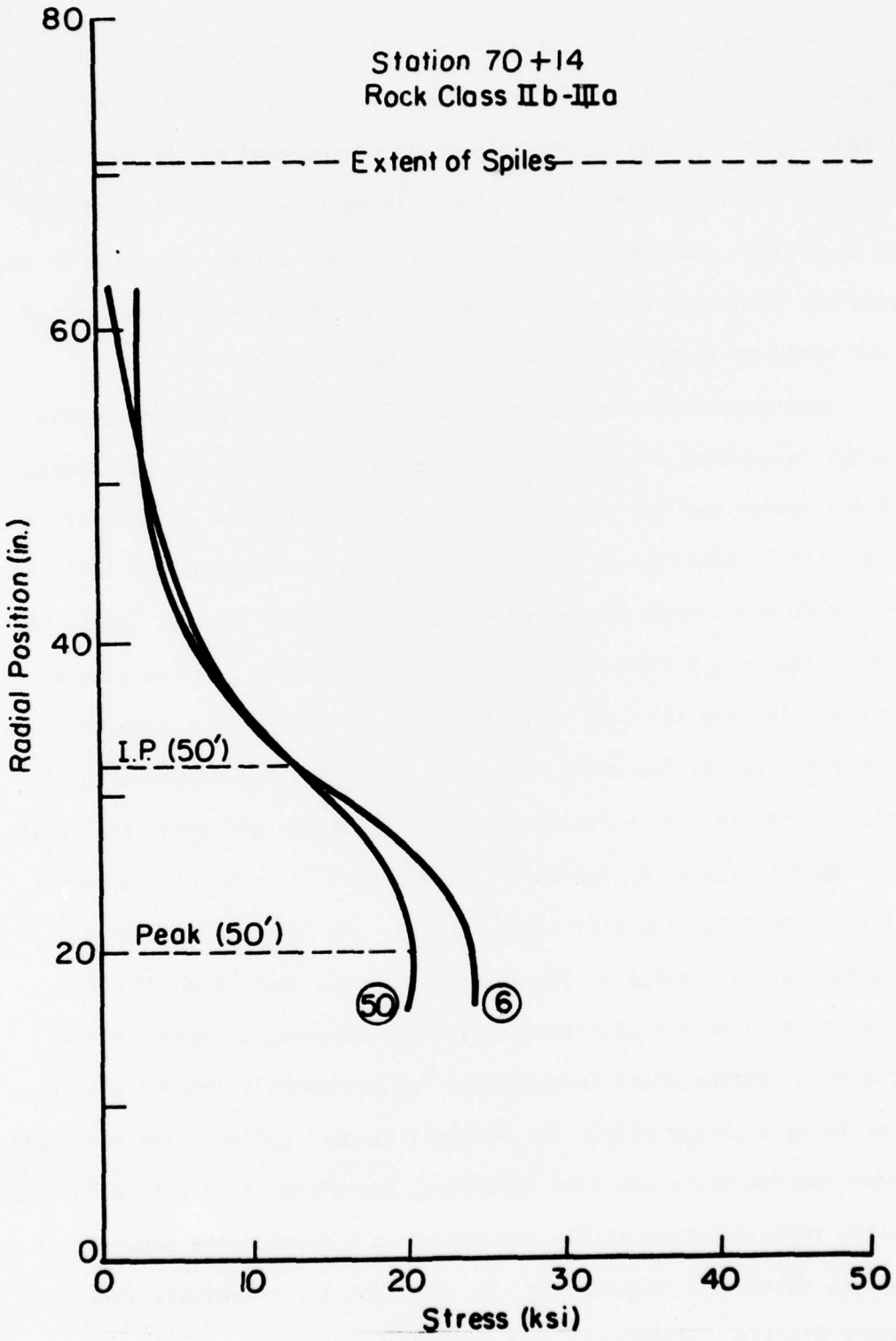

FIG. 3-9. Test Station 70+14, Radial Stress Distribution Comparison: 6 ft. Advance and 50 ft. Advance (summary of Fig. A5-15, 16)

Instrumented spiles installed at station 63+01, the first of two test stations placed in type IIIb-IVa ground, recorded a very large stress increase immediately after advancement of the heading, Figure 3-10. The average peak stress increase was more than 40 KSI, an equivalent tensile force of 30 tons in each spile. Location of the peak was at nearly three feet from the opening, considerably farther than observed in test stations in more competent ground.

Upon continued advancement of the face, there was considerable stress relaxation, Figure 3-10. Close to the opening the percentage of relaxation was not as great as at the peak position. Consider the excerpt from Appendix 7, Figure 3-11, to further examine the influence of the reinforcement stress relief on the measured support loads. As shown, the stress history of the instrumented steel set revealed an increase in load followed by a period of relaxation in a similar manner to the reinforcement. However, there was a time phase shift between the start of relaxation within the spiles and steel set, with the support lagging by approximately 40 hours. There are two major reasons for this time difference. First, the instrumented set was placed four feet ahead of the initial position, more than 24 hours after installing the instrumented spiles. Second, a change in the rock mass-reinforcement response was not necessarily immediately reflected by a change within the internal support system. The rock mass under consideration was time dependent, therefore it took time for the energy redistribution within the ground to influence the support system, especially considering the imperfect and relatively soft wooden blocking between the rock and steel set.

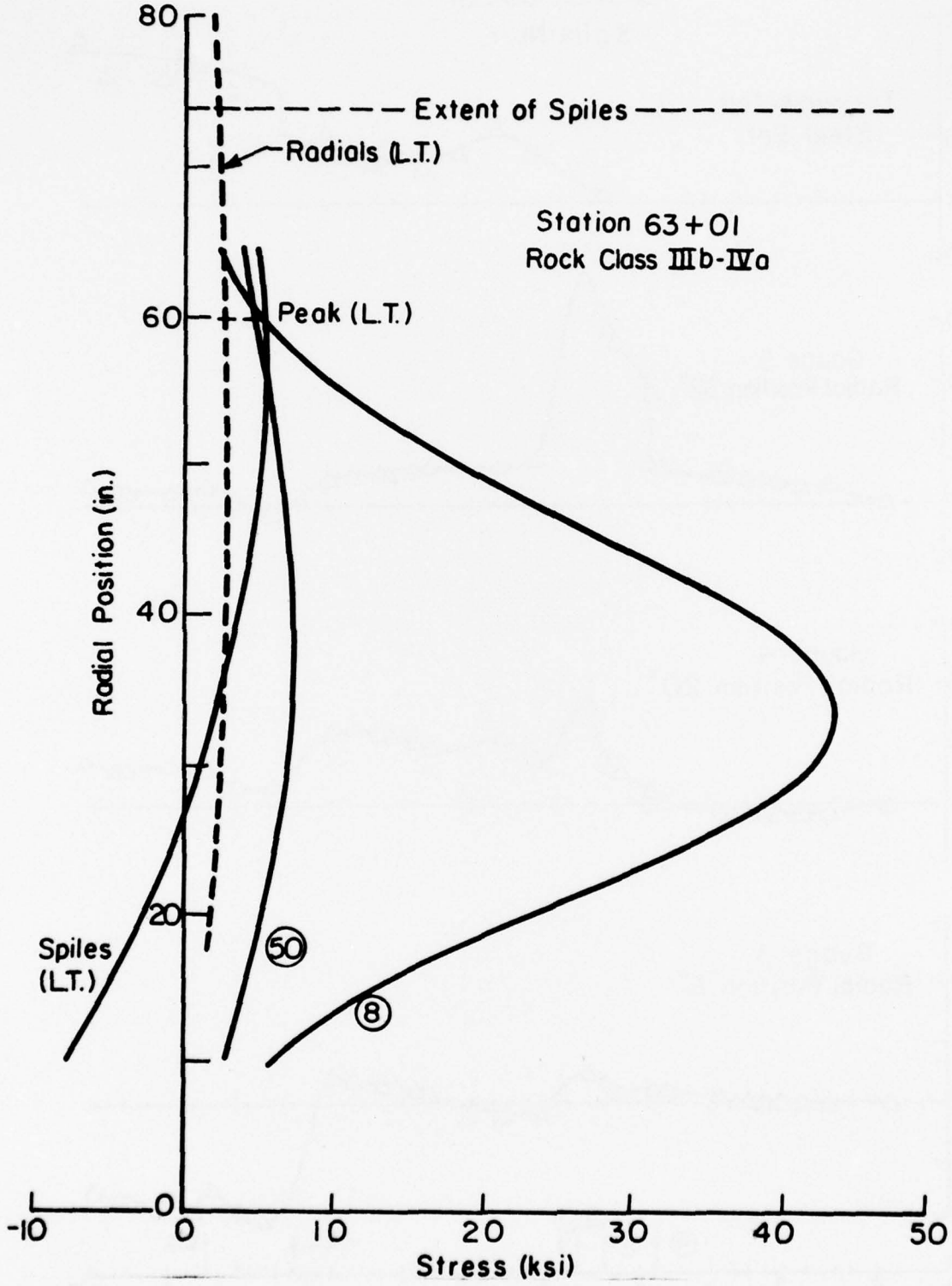

FIG. 3-10. Test Station 63+01, Radial Stress Distribution Comparison: 8 ft. Advance, 50 ft. Advance and Long Term (summary of Fig. A5-12 to 14, 28)

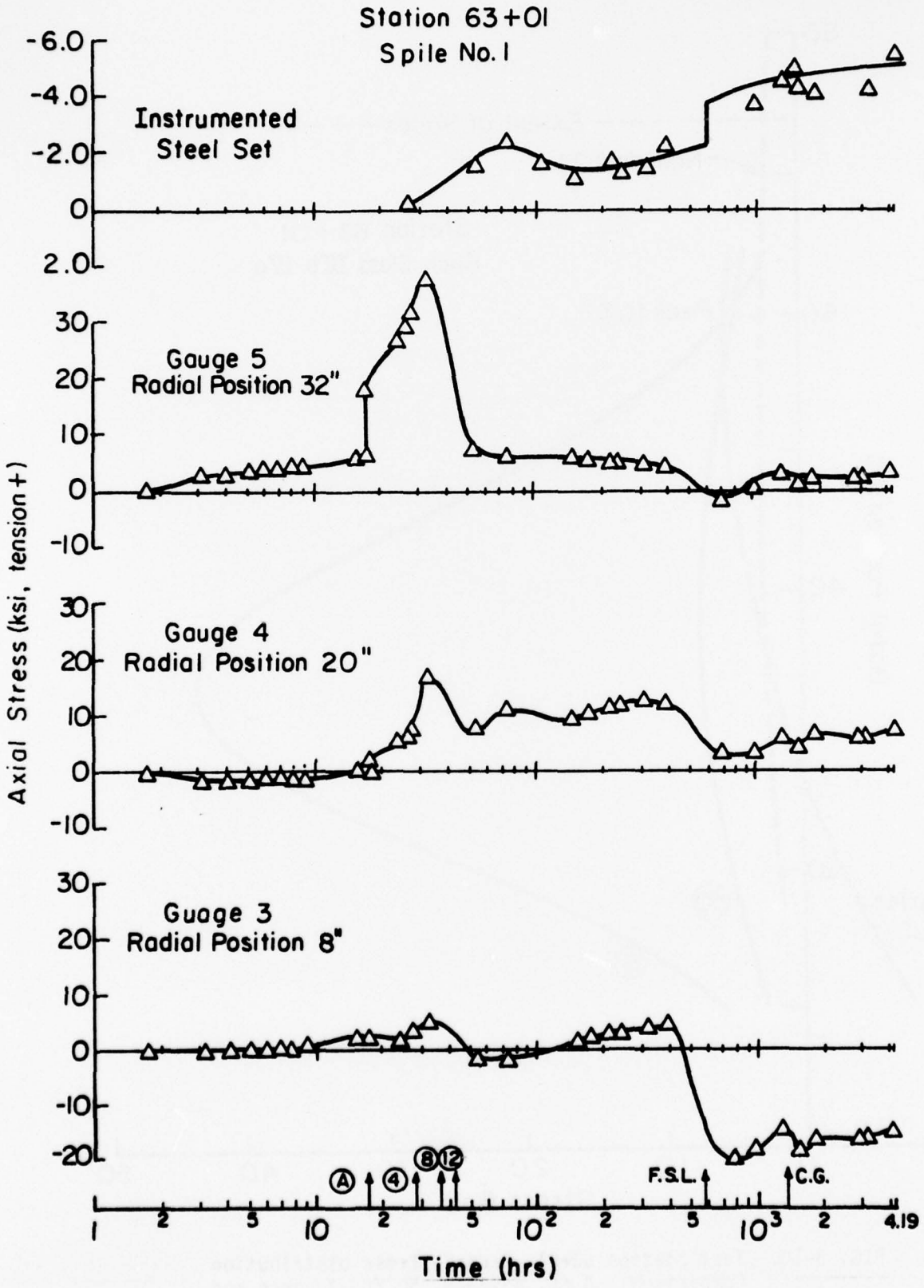

FIG. 3-11. Test Station 63+01, Stress History of Instrumented Spile and Steel Set (excerpt from Appendix 7)

If it was assumed that the peak stress drop of over 36 KSI was released as an equivalent weight of rock requiring support, the instrumented steel set would have shown a stress increase of over 12 KSI (method of computation in Appendix 6). Instead, the set revealed some degree of relaxation. In summary, the total stress relaxation within the reinforcement was not directly related to a total load increase within the support.

With increasing time, the stress distribution peak migrated away from the opening, close to the extent of the spiles, Figure 3-10. Difficulties in grouting resulted in one to two feet of overbreak exposing nearly four feet of spile. Consequently, the reinforced arch was not as thick as planned.

Instrumented radial bolts installed 50 feet behind the face exhibited a relatively small increase in stress over the long term, Figure 3-10. This indicated a stable arch. There is little question that the bolts would have been more useful if installed much closer to the face.

Additional relaxation of the ground nearest the tunnel occurred after placing the first stage concrete liner (F.S.L.). Strain gauges closest to the opening recorded compression of the reinforcement as the ground loaded the support system, Figure 3-11. The magnitude of this relaxation roughly corresponded to the load increase within the internal support (details given later in the chapter).

Results from the second test station in similar ground, confirmed much of the previously discussed behavior. The location of the stress peak immediately after excavation, the stress relaxation, and the migration of the peak and inflection point with increasing time were

all the same, Figure 3-12. However, important differences were observed. Although the magnitude of the stress peak immediately after excavation was lower, the amount of stress relaxation upon advancement of the heading was considerably less. Instead of relaxation occurring throughout the reinforced region, the position of peak stress migrated away from the opening at almost constant magnitude. In the long term, the stable position of the peak was slightly more than 50 in. from the crown, while at station 63+01 it was at 60 in.

In comparison to the reinforced ground response at station 63+01, the second test station 72+36 behaved in a more orderly manner without the extreme changes previously noted. Basically, station 72+36 exhibited the fundamental response of a properly reinforced arch in problematic ground. A major factor in the different behavior of the two test stations in similar ground was the thickness of the reinforced arch. At a radial position of 74 in. from the opening, the extent of the spiles at station 63+01, there was considerable ground activity recorded at the second station, Figure 3-12. The arch thickness would have been increased by 20 percent if the total length of the spiles were embedded at the first station.

Instrumented radial bolts installed 50 feet behind the face exhibited more activity than those installed at the first test station. Considering stress induced from radial deformation alone, the stress increase that occurred between the 50 foot advance and long term spile distribution curves was roughly equivalent to the bolt stress beyond 50 in. from the opening. As in the case of the last test station, earlier installation of the radial bolts would have resulted in a more significant contribution.

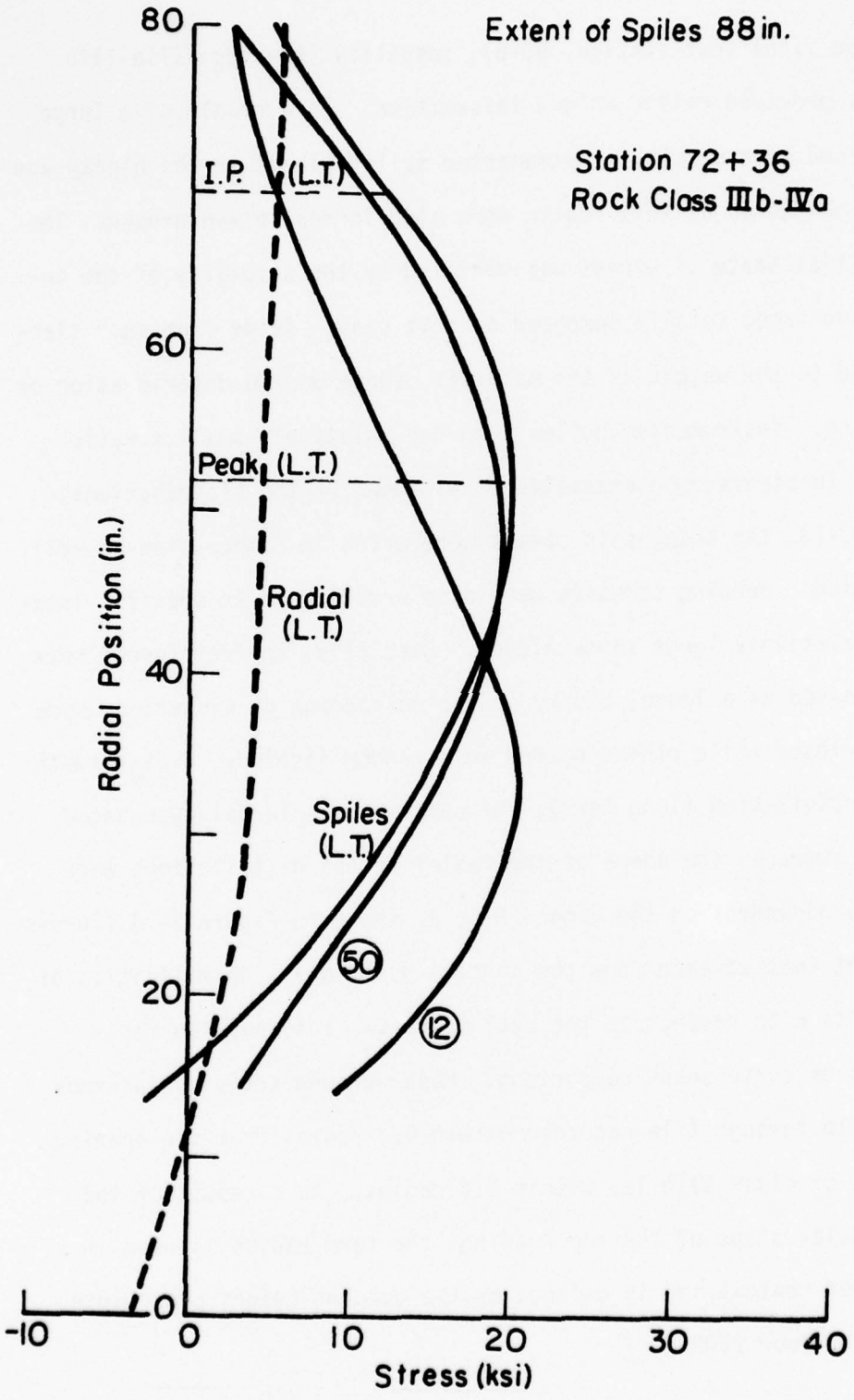

FIG. 3-12. Test Station 72+36, Radial Stress Distribution Comparison: 12 ft. Advance, 50 ft. Advance and Long Term (summary of Fig. A5-18 to 20, 29)

The final test station, 80+87, installed in a type IIIa-IIIb ground, provided rather unique information. As a result of a large destressed zone of clay, instrumented spiles placed in the blocky and seamy rock ahead of this region were also in destressed ground. The low initial state of stress was verified by the stability of the unsupported face, totally composed of soft clay. Aside from some slabbing due to the weight of the material, there was no deterioration or squeezing. Instrumented spiles recorded relatively small erratic changes in stress upon excavation. As shown by the distributions, Figure 3-13, the changes in stress were often in compression as well as tension. Bending stresses were also erratic and in specific locations relatively large in magnitude. Bascially, the reinforced rock mass behaved as a loose, blocky ground responding to vibration, some joints closed while others opened in a random fashion. Over a month after installation (long term), the behavior was largely unchanged.

In summary, the shape of the radial stress distributions were strongly dependent on the ground type as shown in Figure 3-14 (curves for eight foot advance from the initial position). Normalization of the stress with respect to the peak value was incorporated for purposes of curve shape comparison. Major ground activity for rock classes Ib through IIIa occurred within 0.2 radius from the opening and that of class IIIb-IVa within 0.4 radius. As a result of the semicircular shape of the top heading, the term radius is used in a normalized context and is defined as the opening height plus width divided by four (200 in.).

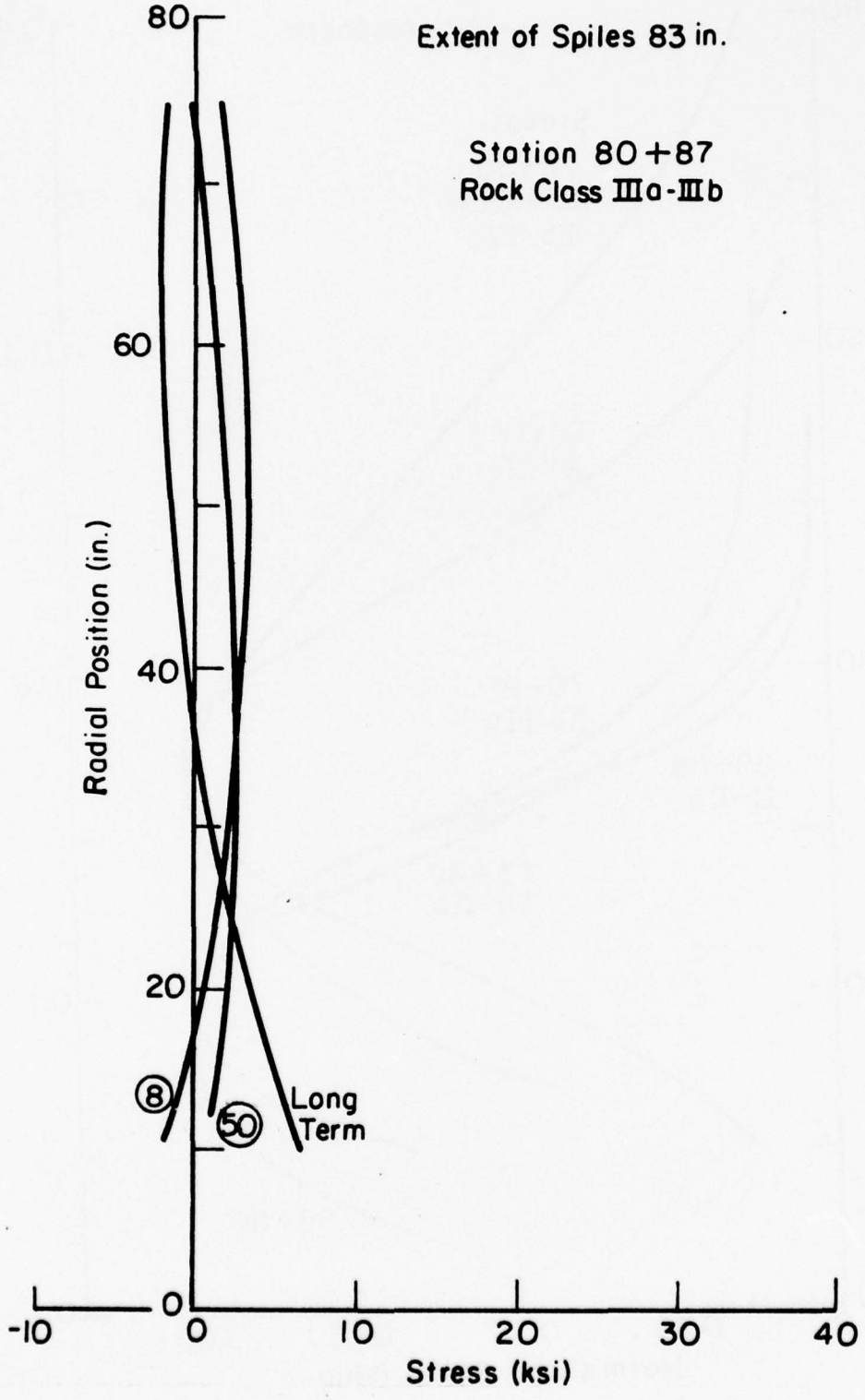

FIG. 3-13. Test Station 80+87, Radial Stress Distribution Comparison: 8 ft. Advance, 50 ft. Advance and Long Term (summary of Fig. A5-25 to 27)

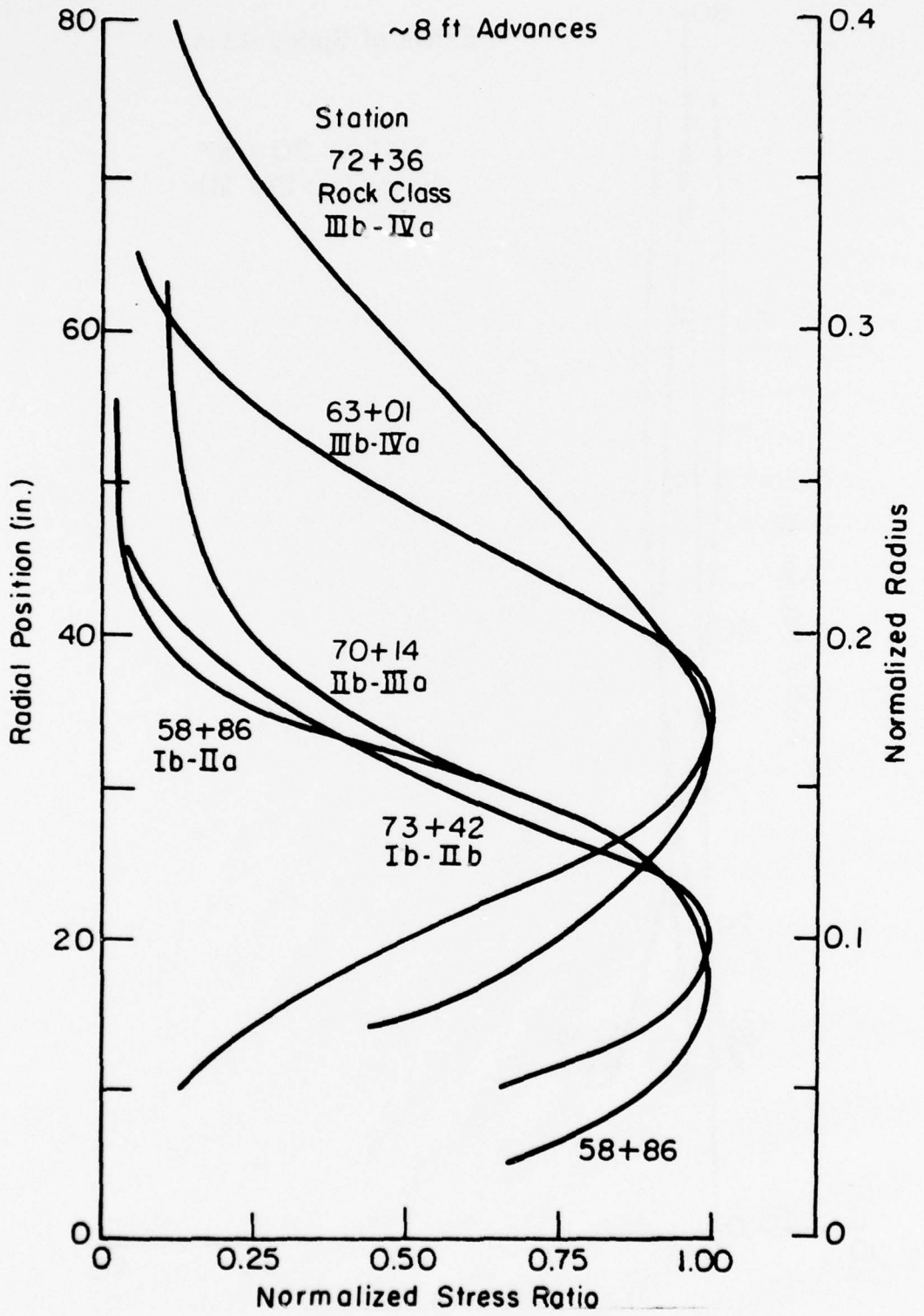

FIG. 3-14. Normalized Stress Ratio (measured to peak stress) Distribution Comparison: Absolute Radial Position and Radii (one radius equals top heading height plus width divided by four, 200 in.), All Test Stations after 8 ft. Advance

The magnitude of force developed within the rock mass-reinforcement system in response to excavation was also related to ground type, Table 3-III. To consider the relation it was necessary to present the results in terms of an equivalent pressure, defined as the peak spile force divided over the tributary area reinforced by the bar. As shown, the lower the rock mass quality, the higher the developed pressure. Developed pressure or spile force also depends on additional factors related to the time of installation with respect to the age of the heading, quality of installation, damage resulting from excavation, and the initial state of stress. The percentage of stress readjustment, either in terms of reinforcement relaxation or gain, at a specific radial position was considerably less in competent ground.

With the exception of station 80+87, the average bending stresses recorded at all other test stations in all types of ground were minor relative to the tensile stresses. During excavation under the cover of the spiles, the bending stresses were often positive, indicative of a concave deflected shape facing downward. With continued advancement, the reinforcement would tend to revert back to its undeflected shape, occasionally continuing beyond, resulting in slightly negative bending stresses.

When conditions permitted it was possible to monitor the response of the instrumented spiles for several hours after installation and before advancing the first round. The results provided strong evidence for the effectiveness of spiling reinforcement in the stabilization of ground at and ahead of the tunnel face. An average distribution of the axial stress increase per hour for the first five hours after installation is shown in Figure 3-15 for three test

TABLE 3-III

Reinforcement System Peak Equivalent Pressure

Test Station	Rock Class	Peak Equivalent Pressure (KSF)	
		8 Ft. Advance	Long Term
58 + 86	Ib - IIa	1.9	1.5
73 + 42	Ib - IIb	3.1	2.5
70 + 14	IIb - IIIa	3.7	3.0
80 + 87	IIIa - IIIb	-	-
72 + 36	IIIb - IVa	6.2	6.0
63 + 01	IIIb - IVa	13.2	1.8

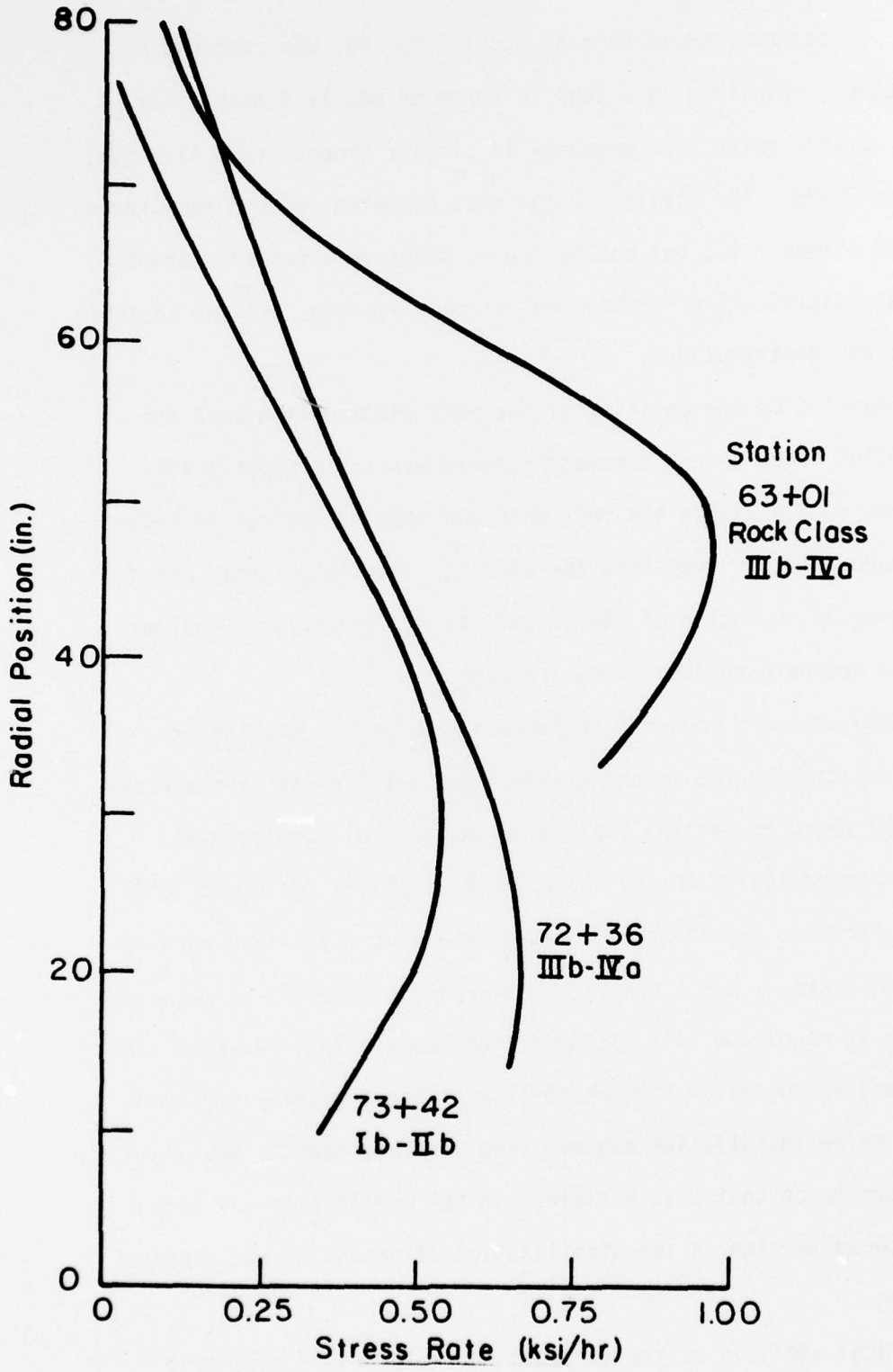

FIG. 3-15. Pre-Excavation Stress Rate Distribution Comparison: Test Stations 63+01, 72+36 and 73+42, First 5 hrs. after Installation

stations. A maximum stress rate of about 1 KSI/HR. was recorded at station 63+01, resulting in a tensile force of nearly 4 tons after 5 hours. Lesser rates were measured in similar ground, type IIIb-IVa, at station 72+36. The station in the most competent ground registered the lowest stress rate, but not as low as might be expected. Shapes of the rate distribution curves were, in many aspects, similar to their radial stress distributions.

As revealed by the position of the rate distribution peak for station 63+01, even before excavation there was an incompatibility between the strain within the rock mass and that of the reinforcement to a distance of four feet from the opening. Partially, this was due to the observed squeezing of the ground at the heading and problems related to adequate reinforcement grouting.

Bending stresses recorded prior to advancing the heading provided information on the ground displacement field ahead of the excavation. No measured bending implied the absence of displacement gradients perpendicular to the spile. Both stations 72+36 and 73+42 showed no bending. Station 63+01 revealed a slight positive bending stress, indicating a small displacement gradient oriented downward and decreasing in magnitude with distance from the opening. Overall, the lack of bending suggested the suitability of the typically employed 30 degree spile installation angle. Used for convenience, the angle also appears to be that most efficient in the mobilization of deformation induced tension in the stabilization of ground at and ahead of the opening.

Numerical analysis of the deformation field around advancing tunnels in elastic and elasto-plastic media, (Ranken and Ghaboussi,

1975), also implies the effectiveness of spiling reinforcement. Depending on the position of the support system with respect to the advancing face, the total displacement vector of the medium nearest the opening was oriented between 20 and 70 degrees from the tunnel axis. The lower bound corresponds to openings in which the support extends to the face and the upper bound to tunnels which remained unsupported to within one radius of the face. A spile installation angle that would maximize the deformation induced tension resulting from the gradient of the ground displacement is located within the bounds considered. Further, it depends on complicating factors such as support system stiffness, ground type, and the time dependent response of the rock mass.

Maximization of the induced tension, however, may not result in sufficient stabilization of the heading upon advancement under the cover of the previously installed spiles. Using a reasonable length of spile, a high installation angle does preclude the reinforcement of ground ahead of the new face. A compromise between these factors and additional constraints related to installation problems at high angles, results in a practical angle of between 25 and 45 degrees, the higher value to be used in competent ground.

b. Reinforced Arch-Supported System Interaction

The relationship between the loads measured on the internal support system, the magnitude of the spile stress relaxation, and the shape of the spile stress distribution curve is complex. In order to consider the topic for application in design, simplifying assumptions were required.

Calculation of the loads measured on the support system was divided into two parts. Immediately prior to placement of the first stage concrete liner (before F.S.L.) the system consisted of blocked steel sets. At this point in time, vertical rock loads were obtained directly from the instrumented sets as described in Appendix 6. Once the concrete liner was in place (after F.S.L.) the long term calculation of loads was possible, but with a greatly reduced accuracy. Although numbers were tabulated, they are subject to errors. The method, assumptions, and problems of the computations are considered in Appendix 6.

Forces measured as an external load on the support system must be transmitted through the rock mass within the immediate vicinity of the opening. In this region, the instrumented reinforcement directly responded to changed conditions within the support system. Reasonable values of load were obtained if it was assumed that all relaxation of spile stresses nearest the opening eventually resulted in load on the support. In the calculations of the average stress relaxation, only the region between the position of peak stress, as derived from the stress distribution after eight feet of advance beyond the initial position, and the tunnel wall was considered. This ground had deteriorated to a certain degree and as a result, it strongly influenced support behavior. Relaxation occurring within the reinforcement beyond the position of peak stress was largely related to energy redistribution within the rock mass, as previously described and illustrated, and to a lesser degree support system loads. If this relaxation had an influence on the support system, it would be recorded by the reinforcement nearest the opening.

Conversion of stress relaxation to support load in terms of the equivalent weight of a column of rock of height H_p is considered in Appendix 6. Basically, the rock load H_p was the spile relaxation stress resolved into a vertically directed force, divided by the tributary area reinforced by the spile and the unit weight of the rock mass.

A comparison between the calculated rock load H_p as derived from the instrumented steel set and the measured spile stress relaxation, for both before F.S.L. and in the long term, revealed good correlation at all test stations except station 80+87, Table 3-IV. Steel sets in competent ground acquired no additional load after placement of the liner. Those in type IIIb-IVa ground indicated increased loads despite the stabilized behavior of the support-reinforcement system as recorded by instrumented sets and spiles. The additional loading was related to the character of the rock mass and the relative stiffness of the reinforced arch-support system.

As shown by the stress histories at station 63+01, Figure 3-11, after the large stress relaxation of the spiles, the reinforcement-support system continued to take load at a decreasing rate (note: logarithmic time scale). This was characteristic behavior for a ground exhibiting a significant time dependent response, or squeeze. With the addition of the concrete liner, the stiffness of the support system to thrust was increased by a factor of nearly four. Consequently, with the increased stiffness, the previously established steady state equilibrium between the reinforced rock mass and internal support was forced to readjust. Since the reinforced rock nearest the opening was not as stiff as the new support system, load was

TABLE 3-IV

Measured, Predicted and Anticipated Rock Loads on Internal Supports

Test Station	Rock Class	Rock Load H_p (FT.)					Spile Stress Distribution Long [illegible] (FT.)	
			Steel Set		Spile Relaxation			
		Anticipated *	Before F.S.L. **	Long Term **	Before F.S.L. ***	Long Term ***	Peak Pt.	Inflection Pt.
58+86	Ib-IIa	6	0.9	0.9	0.7	1.1	1.3	2.3
63+01	IIIb-IVa	60	6.1	17.4	9.8	17.4	5.0	> 5.5
70+14	IIb-IIIa	12	2.1	—	0.0	—	1.7	2.7
72+36	IIIb-IVa	60	5.1	8.6	4.1	7.9	4.3	5.8
73+42	Ib - IIb	9	1.8	1.8	1.9	1.4	1.8	2.6
80+87	IIIa-IIIb	28	4.6	11.6	0.5	0.8	—	—

* From Table 3-I

** Measured from instrumented steel sets

*** Predicted from measured spile relaxation

transferred off the reinforced arch onto the support (Figure 3-11, time at F.S.L.). A short time after placing the liner, a new steady state was established (time 2 to 4 thousand hours). As a result, the magnitude of the additional loads acquired by the composite support system were dependent on the stiffness of the system and the time of installation. The stiffer the system and the earlier the installation, the higher the expected loads.

As described in Chapter 2, the position of the spile stress distribution inflection point marked the boundary at which a significant incompatibility existed between the strain within the rock mass and the reinforcement. Consequently, the ground between the opening and this point had deteriorated from its initial state and, to a certain degree, loosened. Since this region of ground had a relatively low stiffness, the likelihood of it becoming a load on the support system was considerable. Therefore, a simple method by which to predict the loads on support systems was to determine the total weight of this region of ground. Results derived from the long term distribution curves and measured rock loads were in good agreement just prior to placement of the concrete liner, Table 3-IV (before F.S.L.). As shown, the measured rock load height H_p was near or between the position of peak and inflection point. In competent ground this was also the result in the long term. Test stations 63+01 and 72+36, located in ground exhibiting a significant squeezing behavior, took additional load subsequent to lining the tunnel for reasons previously described. The increase in load can be conservatively computed by employing the increased stiffness of the support system as a multiplication factor applied against the calculated load (before F.S.L.).

For the system under consideration the factor was four, and as applied to the position of peak stress it results in a conservative estimation of the long term rock load.

There was no direct method by which the capacity of the reinforced arch could be measured. Consequently, its capacity was based on the conservative assumption that all load measured on the internal support, as previously described, was necessarily that which the reinforcement system could not facilitate. The difference between the measured rock loads on the supports and that of the anticipated loads was an indirect indication of the reinforced arch capacity.

Strong evidence for the overall effectiveness of spiling reinforcement or system capacity is presented by this comparison between measured and anticipated loads, Table 3-IV. Anticipated rock loads were based on the lower bound values derived from the application of Terzaghi's classification system, Table 3-1. On the average, the long term measured loads were less than 25 percent of the anticipated loads, while the loads on the steel sets alone (before F.S.L.) were less than 15 percent. Bascially, this revealed that the rock mass-reinforcement system was the primary factor in the permanent stabilization of the tunnel opening; whereas, the internal support system performed a secondary, though necessary, role in the control of local loosening.

CHAPTER 4

COMPARISON: RESULTS FROM BONNEVILLE & EISENHOWER TUNNELS

Comparison of the results from the North Bonneville Pilot Tunnel with those of the Eisenhower Tunnel was of significance, considering the difference in size of the openings and in the amount of overburden. The Eisenhower Tunnel was more than four times the size and at eight times the depth of the Pilot Tunnel.

Station 70+14 in the Eisenhower Tunnel and the Pilot Tunnel test stations were both located in moderately to very blocky and seamy ground. Normalized stress distributions of the early response from each station were plotted in terms of absolute radial position and radii from the opening, Figure 4-1. As shown, the comparison of distributions on an absolute scale were in excellent agreement, while those with normalized radii revealed no similarity. Despite the differences in tunnel size, shape, and overburden the thickness of the reinforced arches were roughly the same. This implied that for a given type ground, those factors related to geometry and initial state of stress had a relatively weak influence on arch thickness. As described in the previous chapter, however, the thickness was strongly dependent on changes in ground type (Figures 3-14).

Although the reinforced arches from the two tunnels were composed of a similar type ground and had the same thickness, they performed at different capacities. The equivalent pressure of the system at station 70+14 (Table 3-III) was three times that of the Pilot Tunnel. Consequently, the capacity at which the system was required to operate was strongly dependent on the opening size, shape, and initial state

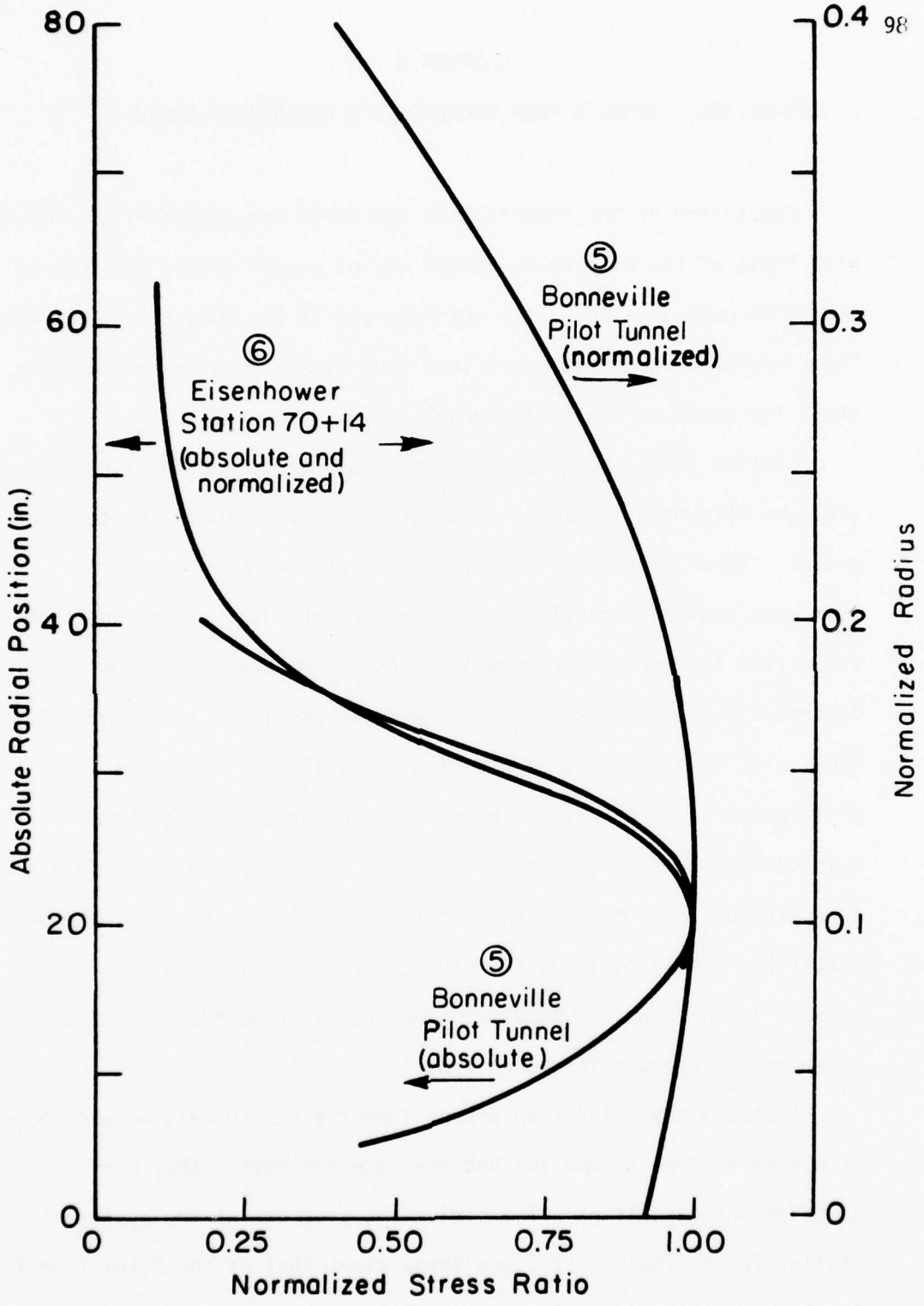

FIG. 4-1. Normalized Stress Ratio (measured to peak stress) Distribution Comparison: Absolute Radial Position and Radii (one radius equals top heading height plus width divided by four; Eisenhower Tunnel = 200 in., Pilot Tunnel = 50 in.)

of stress.

The rock mass-reinforcement system is basically self-equilibrating, a closed loop system with negative feedback. Increased deformation results in increased system resistance and consequently, a reduction in deformation. The formation of a stable arch involves a specific region of material within the immediate vicinity of the opening, the thickness required being largely related to ground type. As a consequence, the extent of the designed arch or length of reinforcement is strongly dependent on ground type. The same dependency applies to the reinforcement spacing and/or pattern. Arch capacity is related to size, shape, and depth of the opening. To increase the capacity, increase the size and/or number of reinforcement bars.

CHAPTER 5

CONCLUSIONS

Findings from this investigation are divided into the categories of rock mass-reinforcement system mechanisms, reinforced ground-support system interaction, and reinforced arch design considerations.

Rock Mass-Reinforcement System Mechanisms

Deformation induced tension within the reinforcement is the major mechanism by which spiling reinforcement effectively contributes to the immediate and permanent stabilization of an opening. Both the rate and magnitude of the measured tensile force, upon advancement of the excavation under the cover of the spiles, was considerable. Immediately on advancing the heading, a tensile force of two tons was recorded at test stations within the small Bonneville Pilot Tunnel, and of 15 to 30 tons at the larger Eisenhower Tunnel. Even before advancing under the cover of the spiles, immediately after installation the reinforcement acquired tensile stress at rates of up to 1 KSI/HR. in response to deformation at and ahead of the face.

Aside from providing information on the ground displacement field, bending stresses resulting from excavation are insignificant relative to the magnitude of the tensile stresses. This point emphasizes the difference between spiling reinforcement and forepoling, a temporary ground support method. The lack of recorded bending also implies the absence of significant displacement gradients perpendicular to the spile, which substantiates the suitability of the typically employed 30 degree installation angle.

Compatibility of the rock mass and reinforcement strains was investigated by the comparison of radial distributions, obtained with the aid of extensometers and instrumented spiles. Distributions of stress or strain increase, derived from instrumented spiles, were similar in form to bell shaped probability distributions. The position of the inflection point represents the point at which there is a break in compatibility. At distances from the opening greater than the inflection point, the rock mass-reinforcement system behaves primarily as a continuum. Between the inflection point and the tunnel opening the system displacement field is basically inhomogeneous. The position of peak stress represents the point at which the response of the reinforcement to rock mass deformation is at maximum. Positions of the peak and inflection point are strongly dependent on ground type; the more competent, the closer to the opening.

The changing shape of the distribution curves as characterized by the position and magnitude of the peak and inflection point provided considerable insight into the rock mass-reinforcement behavior. After the instantaneous stress increase and with continued excavation, stress is partially relieved in the reinforcement nearest the opening, and increased in that farthest from the opening. The magnitude of the change is largely a function of ground type, and is related to energy redistribution and loosening within the rock mass immediately around the tunnel. Relaxation is not indicative of reinforcement failure, but rather of the establishment of a new stable equilibrium.

In difficult ground, the position of the peak and inflection points, with increasing time after excavation, migrate away from the opening to a stable position. If the reinforced arch is too thin,

the peak extends beyond or towards the end of the reinforcement. This results in an inefficient rock mass-reinforcement system.

Reinforced Ground-Support System Interaction

Forces measured as an external load on the support system are transmitted through the rock mass within the immediate vicinity of the opening. Within this region and below the position of peak stress, instrumented reinforcement responds directly to changed conditions in the form of stress relaxation. A comparison of measured loads on the support system and spile relaxation revealed good correlation. Consequently, instrumented reinforcement is a method by which to predict loads on internal support.

The magnitude of the loads developed on the support system is dependent on the system stiffness and ground type. With a relatively flexible system, such as steel sets with blocking, the measured loads are related to the position of the spile stress distribution inflection point. This point marks the boundary at which a significant incompatibility exists between the strain within the rock mass and the reinforcement. Consequently, the ground between the opening and the inflection point deteriorates to a certain degree. Since this region of ground has a relatively low stiffness, a proportion of this zone becomes a load on the support system. Therefore, a verified simple method by which to predict the load is to determine the total weight of this region of ground.

In competent ground, this method is applicable to support systems of any stiffness. In ground exhibiting a significant squeezing behavior, increasing the stiffness upon placement of the concrete liner results in additional loads. Since the reinforced rock

nearest the opening is not as stiff as the new composite support system, load is transferred off the reinforced arch onto the support. The additional load can be conservatively computed by employing the increased stiffness of the support system as a multiplication factor applied against the predicted load based on a flexible system.

Reinforced Arch Design Considerations

Formation of a stable reinforced arch is basically a self equilibrating process, involving a specific region of material within the immediate vicinity of the opening. The required thickness of the arch is strongly related to ground type and construction method, and less to the opening size, shape, and depth. Increased rock mass activity associated with difficult ground requires an arch of increased extent. Based on the Eisenhower and Bonneville tunnels, the range of thickness depending on ground type was from three to eight feet. Designed or installed arch thickness can be significantly different from the in situ condition after excavation. Damage resulting from excavation can destroy up to three feet or more of otherwise effective arch. This can be avoided with effective control and proper blast design.

Arch capacity, related to induced forces within the reinforcement, is strongly dependent on the opening size, shape, and initial state of stress. To increase the capacity, increase the size and/or number of reinforcement bars.

If the continuity, thickness, or capacity of the rock mass-reinforcement system is insufficient for a particular opening the system will not work effectively. This was demonstrated by the results from the main bore of the North Bonneville Tunnel. Upon

excavation, the strains within the rock mass beyond the extent of the spiles were large relative to the reinforced ground, indicative of a discontinuity between the reinforced arch and surrounding rock mass. Normally, the strains were monotonically increasing with decreasing distance from the opening. This was also preceded by the migration of the position of the peak and inflection point to beyond the extent of the spiles. Either instrumented reinforcement or extensometers can be employed to monitor the behavior of a reinforced arch, and should be routinely used to check the design.

In problematic ground, it is important to install the reinforcement as soon as possible. Rock mass deterioration resulting from deformation at and ahead of the face is restrained upon the installation of the spiles, as revealed by the subsequent stress increase within them. This applies equally to before and after advancement of the excavation under the cover of the reinforcement. Untensioned, radial bolts installed behind the face have a minor influence on the stabilization of an opening. Since spiles are easier to install with the available equipment on a jumbo, they can be placed long before radial bolts.

Strong evidence for the overall effectiveness of spiling reinforcement at the Eisenhower Tunnel was presented in the comparison between the measured rock loads on the supports and that of the anticipated loads. The long term measured loads were less than 25 percent of the anticipated loads, while the loads on the steel sets alone were less than 15 percent. Basically, this reveals that the rock mass-reinforcement system was the primary factor in the permanent stabilization of the tunnel opening; whereas, the internal

support system performed a secondary, though necessary, role in the control of local loosening.

REFERENCES

1. Bjurstrom, Sten (1974) "Shear Strength of Hard Rock Joints Reinforced by Grouted Untensioned Bolts," Proc. 3rd Cong. Int. Soc. Rock Mech., Denver, Pt. 11B, pp. 1194-1199.

2. Brekke, T.L., and Korbin, G.E. (1974) "Some Comments on the Use of Spiling in Underground Openings," Proceedings of the Second International Congress of the International Association of Engineering Geology, San Paulo, Brazil, Vol. 2, No. VII-PC-4, Aug.

3. Dunham, R.K. (1976) "Anchorage Tests on Strain-Gauged Resin Bonded Bolts," Tunnels and Tunnelling, Vol. 8 No. 6, Sept./Oct., pp. 73-76.

4. Geological Survey Professional Paper 815 (1974) "Engineering Geologic, Geophysical, Hydrologic, and Rock-Mechanics Investigation of the Straight Creek Tunnel Site and Pilot Bore, Colorado," Lib. of Cong. Cat.-Card No. 73-600330. U.S. Govern. Printing Office, Washington D.C.

5. Hopper, R.C. Lang, T.A., and Mathews, A.A. (1972) "Construction of Straight Creek Tunnel, Colorado," Proceedings, First North American Rapid Excavation and Tunneling Conference ASCE and American Institute of Mining, Metallurgical, and Petroleum Engineers, Vol. 1, June, pp. 501-538.

6. Korbin, G.E. and Brekke, T.L. (1975) "A Model Study of Spiling Reinforcement in Underground Openings," Technical Report MRD-2-75, Missouri River Division, Corps of Engineers, Omaha, Nebraska, April.

7. Korbin, G.E. and Brekke, T.L. (1976) "Model Study of Tunnel Prereinforcement", Journal of the Geotechnical Engineering Division, ASCE, Vol, 102, No. GT9, Proc. Paper 12415, Sept., 1976, pp. 895-908.

8. Lang, T.A. (1961) "Theory and Practice of Rock Bolting," Transactions of the American Institute of Mining, Metallurgical, and Petroleum Engineers, Society of Mining Engineers of AIME, Vol. 220, pp. 333-348.

9. Londe, P. and Bonazzi, D. (1974) "Reinforced Rock," Proc, 3rd Cong. Int. Soc. Rock Mech., Denver, Pt. IIB, pp. 1208-1211.

10. MacDonald, R.D. (1976) "Pilot Tunnel Construction Report," U.S. Army Engineer District, Portland, Bonneville Area Office, North Bonneville, Wash., unpublished.

11. Mathews, K.E. and Meek, J.L. (1975) "Modelling of Rock Reinforcement Systems in Cut and Fill Mining," Proc. 2nd A.N.Z. Conf. on Geomech., Brisbane, Australia, pp. 42-47.

12. Palmer, W.T., Bailey, S.G. and Fuller, P.G. (1976) "Experience with Preplaced Supports in Timber and Cut and Fill Stopes," Research Paper No. 278 of the Division of Applied Geomechanics, Commonwealth Scientific and Industrial Research Organization, Melbourne, Victoria, Australia.

13. Post, J.D. (1973) "Geological Report on the Straight Creek Tunnel," Colorado Div. of Highways, Denver, Colorado, unpublished.

14. Ranken, R.E. and Ghaboussi J. (1975) "Tunnel Design Considerations: Analysis of Stresses and Deformations Around Advancing Tunnels," Report FRA-OR & D 75-84, Dept. of Transportation, Federal Railroad Administration, Washington, D.C.

15. Stateham, R.M. and Sun, M.C. (1976) "Temperature Investigation of Resin-Anchored Bolts," Report of Investigations 8178, U.S. Bureau of Mines, Washington D.C.

16, Stillborg, Bengt (1977) Personal Communication, Research Engineer, University of Lulea, Lulea, Sweden.

17. Terzaghi, K. (1946) "Rock Defects and Loads on Tunnel Supports," Rock Tunneling with Steel Supports, R.V. Proctor and T.L. White, Vol. 1, Commercial Shearing and Stamping Co., Youngstown, Ohio, pp. 17-99.

APPENDIX 1

INSTRUMENTED SPILE DESIGN AND CONSTRUCTION

Designing a rugged instrumented spile which would survive the abuse of installation and the harsh tunnel environment for several years was by itself a significant aspect of the total research effort. The procedure by which this was eventually achieved was somewhat evolutionary in nature. Although it was possible to simulate certain aspects of the tunnel environment in the laboratory, it was not practical to simulate spile installation. Consequently, the performance of bars installed early in the research program was used in the evaluation of the design. Unfortunately, this trial and error procedure is expensive both in terms of cost and the quantity of usable data obtained. A difficult problem of strain gauge survival during spile installation resulted in the malfunction of approximately half of all gauges installed in the Bonneville Tunnel. It was not until the second test station in the Eisenhower Tunnel that this problem was finally resolved.

Basically, an instrumented spile consists of a length of reinforcing steel (rebar) instrumented at various positions with resistive type strain gauges. A machined instrument head is securely welded to one end of the rebar, Figure A1-1. The head is used for installing the spile and provides protection for the electrical connections between the strain gauges, bridge completion resistors, and receptacle.

As shown in the wiring schematic, Figure A1-2, 120 ohm quarter bridge strain gauges incorporating a three lead wire system were employed. Gauges were of a weldable type with integral leads. Gauge

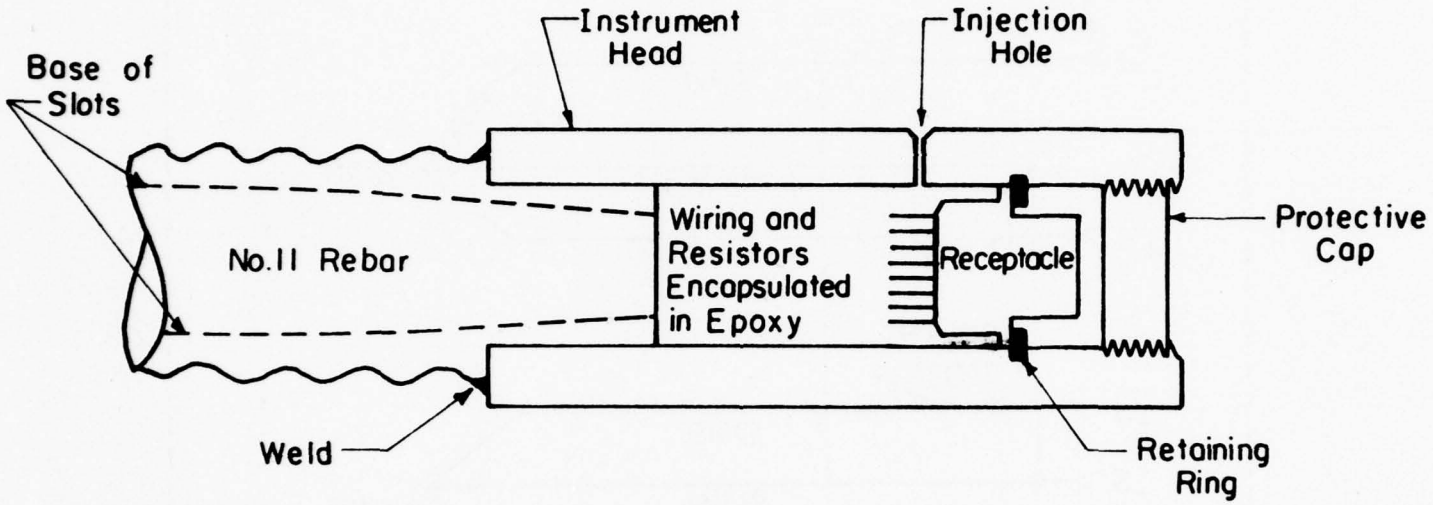

FIG. A1-1. Section of Instrument Head, General Layout

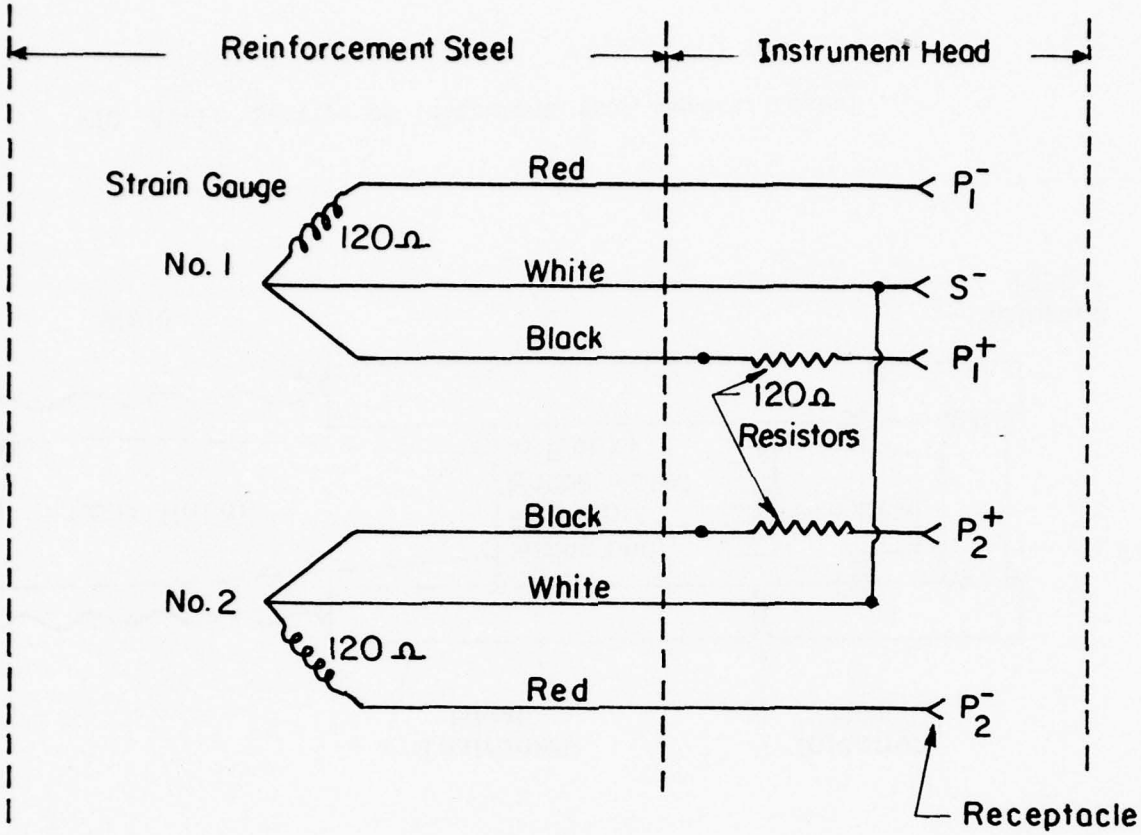

FIG. A1-2. Instrumented Reinforcement Wiring Schematic

leads routed to within the instrument head were connected to 120 ohm resistors and the receptacle. The resulting wiring configuration is a half bridge. When compared to a quarter bridge system, the half bridge has advantages of reduced sensitivity to variations of temperature and receptacle to plug contact resistance. Both the receptacle and mating plug used to connect the external readout instrumentation were of a waterproof design. Waterproofing and vibration protection for the elements within the instrument head were assured by encapsulating everything in a low viscosity epoxy.

North Bonneville Pilot Tunnel Instrumented Spiles

Spiles instrumented for the Bonneville Tunnel were eight foot long, number seven thread bolts. As a result of the small cross sectional area of the number seven bar, strain gauges and integral leads used to run wires between the gauges and instrument head were fixed to the surface of the rebar. Machining a slot or keyway along the length of the bar would have significantly reduced the cross sectional area. The thread bolt has two diametrically opposed flat regions along which there are no deformations. This provided a convenient surface on which to attach the gauge and integral lead. Integral lead wires were sealed within a 0.93 inch diameter stainless steel tube for protection against damage during installation and water. Two gauges and leads were installed on each of the two flat surfaces. The steel tube with gauge wires entered the instrument head through four holes as sketched in Figure A1-3. Integral leads were fixed to the rebar with spot welded metal straps spaced at intervals of six inches. For additional support and protection against damage, the gauges and steel tubes were covered with a structural adhesive

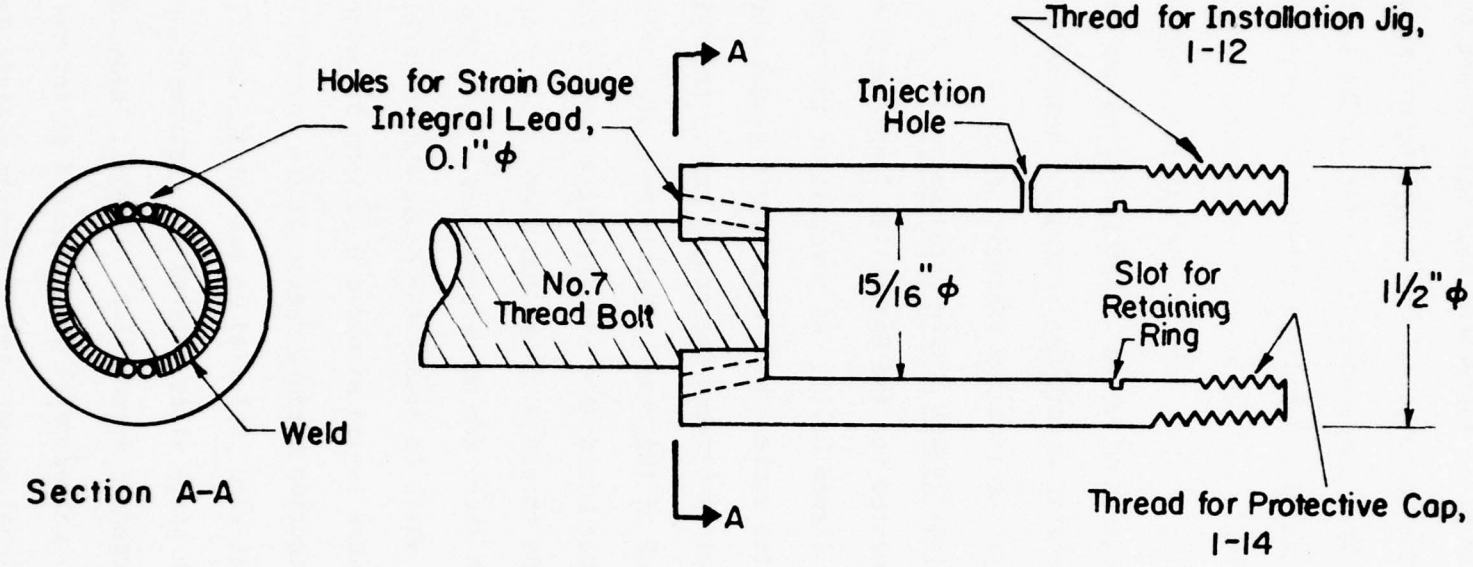

FIG. A1-3. Section of Instrument Head, Shop Drawing, Design Employed at Bonneville Pilot Tunnel

smoothly contoured so as to reduce the chance of getting snagged during installation.

As previously mentioned, nearly half of all gauges installed at the first pilot tunnel test station malfunctioned. Measurements indicated an open circuit within the strain gauge to be the problem. Once in place, it was not possible to determine if the break was due to an internal situation related to vibration or to excessive abuse of the gauge and/or integral lead during installation. At that point in time, vibration was not suspected. Consequently, attention was directed to strengthening the method by which the integral lead was attached to the rebar. Small diameter rods welded along the entire length of the rebar, acting as a trough for the gauges and leads, were incorporated on spiles constructed for the second test station.

Results upon installation were the same, with half the gauges malfunctioning. A closer examination revealed that the malfunctioning gauges belonged to one purchase in which the lead wires within the steel tube were fiberglass insulated solid conductors. The second purchase incorporated PVC insulated wires with stranded conductors in a slightly larger diameter tube (.125 inches). None of the gauges in the second purchase failed, while all but one of the gauges in the first group did. It was evident that the pulsating torsion created by the air driven drill upon rotation was resulting in severe vibration of the wires inside the steel tube. With gauges employing the relatively rigid solid conductors, the vibration was transmitted through a swage designed to isolate the connection between the lead wires and the strain gauge. The magnitude of the vibration was sufficient to break the connections resulting in an open curcuit. In the case of

gauges incorporating the relatively flexible stranded conductors, not enough energy was transmitted past the swage to damage the connections.

Eisenhower Tunnel Instrumented Spiles

With the completion of the two test stations at the North Bonneville Pilot Tunnel, attention was directed to the Eisenhower Tunnel, the site of all future spile installations. Spiles were hefty sixteen foot long number eleven rebars. Considering the large cross sectional area of the rebar, it was possible to mill protective keyways along its length without reducing the area by as much as ten percent. Two diametrically opposed slots approximately one-tenth to one-eighth inch deep and three-eighths inch wide provided adequate cover for the gauges and leads. Four gauges would fit in each keyway.

Aside from increasing the size, the instrument head was modified to accomodate a more efficient drive system. By employing steel hex stocks, Figure A1-4, a standard socket was used to drive the spile during installation. Previously, the outside of the instrument head was threaded to receive a special socket, Figure A1-3. With the addition of keyways it was no longer necessary to drill holes for lead wire access into the head.

Problems of strain gauge failure due to vibration during installation at the Eisenhower Tunnel were likely to be more severe than that encountered earlier. It would take much more force to drive the larger spile. Even though the gauges and leads would be buried within the keyway, it was believed that the extra protection afforded by the steel tube was worth retaining. The gauges using stranded PVC insultated wires required a larger diameter tube and were more costly

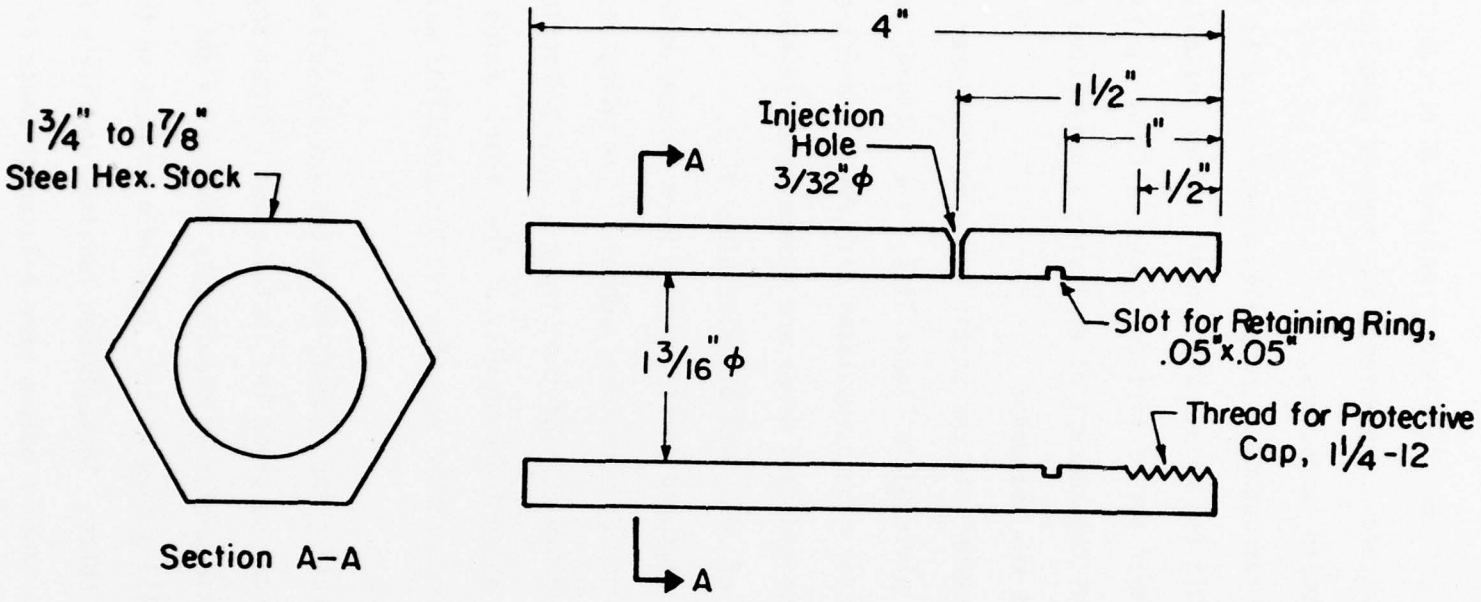

FIG. A1-4. Section of Instrument Head, Shop Drawing, Design Employed at Eisenhower Tunnel

both in terms of price off the shelf and a required 50 percent increase in slot dimensions. Therefore, an attempt was made to redesign the swage on gauges using solid conductors.

With redesigned strain gauges, two spiles were fabricated for the first test station within the Eisenhower Tunnel. After installation, measurements revealed that out of fifteen gauges, all but one had open circuits. At this point the concept of employing a protective steel tube for the lead wires was abandoned.

Working in conjunction with the strain gauge manufacturer resulted in a new design pictured in Figure A1-5. The integral lead is a stranded three conductor ribbon insulated with PVC. Connections between the strain gauge and lead wires are encapsulated in epoxy within a short section of .093 inch diameter steel tube.

Gauges mounted as pictured in Figure A1-5 were covered with at least one-tenth of an inch of structural adhesive. Mounting gauges in this manner prevented any part of the strain gauge, connections, or lead wires from vibrating independently of the rebar. Aside from providing protection against abuse the adhesive had excellent water proofing characteristics.

One spile incorporating the redesigned gauges was installed at station 58+86. All gauges survived the installation without any signs of damage and have performed flawlesssly for over eight months. With this experience, 113 gauges of this type were mounted on thirteen spiles and four radial bolts. Installation resulted in only a few cases of gauge failure. Most problems were related to abuse of the instrument head during driving. For example, excessive percussion, sometimes used to drive a jammed bar, could deform the head or break

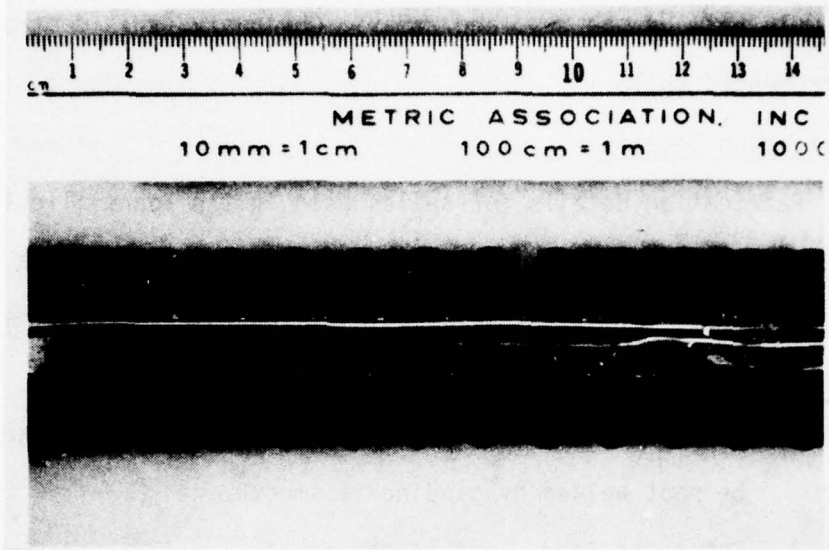

FIG. A1-5. Weldable Strain Gauge Installed within Reinforcement Steel Slot

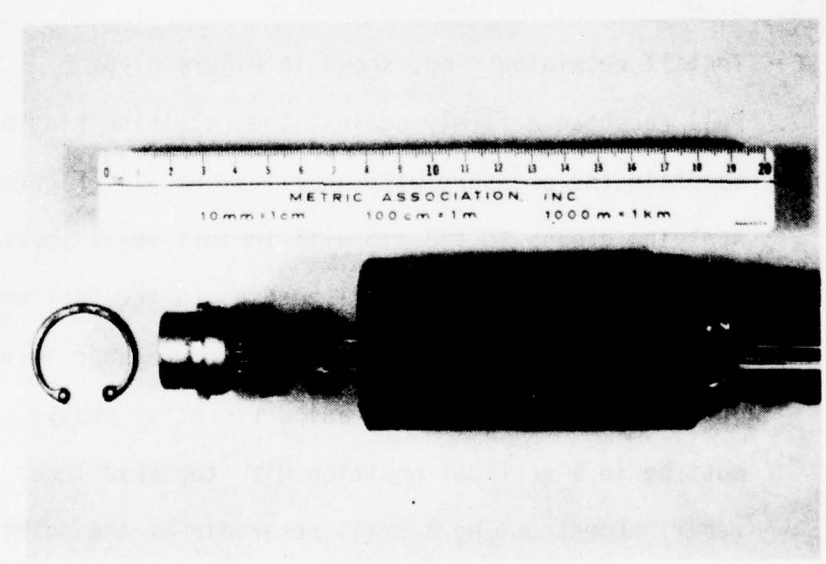

FIG. A1-6. Wired Receptacle and Retaining Ring Ready for Insertion within Instrument Head

the weld between the head and rebar. Obviously, this destroyed the instrumented spile.

Fabrication Details

Fabrication details for spiles used in the Bonneville Tunnel were essentially the same as for the Eisenhower Tunnel. Given a clean machined rebar (if keyway is used) with instrument head, the construction details are as follows:

1. Locate and prepare the area to which the strain gauge is to be spot welded by sanding it smooth.
2. Cut gauge lead wires to the proper length.
3. Feed lead wires through the slots or holes into the instrument head.
4. Wire gauges to bridge completion resistors and to the receptacle, Figure A1-6.
5. Slide receptacle into the head.
6. Install retaining ring, shown in Figure A1-6.
7. Pull receptacle firmly against the retaining ring and maintain the pressure with an alignment jig, Figure A1-7. Applying grease to the jig will inhibit small leaks of epoxy and prevent accidental bonding to the instrument head.
8. Encapsulate the instrument head and keyways or holes leading into the head by injecting a low viscosity epoxy. The spile must be in a vertical position with the head lower than the rebar. Constructing a small reservoir at the point where the keyway enters the head will reduce the possibility of voids by supplying extra epoxy for shrinkage or small leaks past the receptacle.

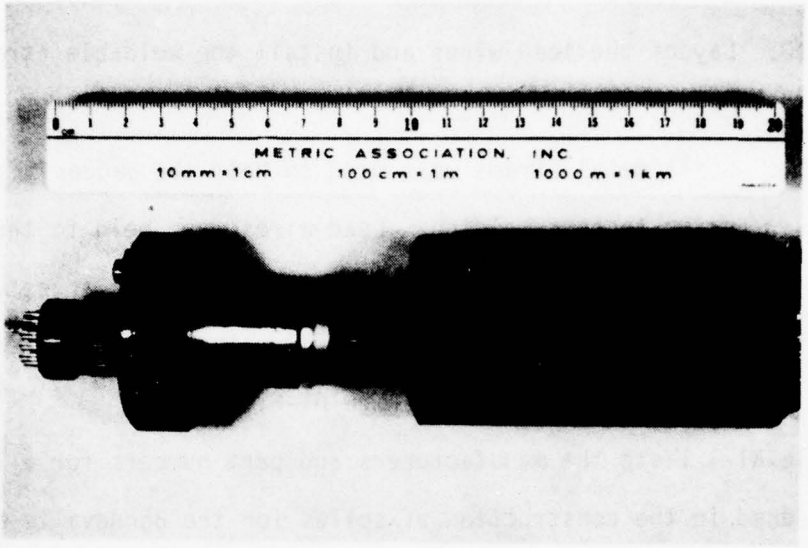

FIG. A1-7. Alignment Jig Used to Position Receptacle after Setting Retaining Ring

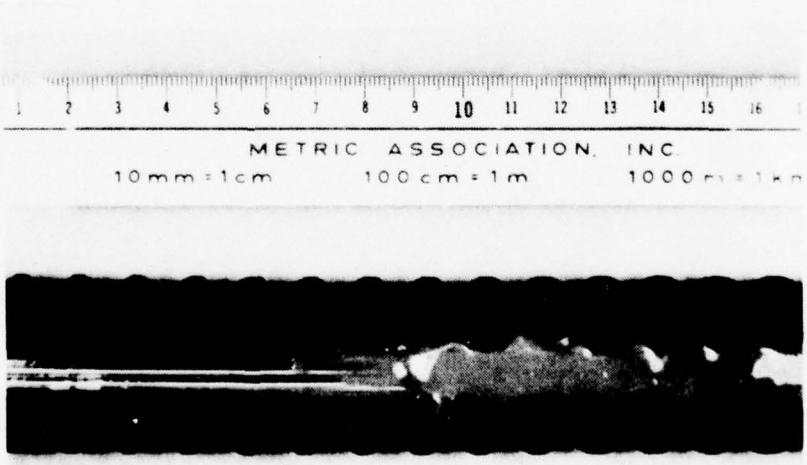

FIG. A1-8. Filling Slot Containing Strain Gauge Lead Wires with Structural Adhesive

9. Allow epoxy to harden.
10. Layout the lead wires and install the weldable strain gauges, Figure A1-5.
11. Small metal straps were used to hold the gauges in place prior to spot welding. Lead wires were held to the keyway base with a thin layer of structural adhesive.
12. Cover gauges and leads by filling the slot with a structural adhesive, Figure A1-8.

Table A1-1 lists the manufacturers and part numbers for all products used in the construction of spiles for the Bonneville and Eisenhower Tunnels.

TABLE A1-1 Instrumented Reinforcement Components List and Parts Manufactor

Spile Components	North Bonneville Pilot Tunnel	Eisenhower Tunnel
Reinforcing Steel	Dyckerhoff & Widmann, 22 mm Thread bolt, Grade 60	Judson Steel, No. 11 rebar, Grade 60
Instrument Head	1018 steel, cold rolled clindrical stock	1018 steel, cold rolled hexagonal stock
Retaining Ring	Waldes Truarc, N5000 - 93	Waldes Truarc, N5000 - 118
Protective Cap	Lucite plastic rod	Lucite plastic rod
Strain Gauge	Ailtech, SG 128 - 011A	Ailtech, SG/28/10
Receptacle	Amphenol, model 165-12	Amphenol, model 165-28
Plug	Amphenol, model 165-9	Amphenol, model 165-25
Resistor	Micro Measurement, S-120-05	Micro Measurements, S-120-05
Structural Adhesive	Scotch Weld, 1838 B/A	Scotch Weld, 1838 B/A
Injected Epoxy	Armstrong C-7, Activator A	Armstrong C-7, Activator A
Readout Cable	Belden, model 8778	Alpha, model 6014 Belden, model 8774
Readout Instrument	Vishay Instruments, P-350A modified by Terrametrics	Vishay Instruments, P-350A modified by Terrametrics

APPENDIX 2

INSTRUMENTATION PERFORMANCE AND CALIBRATION

Several laboratory tests were designed to check the instrumentation system performance under simulated field conditions. As described in Appendix 1, it was not practical to test all aspects within the laboratory, especially those concerned with durability upon installation. Tests were performed to measure residual strain and temperature change resulting from grouting, influence of water, and repeatability. Other tests were designed to check the strain gauge calibration and determine the reinforcing steel modulus. Information on gauge creep and stability was also obtained.

System Performance

Residual strains resulting from the temperature increase during cure of the polyester resin grout and/or non-temperature related grout shrinkage or expansion was investigated as a possible source of error. A two foot long, four by six inch block of granite was cored along its length. The one and one-half inch diameter hole was filled with resin cartridges (Celtite, 15-30 minutes set time). A specially constructed three foot long instrumented spile with two diametrically opposed strain gauges and an iron-constantine thermocouple mounted on 22 mm threadbolt was driven into the resin filled hole.

After installation, measurements of temperature and strain were recorded at regular intervals. A maximum temperature rise of three degrees Centigrade was noted after 40 to 50 mintues. The corresponding average residual strain amounted to only three microstrains in compression and was of no concern.

Temperature investigations on resin grouted bolts installed in the White Pine mine using a faster setting resin revealed increases of three to five degrees Centigrade (Stateham and Sun, 1976). The magnitude of the temperature rise depends on the type of resin, set time, size of resin column, and rock mass conductivity. Even with increases up to five degrees, residual strains are negligible.

Additional tests, incorporating the block of granite with embedded spile, were performed to investigate the adequacy of the electrical waterproofing. The entire system with readout cable inserted into the instrument head was placed in a constant temperature wet room. After two months of nearly 100 percent humidity, no signs of electrical instability were observed.

From time to time the waterproof readout plug was removed and then reinserted into the instrument head. This served as a check on the moisture seal and differences in strain measurements related to small changes in pin contact resistances. Readings taken before and after plug removal were always repeatable to within a few microstrains.

Strain Gauges

As shown in Figure A1-2 of Appendix 1, the quarter bridge strain gauges incorporated a three lead wire system. This system is imperative if errors resulting from resistance changes within the lead wires are to be cancelled by adding the resistance error to each leg of the half bridge completed in the instrument head. Sources of resistance error are changes in wire temperature, straining the lead wires, and plug contact resistance.

Desensitization errors result from the added resistance of long readout cables. This was corrected by a calculated reduction of the gauge factor.

Two diametrically opposed gauges mounted on a length of 22 m thread bolt were tested in direct tension and bending. Strains measured by the gauges and those recorded independently with linear variable differential transformers were compared. At up to 50 percent of the rebar yield strength (1,000 micro-strains), strains correlated to within three percent. The elastic modulus of the steel was calculated as 30.5 million pounds per square inch.

Information on the long term gauge creep and stability was obtained through a personal communication.* Gauges welded to a specially treated cantilever beam were subjected to an initial strain of 1,000 micro-strains. After two years at constant load and temperature (21°C), creep resulted in 1.5 percent decrease in measured strain.

Of all the possible error producing factors considered in this appendix, none were significant enough to merit correction of the strain data.

---

* Al Johnson, Pacific Gas and Electric Research Station, San Ramon, California.

APPENDIX 3

EXTENSOMETER DESIGN, CONSTRUCTION, AND INSTALLATION

Design and Construction

Design and construction of the four position rod type extensometers used at the North Bonneville Tunnel were carried out to specifications by Terrametrics. As illustrated in Figure A3-1, the extensometer was basically composed of six principal components. These are:

1. A wooden telltale attached to the first anchor. It was used to locate the extensometer from within the tunnel.
2. Four hydraulically activated anchors and hydraulic tubing. As pictured in Figure A3-2, each anchor consisted of three expandable copper jackets. When inflated, the jackets can extend up to five inches into the surrounding material, Figure A3-1. Hydraulic pressure to set the anchors was obtained through a small diameter tube connected to the anchor and to a pump on the surface, Figure A3-3.
3. Four three-eighths inch diameter aluminum measuring rods. Each of the rods were attached to one of the four anchors. Rod lengths between the anchors and reference head, Figure A3-4, varied between 150 and 190 feet.
4. One inch diameter sealtite conduit. For protection, the four measuring rods were encased in oil filled conduit. The diameter of the rods and conduit were such that the rods moved freely, but did not have excessive lateral motion.

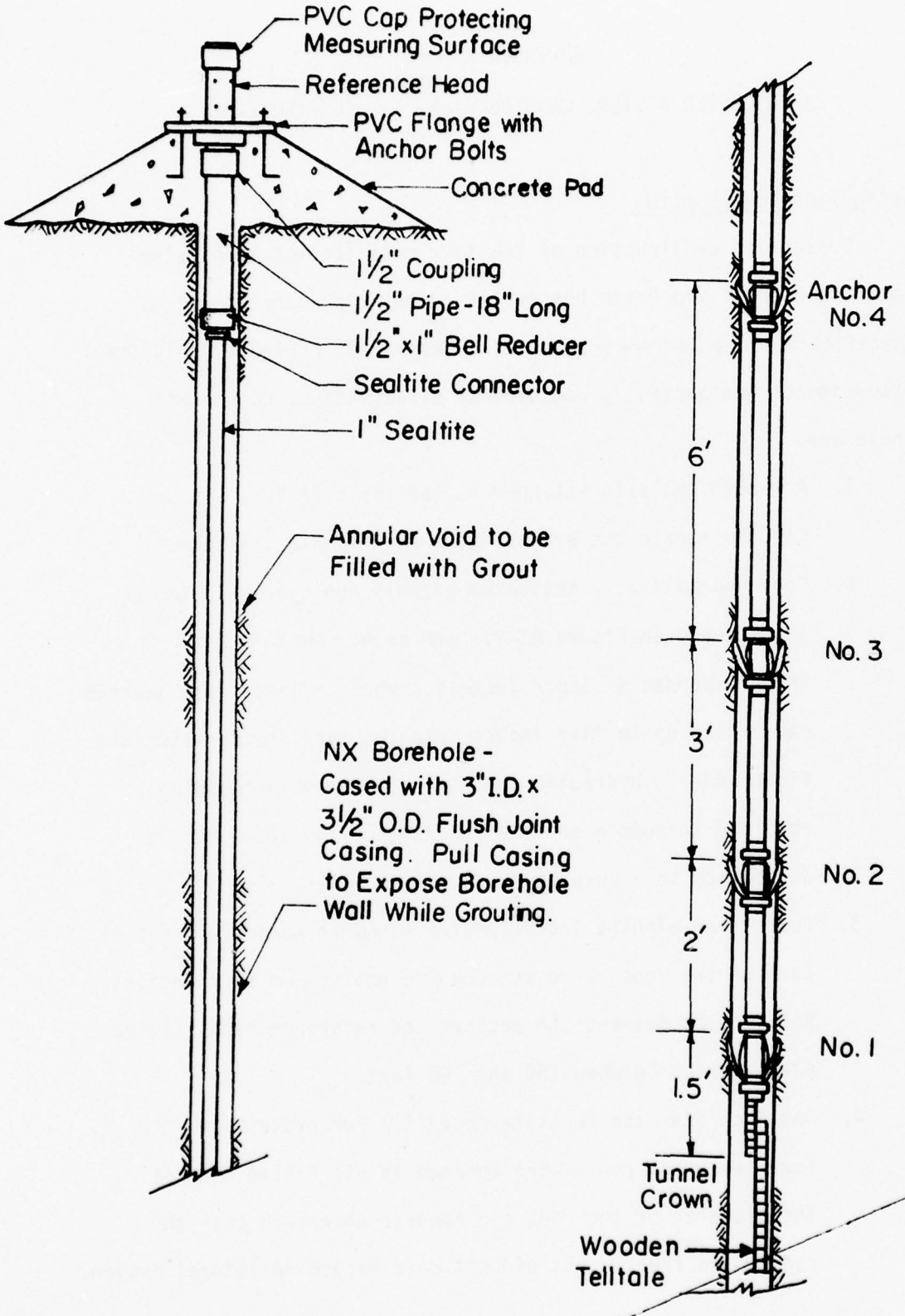

FIG. A3-1. Extensometer Design, Construction, and Installation (Terrametrics Inc.)

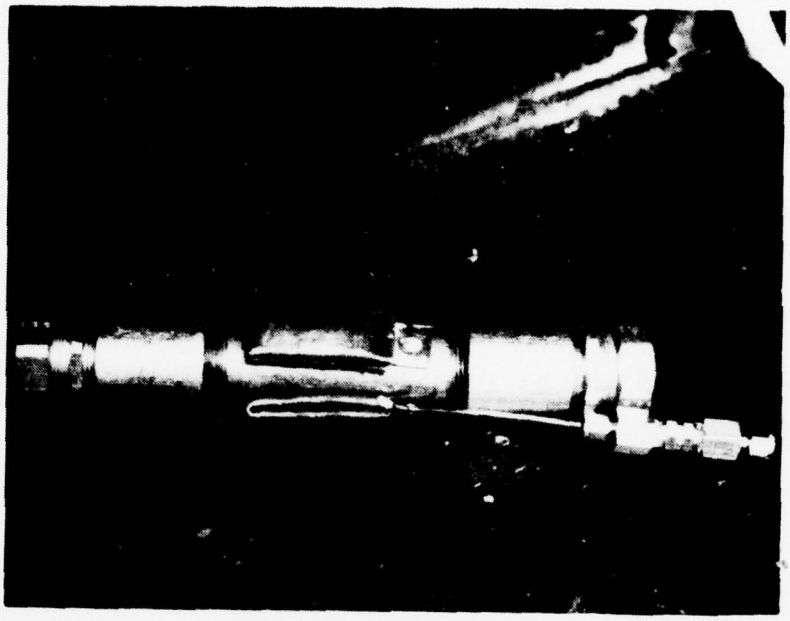

FIG. A3-2. Extensometer Anchor, Hydraulicly Activated

FIG. A3-3. Setting Anchors with Hydraulic Pump

This reduced errors resulting from the spiraling of the buckled rods within the conduit. Oil helped to reduce friction between rods and prevent corrosion.

5. Galvanized collar anchor standpipe and PVC flange. This portion was encased within the concrete pad, Figure A3-1.
6. Reference head with stainless steel measurement surface. Pictured in Figure A3-4, the head was the reference point at which the rise and/or fall of the rods were measured. A protective cap was placed over the measurement surface to keep out dirt and water.

The readout unit was simply a mechanical depth micrometer placed on the measurement surface. It had an accuracy of one-thousandth of an inch and, with extension rods, was capable of recording a measuring rod change of up to six inches. The extensometer was designed to accomodate a maximum of six inches of relative displacement between the anchors and reference head. Overall accuracy of the extensometer was believed to be about ten-thousandths of an inch. This was mainly a function of the measuring rod length.

Installation

Vertical holes drilled from the surface, directed to intersect the tunnel center line were used for subsurface exploration as well as extensometer installation. The recovered core was examined to determine the suitability of the ground above the future tunnel crown. It was desirable to have the entire test station of spiles and extensometer anchors within a relatively homogeneous rock mass. Since the ground was of poor quality, it was necessary to case the

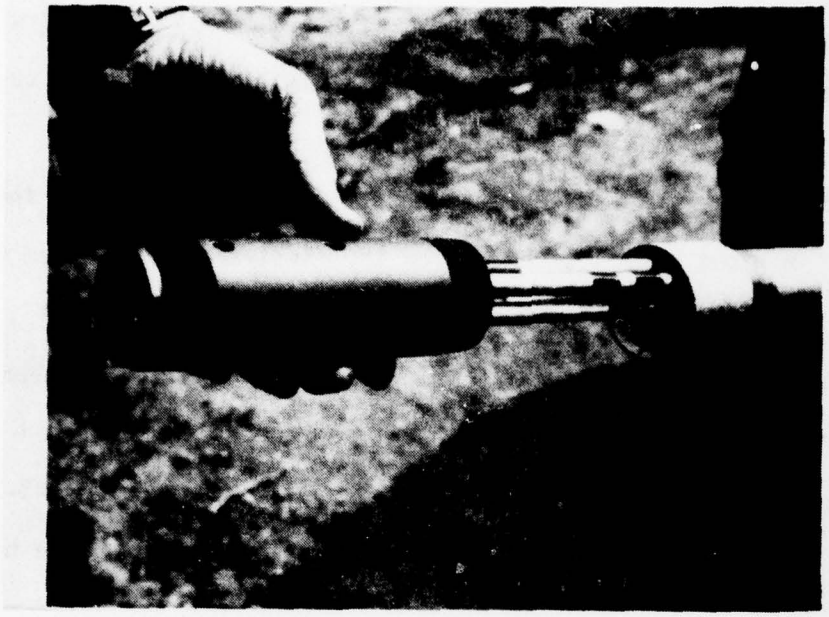

FIG. A3-4. Reference Head and Measuring Rods

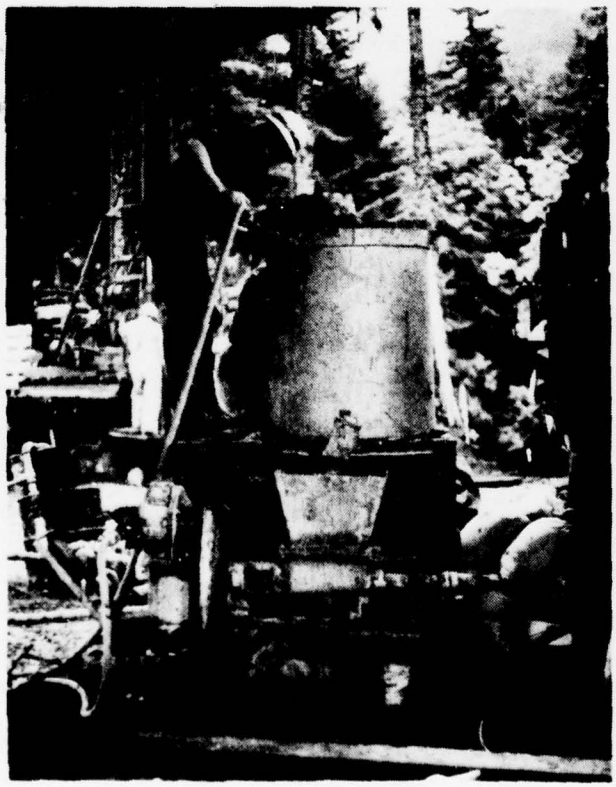

FIG. A3-5. Grout Mix Tank and Pump

entire length of the hole. Once completed, the hole was surveyed with an inclinometer to make sure that it was reasonably close to the tunnel center line.

The extensometer was assembled on the site and lowered into the cased hole. A grout line attached below the first anchor was used to nearly fill the hole with a weak bentonite-cement grout. Several lengths of casing were subsequently removed and more grout was added. This was repeated until all casing was out and the hole was filled with grout. All anchors were set with a hydraulic pump, Figure A3-3. Finally, a small concrete pad was constructed below the reference head.

Grout, used to fill the void between the bore hole and extensometer, was a low strength bentonite-cement mix. A low strength mix was necessary to insure that the grout would not significantly strengthen the surrounding rock mass, either through the grout column itself or by cementation of joints intersecting the hole. Inspection of the rock surrrounding the extensometer following tunnel excavation revealed many joints filled with grout. This was expected, considering the large amount of material placed with respect to the volume of the hole. The grout mix tank and pump are pictured in Figure A3-5.

Proportions of water, bentonite and cement by weight were 4.5 : 0.4 : 1.0. Strength tests on 90 day old field cast specimens resulted in average unconfined compressive strengths of 65 psi and tensile strengths of 19 psi.

After the grout had become firm, usually in two days, the measuring rods were released from the reference head. Initial readings were taken, followed by daily monitoring until the system

stabilized. This required approximately seven days, at which point the extensometer was ready for service.

APPENDIX 4

DATA REDUCTION

Spiles (Bonneville and Eisenhower Tunnels)

Spiles instrumented with weldable strain gauges measured the average change in strain due to the axial shortening or lengthening over a distance of one inch. With the proper gauge factor, including compensation for readout cable desensitization, the strain was obtained directly from the external instrumentation.

For those spiles designed to record bending as well as axial strain, the bending strain is the average of the difference between the bottom and top gauges. Axial strain is the simple average of the bottom and top gauges. To change from strain to stress, the strain is multiplied by the elastic modulus of steel, thirty million pounds per square inch.

Extensometers (Bonneville Tunnel)

Extensometers installed from the ground surface prior to tunnel excavation supplied the ground deformation history for a vertical line above the crown. To correlate the strain within the rock mass (as deduced from extensometer data) for a particular position, direction, and time with that measured within the spile required transformation of the extensometer data. First, it was necessary to reduce the vertical distributions of deformation to strain. Second, transform the strain distributions from the vertical direction to the direction of the spile. Last, interpolate the data in position and time as required to match a particular spile strain gauge position and time of reading.

Calculating the axial strain from the relative displacement of several extensometer anchors is simple in principle. Consider the example shown in Figure A4-1. Given the displacement of four anchors at a specific time, an approximating continuous distribution curve, $u = f(r, t_1)$, is obtained. The slope of this curve is the strain. Problems arise when the data points fail to depict a smooth, well behaved function. For example, if point 2 is located at A, selecting an appropriate distribution curve is more difficult. Several possible curves could be generated, some connecting all data points and others a form of best fit between the points. Slopes derived from the various curves at a specific position would give rise to different values of strain. Since it was often difficult to pick the "best" curve, several distribution functions were used and compared in obtaining values for strain. Four different functions were used. They are described in the next section of this Appendix.

It is worth noting that incorporating a smooth, continuous function which monotonically decreases with increasing distance from the tunnel opening is appropriate for grounds which behave as a continuum. However, joints and other discontinuities invalidate this concept. The strain may be higher at points farther from the opening than at the surface. This fact complicates strain calculations and further necessitates the use of several approximating functions.

Transformation of the strain distributions from the vertical direction to the orientation of the spile requires two assumptions. First, the vertical direction is a principal direction of strain. Second, the strain along the tunnel axis is assumed to be zero, a

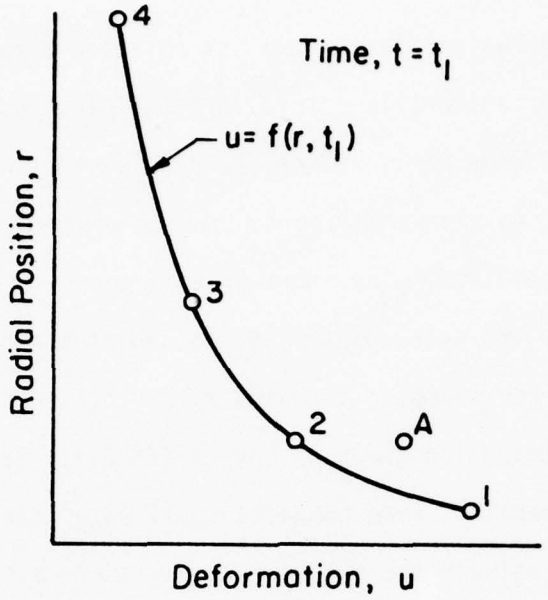

FIG. A4-1. Radial Deformation Distribution as Derived from Extensometer Results

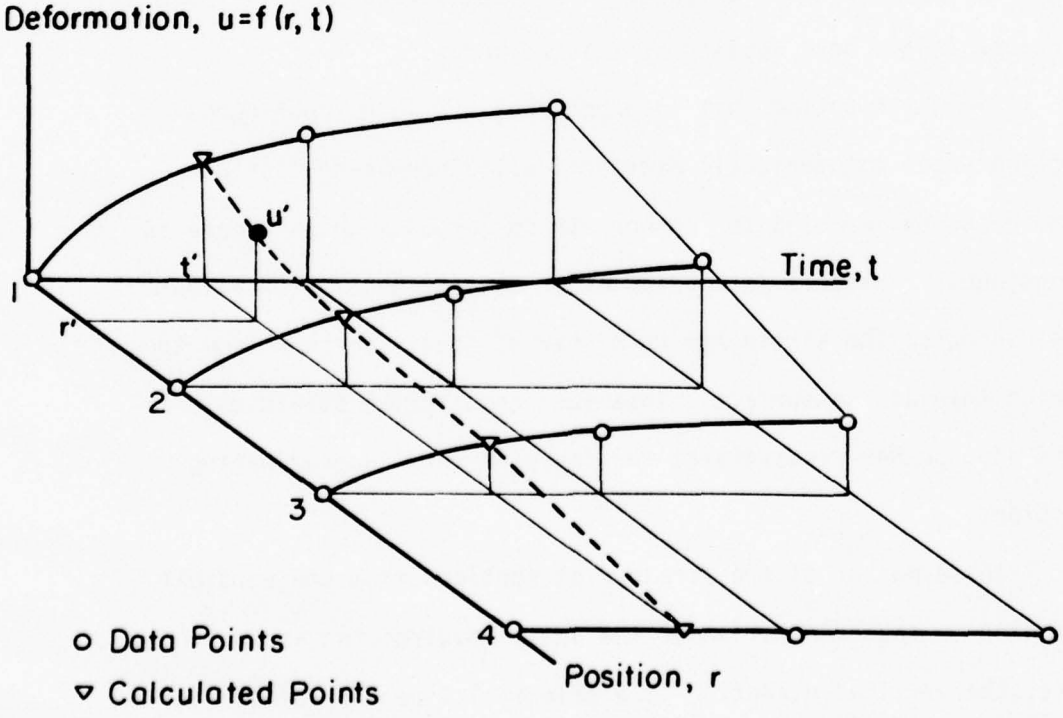

FIG. A4-2. Interpolation on Deformation Surface in Terms of Time and Radial Position

plane strain condition. Both assumptions are close to reality. In the region of the spile, the strain in the orientation of the tunnel axis is not zero, but is small when compared to that in the vertical direction. Based on the previous assumptions,

$$\varepsilon_s \simeq \varepsilon_v \cos^2\theta$$

is the transformation of vertical strain ε_v to strain in the orientation of the spile, ε_s. For bars installed at the test stations the angle θ, measured from the vertical to the spiles, is 60 degrees.

Interpolation Functions

As previously mentioned, the correlation of rock mass and spile behavior required interpolation. This is illustrated with the hypothetical surface in Figure A4-2. "Data Points" represent ground deformation at discrete times and positions as recorded by a four position extensometer. Assume an instrumented spile strain gauge is located at position r' and is read at time t', the points at which the correlation is to be made. The interpolated deformation distribution at time t', required for calculation of strain at u', is derived from the "Calculated Points" as shown by the stippled curve. "Calculated Points" are obtained from interpolation in the deformation-time plane at each of the fixed anchor positions. Hence, a total of two interpolations are needed to find the deformation or strain at u'.

The accuracy of this interpolating scheme rests with the choice of interpolating functions. Four different functions were selected for this study. In order of increasing smoothness imparted to the data the functions employed were:

a) Linear. Linear interpolation is derived from a straight line connecting the two data points which bracket the point in question, Figure A4-3. It provides no smoothing and contains all data. Slopes of the function are constant between data points and are averaged at intersections (e.g. data point 2).

b) Parabolic Fairing. A total of four points are required to apply this technique. As shown in Figure A4-4, two sets of three points each are used to obtain the equations of two parabolic curves with either a fixed horizontal or vertical axis. The two solutions are blended at the point in question, x', by averaging the values of the ordinate. If two consecutive points lie either in a horizontal or vertical line, the routine connects these two points with a straight line. The result is a well behaved trend curve such that there is maintained a one-to-one correspondence between the relative extremes in the data and the relative extremes implied by the curve. This function provides for more smoothing than a straight line, but still contains all data points.

c) Least Square Blend. This scheme is similar to that of parabolic fairing. Instead of combining the solution of two parabolas, two least square solutions to Hoerl's equation are blended. Hoerl's equation,

$$y = ax^b e^{cx}$$

is solved for two sets of three points in a least squares sense. The least square blend results in a smoother function than parabolic fairing. Data points are no longer a part of the function, yet they are within the neighborhood.

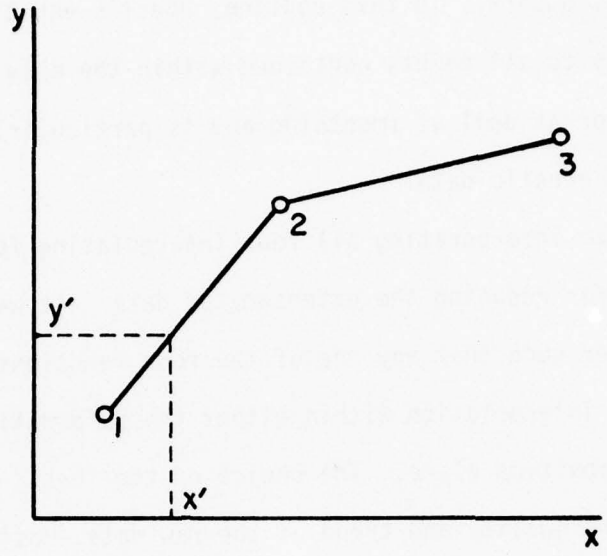

FIG. A4-3. Linear Interpolation

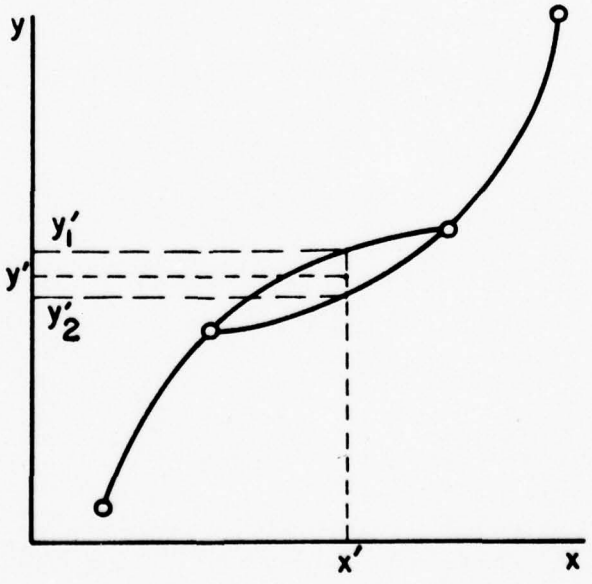

FIG. A4-4. Interpolation by Parabolic Fairing with Blend

d) Least Square. In this routine, Hoerl's equation is again employed only to all points contained within the data set. This provides for a great deal of smoothing and is particularly useful in working with erratic data.

A program incorporating all four interpolating functions was established for reducing the extensometer data. It was written in a general manner such that any one of the four functions could be selected for interpolation within either the deformation-time or deformation-position plane. The choice of the "best" function was related to the quality and trend of the raw data. Most often, several functions were used and the results compared.

APPENDIX 5

INSTRUMENTED REINFORCEMENT STRESS DISTRIBUTIONS

Radial stress distributions were obtained at three separate times and positions of the advancing face for each set of instrumented spiles installed at all test stations. The first distribution was derived after excavating two-thirds of the distance beneath the cover provided by the spiles. This was five feet beyond the initial position for stations at the Bonneville tunnels, and roughly eight feet at the Eisenhower Tunnel. A second distribution was obtained as soon as the face had advanced to a point where it no longer influenced the reinforcement behavior, approximately 15 feet in the pilot tunnel and 25 feet in the main bore at Bonneville, and 50 feet at the Eisenhower Tunnel. The final distribution, identified as long term, was produced from the last recorded set of data.

Distributions were obtained with the aid of a least square routine employing Hoerl's function,

$$y = ax^b e^{cx}$$

where the independent variable was radial position and the dependent variable measured stress. By incorporating a least square routine, the probability of achieving a "best" fit for all data points was increased.

An index to all radial stress distributions is presented in Table A5-1. Also included are the face position and time at which each distribution was derived.

TABLE A5-I

Radial Stress Distribution Index

Tunnel	Test Station	Figure Number	Advance Beyond Initial Position (FT.)	Time (HRS.)
Bonneville Pilot	No. 1&2	A5-1	5	4, 4
		2	15	22, 24
		3	L.T.	8000, 8373
Bonneville Main	No. 1&2	4	-120, -65	0, 0
		5	5	65, 47
		6	25	95, 115
		7	L.T.	4945, 4222
Eisenhower (Spiles)	58+86	8	8	2
		9	50	44
		10	L.T.	5359
	63+01	11	0	1 to 6
		12	8	31
		13	50	151
		14	L.T.	4185
	70+14	15	6	2
		16	50	71
	72+36	17	0	1 to 6
		18	12	85
		19	50	191
		20	L.T.	1970
	73+42	21	0	3 to 8
		22	8	6
		23	50	43
		24	L.T.	1656
	80+87	25	8	16
		26	50	150
		27	L.T.	986
Eisenhower (radials)	63+06	28	L.T.	4185
	72+46	29	L.T.	1970

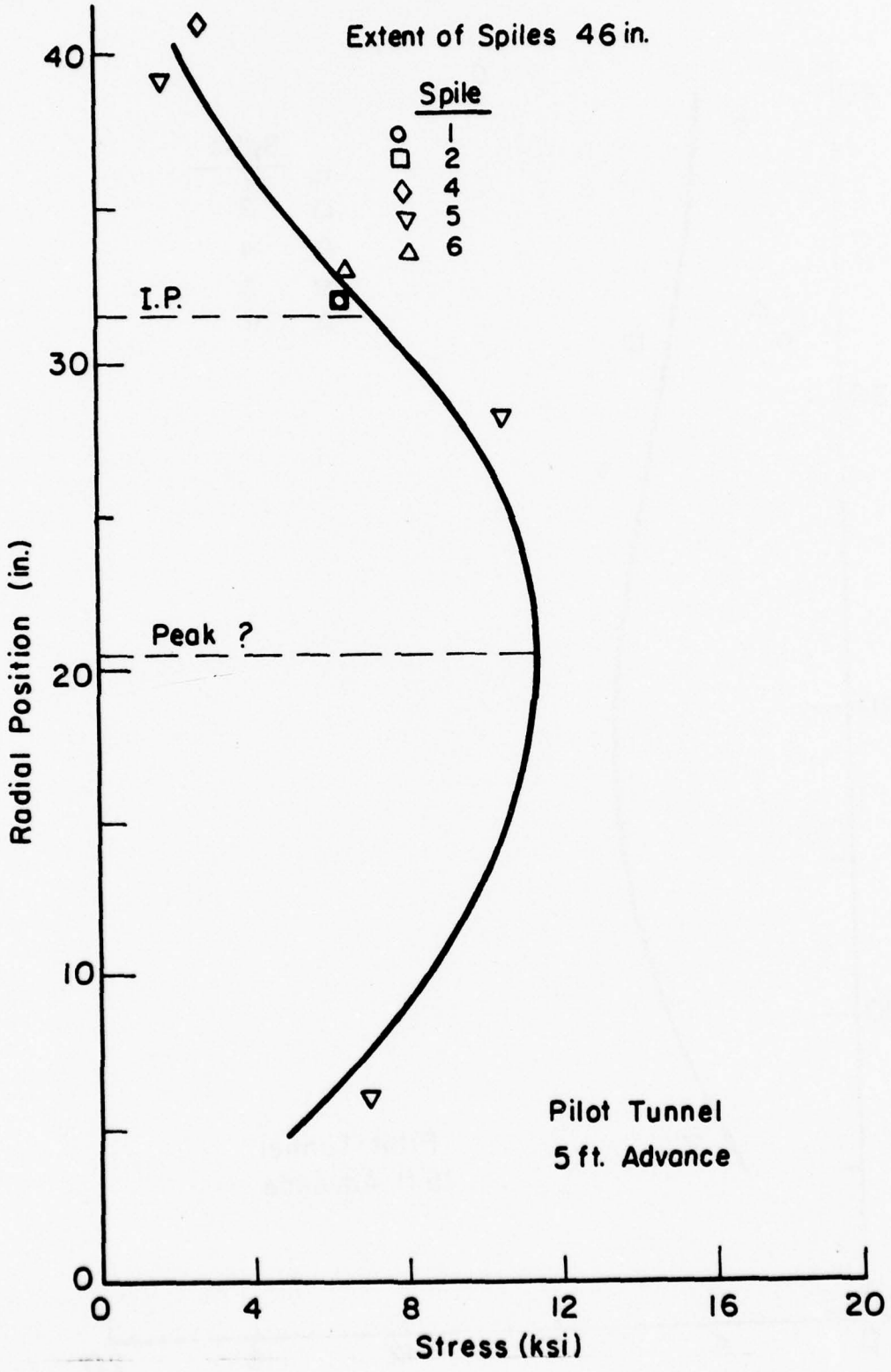

FIG. A5-1. Bonneville Pilot Tunnel Radial Stress Distribution, 5 ft. Advance

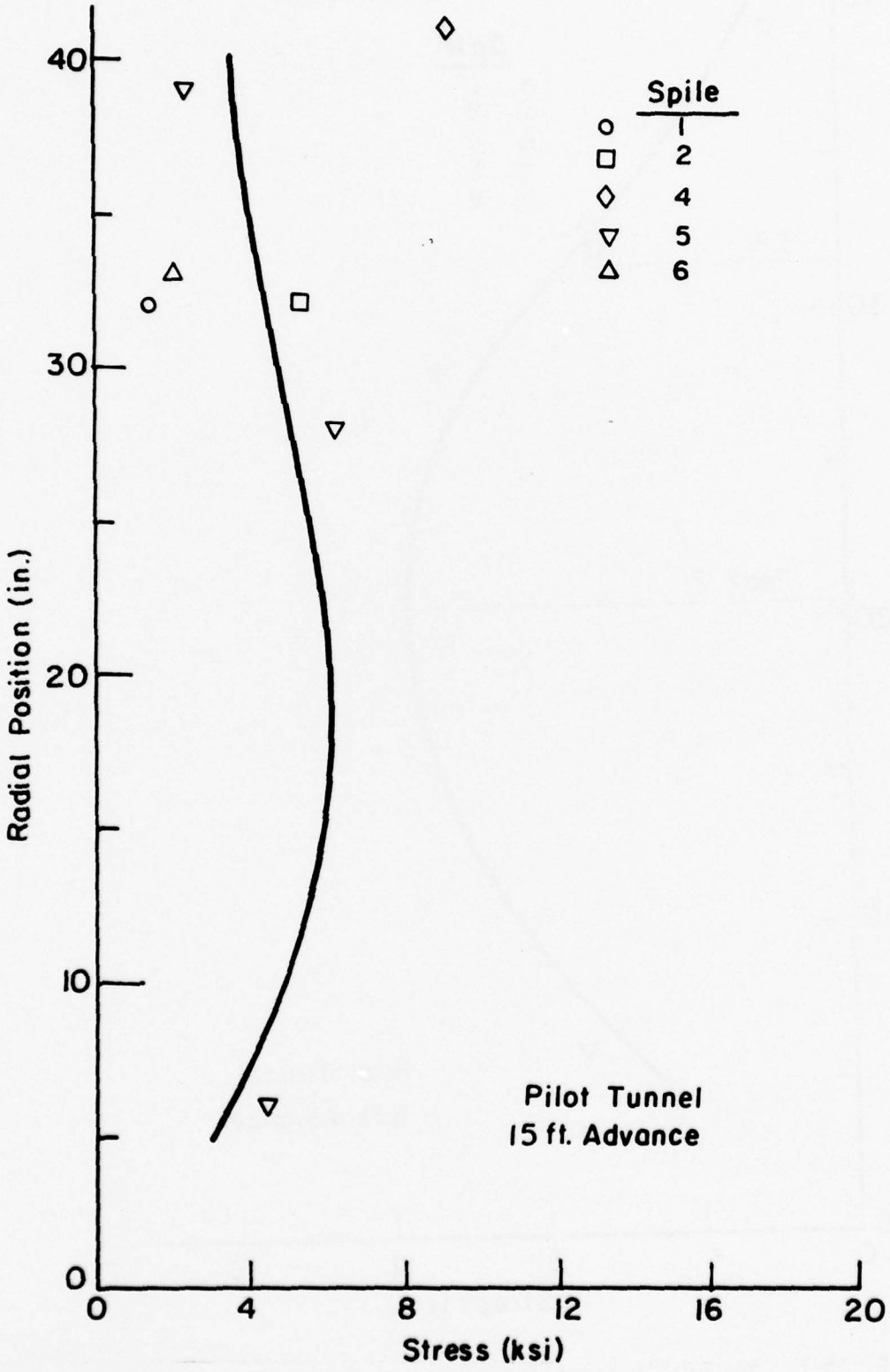

FIG. A5-2. Bonneville Pilot Tunnel Radial Stress Distribution, 15 ft. Advance

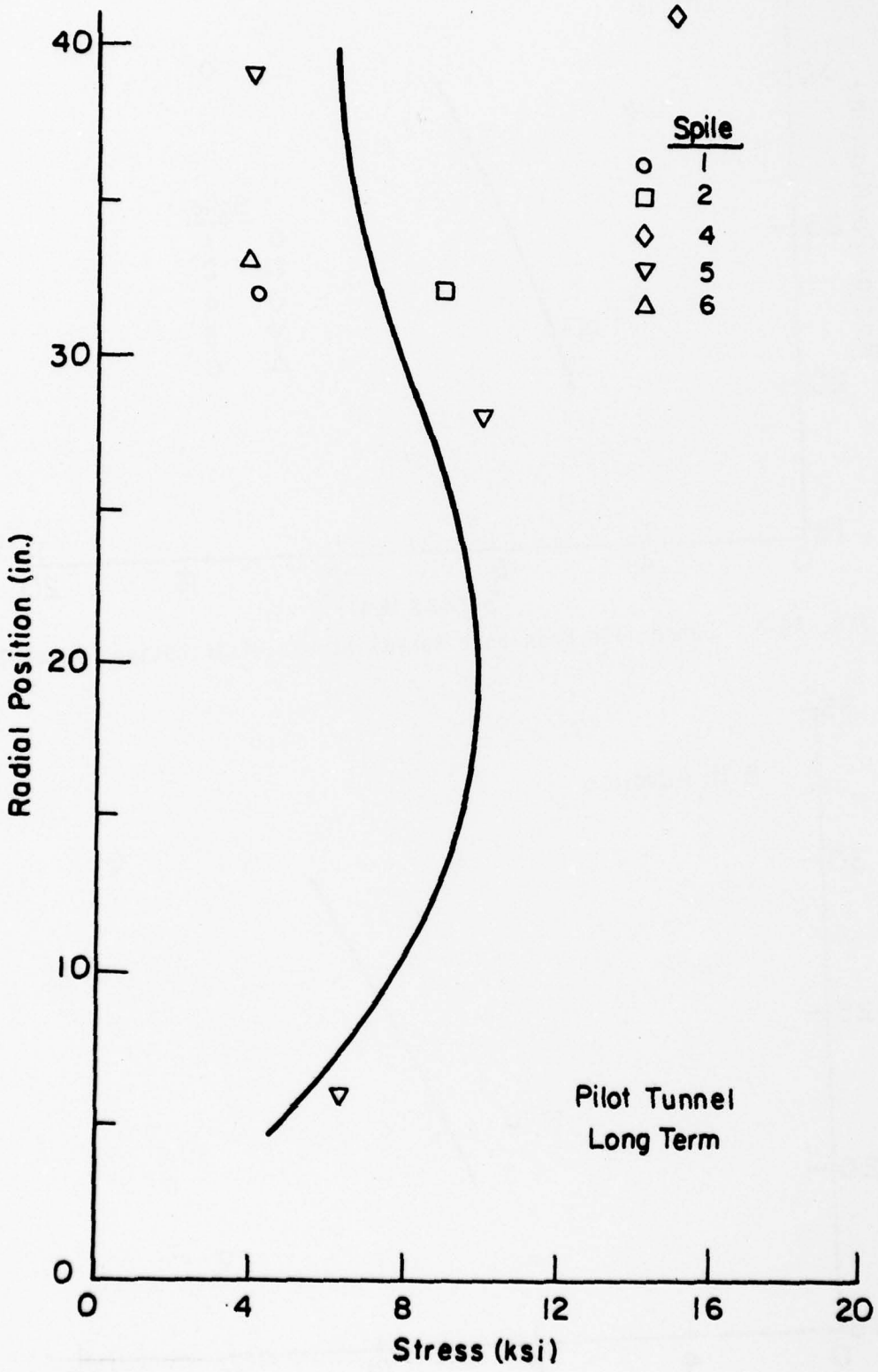

FIG. A5-3. Bonneville Pilot Tunnel Radial Stress Distribution, Long Term

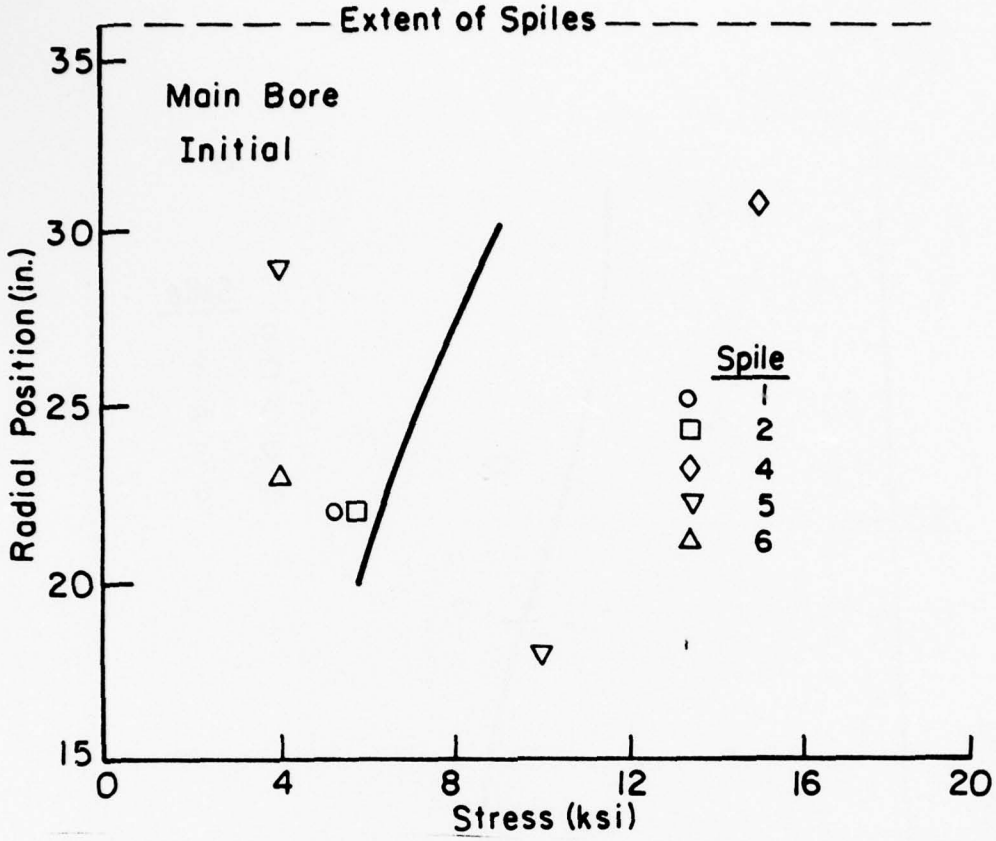

FIG. A5-4. Bonneville Main Bore Radial Stress Distribution, Initial

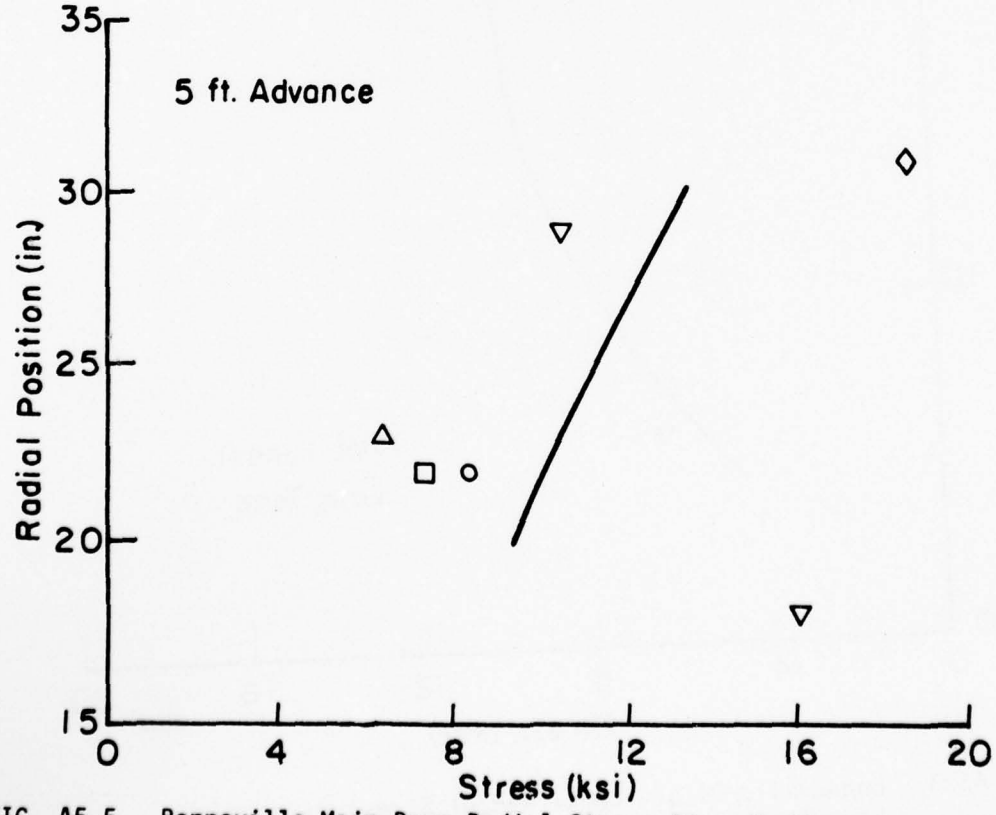

FIG. A5-5. Bonneville Main Bore Radial Stress Distribution, 5 ft. Advance

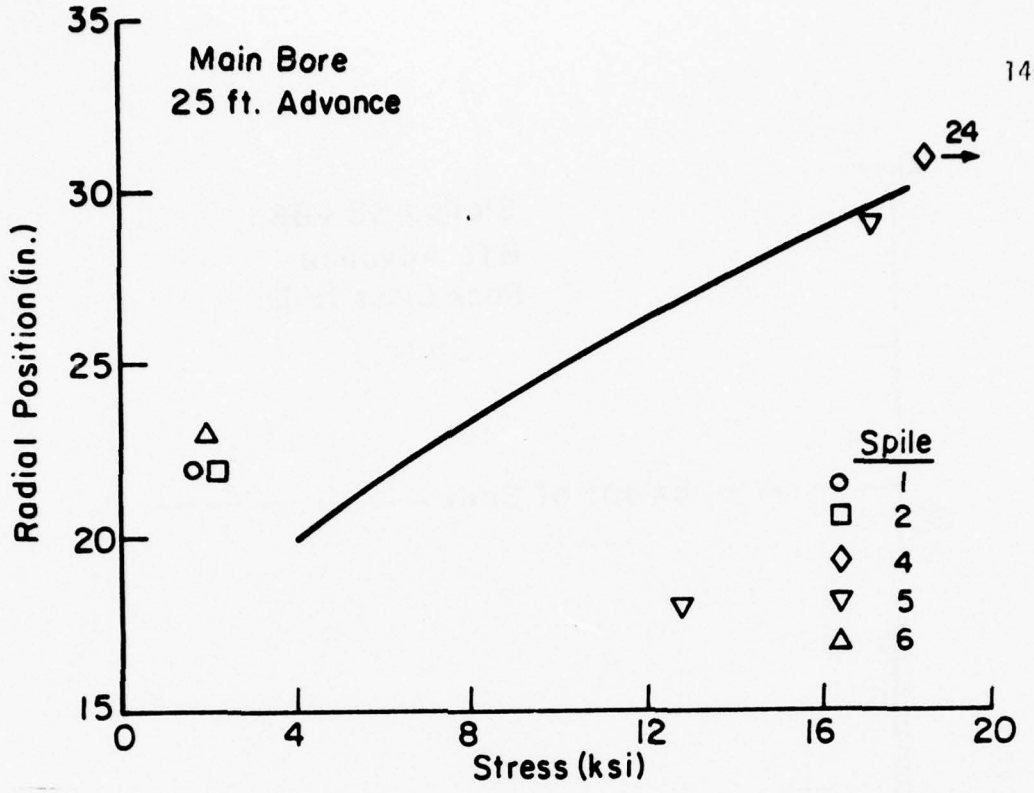

FIG. A5-6. Bonneville Main Bore Radial Stress Distribution, 25 ft. Advance

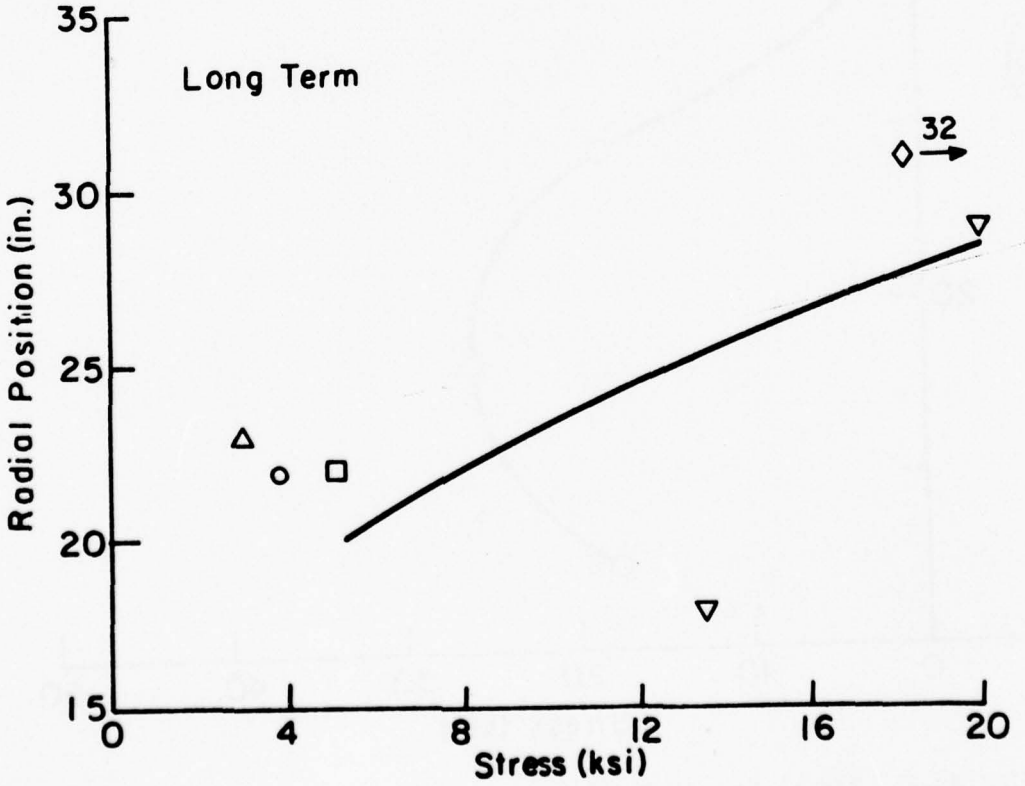

FIG. A5-7. Bonneville Main Bore Radial Stress Distribution, Long Term

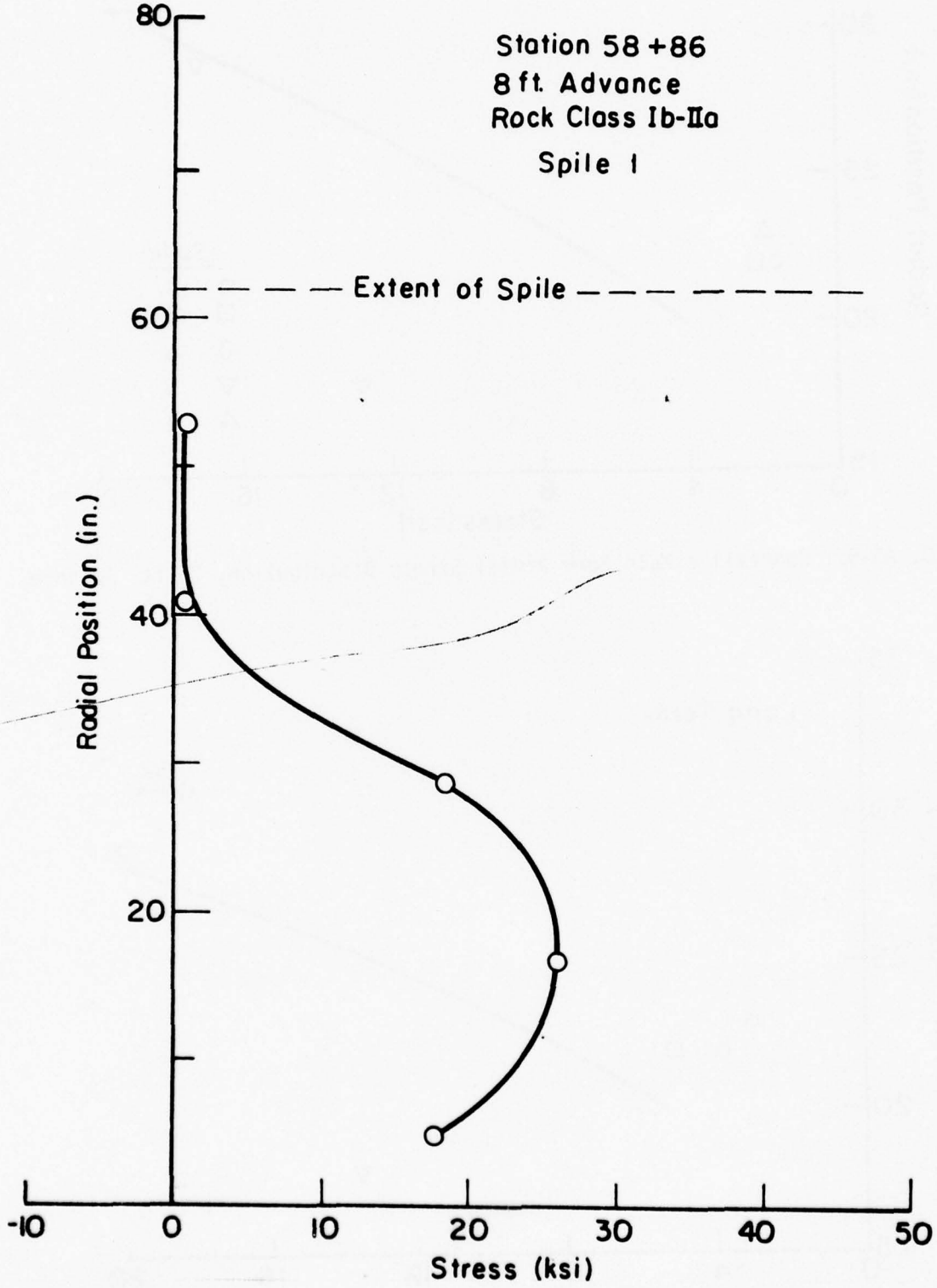

FIG. A5-8. Radial Stress Distribution, Test Station 58+86, 8 ft. Advance

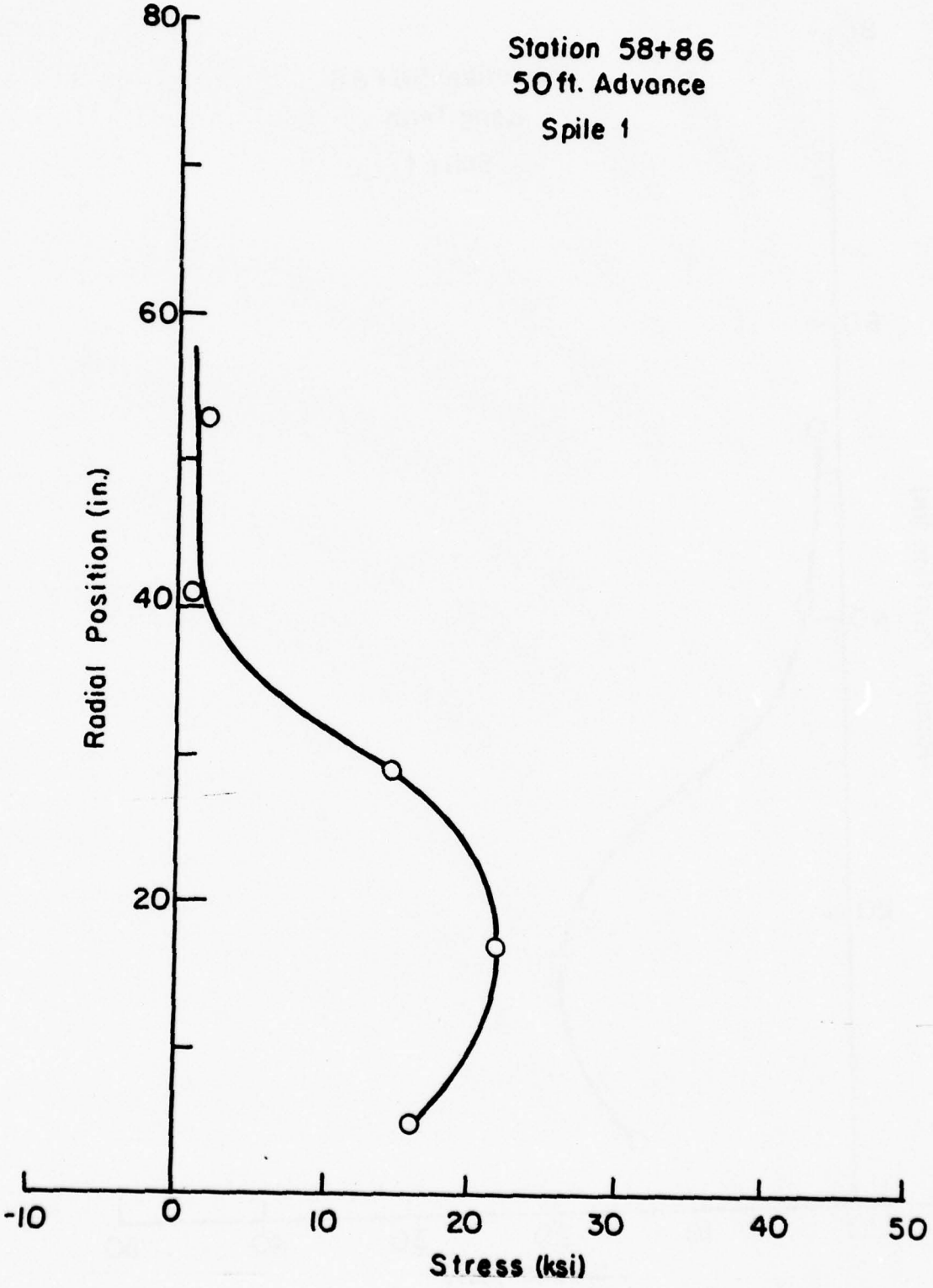

FIG. A5-9. Radial Stress Distribution, Test Station 58+86, 50 ft. Advance

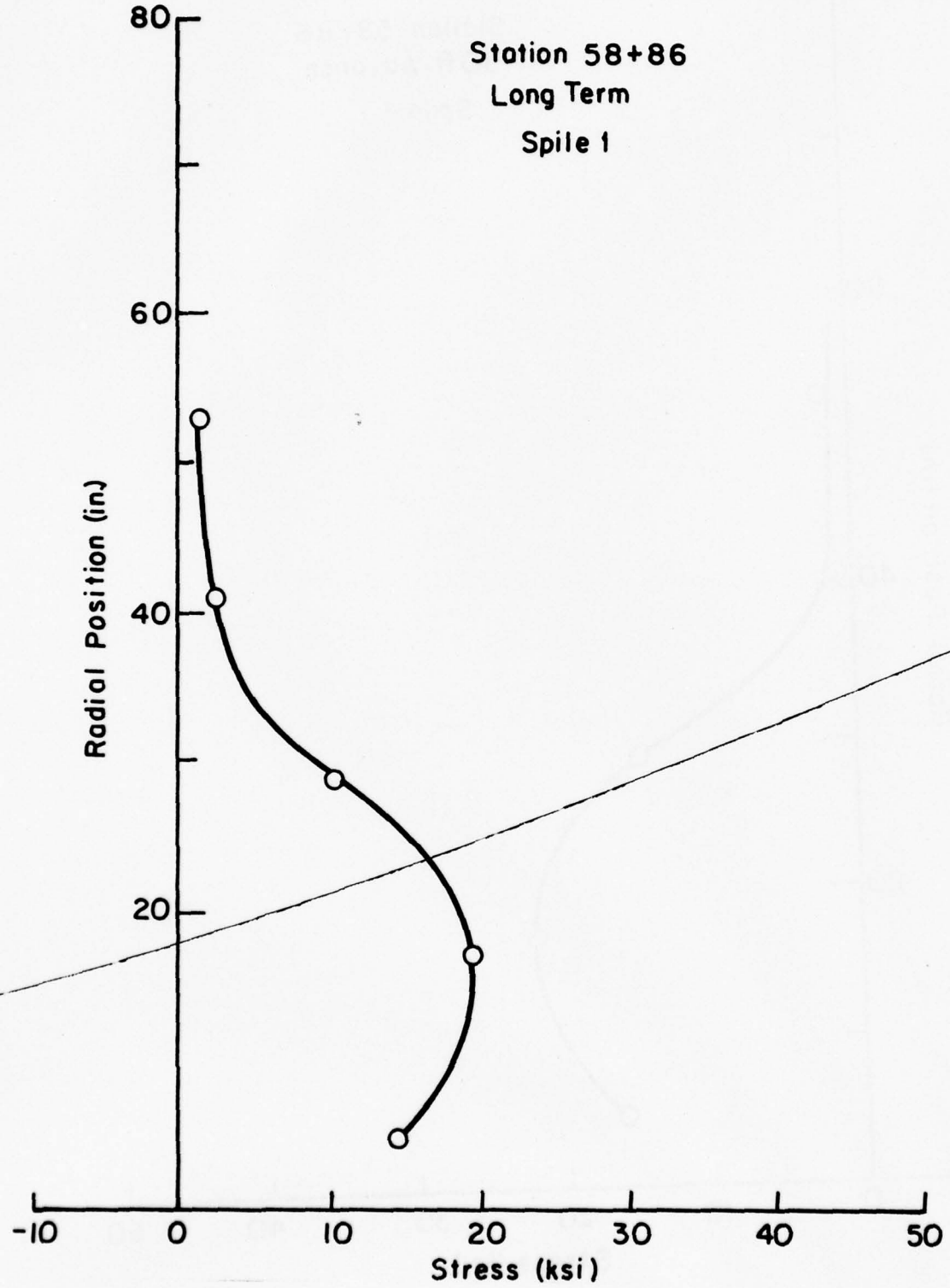

FIG. A5-10. Radial Stress Distribution, Test Station 58+86, Long Term

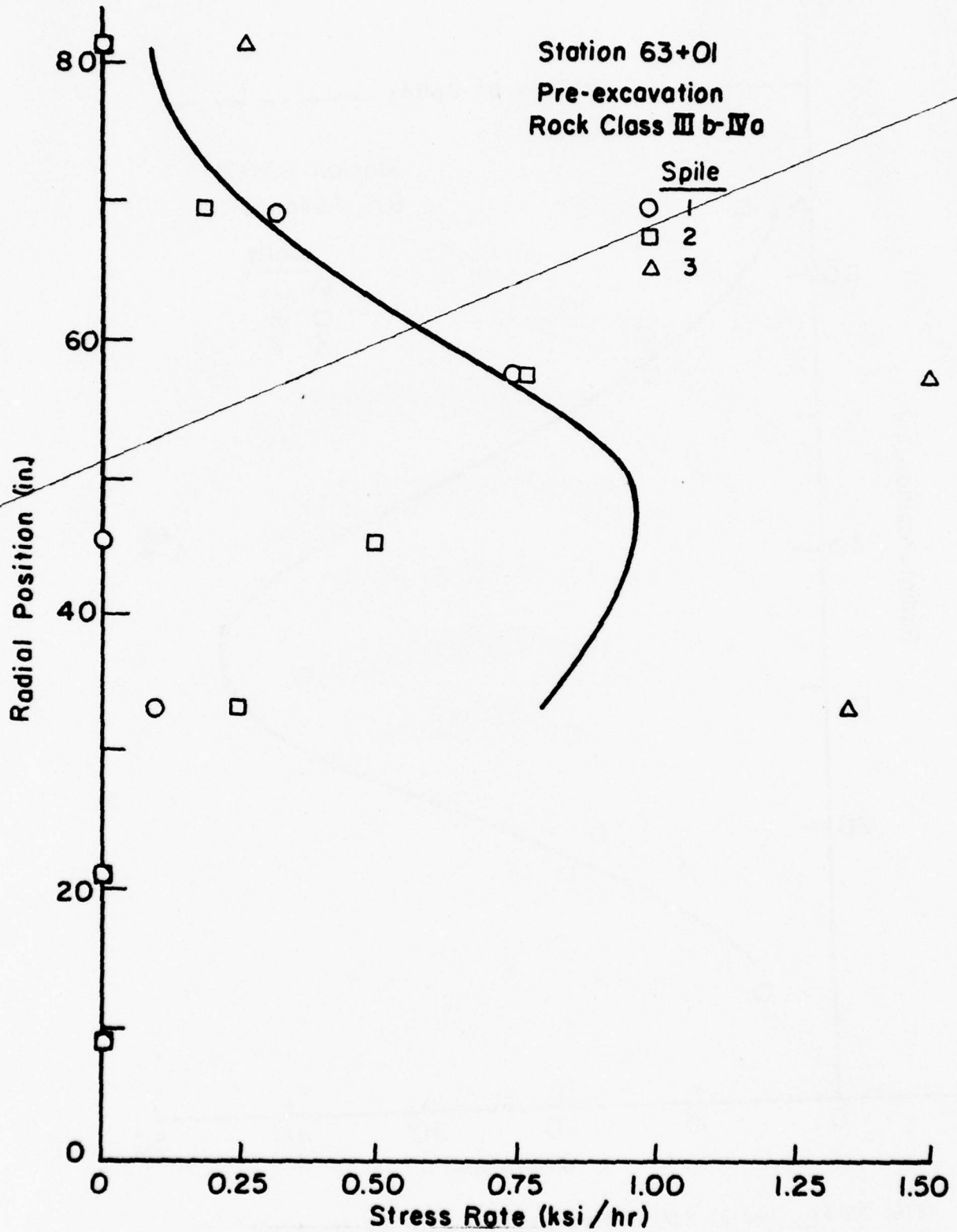

FIG. A5-11. Radial Stress Distribution, Test Station 63+01, Pre-excavation

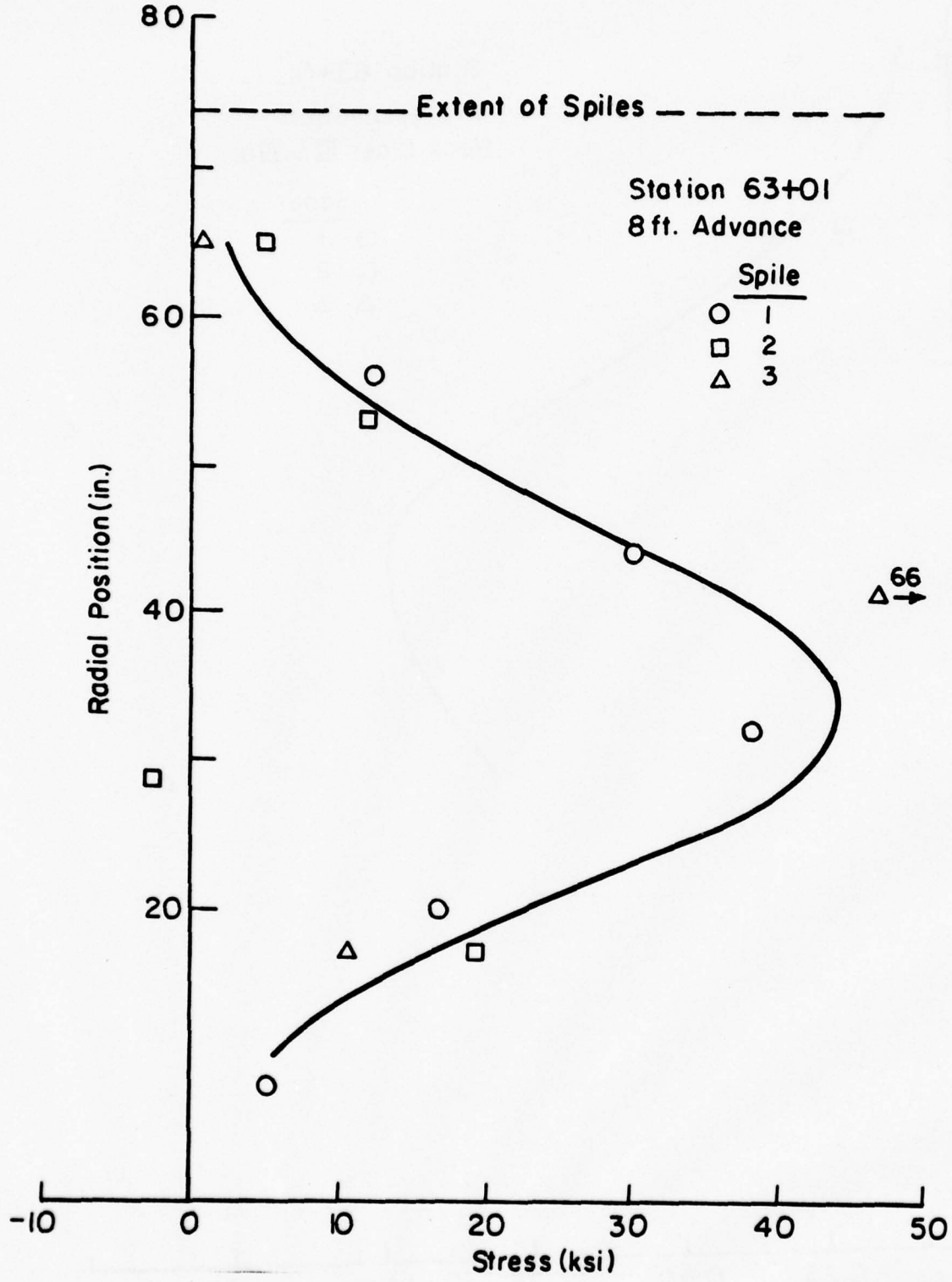

FIG. A5-12. Radial Stress Distribution, Test Station 63+01, 8 ft. Advance

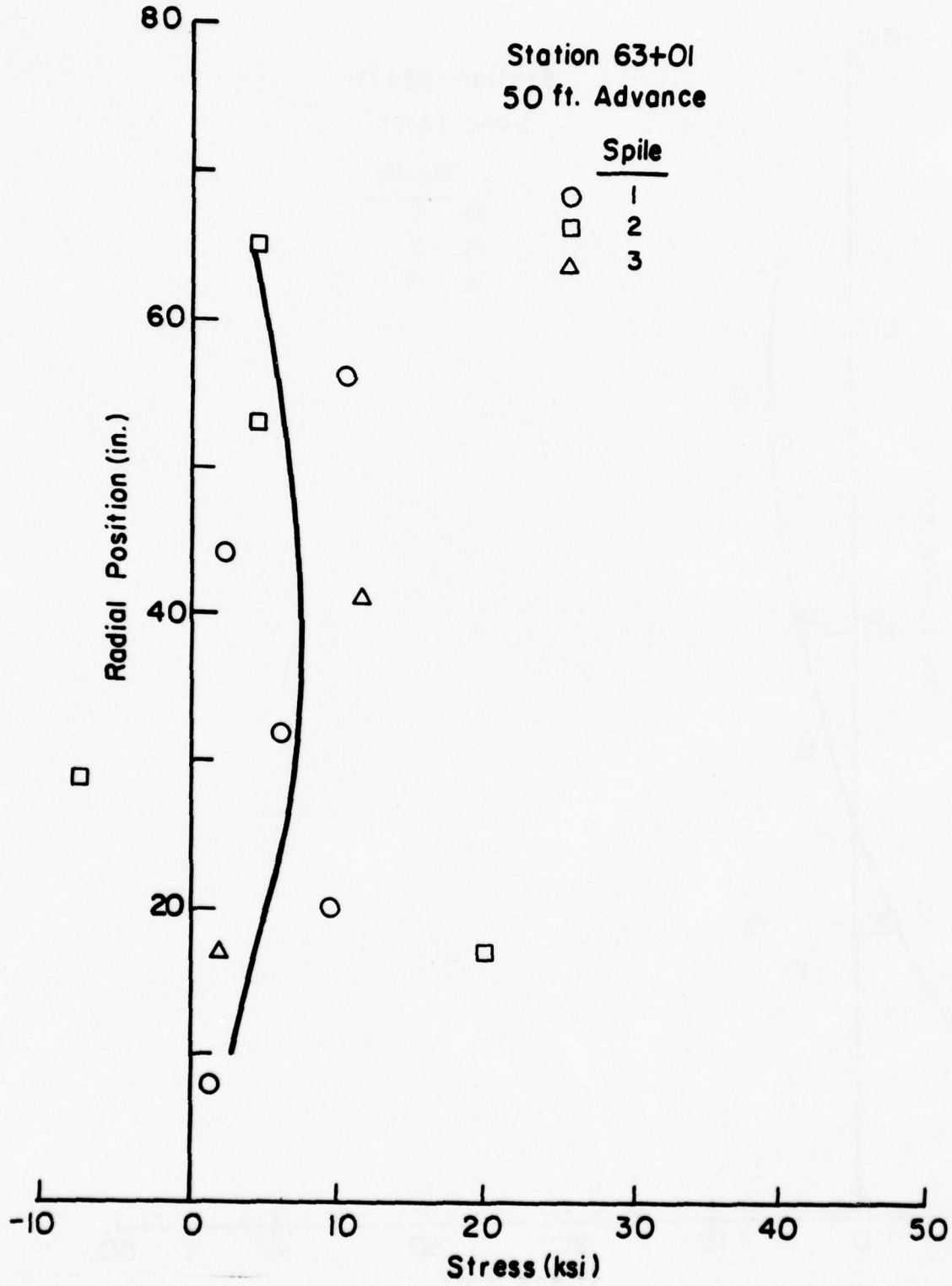

FIG. A5-13. Radial Stress Distribution, Test Station 63+01, 50 ft. Advance

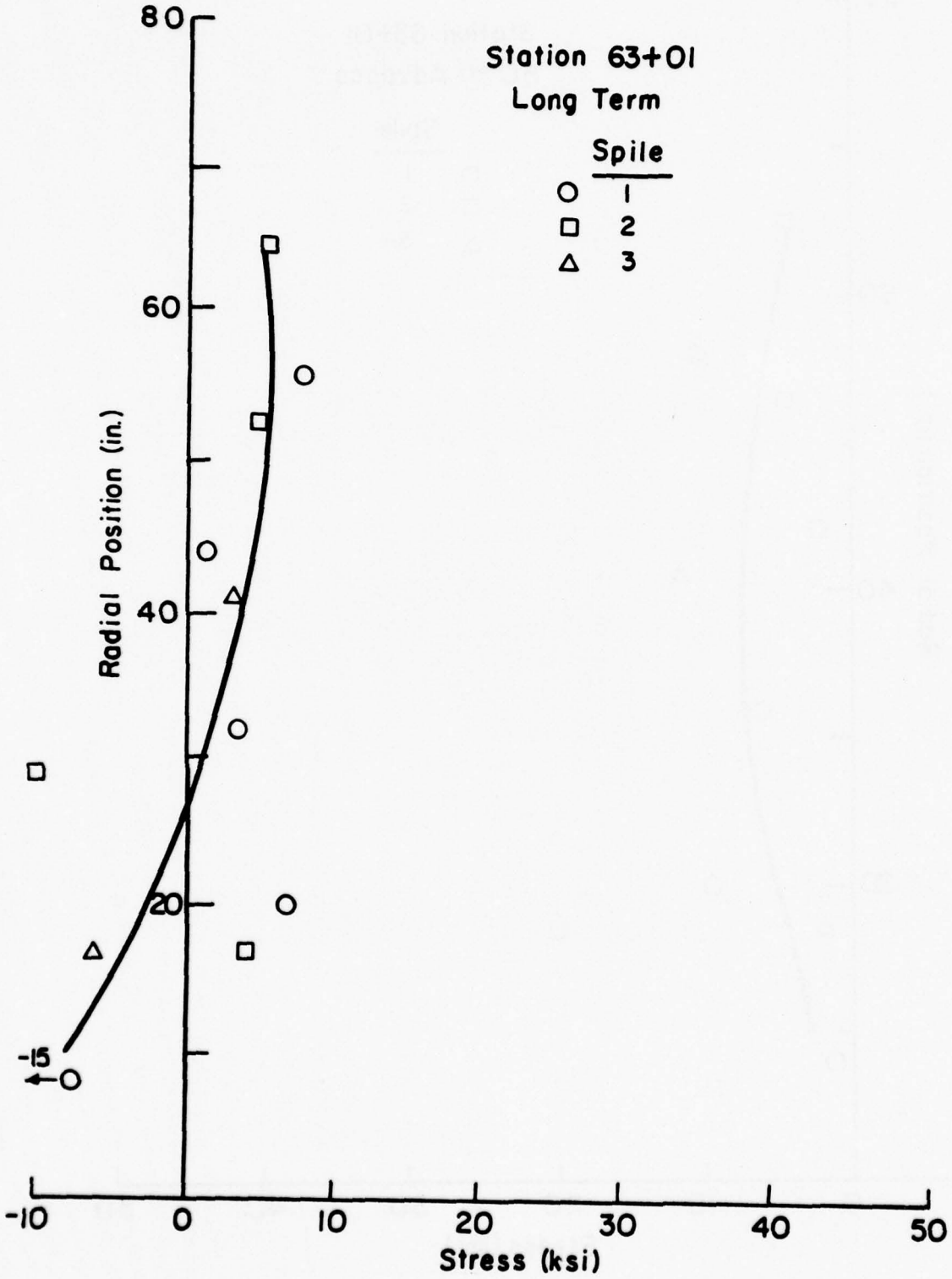

FIG. A5-14. Radial Stress Distribution, Test Station 63+01, Long Term

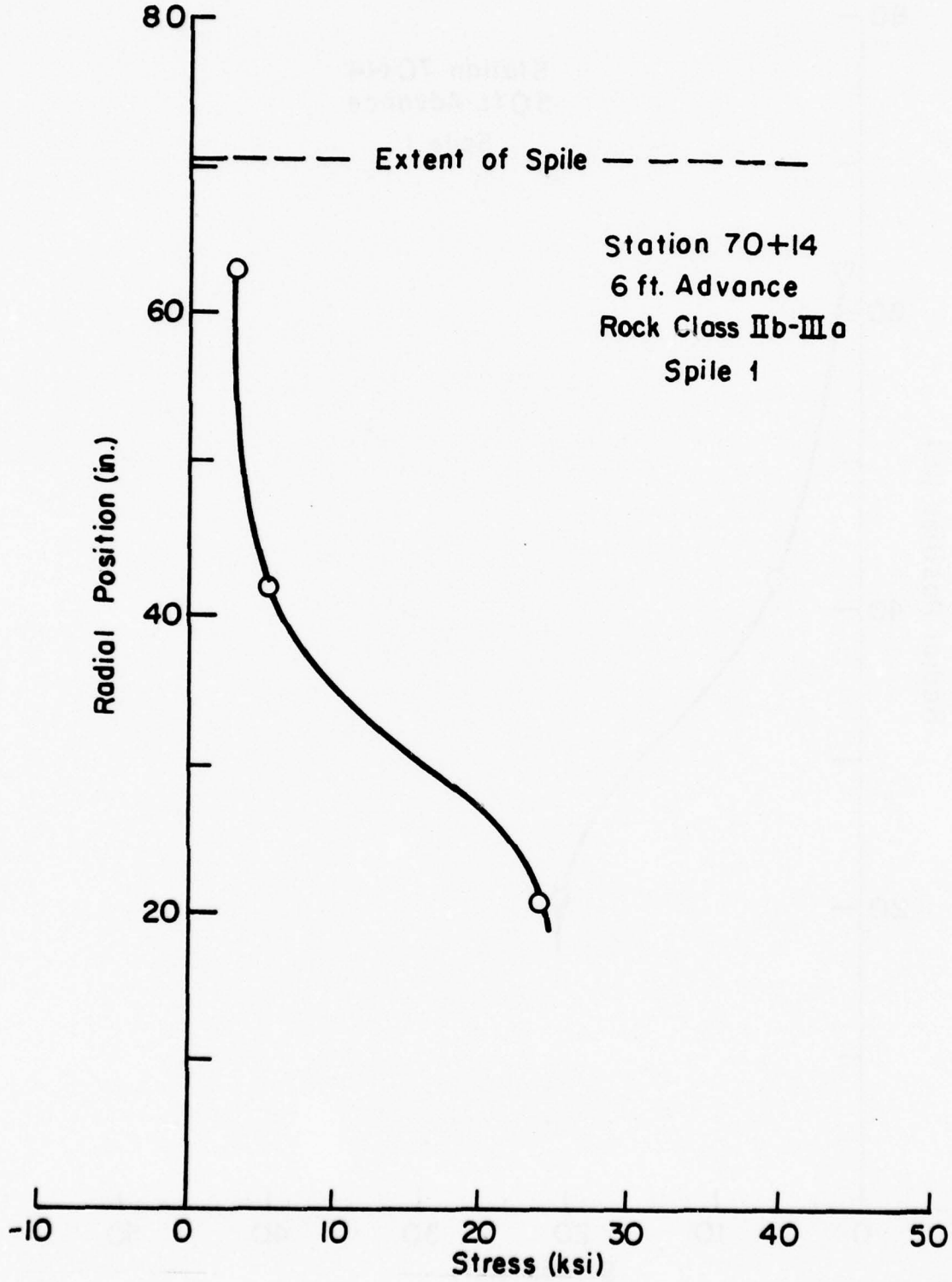

FIG. A5-15. Radial Stress Distribution, Test Station 70+14, 6 ft. Advance

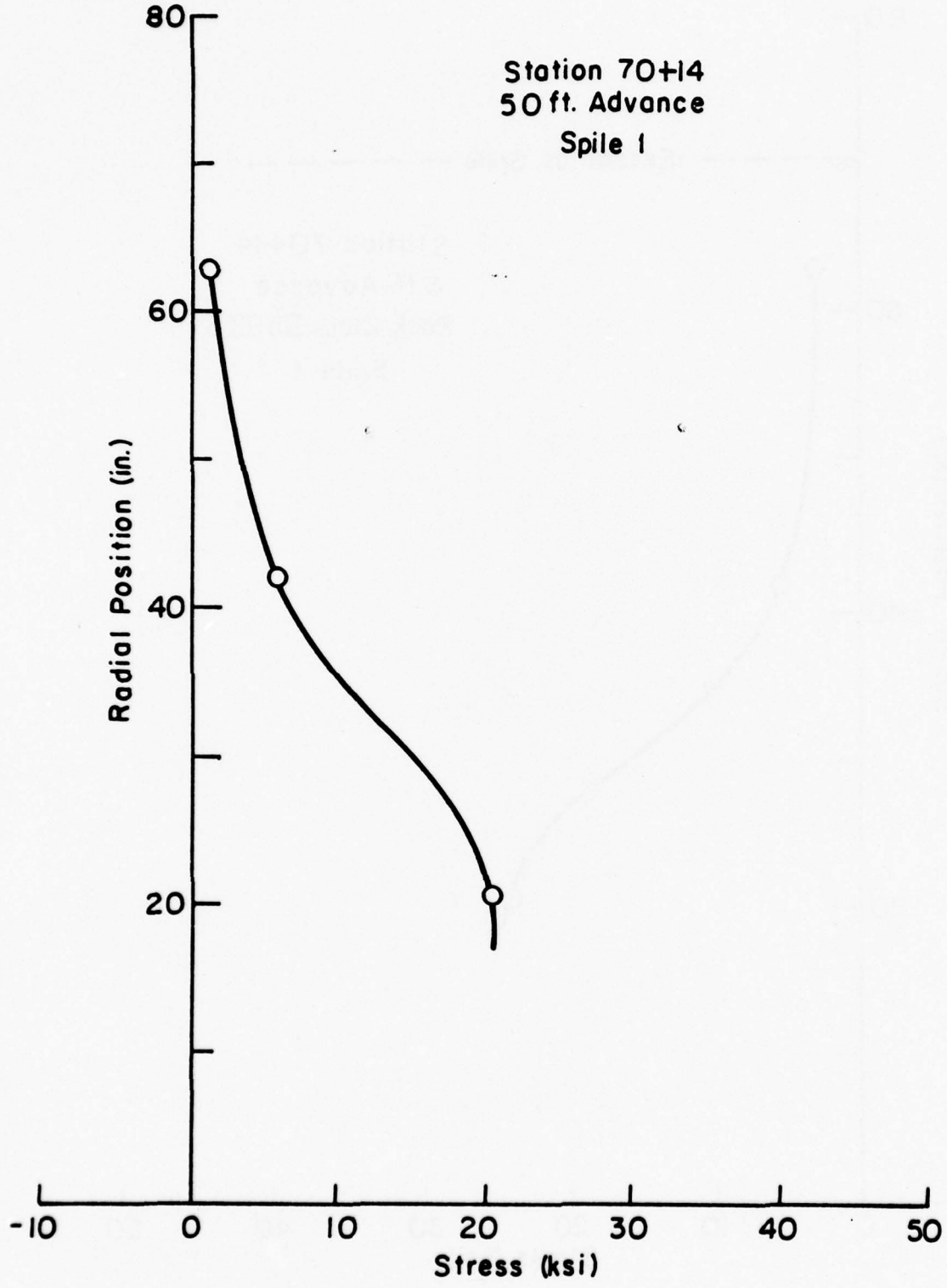

FIG. A5-16. Radial Stress Distribution, Test Station 70+14, 50 ft. Advance

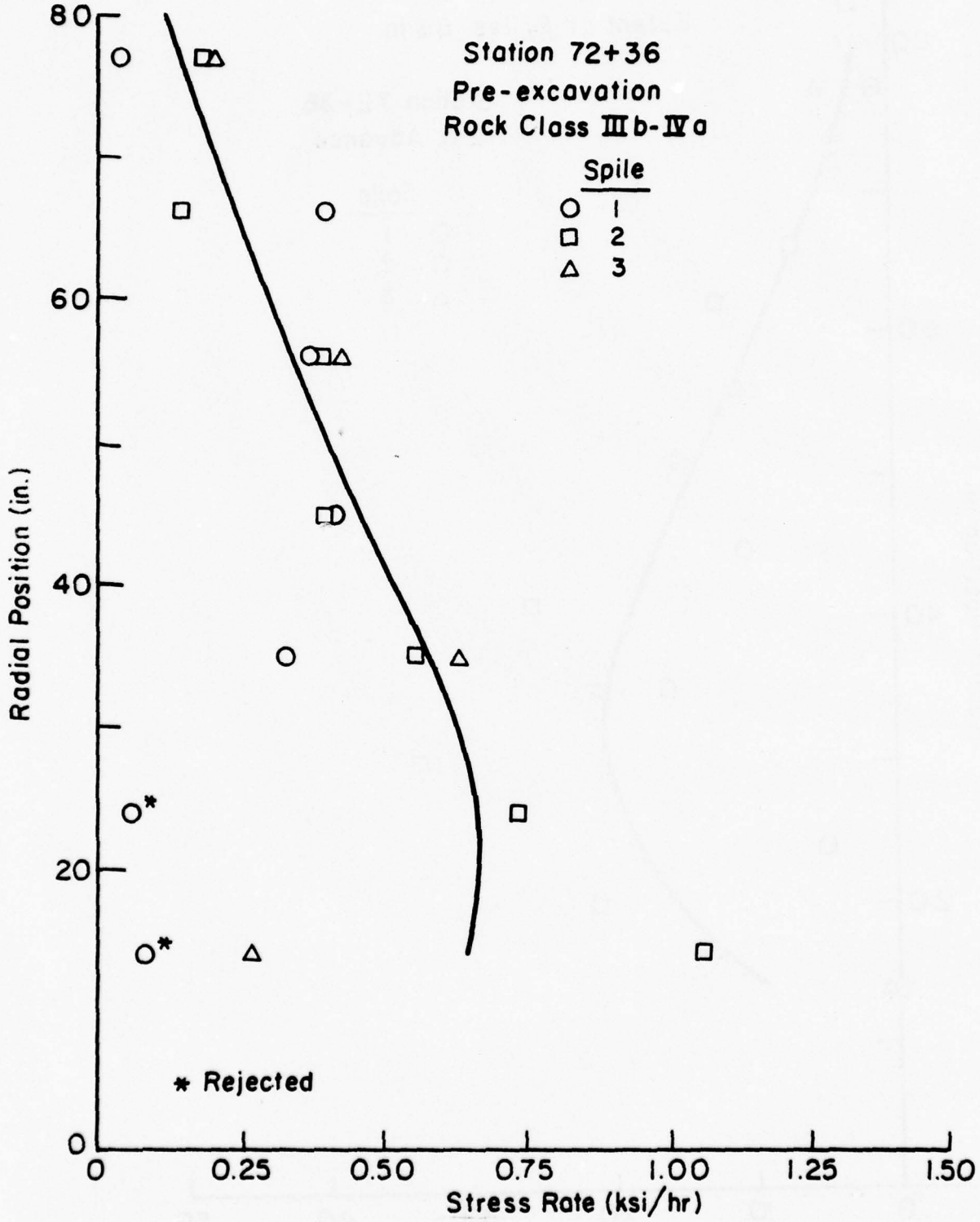

FIG. A5-17. Radial Stress Distribution, Test Station 72+36, Pre-excavation

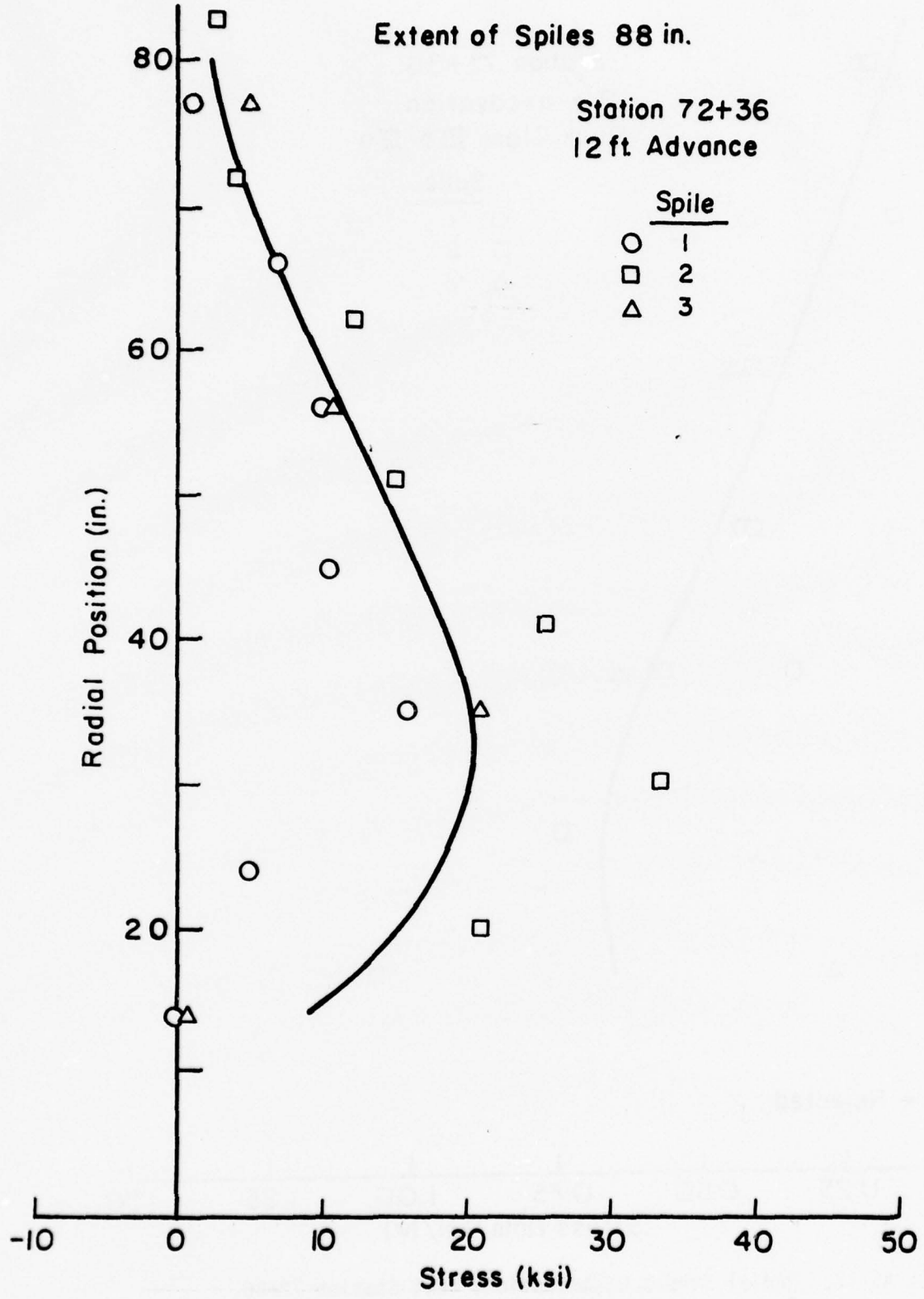

FIG. A5-18. Radial Stress Distribution, Test Station 72+36, 12 ft. Advance

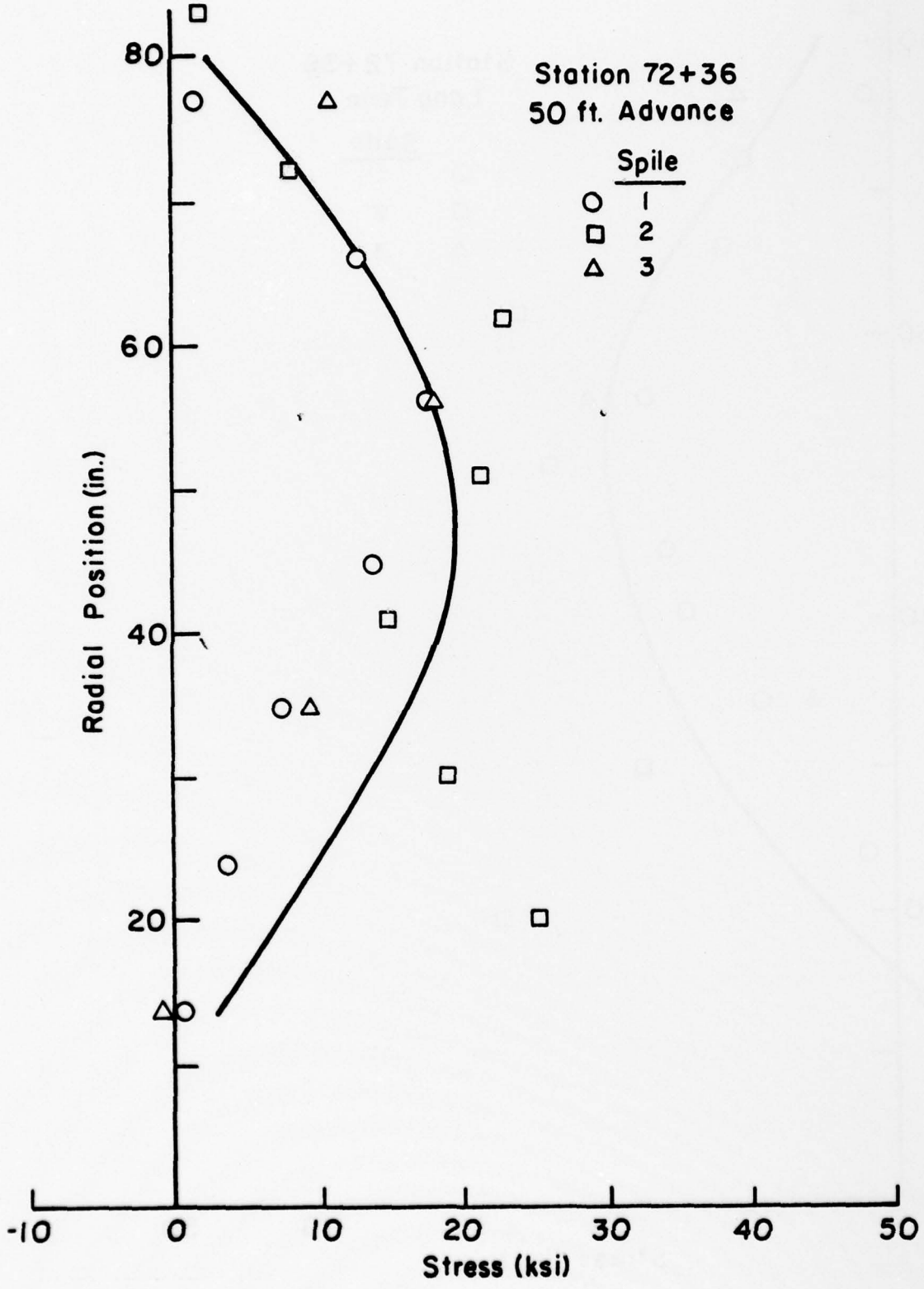

FIG. A5-19. Radial Stress Distribution, Test Station 72+36, 50 ft. Advance

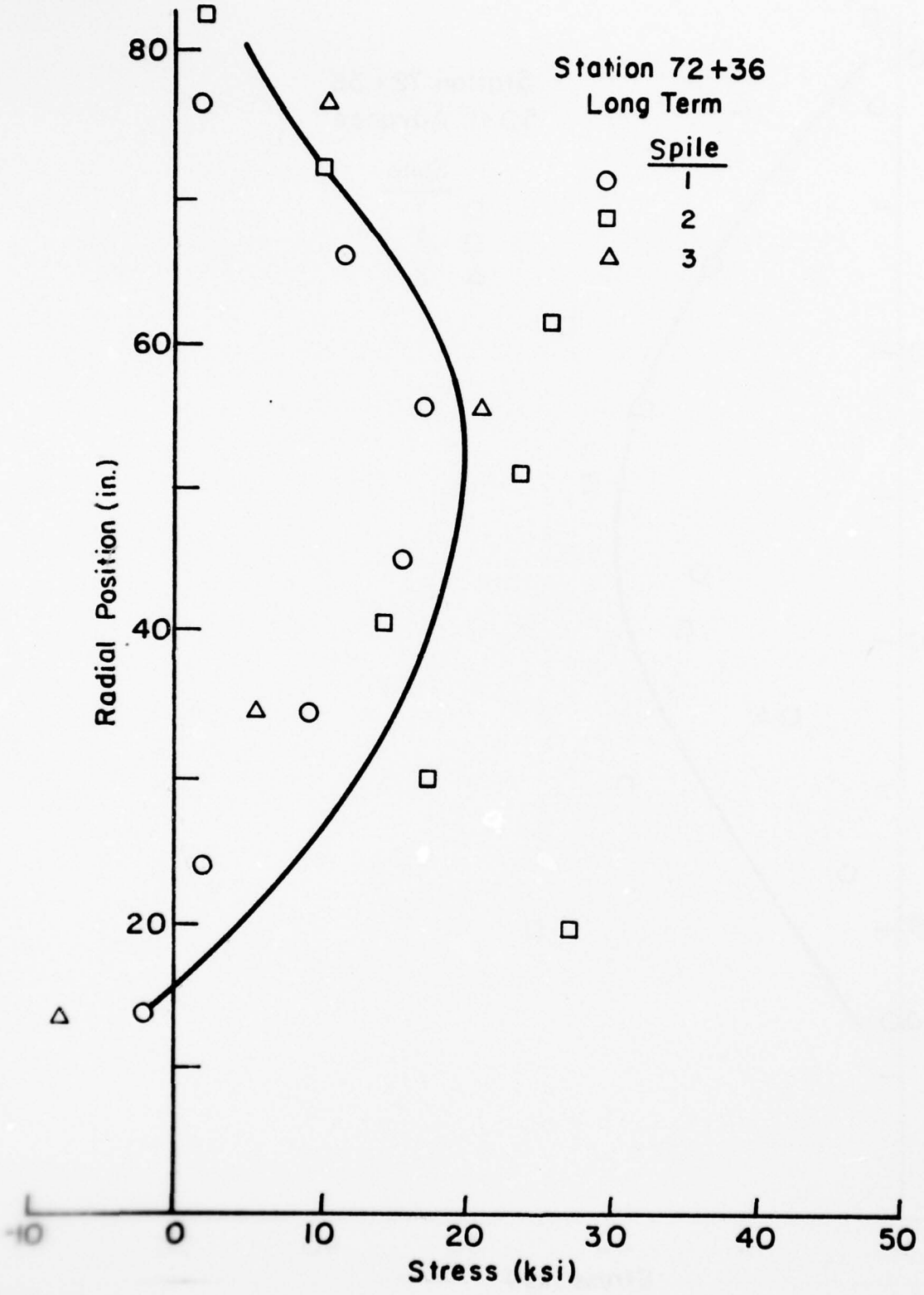

FIG. A5-20. Radial Stress Distribution, Test Station 72+36, Long Term

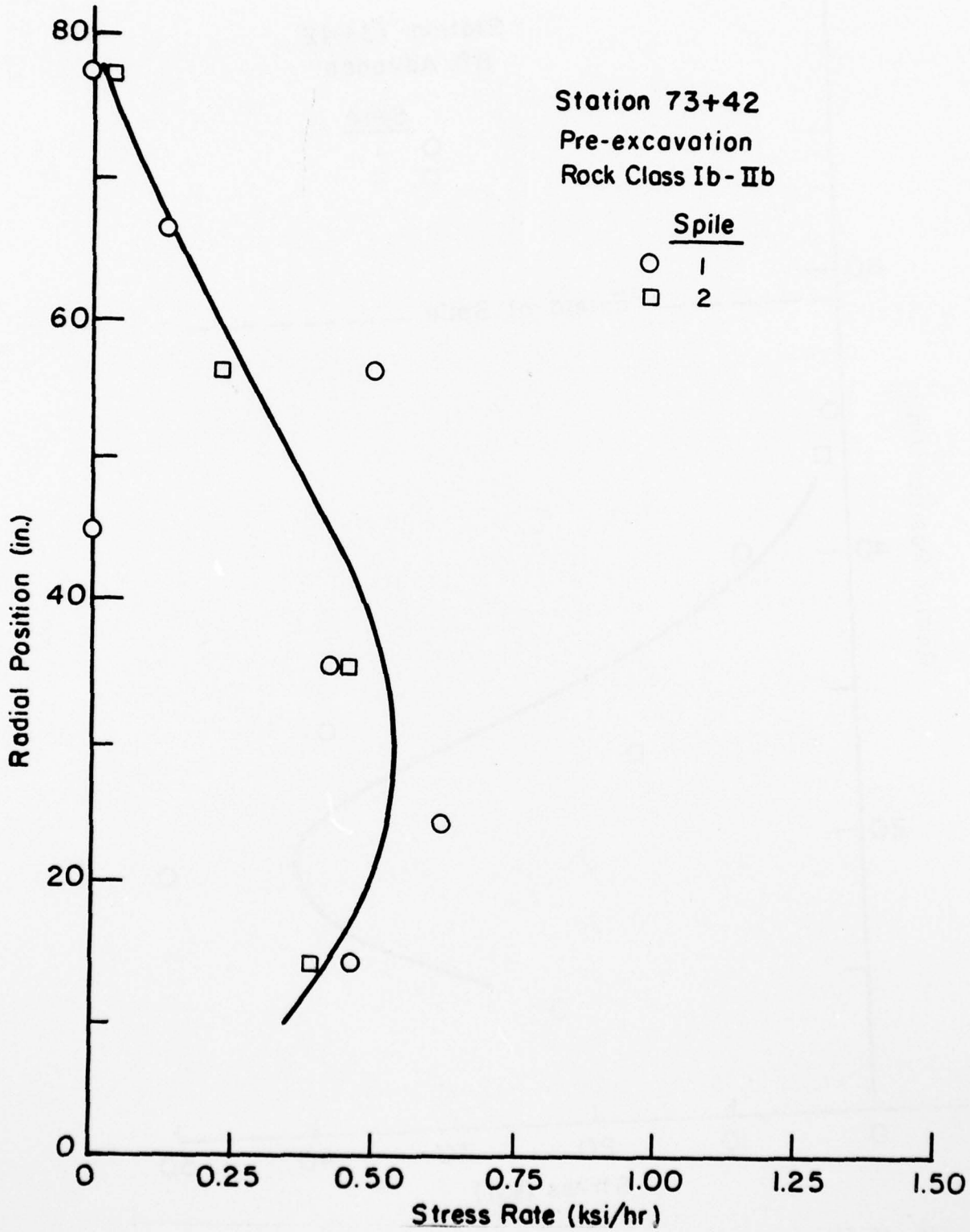

FIG. A5-21. Radial Stress Distribution, Test Station 73+42. Pre-excavation

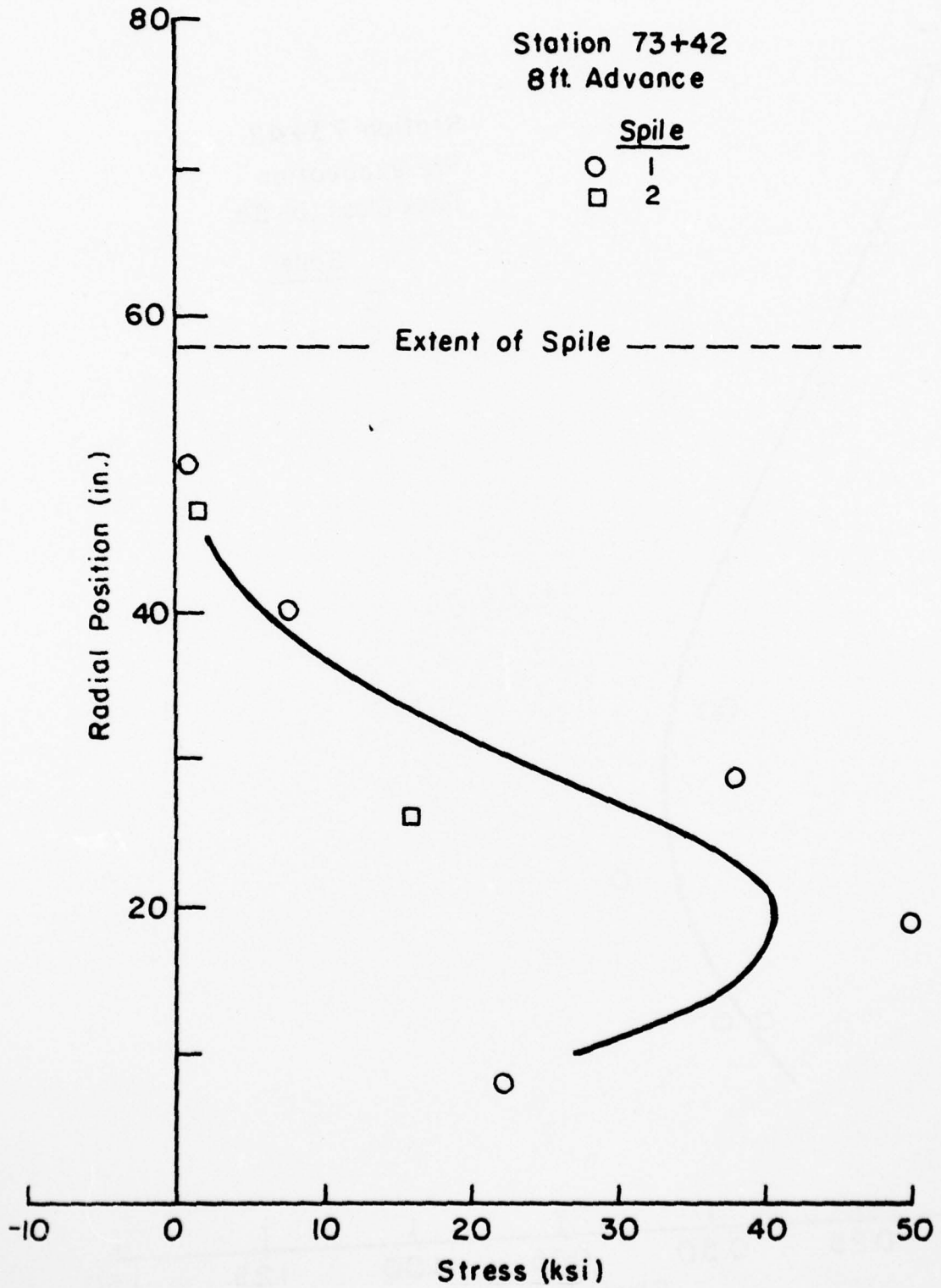

FIG. A5-22. Radial Stress Distribution , Test Station 73+42.
8 ft. Advance

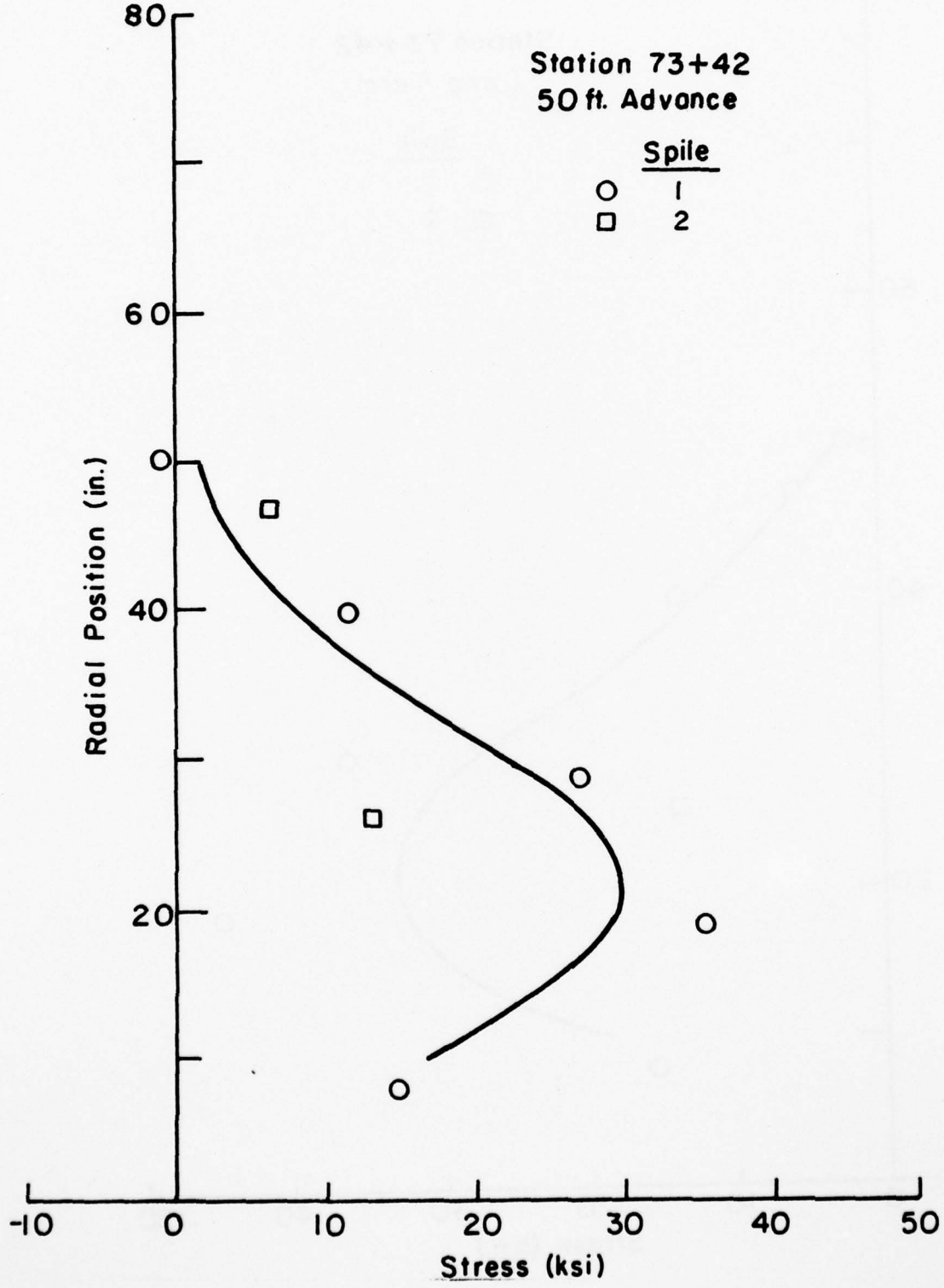

FIG. A5-23. Radial Stress Distribution, Test Station 73+42, 50 ft. Advance

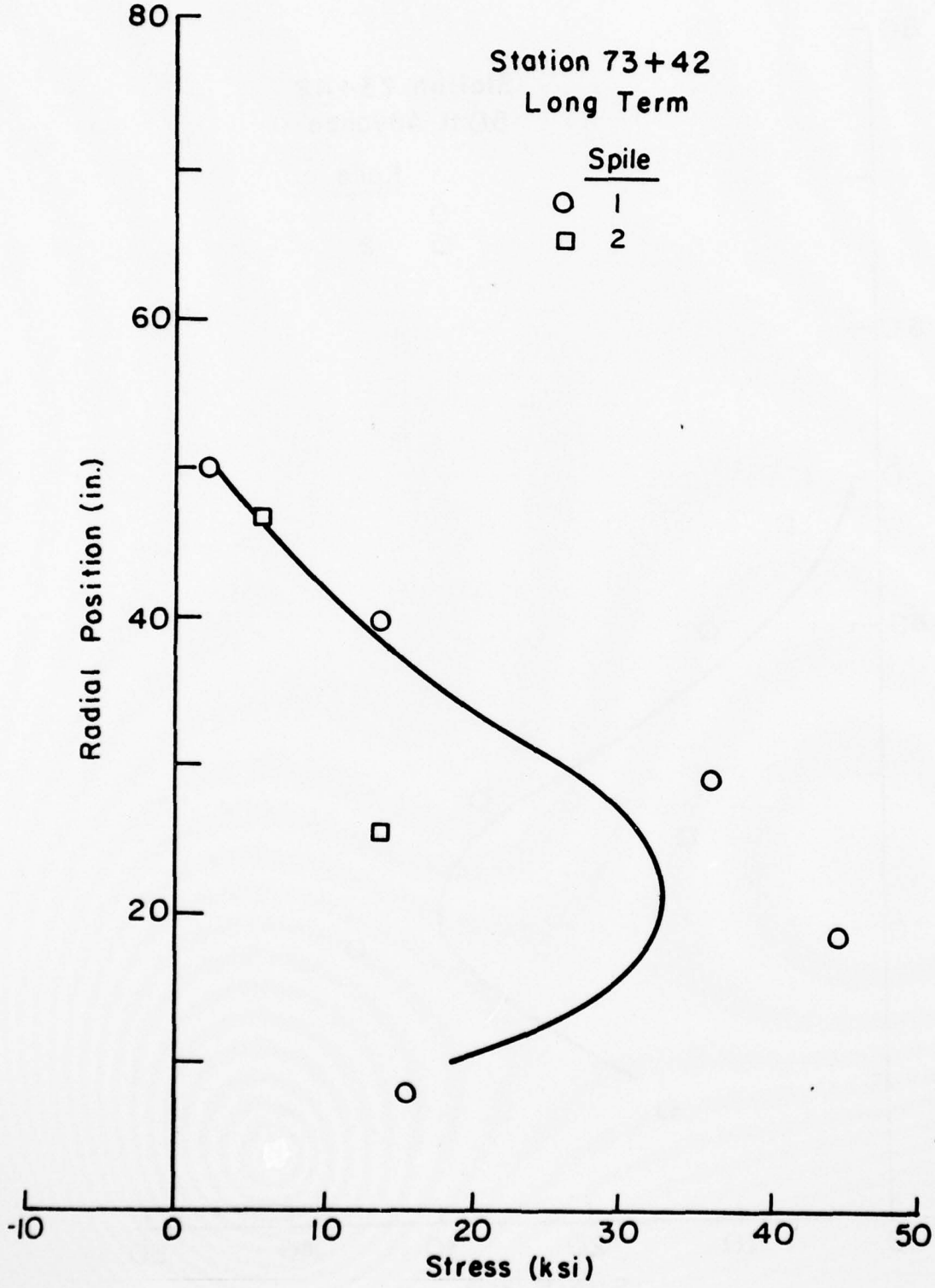

FIG. A5-24. Radial Stress Distribution, Test Station 73+42, Long Term

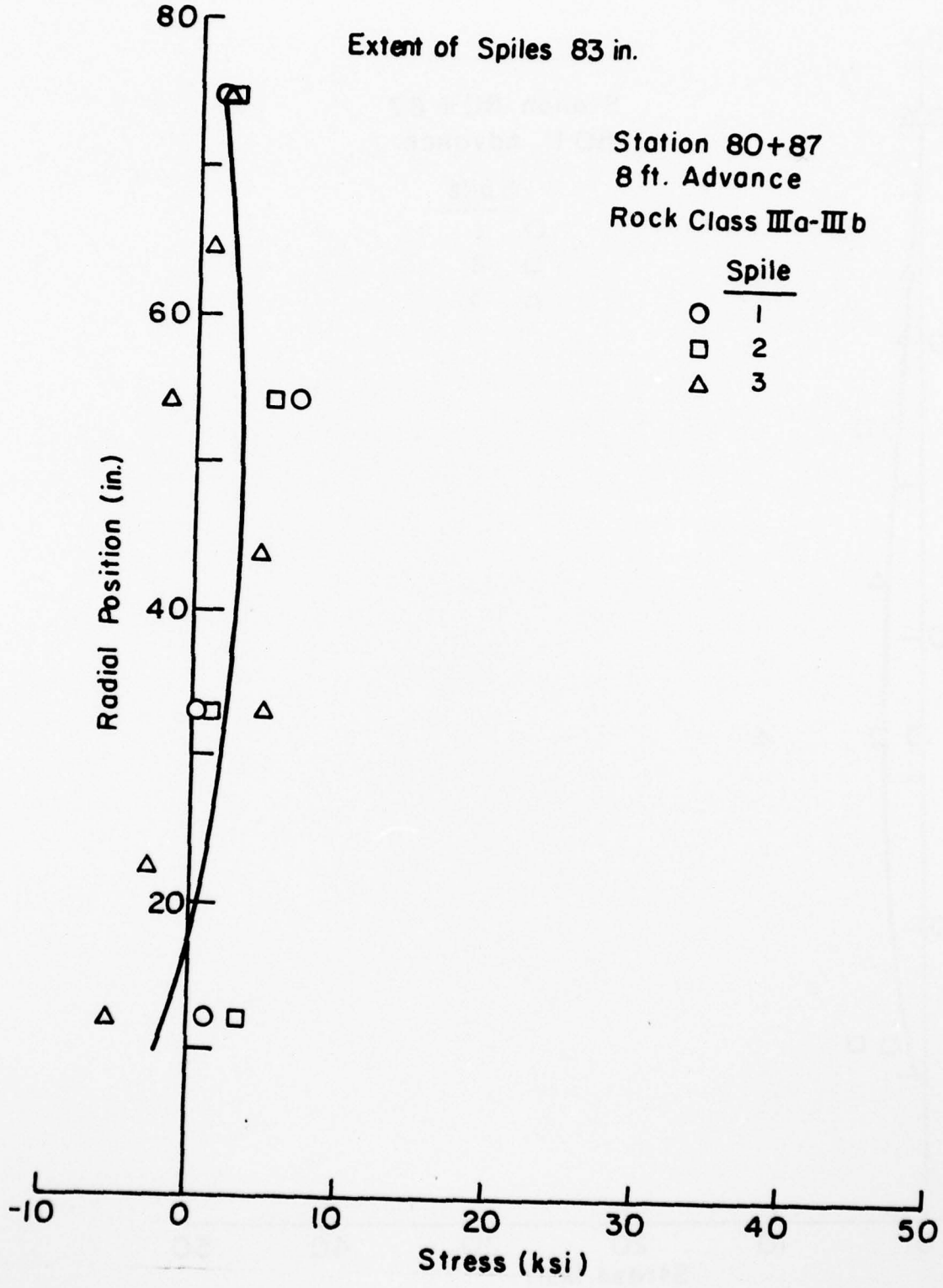

FIG. A5-25. Radial Stress Distribution, Test Station 80+87, 8 ft. Advance

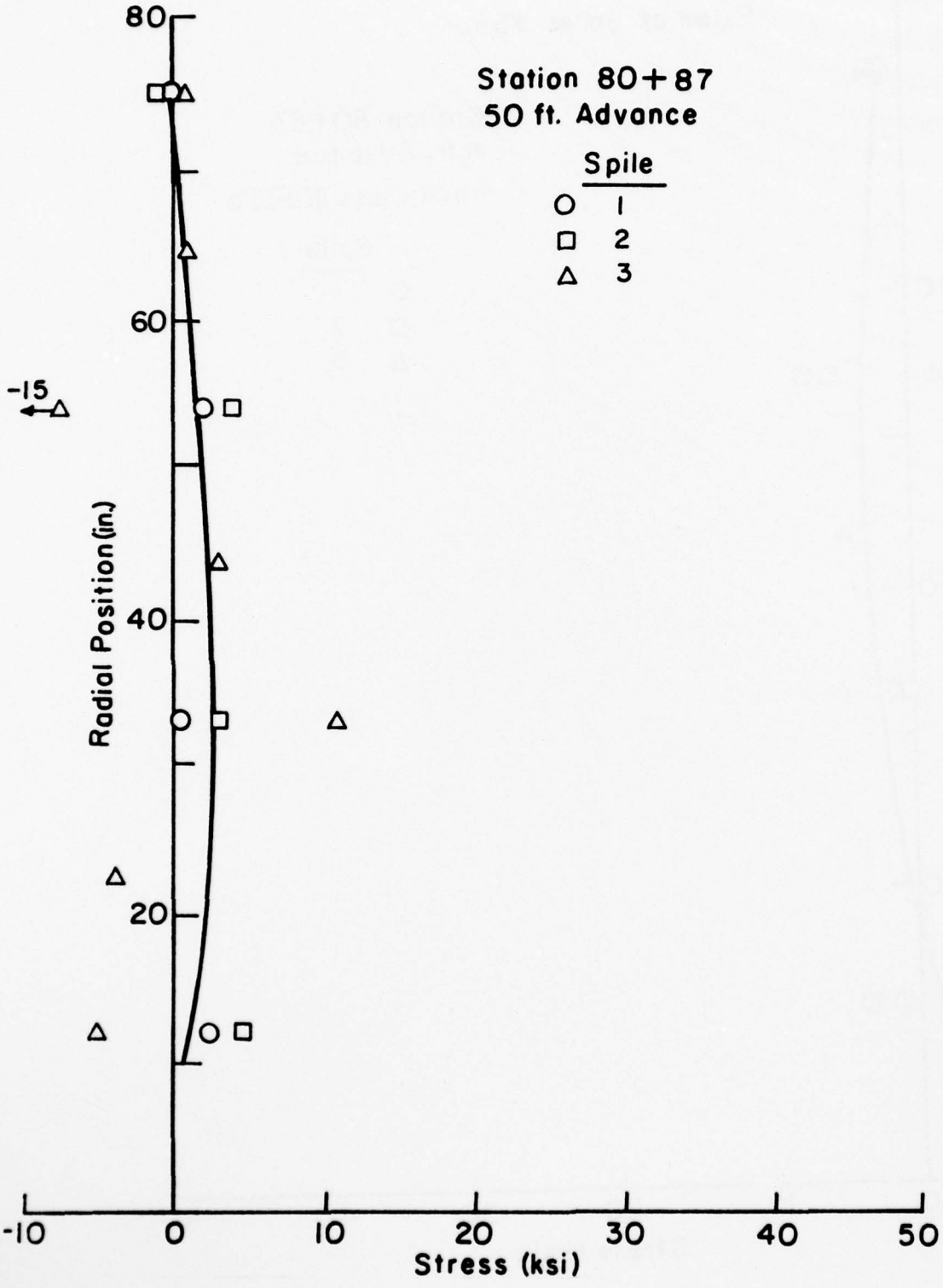

FIG. A5-26. Radial Stress Distribution, Test Station 80+87, 50 ft. Advance

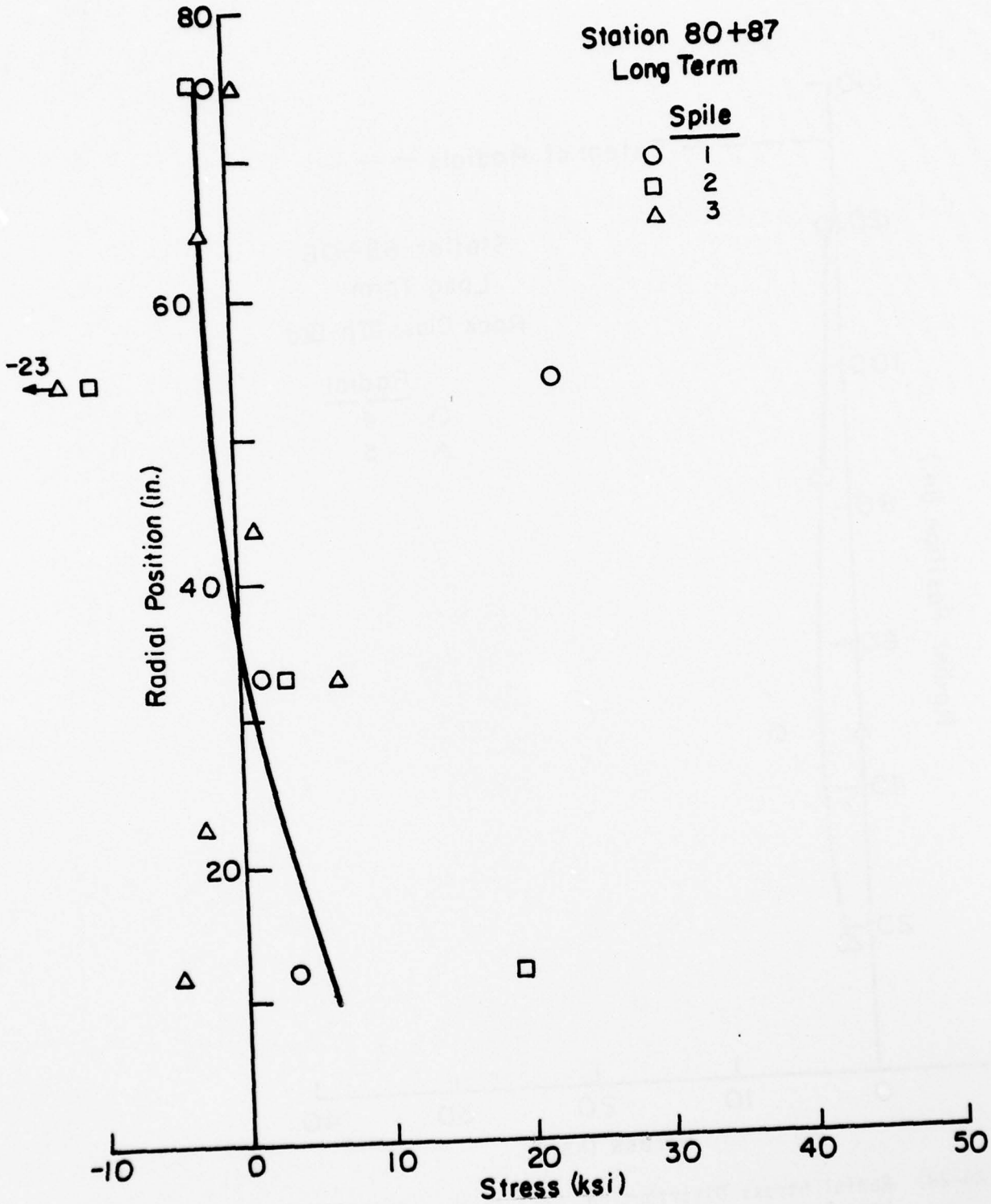

FIG. A5-27. Radial Stress Distribution, Test Station 80+87, Long Term

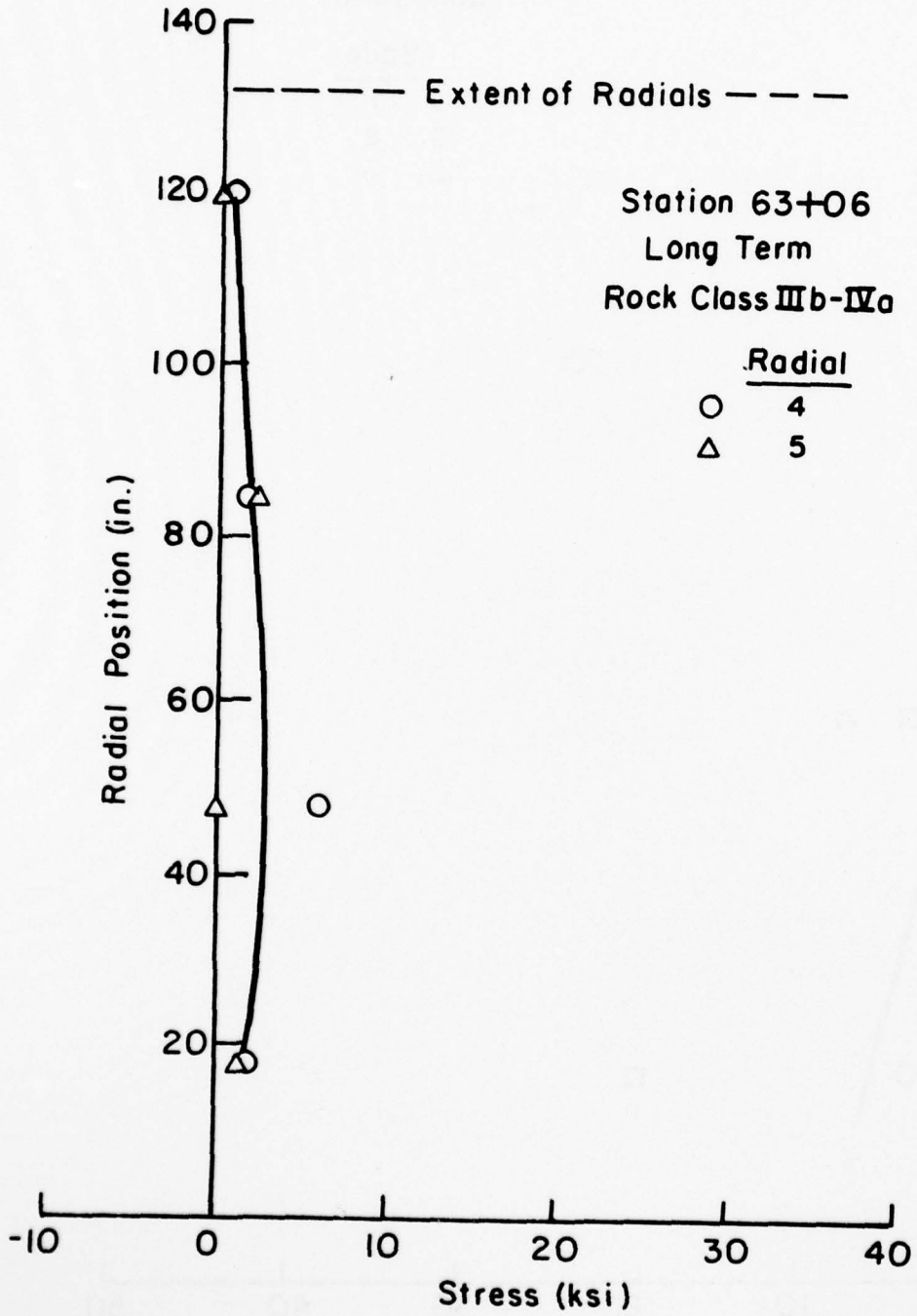

FIG. A5-28. Radial Stress Distribution, Test Station 63+06, Long Term

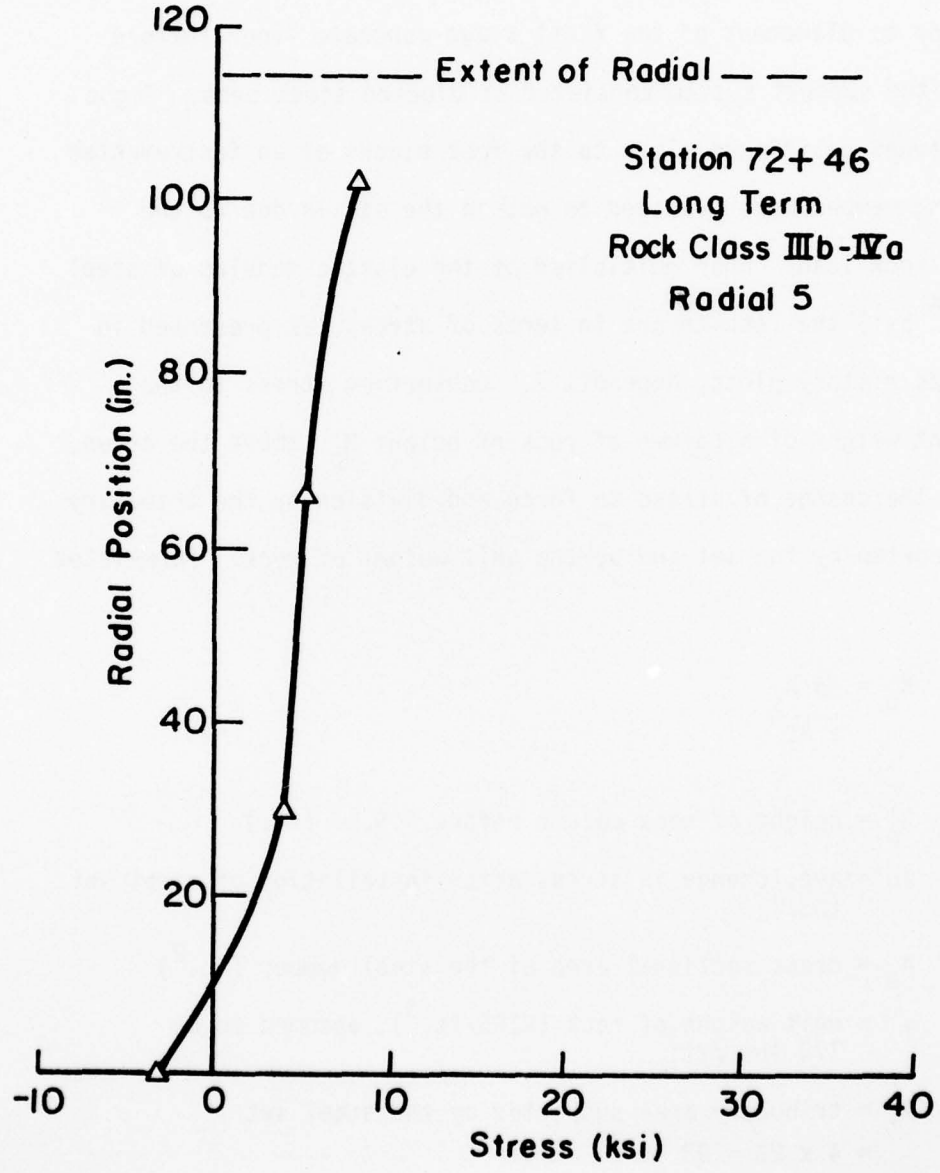

FIG. A5-29. Radial Stress Distribution, Test Station 72+46, Long Term

APPENDIX 6

SUPPORT SYSTEM LOADS

Loads From Instrumented Steel Sets

Prior to placement of the first stage concrete liner (before F.S.L.), the support system consisted of blocked steel sets. Eight strain gauges positioned close to the foot blocks of an instrumented steel ring member were averaged to obtain the strain due to the vertical rock load. When multiplied by the elastic modulus of steel (30×10^6 psi) the results are in terms of stress, as presented in the stress history plots, Appendix 7. Converting stress to the equivalent weight of a column of rock of height H'_p above the crown, involves the change of stress to force and division by the tributary area supported by the set and by the unit weight of rock. Formulated as,

$$H'_p = \frac{\Delta\sigma' A_s}{\gamma A_t}$$

where H'_p = height of rock column before F.S.L. (ft.)

$\Delta\sigma'$ = ave. change in stress after installation of steel set (KSI)

A_s = cross sectional area of the steel member ($in.^2$)

γ = unit weight of rock ($KIPS/ft.^3$), assumed to be 170 $lbs./ft.^3$

A_t = tributary area supported by the steel set
$= 4 \times 23 = 92\ ft.^2$

Immediately after placing the liner, the fluid pressure of the concrete results in a 1 to 3 KSI increase in measured vertical stress.

The lower values are appropriate for the heavier steel members.

Once the concrete has cured, a residual stress is left in the steel set. To an unknown extent, the stress will relax as the weight of the concrete is transferred by creep, from the steel member into the liner itself. This precludes the accurate computation of loads after placement of the liner. As load develops on the composite system of steel set and concrete liner, it can be assumed that the recorded strain within the set is the same as that within the liner. On this basis, the additional cross sectional area of support provided by the liner is the tributary area of the concrete liner multiplied by the concrete to steel modulus ratio. In terms of the height of a rock column,

$$H_p'' = \frac{\Delta\sigma'}{\gamma A_t} \left\{ A_c \left(\frac{E_c}{E_s} \right) + A_s \right\}$$

where H_p'' = height of rock column after F.S.L. (ft.)

$\Delta\sigma''$ = ave. change in stress after placement of liner (KSI)

A_c = tributary cross sectional area of the concrete liner ($in.^2$)

E_c = elastic modulus of concrete (3×10^6 psi)

E_s = elastic modulus of steel (30×10^6 psi)

A_s, γ, and A_t are as previously defined.

In computations, the average change in stress after placement of the liner, $\Delta\sigma''$, did not include the weight of the liner or any proportion thereof due to relaxation.

TABLE A6-I

Values Used in Computation of Rock Load from Instrumented Steel Set Results

Test Station	Steel Set		First Stage Concrete Liner		Steel Stress Change (KSI)		Rock Load H_p (FT.)		
	Member	Area$_2$ (IN.^{2})	Thickness (IN.)	Area$_2$ (IN.^{2})	Before F.S.L.	After F.S.L.	Before F.S.L.	After F.S.L.	Long Term
58+86	W14x61	18	14	672	0.8	0.0	0.9	0.0	0.9
63+01	W14x136	40	20	960	2.4	1.3	6.1	11.3	17.4
70+14	W14x95	28	14	672	1.2	—	2.1	—	—
72+36	W14x136	40	20	960	2.0	0.4	5.1	3.5	8.6
73+42	W14x95	28	14	672	1.0	0.0	1.8	0.0	1.8
80+87	W14x136	40	20	960	1.8	0.8	4.6	7.0	11.6

All values of stress change and support area necessary in the calculation of rock load, before and after F.S.L. are presented for each test station in Table A6-1. The long term load or total rock load is simply the sum, $H_p = H_p' + H_p''$.

Loads From Spile Stress Relaxation

Computation of the rock load H_p from spile relaxation was basically the same in principle as that from the instrumented steel sets. The only significant difference was that the spile force must be resolved into its vertical component (multiplied by sin 30°). This resulted in the formulation,

$$H_p = \frac{A_r \Delta\sigma}{\gamma A_t} \sin 30° = 4.41 \frac{\Delta\sigma}{A_t}$$

where $H_p = H_p'$ or H_p'', height of rock column before or after F.S.L. (ft.)

$\Delta\sigma = \Delta\sigma'$ or $\Delta\sigma''$, ave. spile stress relaxation within the reinforcement nearest the opening before or after F.S.L. (KSI)

A_r = cross sectional area of the reinforcing steel = 1.5 $in.^2$

γ = unit weight of rock (KIPS/$ft.^3$), assumed to be 170 lbs/$ft.^3$

A_t = tributary area reinforced by the spile, one-half the axial spacing multiplied by the circumferential spacing ($ft.^2$)

AD-A046 358 CALIFORNIA UNIV BERKELEY DEPT OF CIVIL ENGINEERING F/G 13/13
A FIELD STUDY OF SPILING REINFORCEMENT IN UNDERGROUND OPENINGS.(U)
JUN 77 G E KORBIN, T L BREKKE DACW45-74-C-0026

UNCLASSIFIED MRD-TR-1-77 NL

3 OF 3
ADA
046358

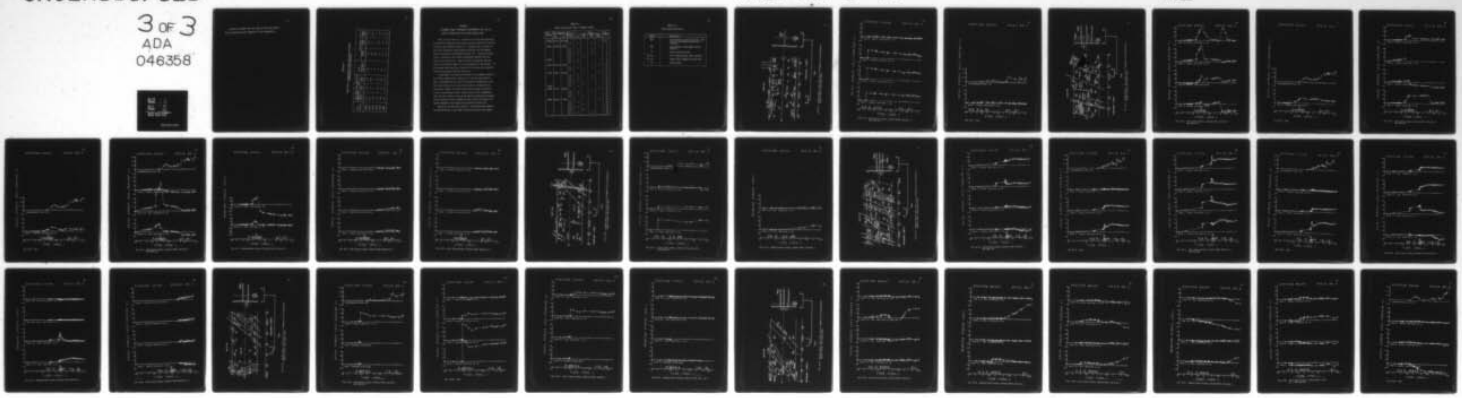

END
DATE
FILMED
12-77
DDC

Table A6-II contains the rock loads for each test station and all associated values necessary for their computation.

TABLE A6-II

Values Used in Computation of Rock Load from Instrumented Reinforcement Stress Relaxation

Test Station	Ave. Spile Stress Relaxation Below Peak (KSI)			Spile Tributary Area ($FT.^2$)	Rock Load H_p (FT.)		
	Before F.S.L.	After F.S.L.	Long Term		Before F.S.L.	After F.S.L.	Long Term
58+86	3.1	1.8	4.9	20	0.7	0.4	1.1
63+01	11.1	8.7	19.8	5	9.8	7.7	17.4
70+14	0.0	—	—	10	0.0	—	—
72+36	4.7	4.3	9.0	5	4.1	3.8	7.9
73+42	8.5	< 0	6.4	20	1.9	< 0	1.4
80+87	0.6	0.3	0.9	5	0.5	0.3	0.8

APPENDIX 7

EISENHOWER TUNNEL INSTRUMENTED REINFORCEMENT AND STEEL SET STRESS HISTORIES AND TEST STATION GEOLOGIC MAPS

Plots of axial stress as a function of time have been developed for each strain gauge position on each spile and radial bolt installed at the six test stations (Figure 3-3). Bending stress is shown for those bars designed to record bending resulting from displacement normal to the tunnel circumference (Figure 2-4). A positive bending stress is defined as one in which compression develops below the neutral axis (Figure 2-8). Radial position was measured from the point of installation normal to the circumference of the opening. All spiles were installed within a few feet of the crown and at approximately thirty degrees from the tunnel axis.

A logarithmic time scale was employed for an expanded viewing of the initial response and a compression of the long term behavior. Data is presented from the time of installation through April, 1977. The stress history plot of each strain gauge is arranged by test station, bar number, and radial position as outlined in Table A7-I. A plot of the average vertical stress history of the instrumented steel set and a sketch in plan of the specific geology and instrumentation location are also included for each station (see Table A7-I). Symbols employed in the Figures are described in Table A7-II.

Basically, the data were unaltered. Extra points were added to provide definition at shot times and obvious outliers were removed.

TABLE A7-I

Stress History Plot Index, Eisenhower Tunnel

Test Station	Zero Reference		Instr. Bar No. & Type	Plot				Fig. Number
	Date	Time		Axial	Bend-ing	Steel Set	Geo-logic	
58+86	9-15-76	12 noon	-				X	A7-1
			1-A	X		X		2
63+01	10-19-76	6 AM	-				X	3
			1-A	X		X		4
			2-A	X		X		5
			3-B	X		X		6
			3-B		X			7
63+06			4-C	X				8
			5-C	X				9
70+14	12-27-76	9 AM	-				X	10
			1-B	X		X		11
			1-B		X			12
72+36	1-20-77	12 noon	-				X	13
			1-A	X		X		14
			2-A	X		X		15
			3-B	X				16
			3-B		X			17
72+46			5-C	X				18
73+42	2-2-77	12 noon	-				X	19
			1-A	X		X		20
			2-B	X				21
			2-B		X			22
80+87	3-23-77	9 AM	-				X	23
			1-B	X				24
			1-B		X			25
			2-B	X				26
			2-B		X			27
			3-A	X		X		28

TABLE A7-II

Figure Symbol Description

Symbol	Description
(A)	face located at initial position, point at which instrumented spiles were installed
(n)	face advanced n feet beyond initial position
↑	time of excavation shot
↑ F.S.L.	first stage concrete liner installed
↑ C.G.	contact grout between rock and liner
J.S.	joint spacing

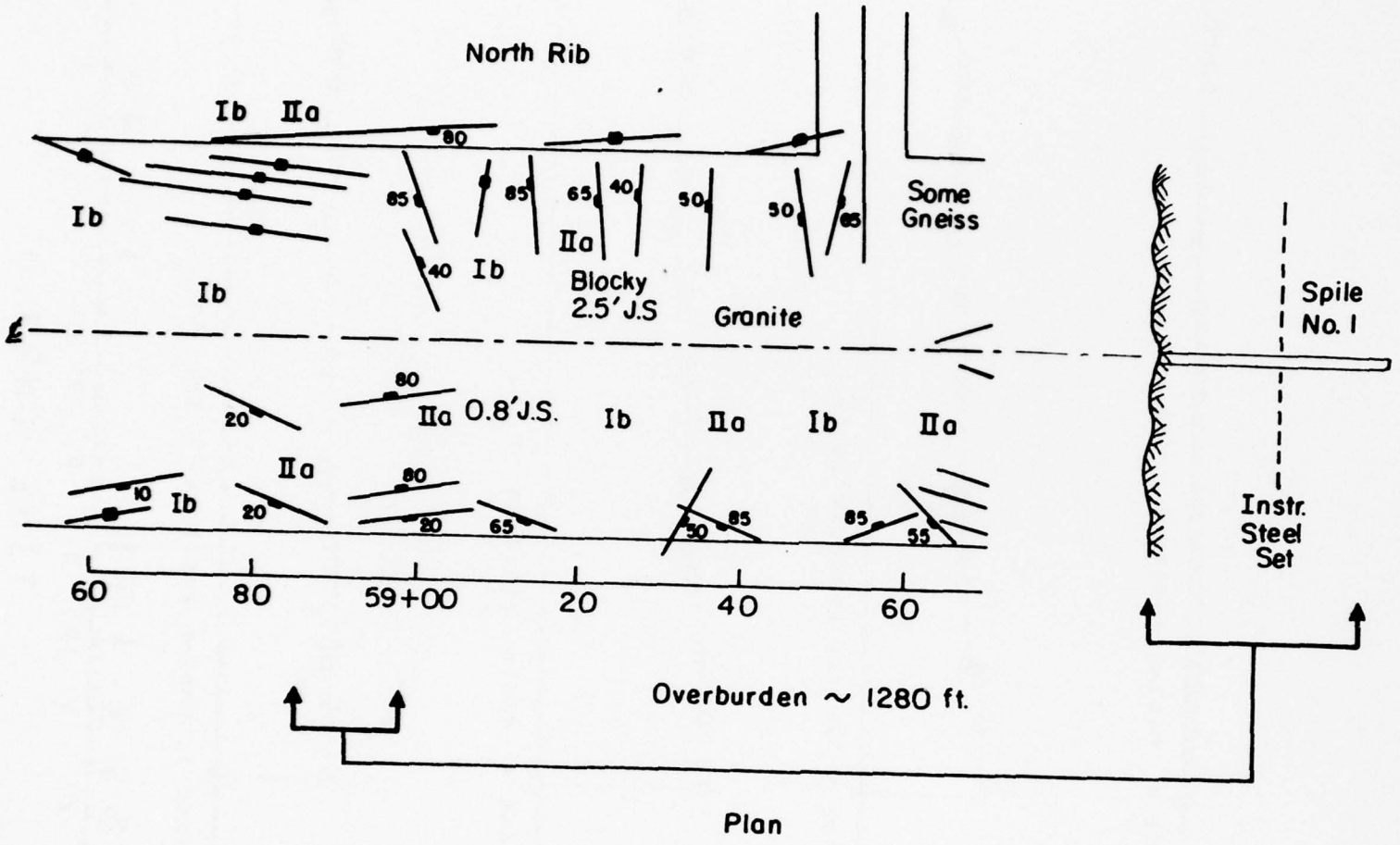

FIG. A7-1. Geologic Map (J. Post, Colo. Div. of Highways) and Instrumentation Layout in Plan, Test Station 58+86

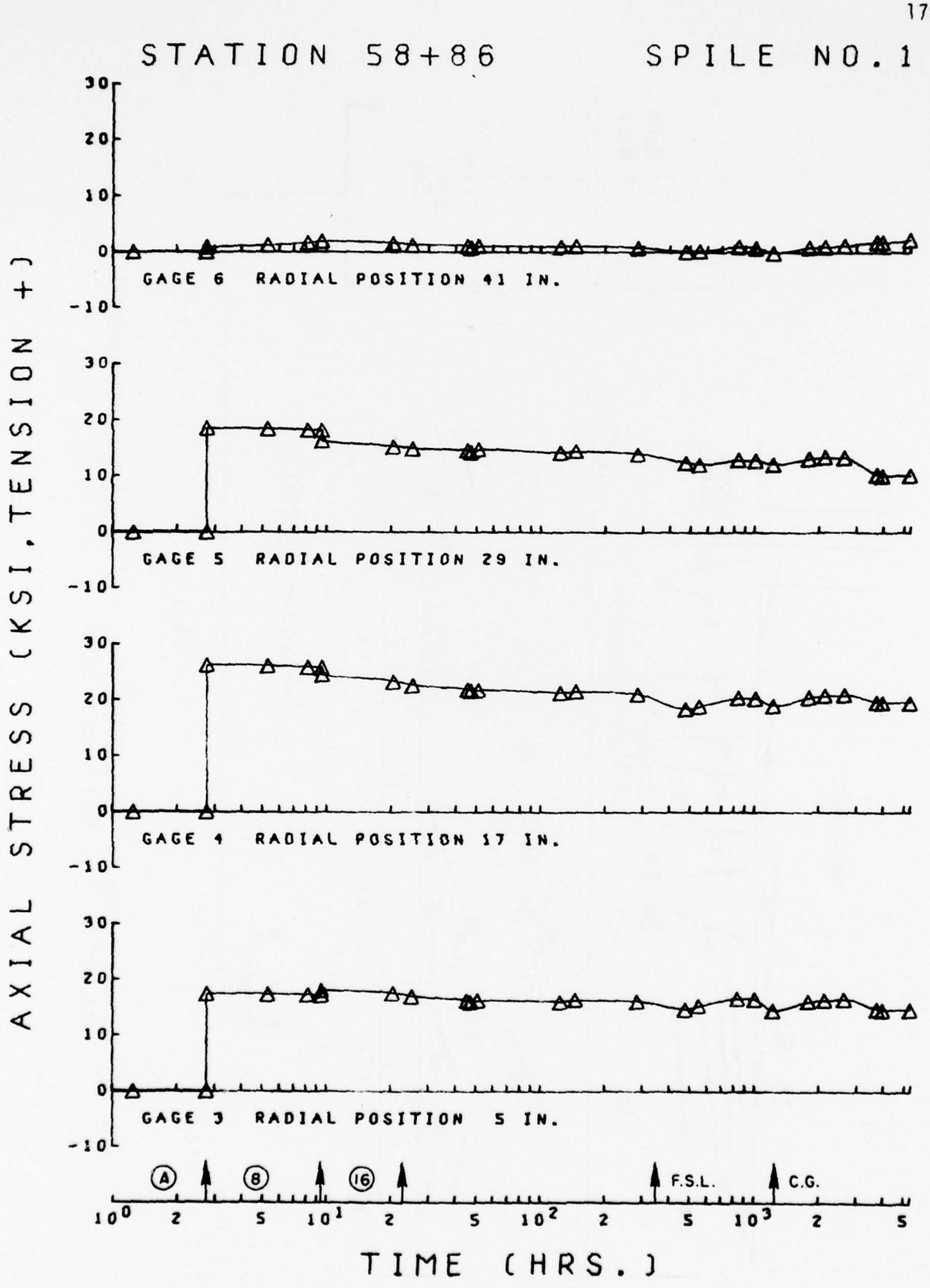

FIG. A7-2. Axial Stress History, Station 58+86, Spile No. 1, and Steel Set

STATION 58+86 SPILE NO. 1

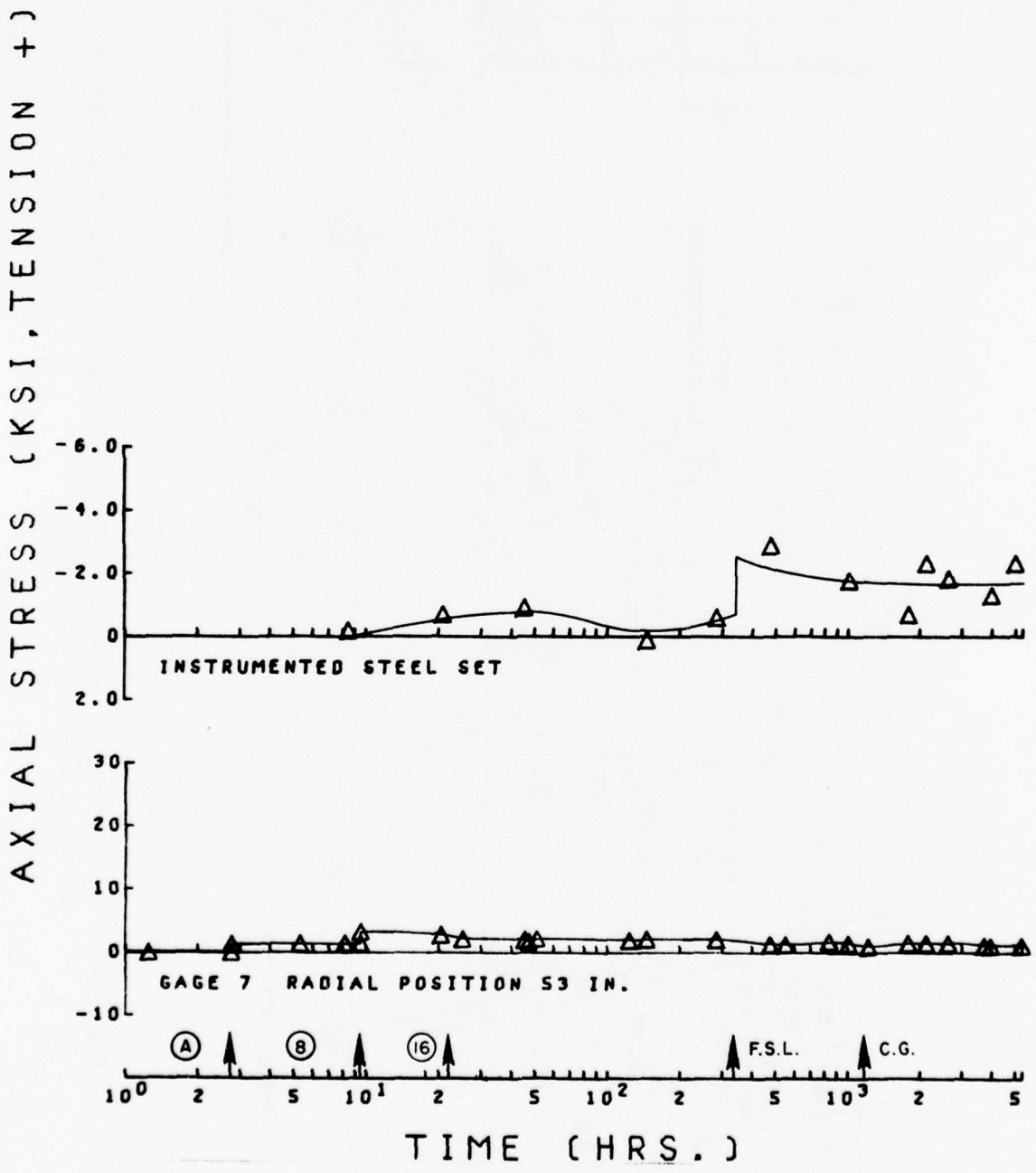

FIG. A7-2. Cont.

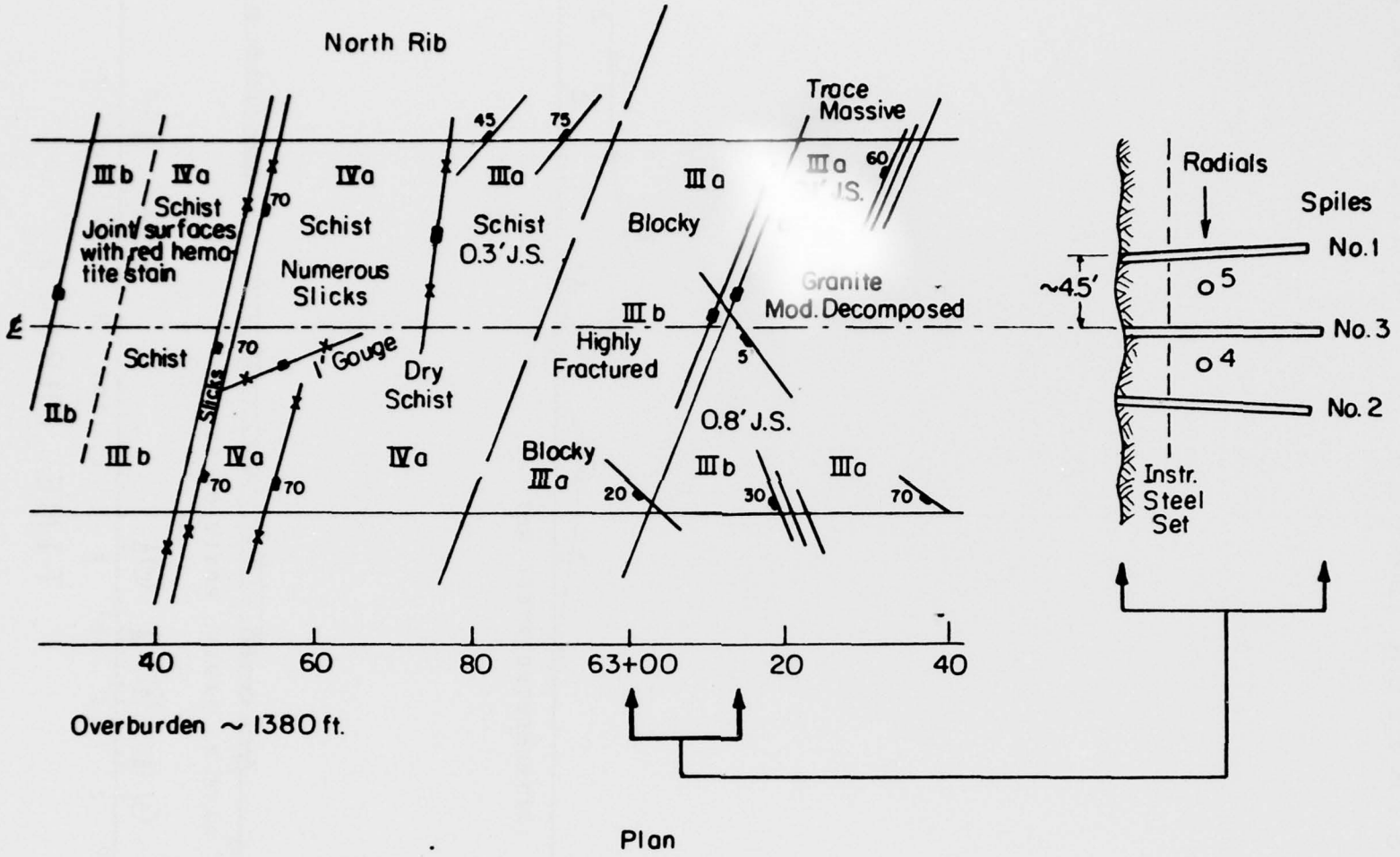

FIG. A7-3. Geologic Map (J. Post, Colo. Div. of Highways) and Instrumentation Layout in Plan, Test Station 63+01

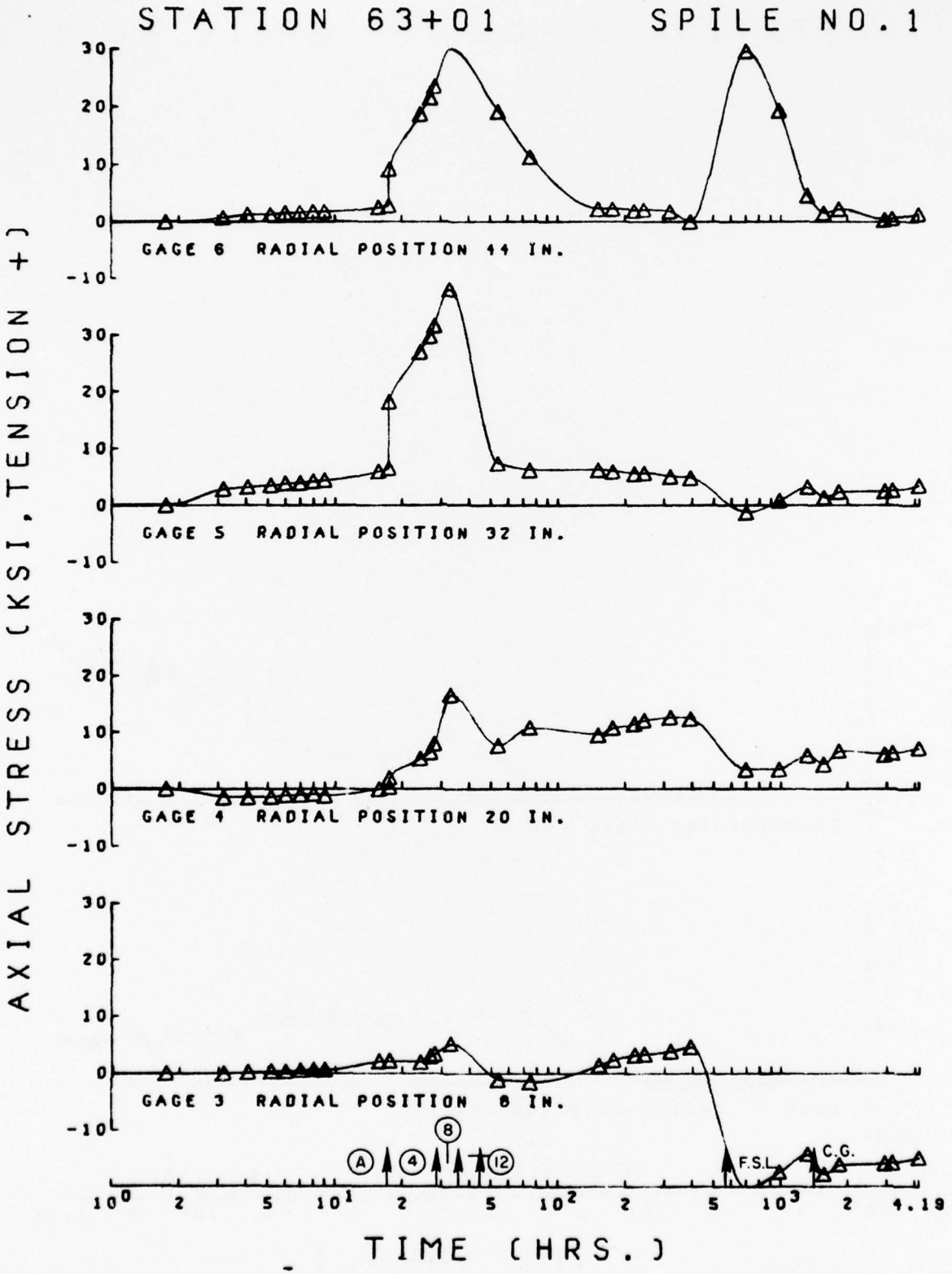

FIG. A7-4. Axial Stress History, Station 63+01, Spile No. 1 and Steel Set

STATION 63+01 SPILE NO. 1

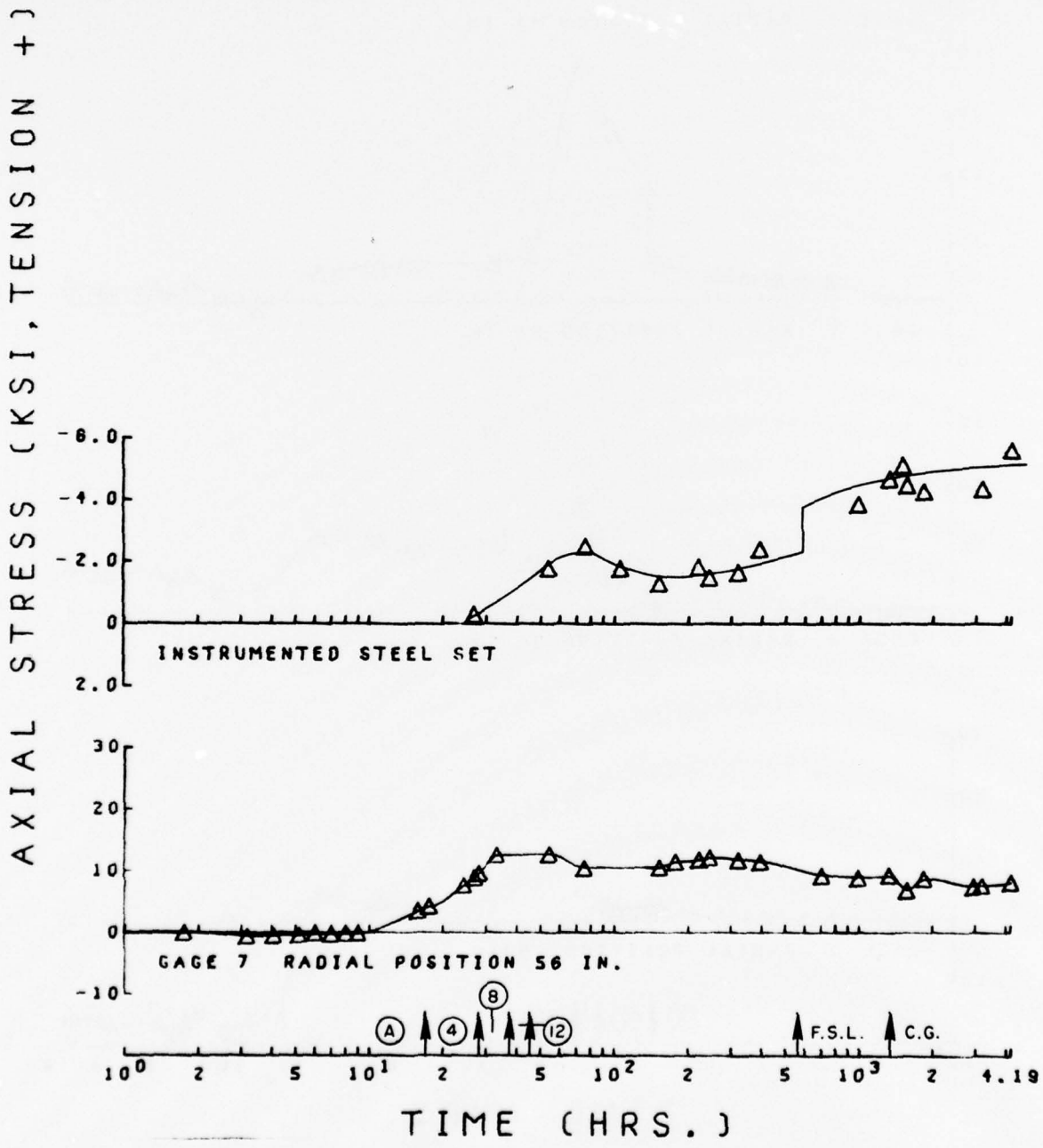

FIG. A7-4. Cont.

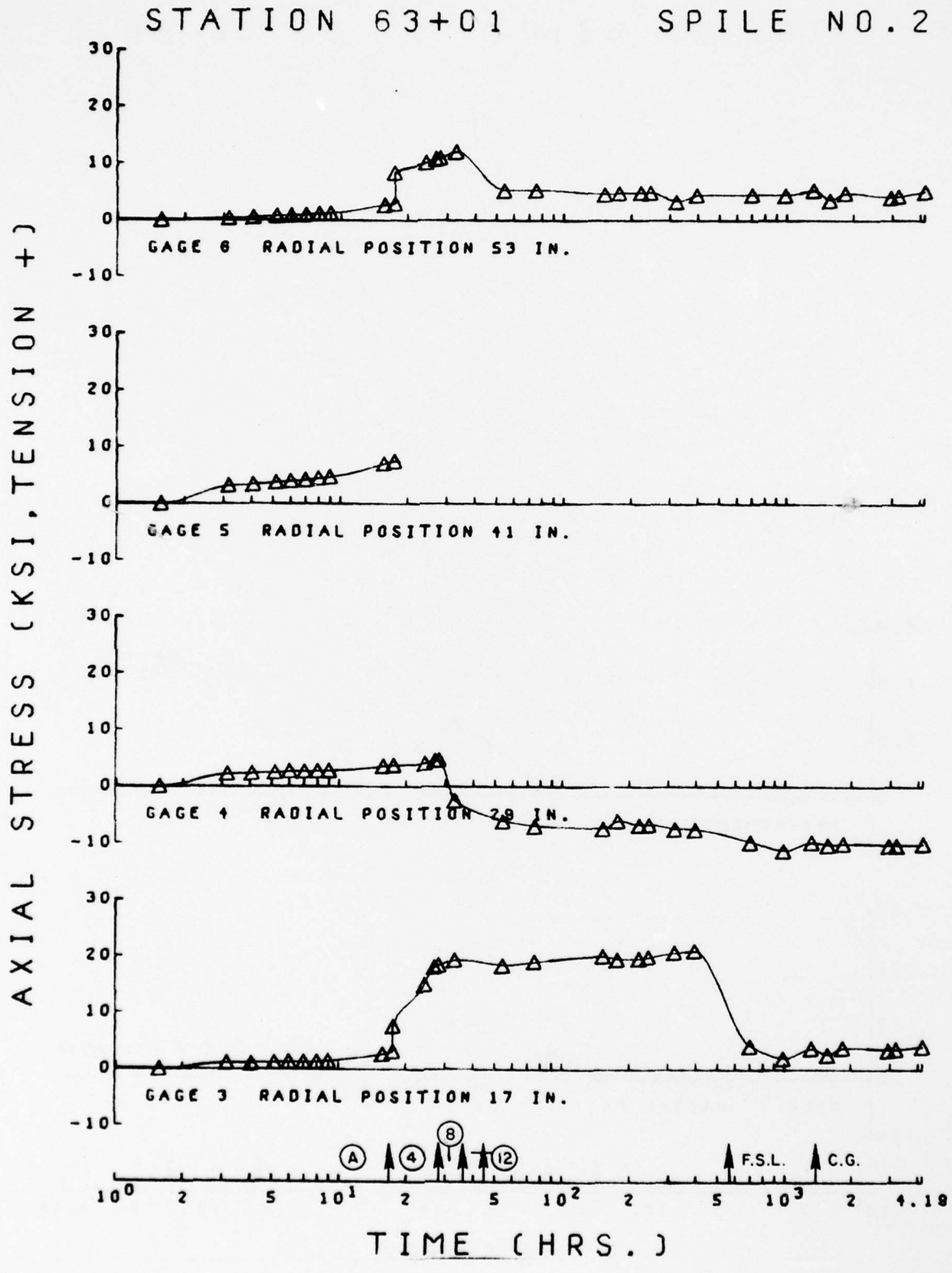

FIG. A7-5. Axial Stress History, Station 63+01, Spile No. 2 and Steel Set

STATION 63+01 SPILE NO. 2

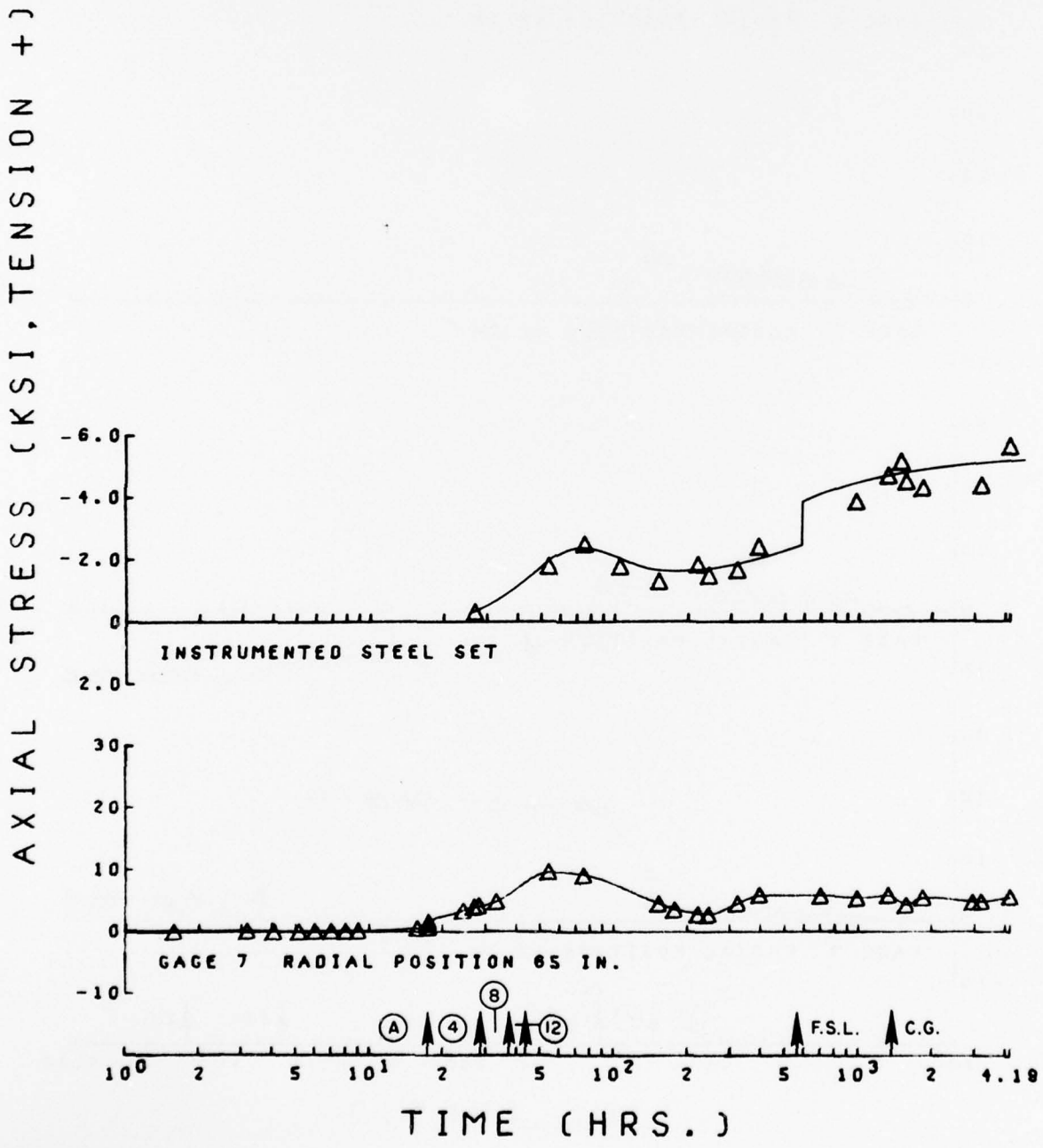

FIG. A7-5. Cont.

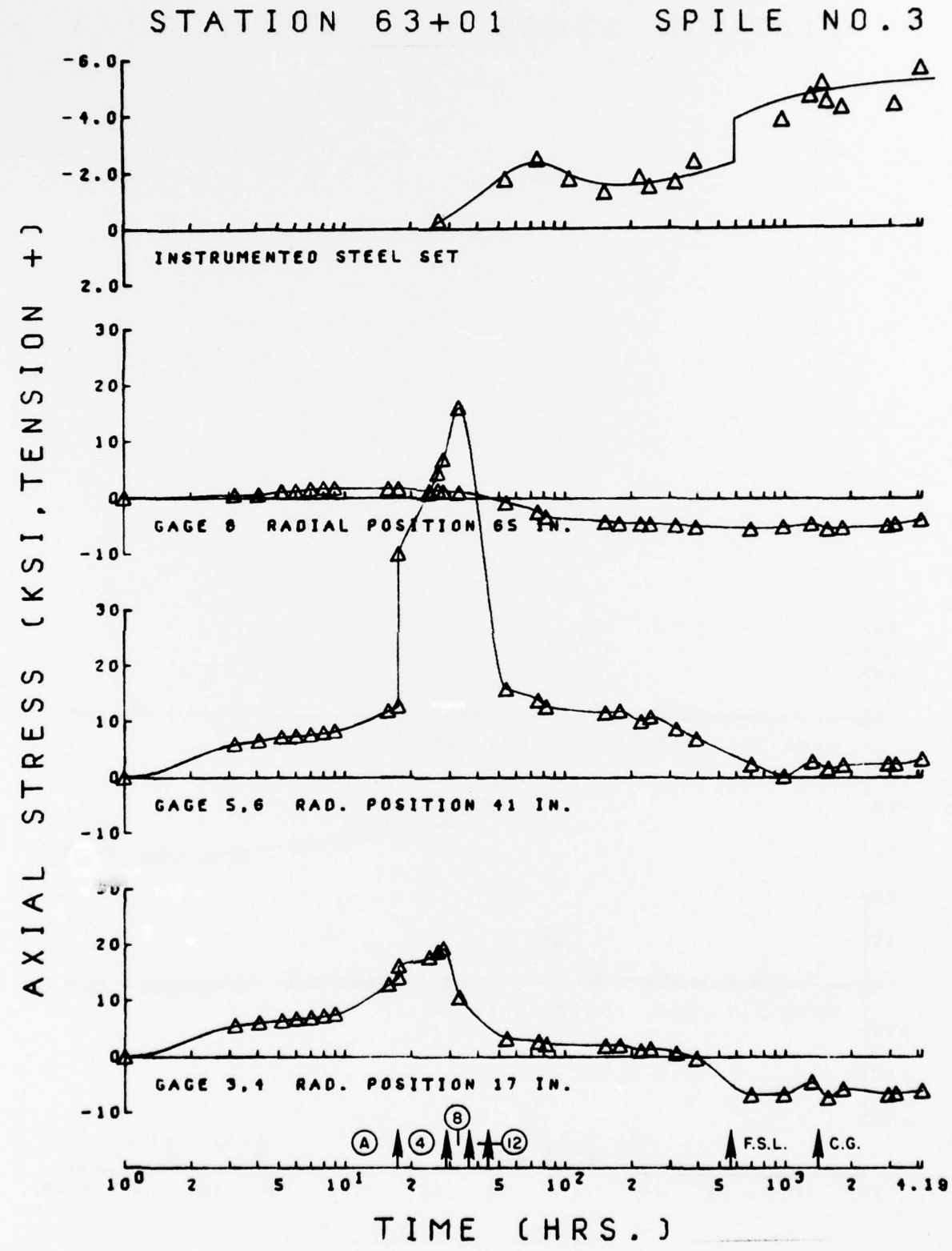

FIG. A7-6. Axial Stress History, Station 63+01, Spile No. 3 and Steel Set

STATION 63+01 SPILE NO. 3

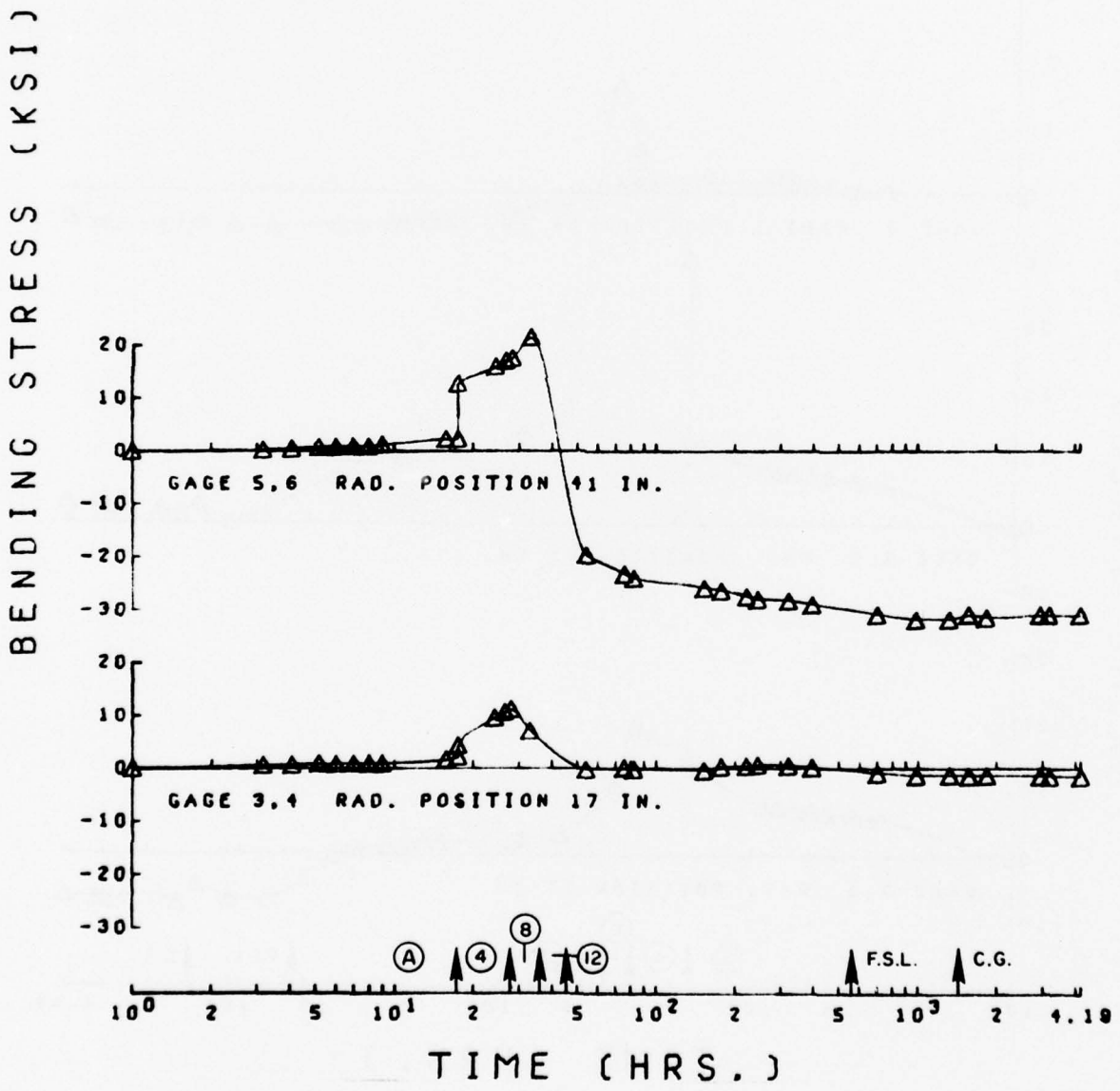

FIG. A7-7. Bending Stress History, Station 63+01, Spile No. 3

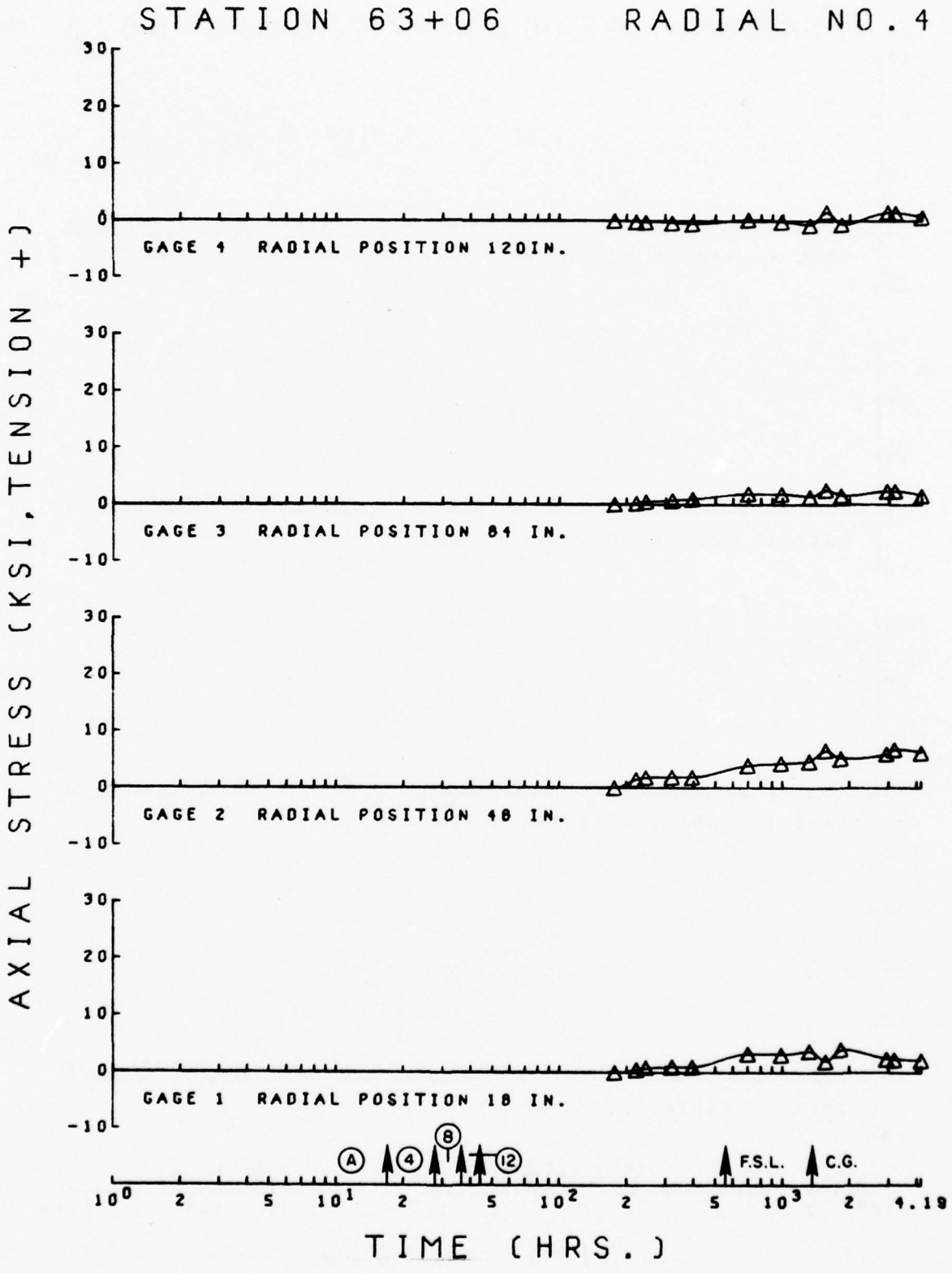

FIG. A7-8. Axial Stress History, Station 63+06, Radial No. 4

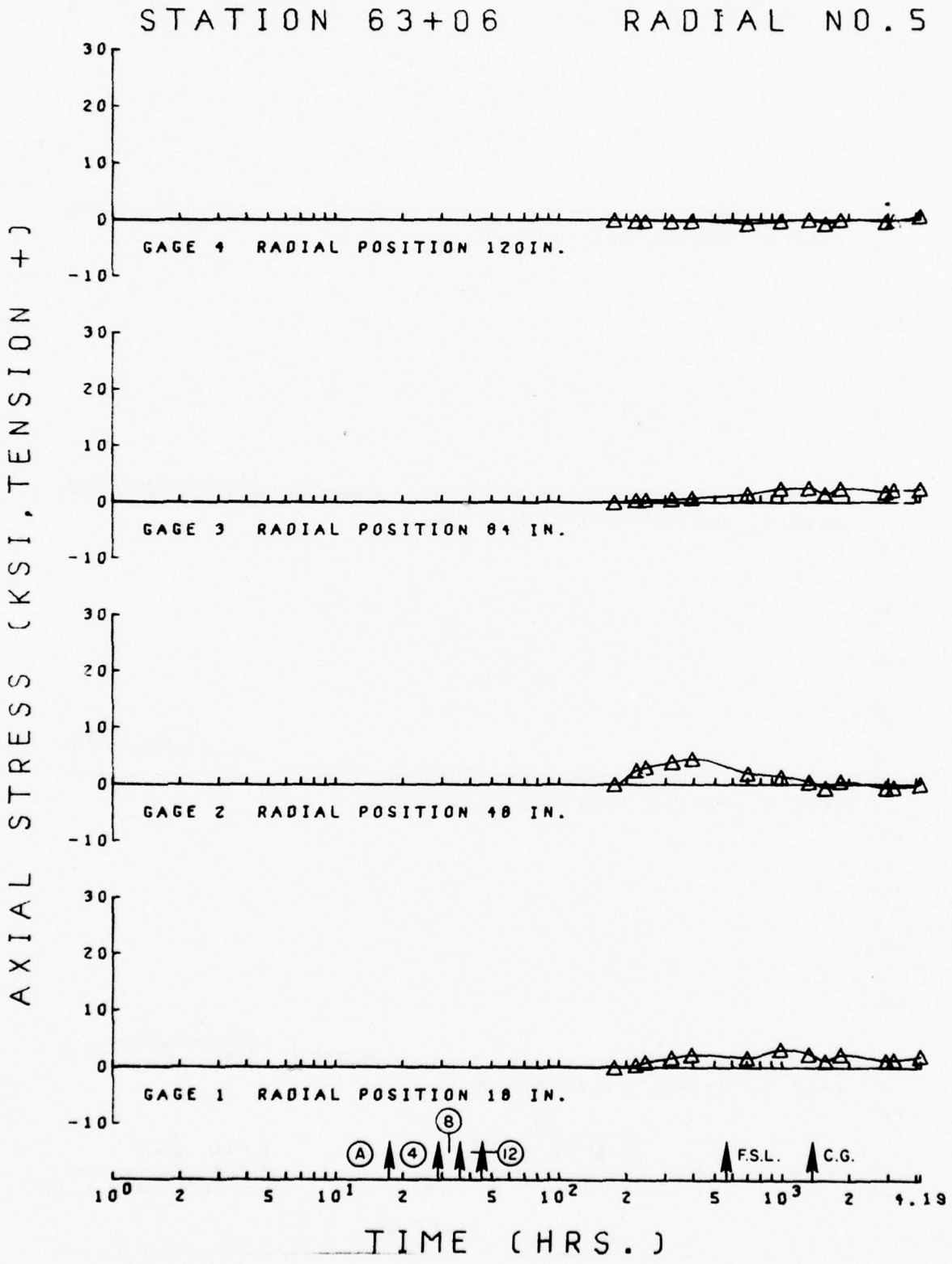

FIG. A7-9. Axial Stress History, Station 63+06, Radial No. 5

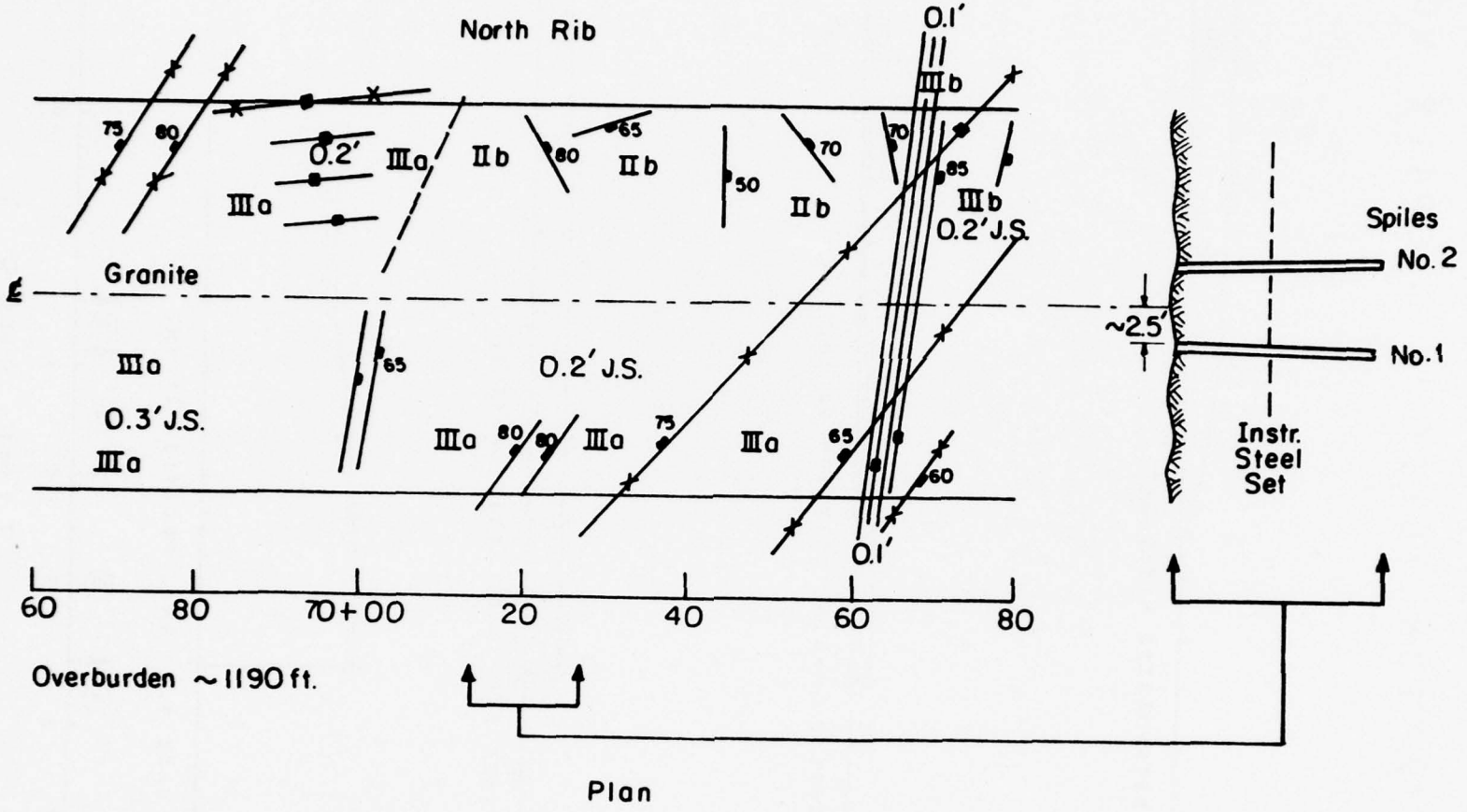

FIG. A7-10. Geologic Map (J. Post, Colo. Div. of Highways) and Instrumentation Layout in Plan, Test Station 70+14

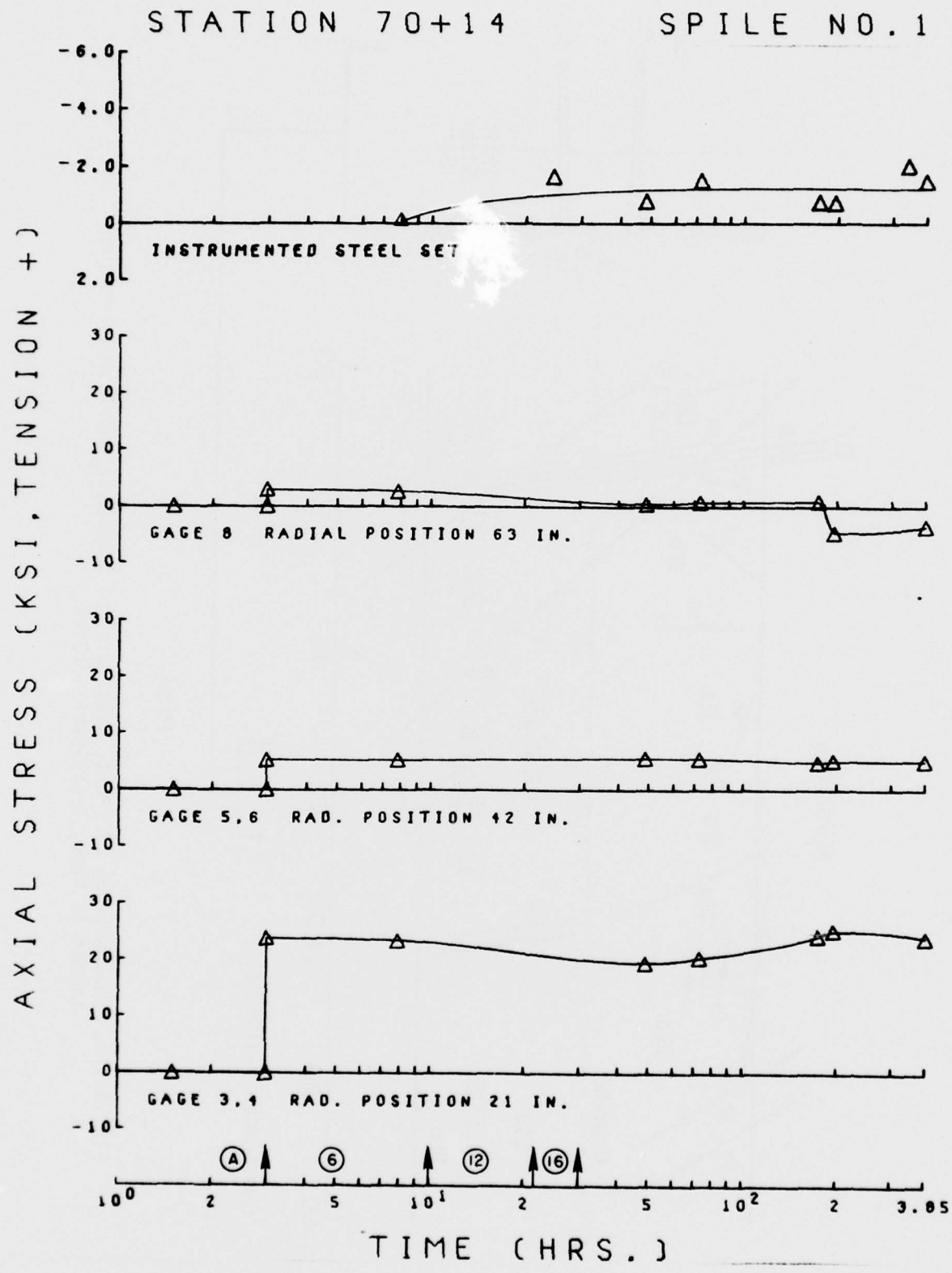

FIG. A7-11. Axial Stress History, Station 70+14, Spile No. 1 and Steel Set

STATION 70+14 SPILE NO. 1

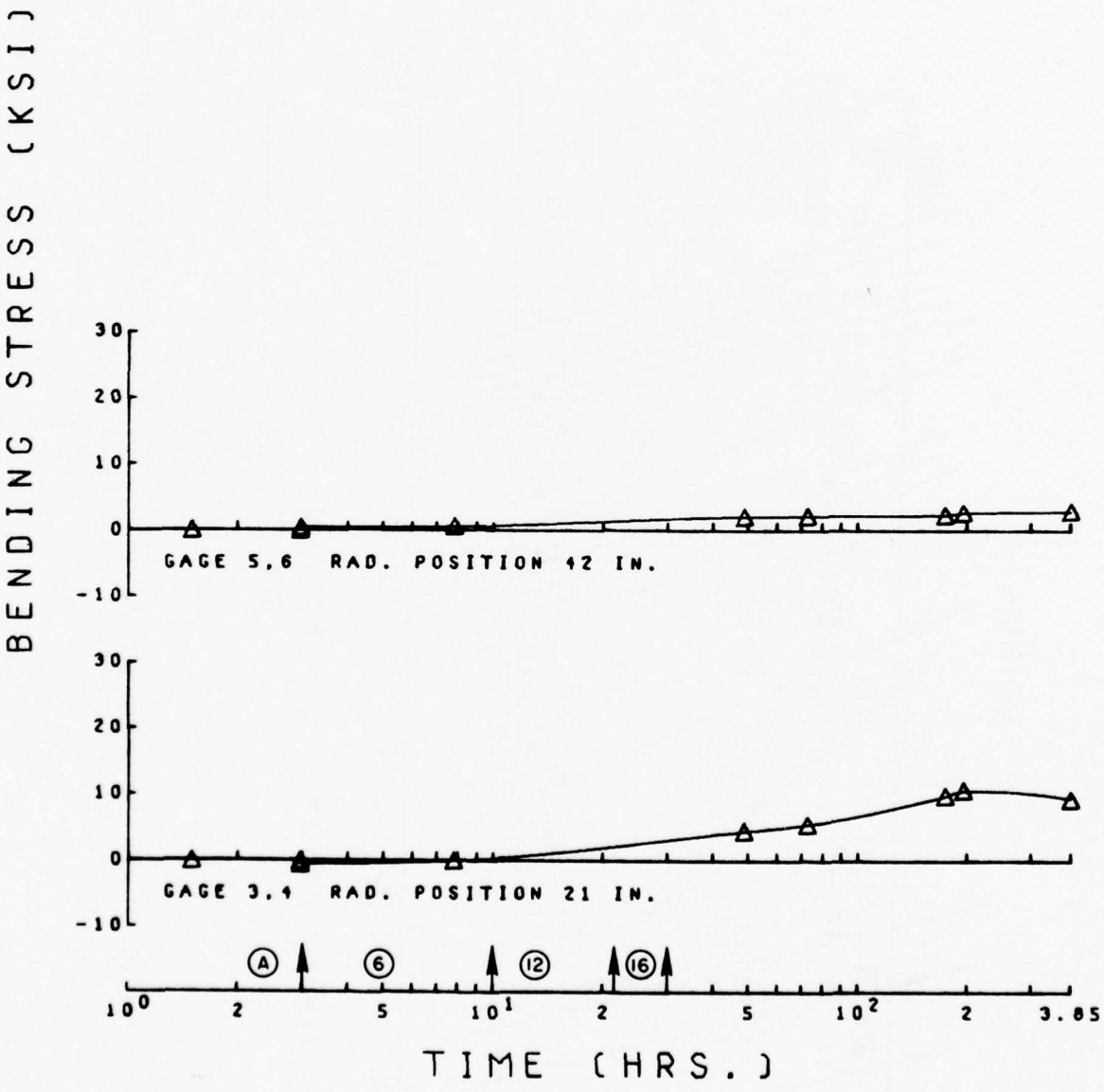

FIG. A7-12. Bending Stress History, Station 70+14, Spile No. 1

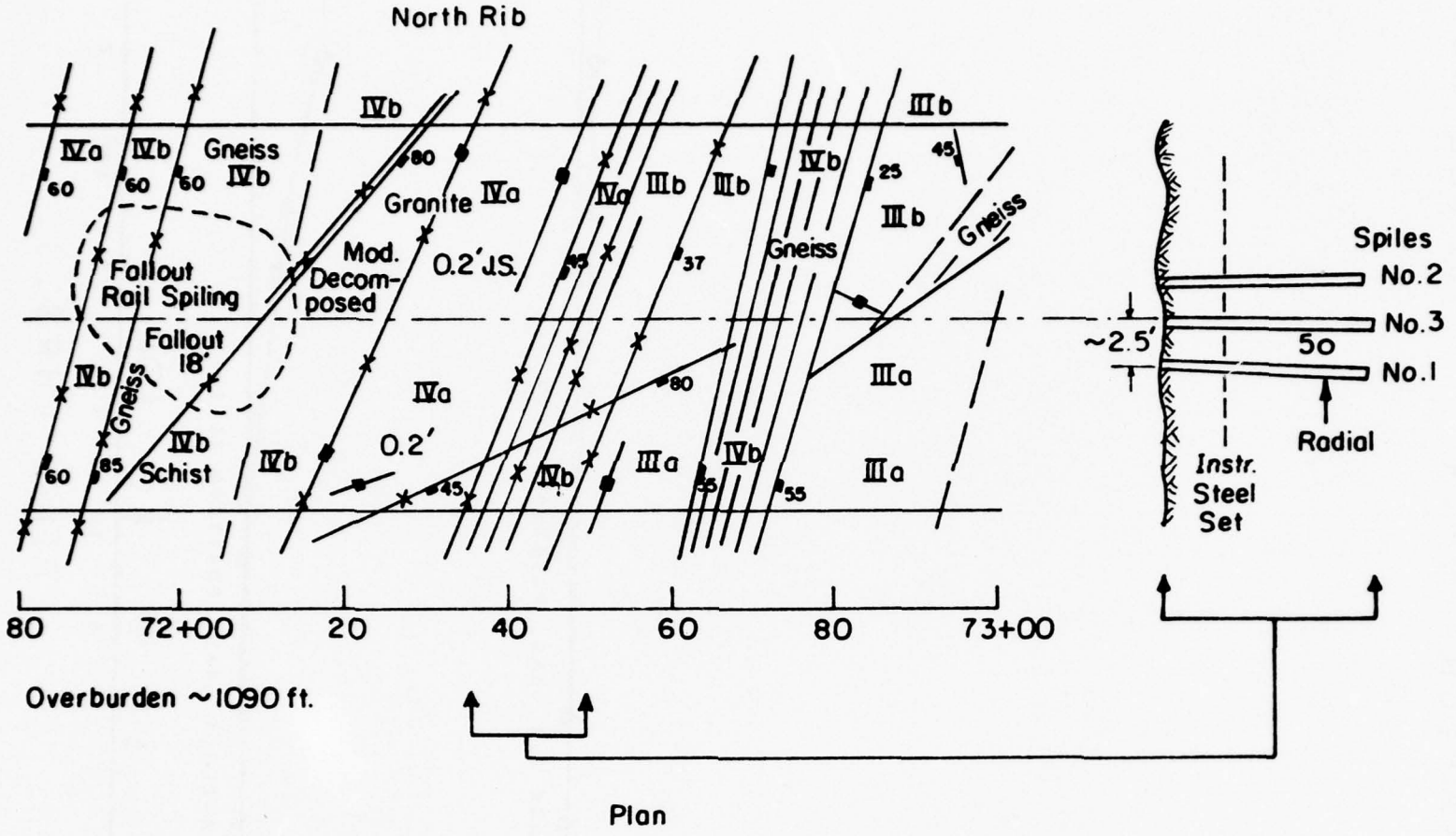

FIG. A7-13. Geologic Map (J. Post, Colo. Div. of Highways) and Instrumentation Layout in Plan, Test Station 72+36

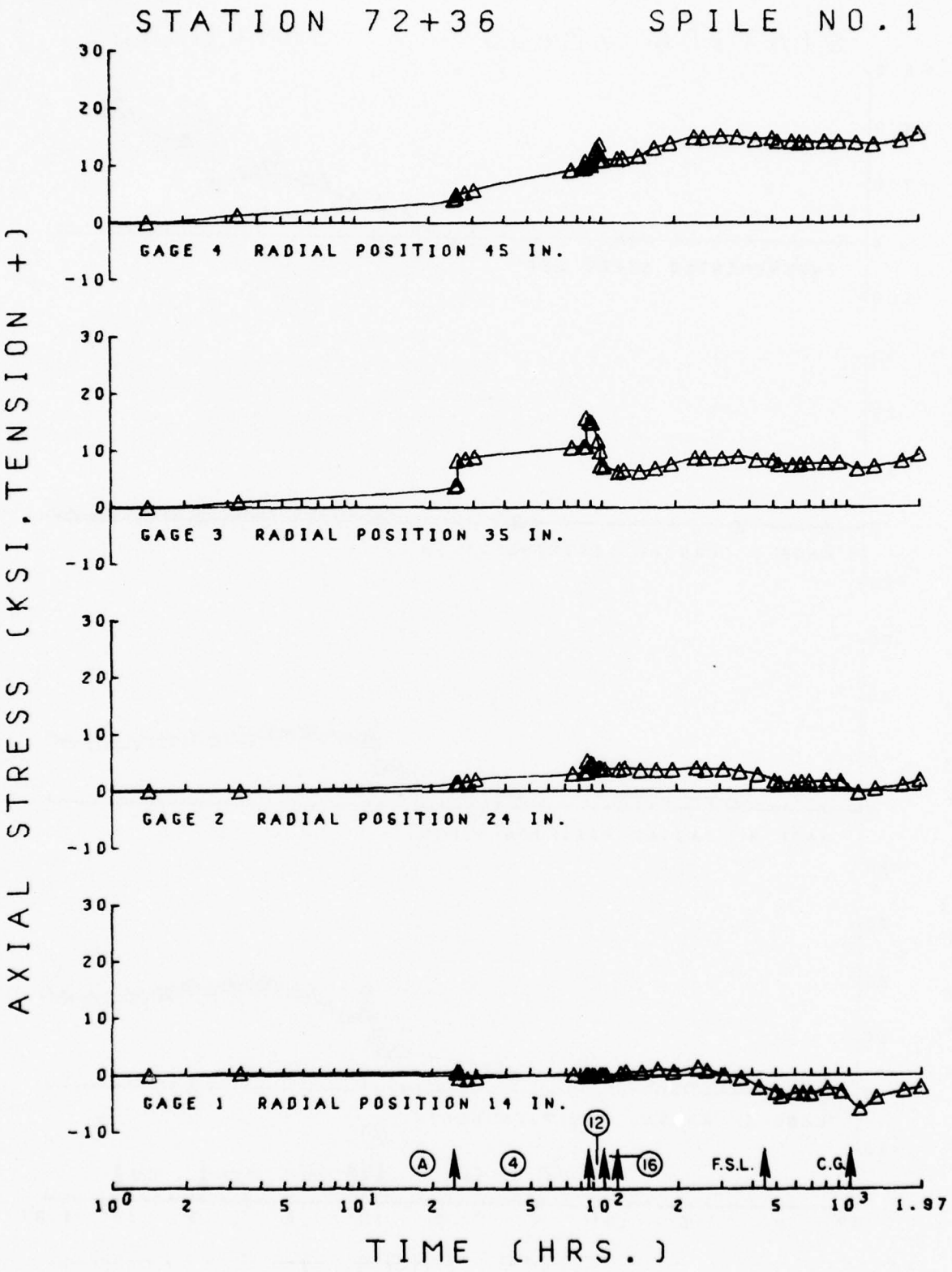

FIG. A7-14. Axial Stress History, Station 72+36, Spile No. 1 and Steel Set

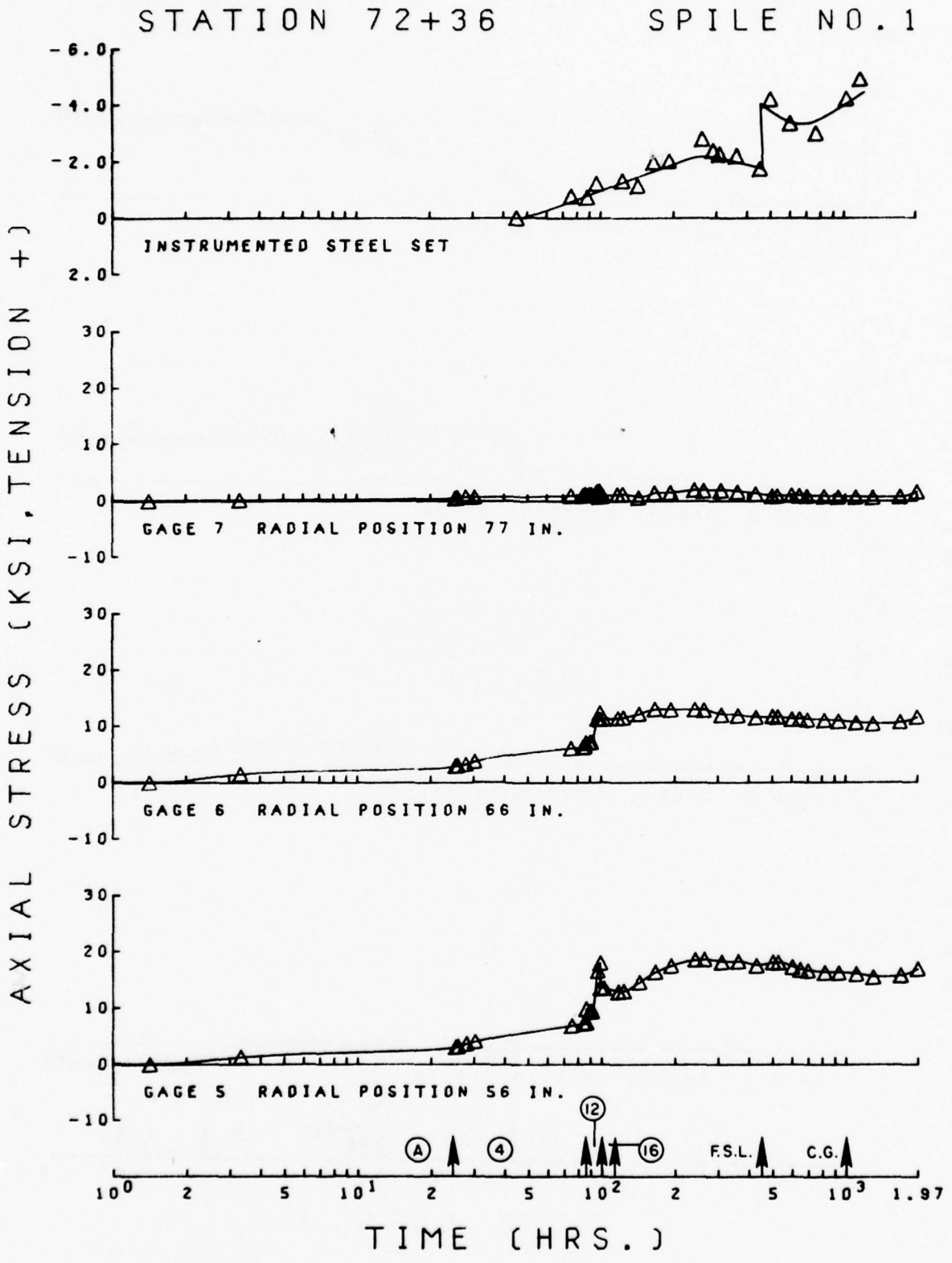

FIG. A7-14. Cont.

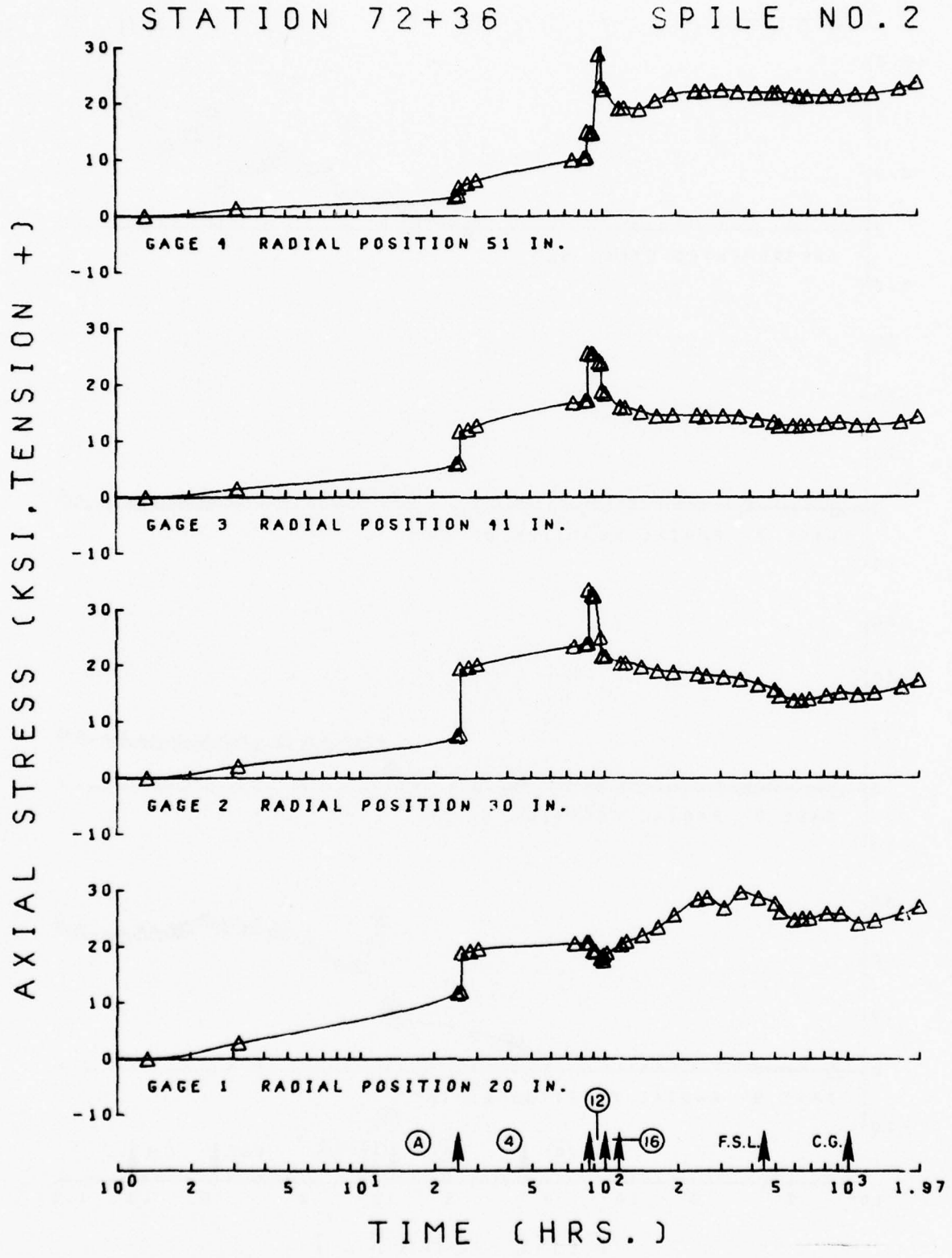

FIG. A7-15. Axial Stress History, Station 72+36, Spile No. 2 and Steel Set

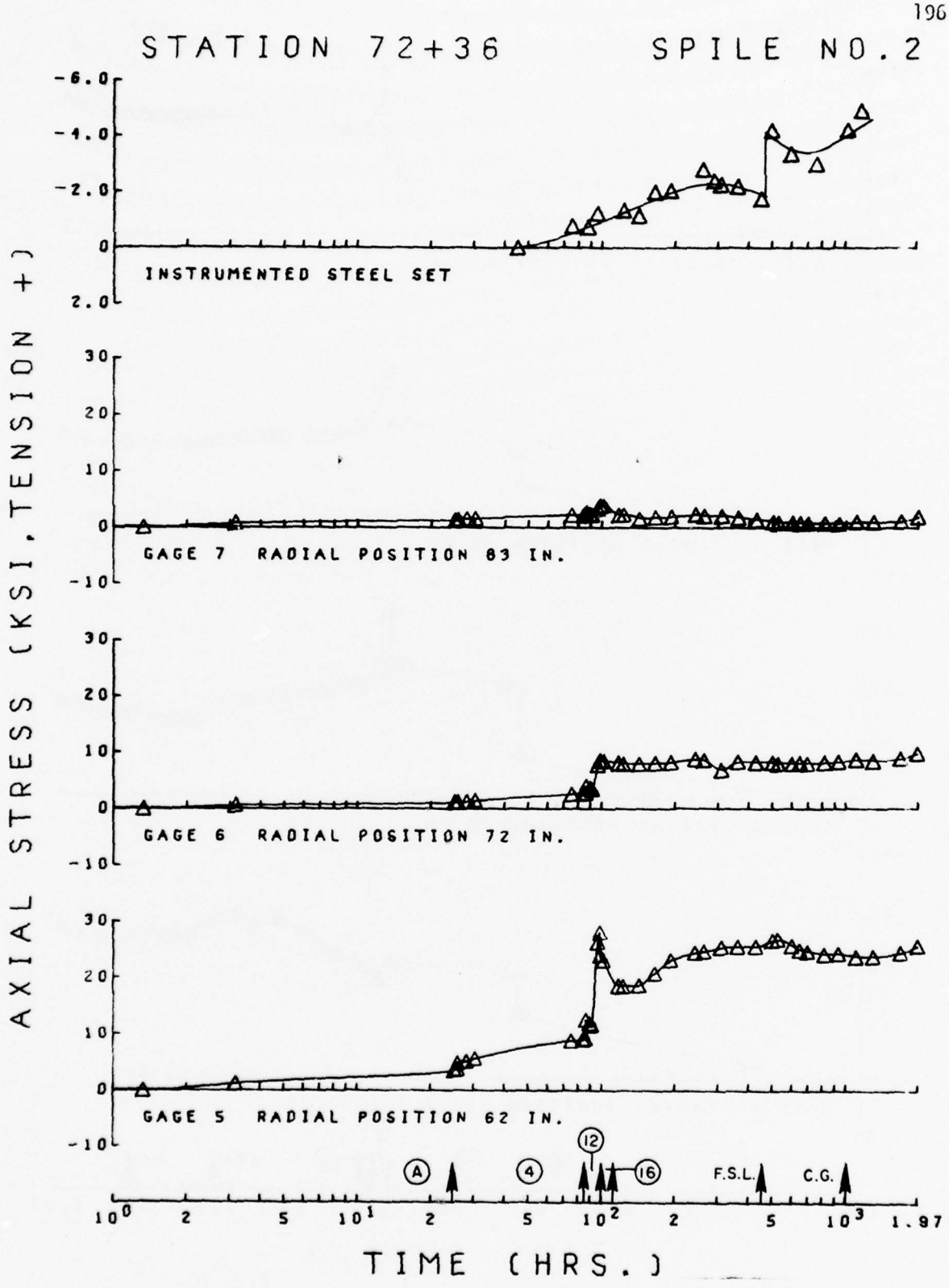

FIG. A7-15. Cont.

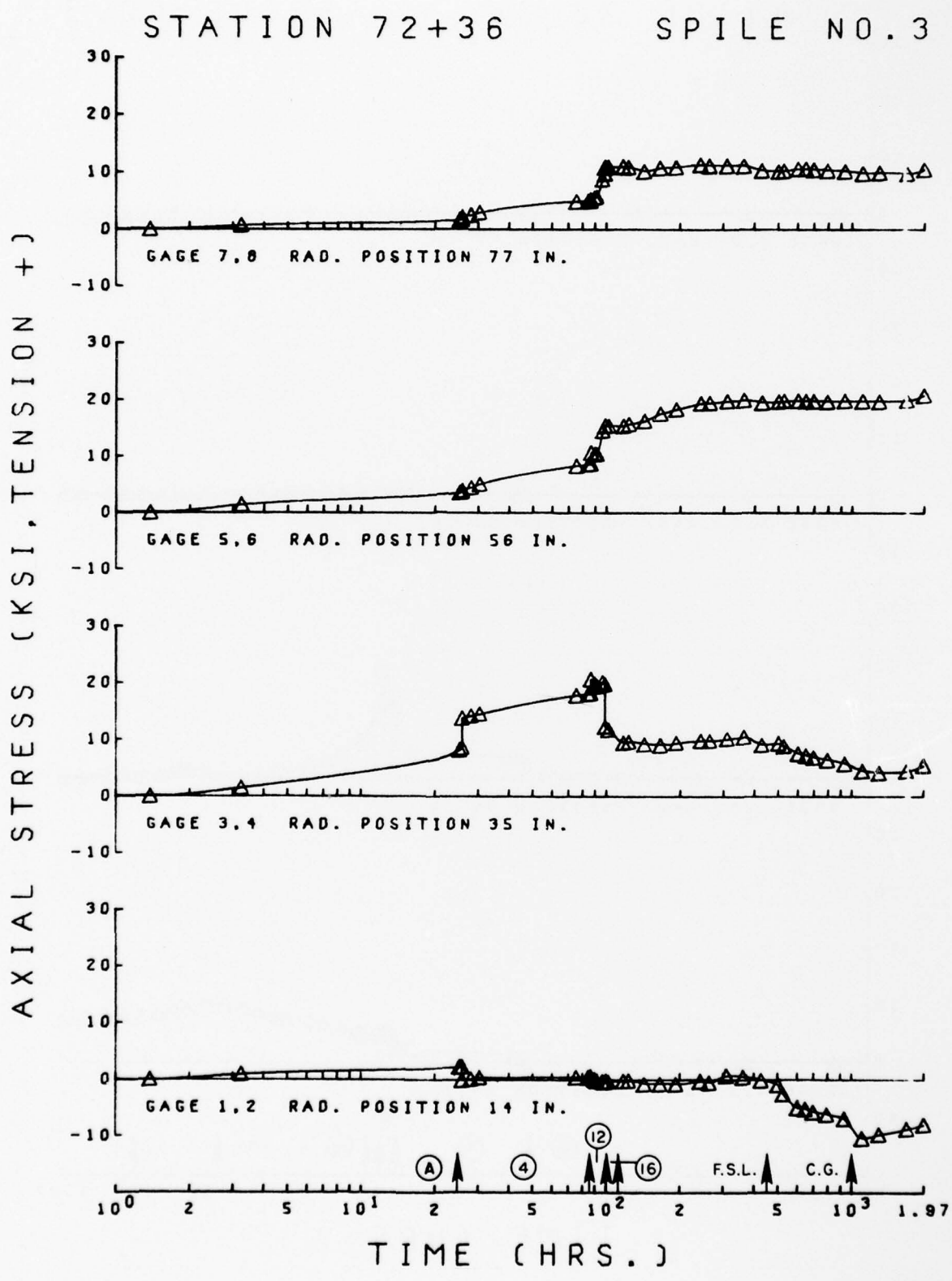

FIG. A7-16. Axial Stress History, Station 72+36, Spile No. 3

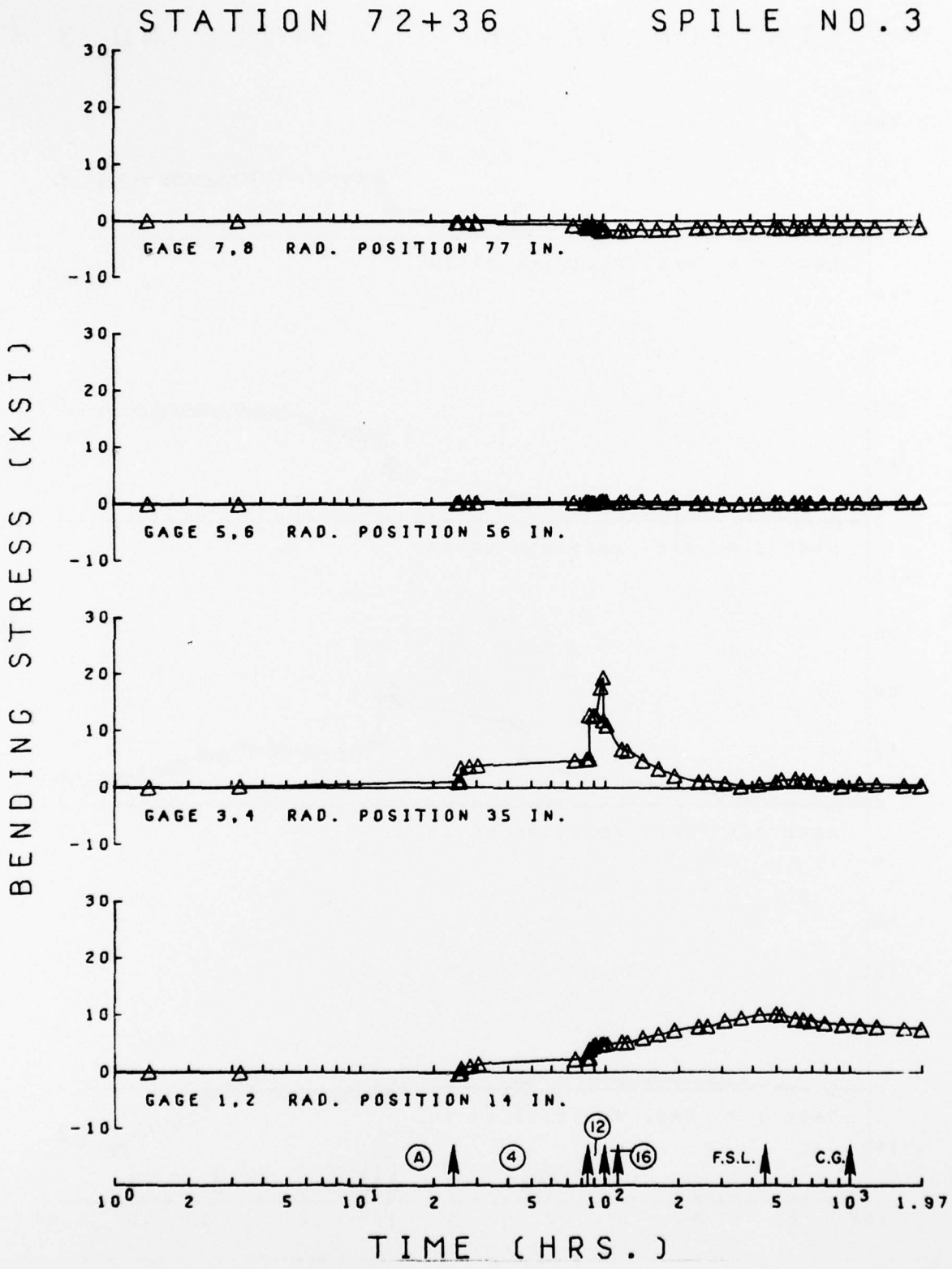

FIG. A7-17. Bending Stress History, Station 72+36, Spile No. 3

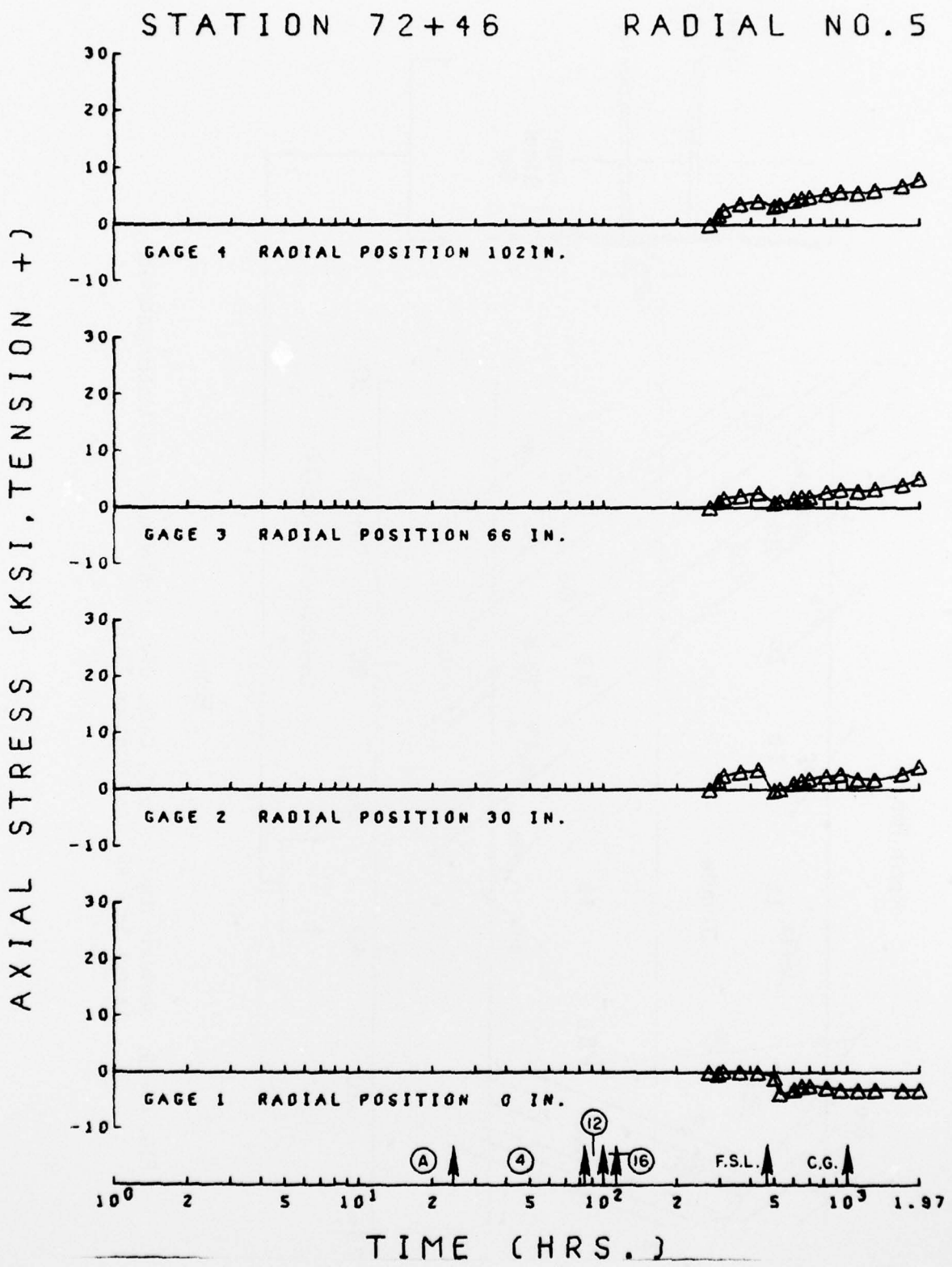

FIG. A7-18. Axial Stress History, Station 72+46, Radial No. 5

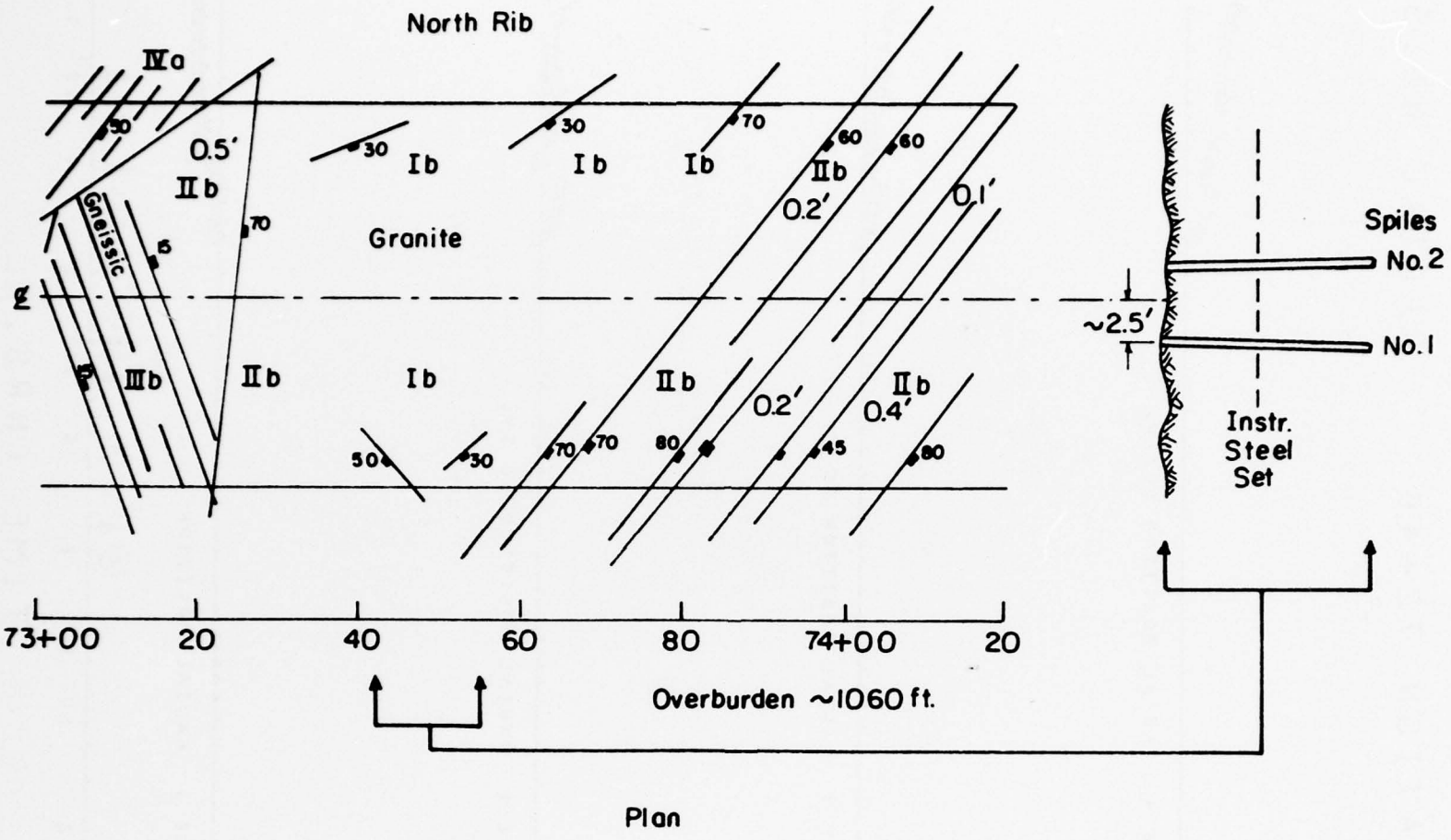

FIG. A7-19. Geologic Map (J. Post, Colo. Div. of Highways) and Instrumentation Layout in Plan, Test Station 73+42

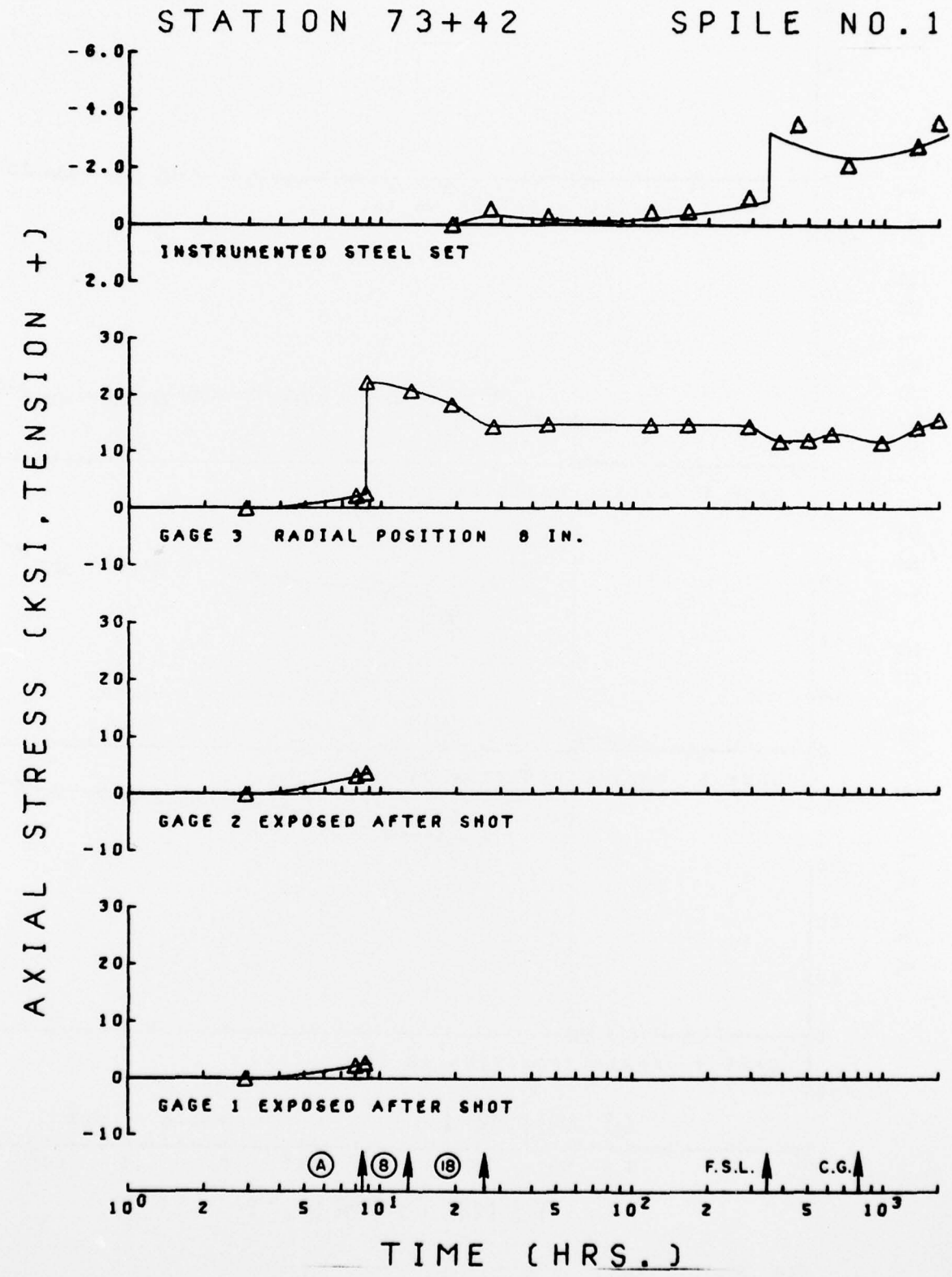

FIG. A7-20. Axial Stress History, Station 73+42, Spile No. 1 and Steel Set

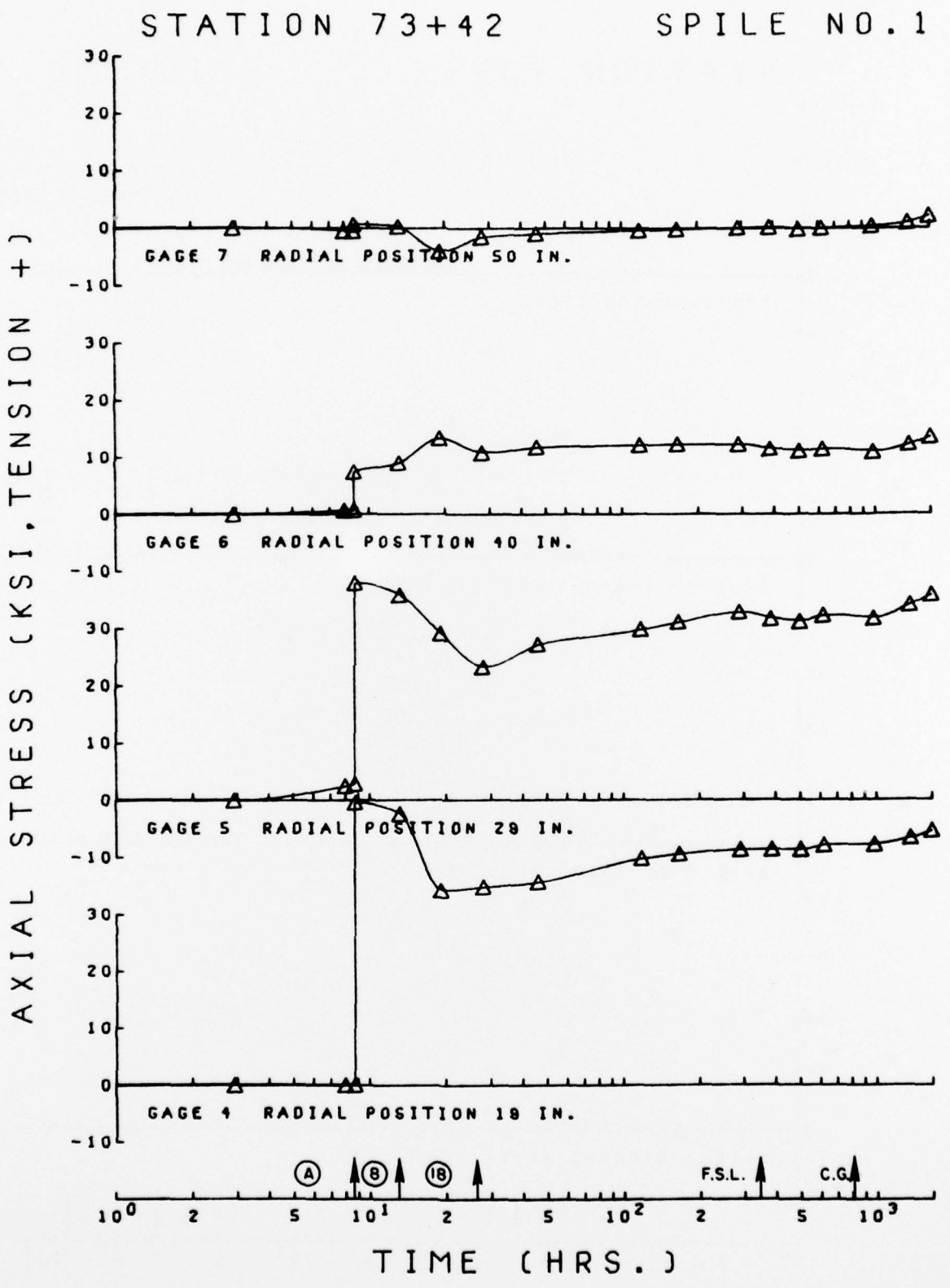

FIG. A7-20. Cont.

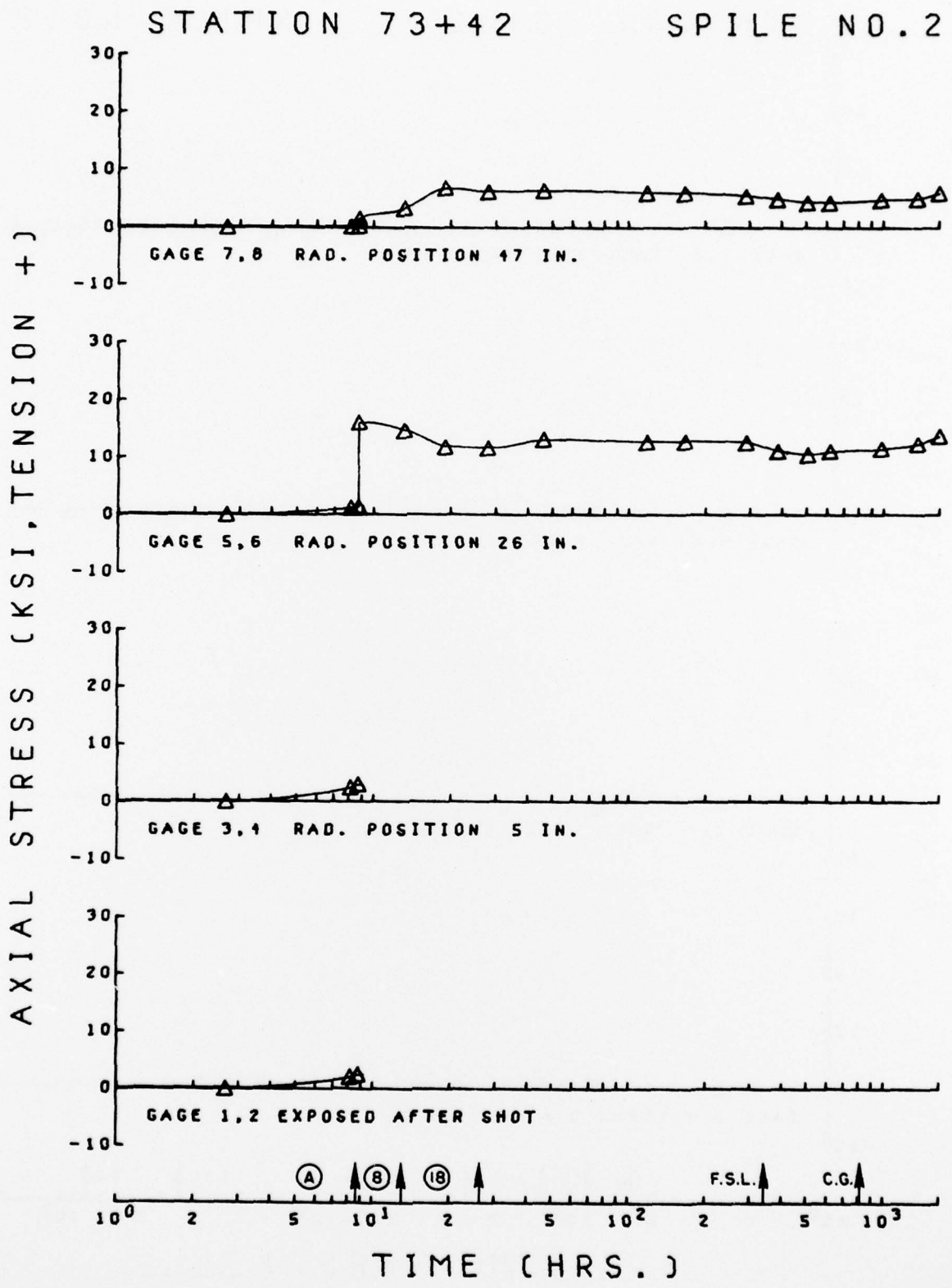

FIG. A7-21. Axial Stress History, Station 73+42, Spile No. 2

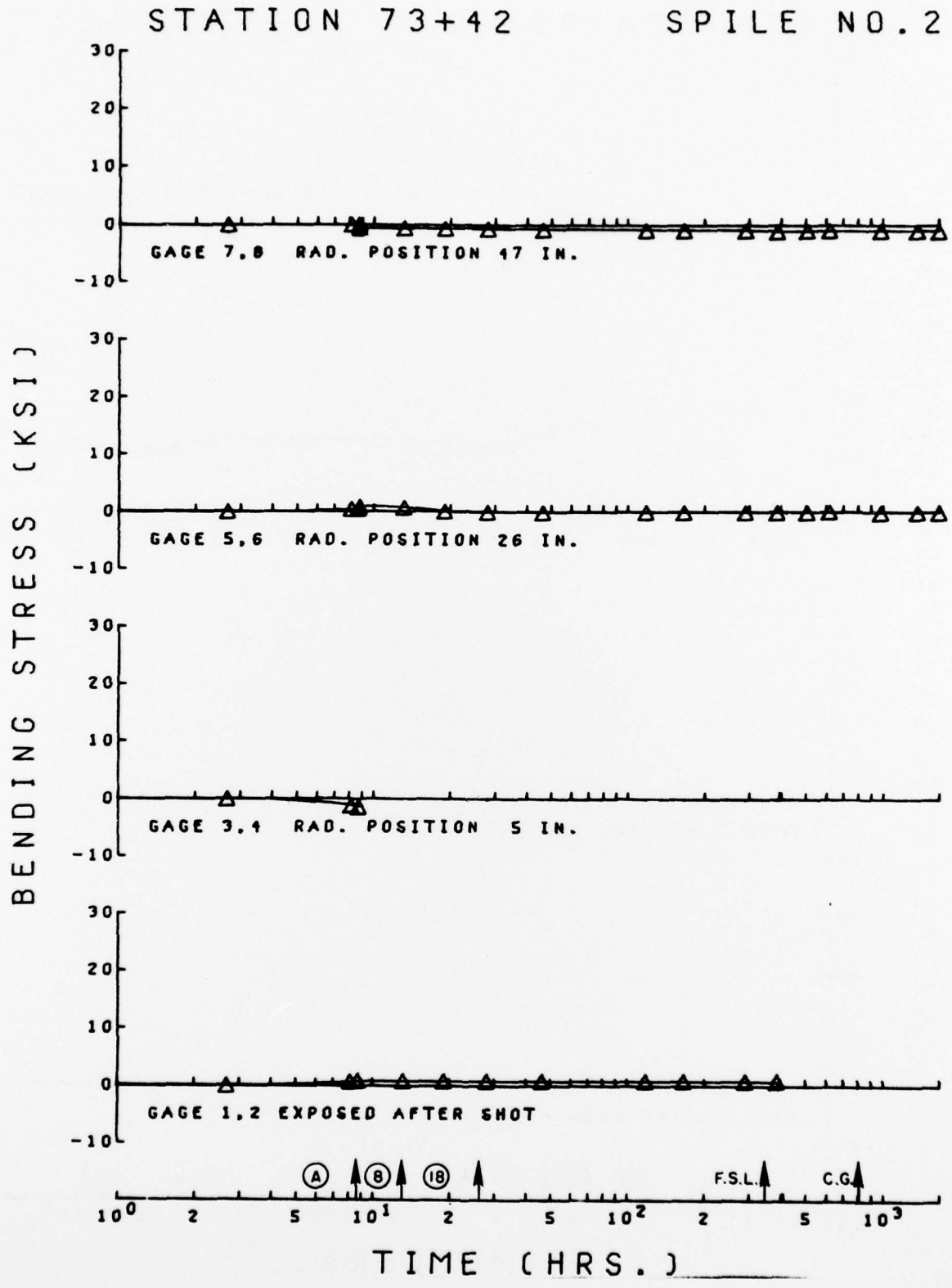

FIG. A7-22. Bending Stress History, Station 73+42, Spile No. 2

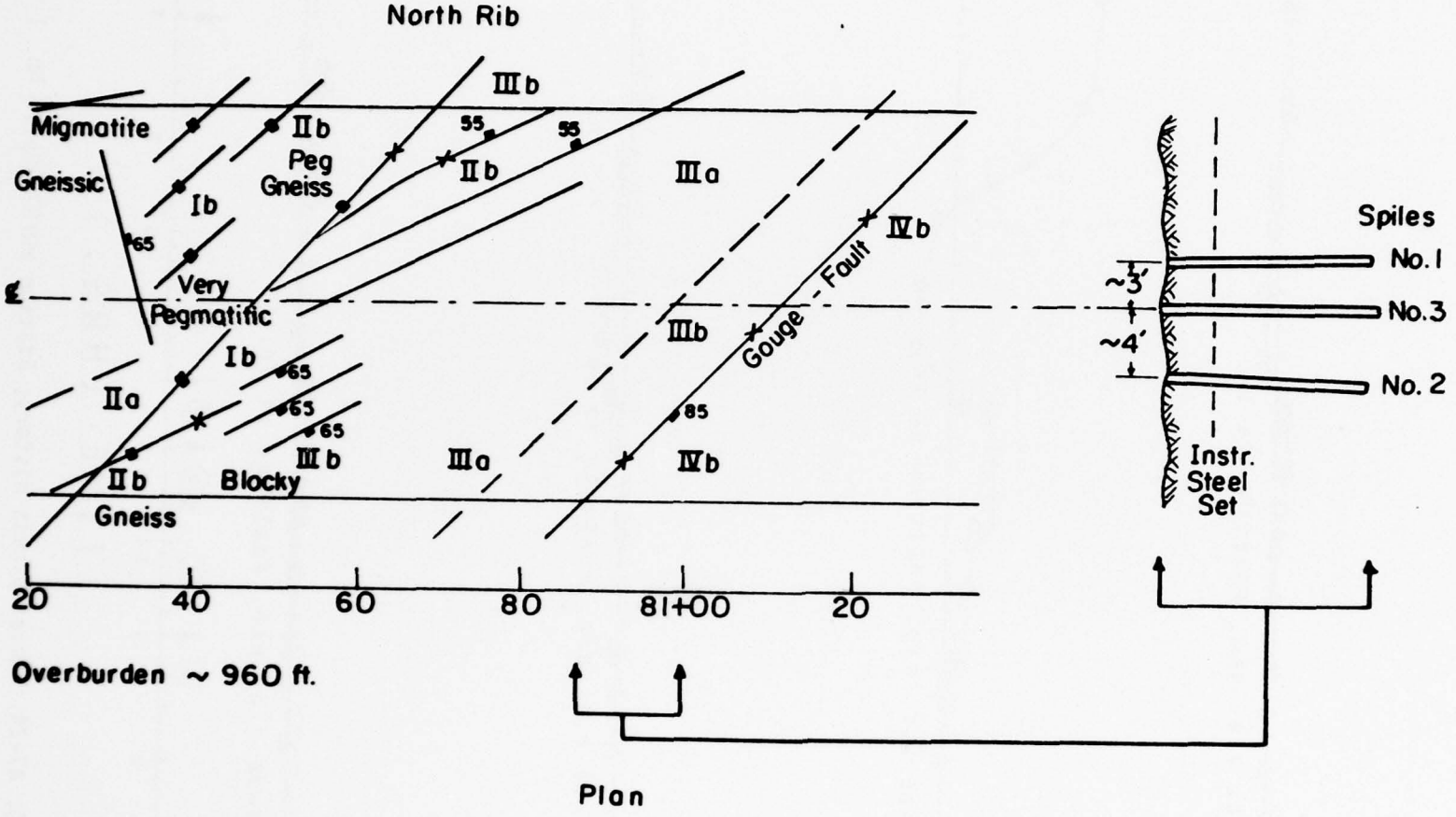

FIG. A7-23. Geologic Map (J. Post, Colo. Div. of Highways) and Instrumentation Layout in Plan, Test Station 80+87

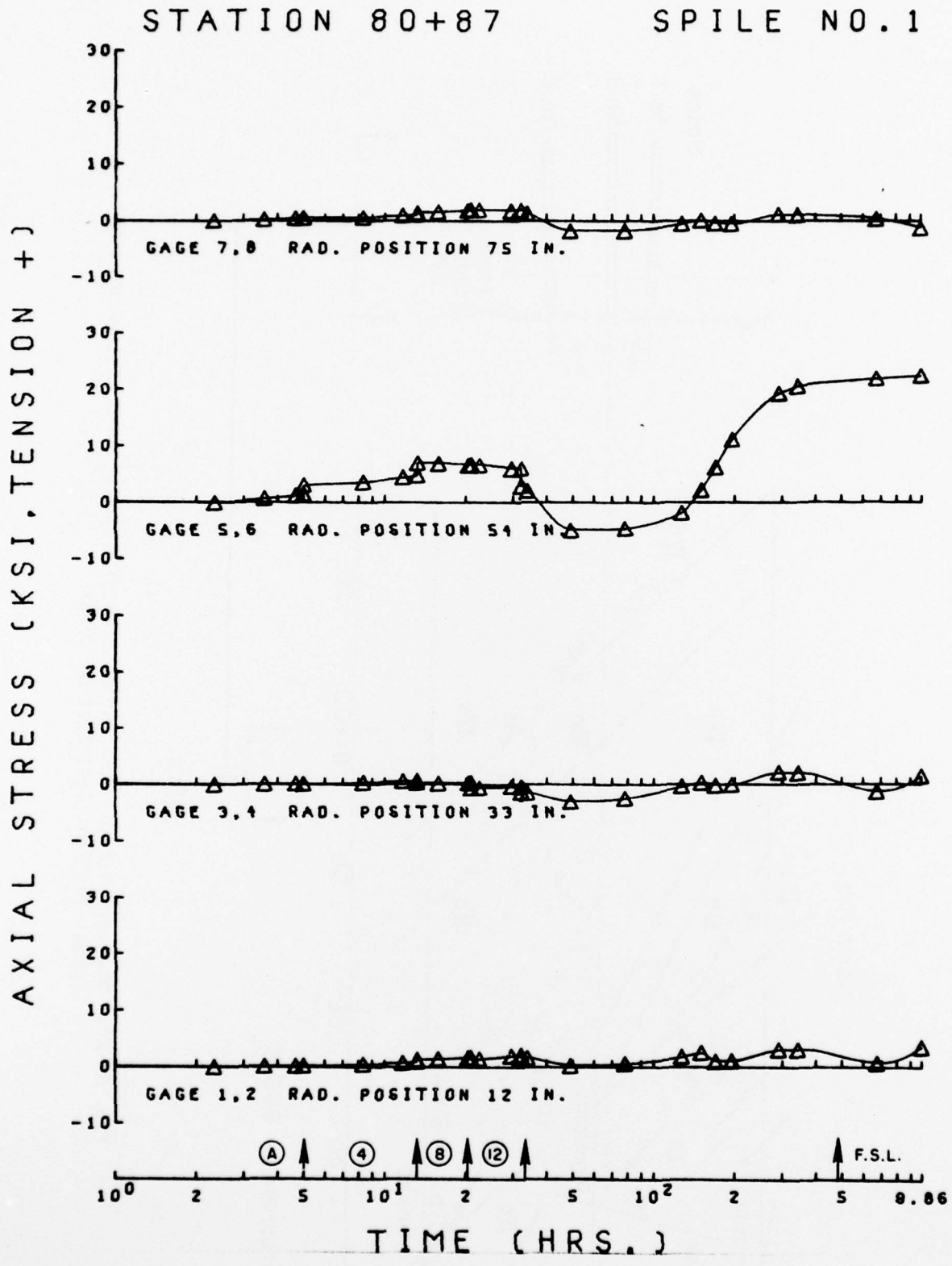

FIG. A7-24. Axial Stress History, Station 80+87, Spile No. 1

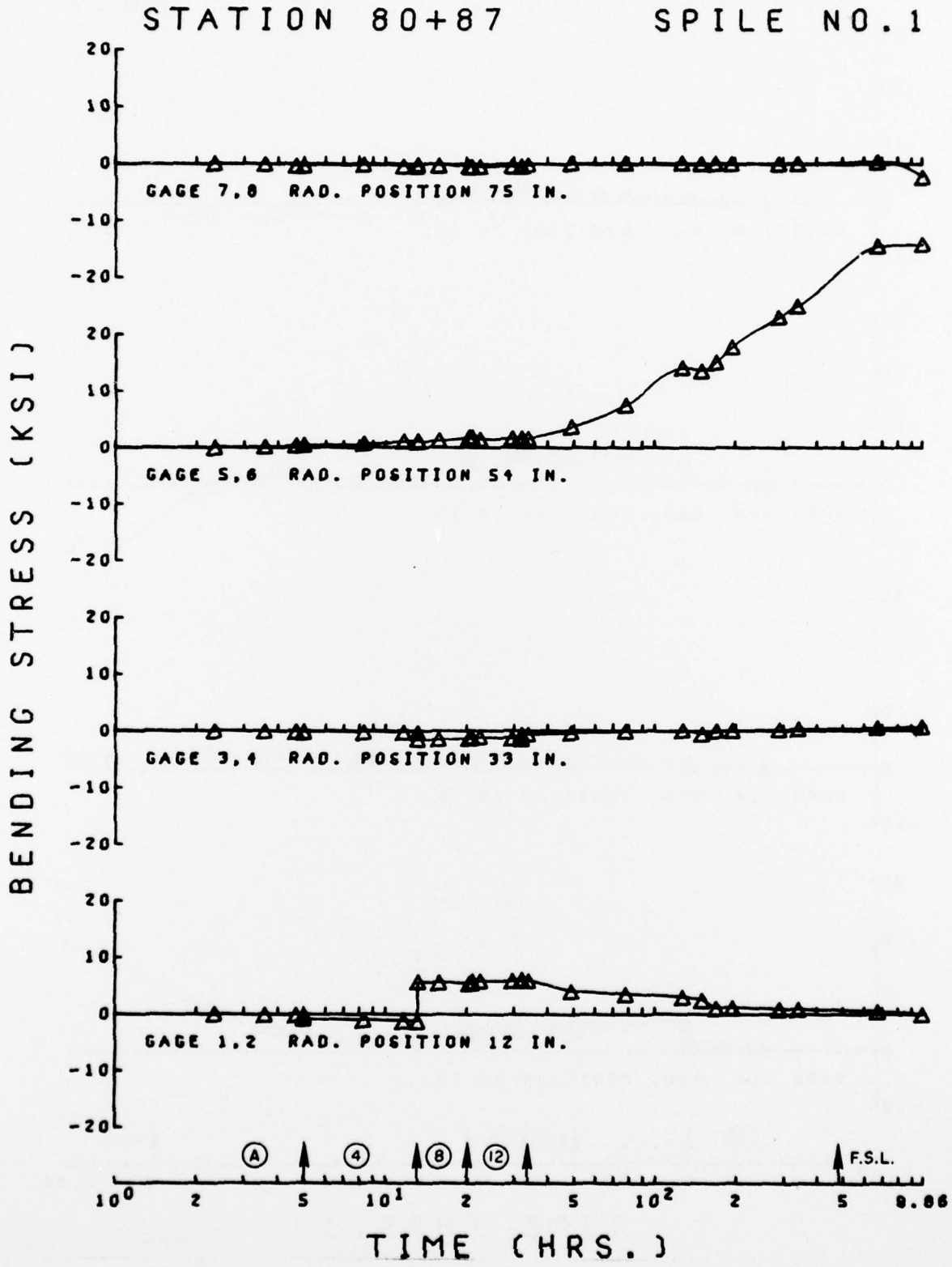

FIG. A7-25. Bending Stress History, Station 80+87, Spile No. 1

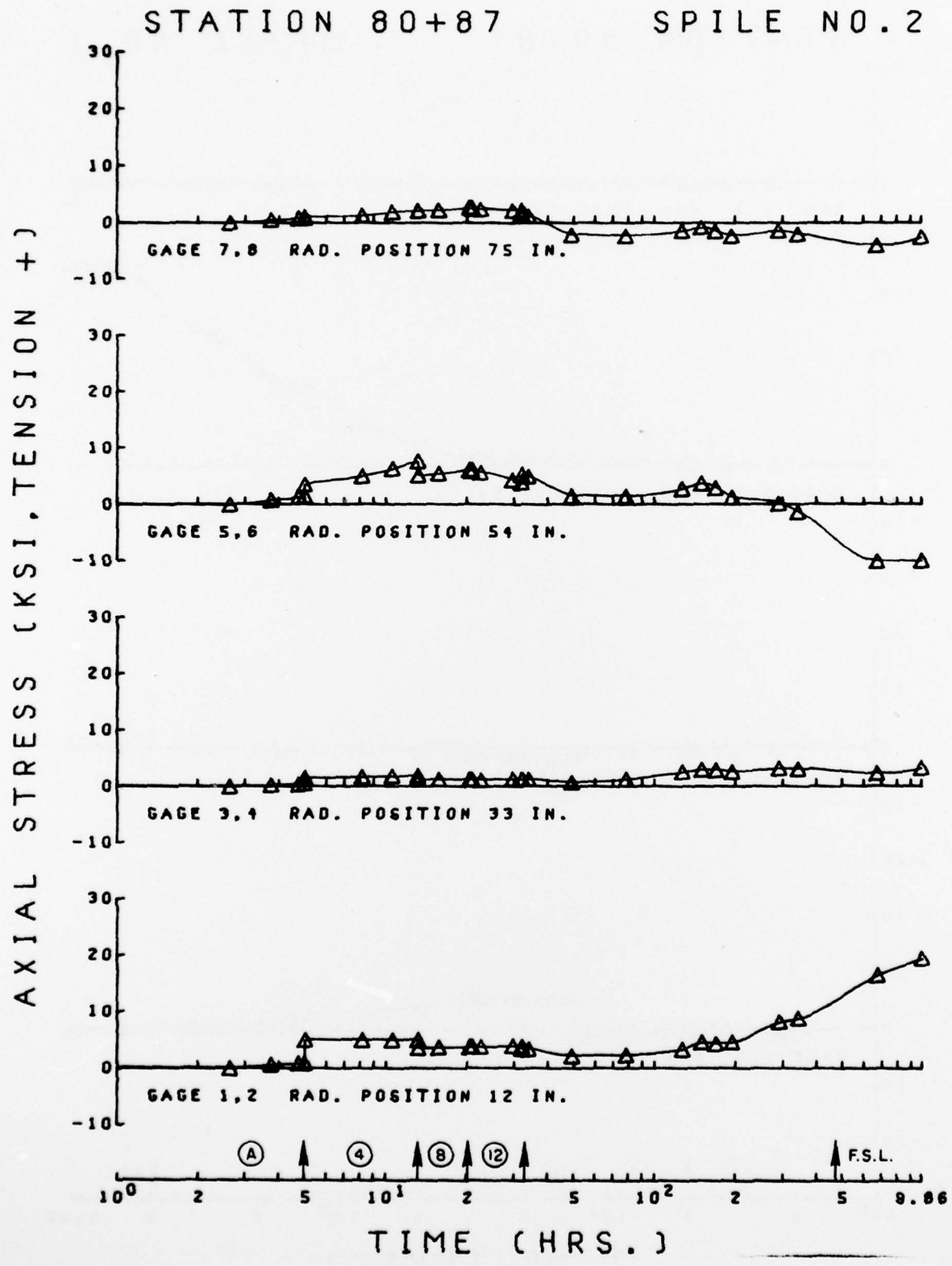

FIG. A7-26. Axial Stress History, Station 80+87, Spile No. 2

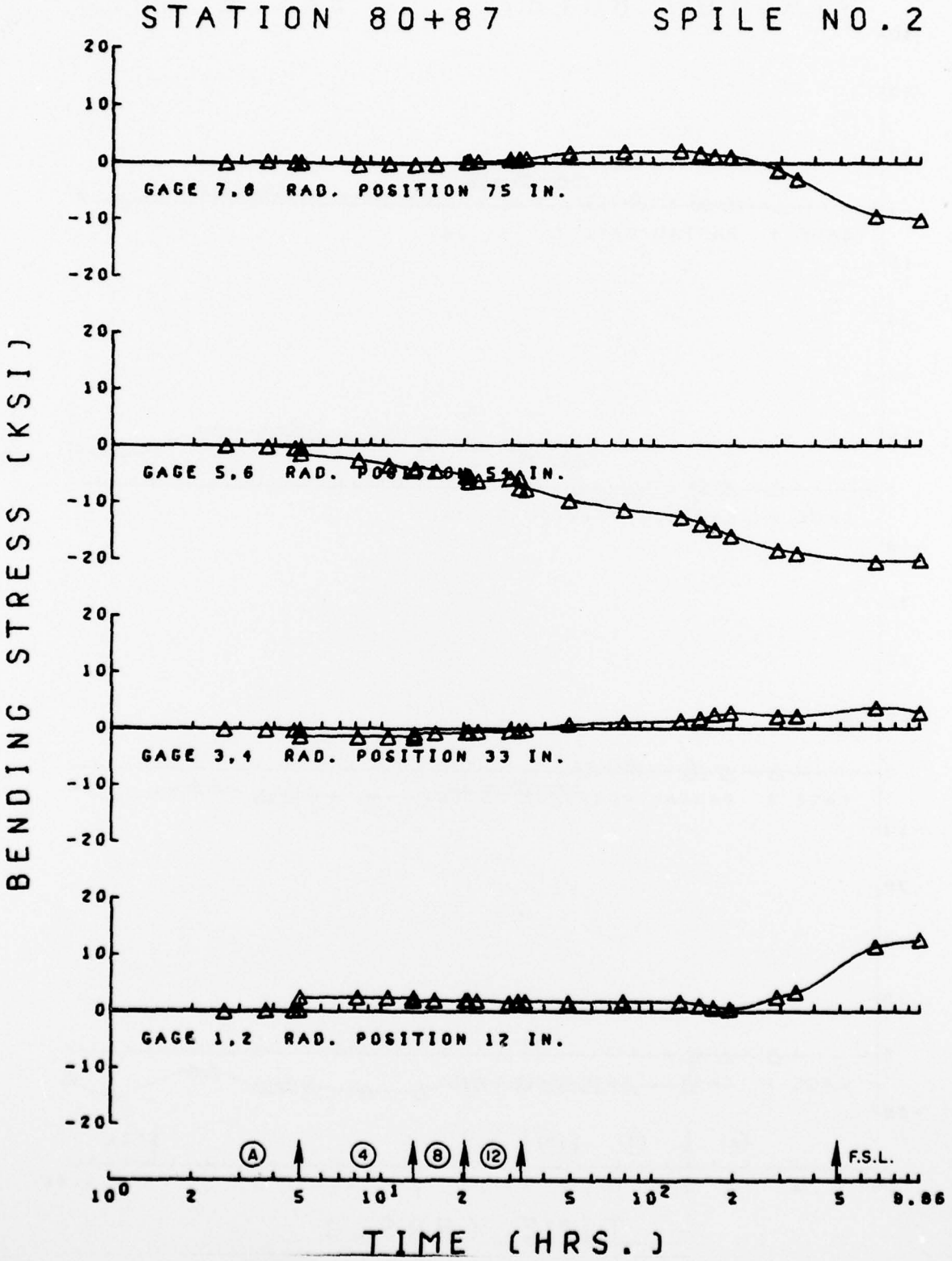

FIG. A7-27. Bending Stress History, Station 80+87, Spile No. 2

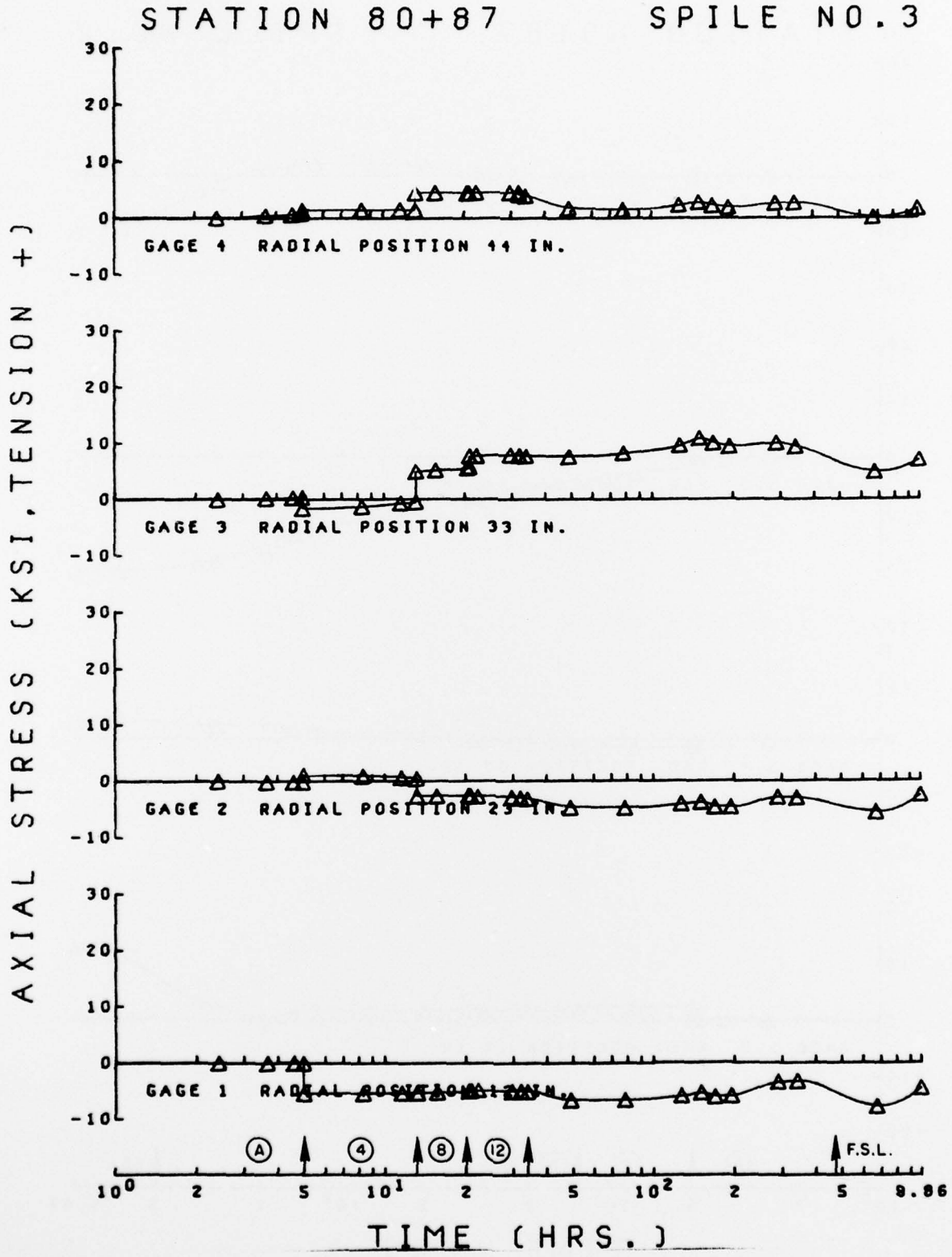

FIG. A7-28. Axial Stress History, Station 80+87, Spile No. 3 and Steel Set

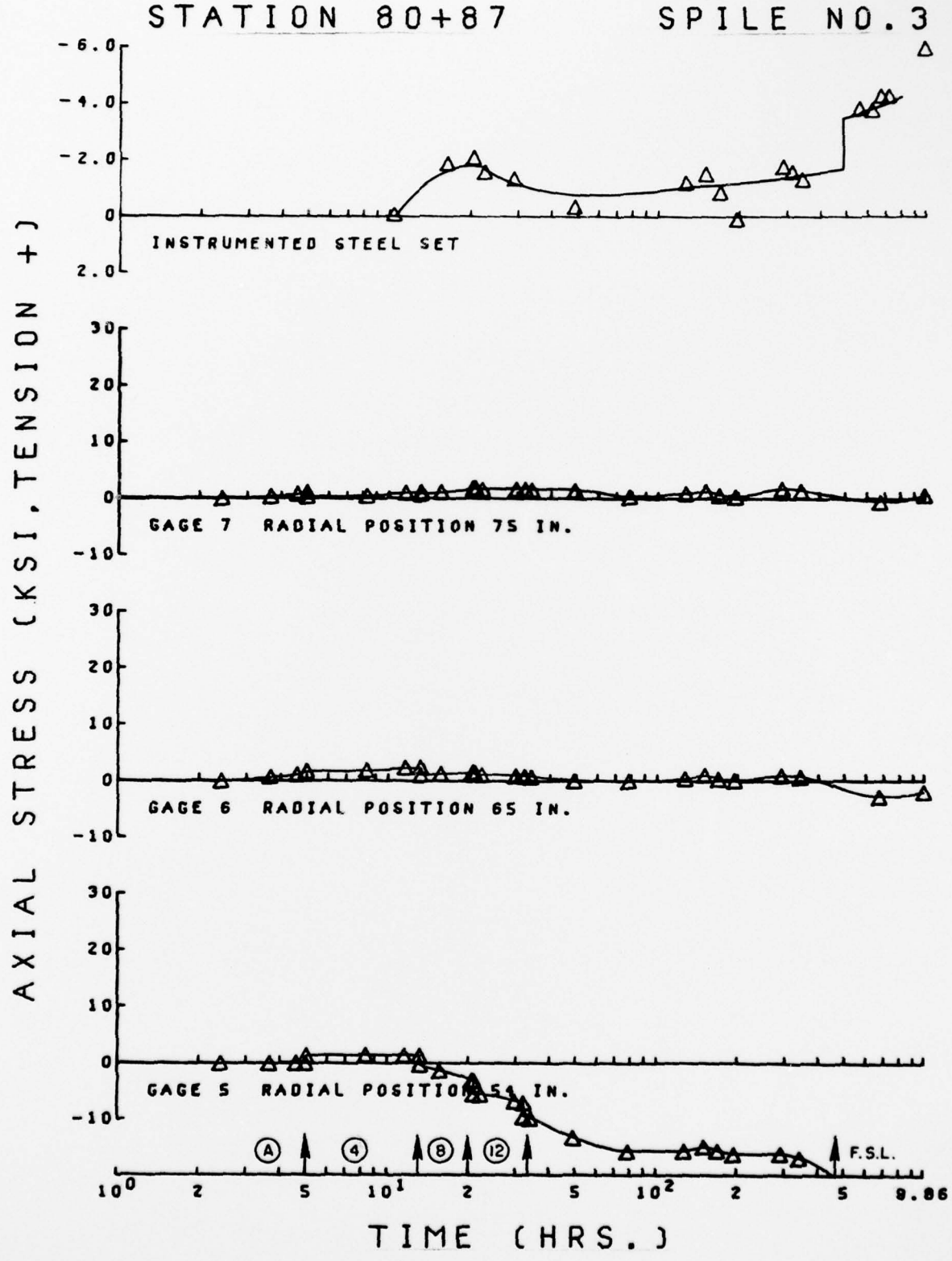

FIG. A7-28. Cont.